UNIVERSITY OF NOTTINGHAM

DEPARTMENT OF CIVIL ENGINEERING

POLYMER GRID REINFORCEMENT OF ASPHALT PAVEMENTS

by

DAVID ARTHUR BRACKEN HUGHES B.Sc.

Thesis submitted to the University of Nottingham

for the degree of Doctor of Philosophy.

May 1986

To Mum and Dad.

CONTENTS

ABSTRACT

The aim of this research was to investigate the possibility of reinforcing asphalt pavements with a polymer grid and develop a better understanding of the mechanisms of reinforcement.

Considerable expertise in the field of pavement engineering exists at the University of Nottingham and facilities were available for testing pilot scale reinforced pavements. A comprehensive laboratory study was undertaken in order to quantify the benefits of reinforcing asphalt and to this end several failure modes were isolated and the effect of reinforcement studied.

Simulative reflection cracking tests were devised and asphalt beams and slabs subjected to loading representative of traffic. It has been shown that reflection cracking can be attenuated by including a polymer grid at the base of a flexible overlay.

The effect on permanent deformation of including the reinforcement has also been examined. It has been shown that, provided the grid is situated at an appropriate position within the depth of the pavement, such deformation can be substantially reduced.

Two pilot scale pavements were constructed in the laboratory and fully instrumented. By comparing the degree of fatigue cracking and rutting in reinforced and unreinforced pavements it was shown that the polymer grid could positively reinforce asphalt pavements.

A large shear box was developed to examine the effect of including the grid at an asphalt interface. The shear strength of this interface was reduced when the grid was included, but not to a significant extent.

The analytical design methods available at the University of Nottingham were adapted to produce a preliminary design guide for polymer reinforced pavements. This was achieved by introducing factors obtained from the laboratory data which quantified the

benefits of including reinforcement, and were used to modify the failure criterion in the design.

Acknowledgements

I am grateful to Professor Peter Pell for providing the excellent facilities of his laboratories and to the members of the Civil Engineering Department for their help and encouragement during my time here.

I am indebted to Professor Stephen Brown, who supervised this project, for his guidance and patience throughout. It was a pleasure to work with the Pavement Research Group at the University of Nottingham, particularly Janet, Keith, Mike, Chris and Simon. I would like especially to thank Barry Brodrick for his invaluable assistance.

I was fortunate to have the technical help of Andy Leyko and Dennis Lockyer, although many other technicians gave a hand, and this was always appreciated.

The dissertation was prepared with the secretarial help of Rosemary Hodges and Sue Punt with assistance from Ann Smith. Despite my appalling handwriting they nearly always got it right! The figures were prepared by Caroline Brayley.

I would also like to thank Helen for her help and support throughout.

Finally the financial assistance of Netlon Ltd. and the S.E.R.C. is gratefully acknowledged, together with the cooperation of the local "black top" industry and the staff of S.W.K.P.E.

SYMBOLS

C.B.R	California bearing ratio
E	Modulus of Elasticity
G_a	Specific gravity of mixed aggregate
G_b	Specific gravity of bitumen
M_A	Percentage of aggregate in mix by mass
M_B	Percentage of bitumen in mix by mass
N	Design life
P_i, P_r	Initial and recovered bitumen penetration
S_b	Bitumen stiffness
S_m	Asphalt mix stiffness
SP_i, SP_r	Initial and recovered softening point of bitumen
V_b	Percentage volume of binder
VMA	Voids in mixed aggregate
V_v	Percentage volume of voids
h	Thickness of layer
ϵ	Strain (suffices denote direction)
σ	Direct stress (suffices denote direction)
ν	Poissons's ratio
τ	Shear stress
ϕ	Angle of internal friction

Suffices

r	radial
t	tangential
z	vertical

Conventions

All compressive stresses and strains are positive

INTRODUCTION

1.1 PAVEMENT DESIGN PHILOSOPHY

Asphalt pavement structures may vary from heavy duty constructions, such as that on an aircraft runway or motorway, through major trunk roads, to single track access roads and country lanes. The first consideration,therefore,for the structural design of a pavement is the class of road and hence volume, speed and weight of vehicles likely to use the route.

To simplify the design process a standard axle weight of 80kN in the United Kingdom (UK) has been specified, and the range of axle loads encountered on any pavement structure are converted to an equivalent number of these standard axles.

One application of an axle load L, is equivalent to F applications of a standard axle load L_s.

where $$F = \left[\frac{L}{L_S}\right]^a \qquad 1.1$$

The value of the power a is commonly 4 or greater.

Having ascertained the damaging power of individual axles it is then possible to convert the damaging power of any particular commercial vechical (i.e. over 1.5 tonnes unladen) to an equivalent number of standard axles. Knowing the damage factor for every type of commercial vechical the number of standard axles on any particular road on any day, may be obtained by counting the number and type of commercial vechicles and applying the previously calculated factor to each. One unique damage factor may be obtained for a road so that when this is multiplied by the total number of commercial vechicles

per day the equivalent number of standard vechicles is immediately obtained. This damage factor depends on the class of road and may vary typically between 0.78 and 3.76 for a trunk route (Powell et al 1984). Damage factors may be obtained as outlined in Road Note 40 (T.R.R.L. 1978).

By estimating the traffic growth rate and knowing the design life of a pavement, usually 20 years, the total number of standard axles likely to use the pavement may be estimated.

The average temperature of the pavement and speed of traffic has an effect on the mechanical properties of bituminous materials, and hence structural design, but these may or may not be taken into account directly, in the design process.

A second consideration in the structural design process is the strength of the subgrade, this plays a major part in determining the level of stresses generated in the pavement. The role of the pavement is to reduce the level of transient stress in the subgrade to some pre-determined permissible value. Obviously if a subgrade is weak a stiffer pavement will be required to reduce the levels of stress than would otherwise be required if the subgrade were strong. Relationships have been derived from back-analysing structures, relating the level of vertical compressive elastic strain in the subgrade under a standard 40kN dual wheel load, to design life of the pavement. (Powell et al 1984, Brown and Brunton 1984(a)). This criterion is regarded as an indication of the likely development of permanent deformation in a pavement.

The most common assessment of subgrade strength is given by the Californian Bearing Ratio (C.B.R.). This may either be obtained insitu or in the laboratory on recovered samples. Taking account of the likely moisture conditions in the pavement during its life, the C.B.R. of the foundation dictates the strength of pavement required.

Where the C.B.R. of the subgrade is less than 5 percent a capping layer may be required to provide an adequate platform on which to construct the pavement. Several relationships have been derived which offer a means of converting a C.B.R. to a modulus of elasticity (E.) such as:

$$E = 17.6 \times (C.B.R.)^{0.64} \quad MPa \qquad 1.2$$

(Powell et al 1984)

or $$E = (C.B.R.) \times 10 \quad MPa \qquad 1.3$$

(Heukelom et al 1962)

(C.B.R. quoted in percent).

Two typical pavements structures are shown in Fig. 1.1. Fig. 1.1(a) illustrates the most common type of construction, whereas Fig. 1.1(b) illustrates a full depth asphalt construction, which obviates the need of a sub-base layer.

Most pavements in the UK are designed by semi empirical methods described in Road Note 29, (Road Research Laboratory 1970) presently being revised, and LR1132 (Powell et all 1984). These methods were developed substantially from full scale pavement design experiments carried out by the Transport and Road Research Labatory (T.R.R.L.) (Thompson et al 1972). Empirical design methods are limited by their lack of versatility when considering temperatures, speed of traffic, subgrade conditions, material properties and different types of structure.

A more fundamental approach to structural pavement design has been developed at Nottingham (Brown and Brunton 1984 (a), (b) and (c), Brown and Brunton 1985). This approach is described further in Chapter 9, and involves using linear elastic layered programs to analyse the critical strains in any pavement structure, hence calculating the life. This approach takes account of the material

properties of each individual bituminous mix, as well as temperature, and the speed of traffic.

1.2 OVERLAY DESIGN AND PHILOSOPHY

The level of serviceability of a pavement declines gradually until a state exists where it is considered unacceptable. As the pavements nears a "critical" condition it is usual to consider some form of rehabilitation. If a pavement has deteriorated too much this may take the form of a complete reconstruction although it is more likely that an overlay or strengthening layer would be considered.

Critical condition is described as a rut depth of 10mm, accompanied by cracking in the nearside wheel track. In the critical state the rate of pavement deterioration is rapid and rehabilition should be undertaken immediately.

Overlay design must take account of the residual life of the existing pavement. The method used in the UK to estimate this residual life, described in LR833 (Kennedy et al, 1978), makes use of the deflection bowl obtained under a standard dual wheel load of 3175 kg as measured by the "Deflection beam". (The "Deflection beam" is fully described in LR834, (Kennedy Fevre and Clarke, 1978)). The deflection of the pavement is used to determine the residual life of a pavement from charts such as that shown in Fig. 1.2(a), and an estimation of the thickness of overlay required to extend the life of the pavement for a specific design life, in numbers of standard axles; can be taken from charts such as Fig. 1.2(b).

More sophisticated analytical methods have been developed using the Falling Weight Deflectometer (F.W.D.) to estimate the strength of an existing pavement (Bohn et al 1972). The deflection bowl recorded under a falling weight is back-analysed to produce values of insitu

stiffness of the pavement layers, hence an estimation of residual life is obtained. A full description of the technique is given by Tam 1985.

1.3 PRINCIPLE MODES OF DISTRESS IN PAVEMENTS

In order to take best advantage of any innovative construction techniques it is necessary to understand the way in which a pavement is likely to fail, and the causes of any failure. The two principal modes of failure, are illustrated in Fig. 1.3. These are permanent deformation, or rutting, controlled by the vertical compressive strain in the subgrade, Fig. 1.3(a), and fatigue cracking, controlled by tensile strain at the base of the asphalt layer Fig. 1.3(b).

A further failure mode, less well catered for in any design method is reflection cracking.

1.3.1 Permanent Deformation.

After a period of time under traffic a pavement surface may exhibit signs of permanent deformation, or rutting. This is caused by the gradual build up of deformation within any or all of the layers in a pavement. Rut depth is measured as the maximum distance between a 2m straight edge and the bottom of the rut and is considered critical at a depth of 10mm.

The visco-elastic nature of bituminous materials is illustrated in Fig. 1.4. A constant stress regime in Fig. 1.4(a) shows the initial immediate elastic strain followed by a viscous strain. When the stress is removed the elastic strain is recovered with some additional delayed recovery over a period of time. Ultimately some residual strain remains, that is the permanent strain, and is irrecoverable. Fig. 1.4(b) shows the response to a load pulse such

as may be experienced by an element of bituminous material in a pavement. It is not possible to seperate the two components of the visco elastic response, but the permanent strain is illustrated. It is the accumulation of permanent strain for each load pulse which results, over millions of load applications, in the formation of rutting.

Bituminous materials become increasingly viscous at high temperatures and behave more elastically at low temperatures. Therefore a combination of high temperature and long loading times are the most conducive to rutting in a pavement. Thus the slow lane on a steep incline is susceptible to rutting as are bus lanes and traffic lights, where traffic is standing for long periods of time in high ambient temperatures.

Viscous deformation can be controlled in a bituminous mixture by judicious mix design. The aggregate type and grading are important as is the penetration of bitumen. This is discussed further in Sections 2.3.2 and 9.2.2.

Rutting is undesirable as it leads to ponding of water and hence dangerous driving conditions. Water collecting on the pavement surface will also more readily permeate through the structure, reaching the foundation.

1.3.2 Fatigue Cracking

Fatigue cracking is the phenomenon of fracture under repeated or fluctuating stress having a maximum value less than the tensile strength of the material. Under traffic loading a pavement structure flexes and the maximum tensile strain occurs at the base of the asphalt layer as shown in Fig. 1.3(b). Cracking initiates at the base of the asphalt layer and manifests itself on the surface of the pavement as interconnected cracks. This is sometimes called

"Alligator cracking", due to the pattern of cracks.

The time to crack initiation in bituminous materials was found to be dependent on the magnitude of strain. (Pell and Cooper 1969, Cooper and Pell 1974). The level of strain varies considerably, under the action of different applied loads in a pavement. It was shown that the use of a linear damage hypothesis such as Miner's Rule was appropriate under compound loading. This is described as:-

$$\sum_{i=1}^{i=j} \frac{n_i}{N_i} = 1 \qquad 1.4$$

Where n_i = number of cycles of strain level $_i$ applied

N_i = number of cycles of strain level $_i$ to produce failure in a simple loading test

J = number of different strain levels.

A method of predicting the fatigue life of bituminous pavements has been developed at Nottingham (Cooper and Pell 1974) and is described in Section 9.2.1.

Fig. 1.5 shows the effect of test and mix variables on the fatigue performance of bituminous materials. The only fundamental change in the fatigue life is brought about by either altering the penetration or volume of binder. Other variables effect the fatigue life only insofar that the stiffness and hence level of strain for a given level of stress is altered.

1.3.3 Reflection Cracking

Reflection cracking is one of the major problems in pavement rehabilitation. It is defined as the cracking of an asphalt overlay placed above existing cracks or joints in a resurfaced pavement. The cracking is initiated by excessive relative horizontal and vertical

movements at the tip of the existing crack, which is at the bottom of the overlay. These movements may be induced either by traffic loading or due to temperature changes in the pavement. Reflection cracking is especially a problem where old jointed concrete pavements or lean mix concrete bases are overlaid with asphalt.

Seasonal variations in temperature lead to the variation in slab length causing movement and hence reflection cracking at joints. This is prevalant in geographical areas which experience Continental climates.

Diurnal variations in temperature cause temperature gradients to be set up over the depth of the pavement. These temperature gradients cause the slab to distort either by curling, if the slab is colder on top, or conversely hogging, if the slab is hotter on top. When any concrete slab has curled, (ie. is concave upwards) movements at the joints are exacerbated by traffic loading.

Cracks in a pavement lead not only to poor riding quality but, through water ingress and spalling, to premature failure of the pavement by weakening the lower layers.

Extensive research has investigated the possibility of reducing reflection cracking and some of the recommendations are discussed in Section 2.3. These include a great variety of fabrics and wire mesh reinforcing.

A more fundamental understanding of crack growth in asphalt pavements has been sought, so that a better indication of the life of an overlay with regard to reflection cracking can be predicted. One such method is the use of fracture mechanics (Molenaar, 1983). There are three basic modes of fracture in a material (see Fig. 1.6(a))

(a) Mode I - opening mode

(b) Mode II - shearing mode

(c) Mode III - tearing mode.

For mode I (Fig 1.6(a)), the components of stress at the point (r,Q) (Fig.1.7) in the vicinity of the crack tip are approximately:-

$$\sigma_{yy} = \frac{K_I}{(2\pi r)^{\frac{1}{2}}} \cos\frac{\vartheta}{2}\left(1 - \left(\sin\frac{\vartheta}{2}\sin\frac{3\vartheta}{2}\right)\right) \qquad 1.5$$

$$\sigma_{xx} = \frac{K_I}{(2\pi r)^{\frac{1}{2}}} \cos\frac{\vartheta}{2}\left(1 + \left(\sin\frac{\vartheta}{2}\sin\frac{3\vartheta}{2}\right)\right) \qquad 1.6$$

$$\sigma_{xy} = \frac{K_I}{(2\pi r)^{\frac{1}{2}}} \cos\frac{\vartheta}{2}\left(\frac{\sin\vartheta}{2}\cos\frac{3\vartheta}{2}\right) \qquad 1.7$$

All the near crack tip stresses are proportional to the same scaling factor, K, which is called the stress intensity factor. K depends on only two quantities, the applied loading and the geometry of the cracked specimen. Brittle fracture occurs when the stress intensity factor reaches a critical value K_c. The critical value is the fracture toughness and may be considered a material property. Relationships may be derived for the three modes of fracture.

Crack growth in a pavement occurs under cyclic loading caused by either traffic or temperature. The rate of crack growth was found to approximate to the relationship (Paris and Erdogan, 1963)

$$\frac{dc}{dN} = AK_I^{\,n} \qquad 1.8$$

K = stress intensity factor $N/mm^{1.5}$

A and n = material constants

The relationship may be extended to cover non linear viscoelastic materials (Shapery 1972). Molenaar describes tests which where used to estimate A and n. From equation 1.8 the life of an overlay may be expressed as:

$$N = \int_{o}^{ho} \frac{1}{A(K_{(c)})^{n}} \, dc \qquad 1.9$$

Where ho = overlay thickness

The stress intensity factor K in relation to crack length C should be known in order to solve equation 1.9. For any pavement situation K may be determined from finite element analysis.

The use of fracture mechanics to predict the rate of crack growth in bituminous overlays is still as yet, a research tool. However, the fundamental understanding of crack growth can only be beneficial to pavement design.

1.3.4 Other Failure Modes

Other failure modes include slippage, that is the breaking down of the bond between layers in a pavement. This is discussed in more detail in Section 8.1. Both slippage and fatigue cracking can cause potholing.

A pavement, although structurally satisfactory may also be in a dangerous condition due to lack of skid resistance, this may be redressed with the application of a surface dressing.

1.4 THE ROLE OF POLYMER GRIDS IN ASPHALT PAVEMENTS

From the previous discussion it has been shown that failure in a bituminous pavement is caused by both viscous flow and cracking. By introducing a reinforcing mesh into the asphalt it may be possible to obstruct the viscous flow, limiting the magnitude of permanent deformation, and reduce the incidence of cracking.

With the advent of high strength polymers such as "Tensar" geogrids it has become possible to construct a composite pavement structure which combines the qualites of both bitumen and grid to produce a more durable pavement. The grid structure allows the mechicanism of interlock between aggregate and grid to hinder

movement in asphalt, a mechanism not present in other reinforcing elements such as fabrics. Futhermore as the polymer grid is not susceptible to corrosion it has an immediate advantage over metal reinforcement.

The University of Nottingham was approached by Netlon Ltd., who manfacture a polymer grid, and a preliminary feasibilty study was completed in 1982 (Brown, Brodrick 1982). Following this a three year research programme was initiated in cooperation with the S.E.R.C. to identify in detail the mechanisms of reinforcement and quantify any particular benefits obtained. This thesis is an account of that research.

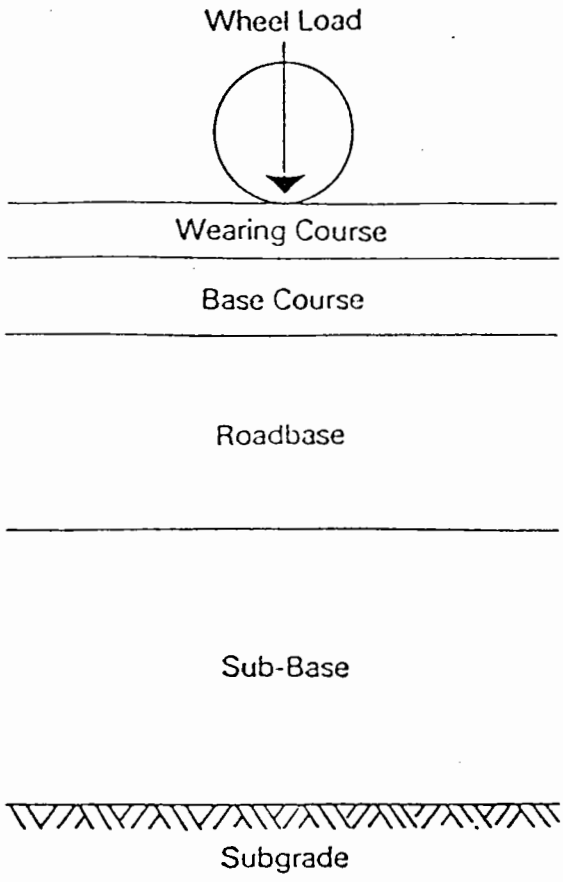

(a) flexible pavement

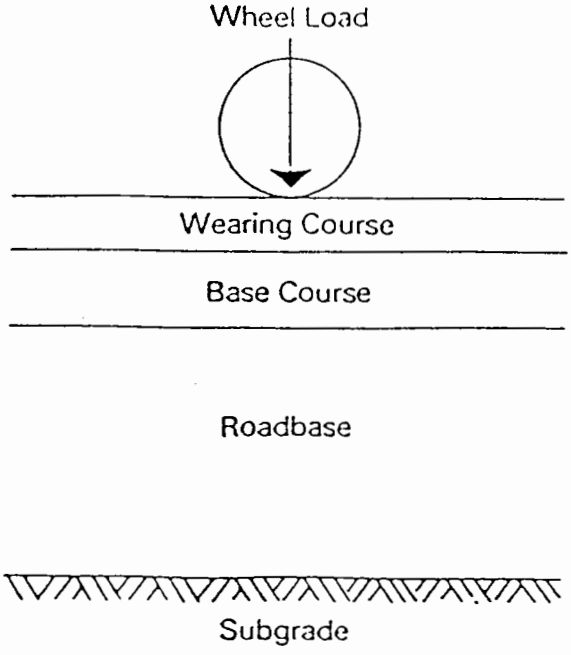

(b) total asphalt

Fig 1.1 Typical pavement constructions

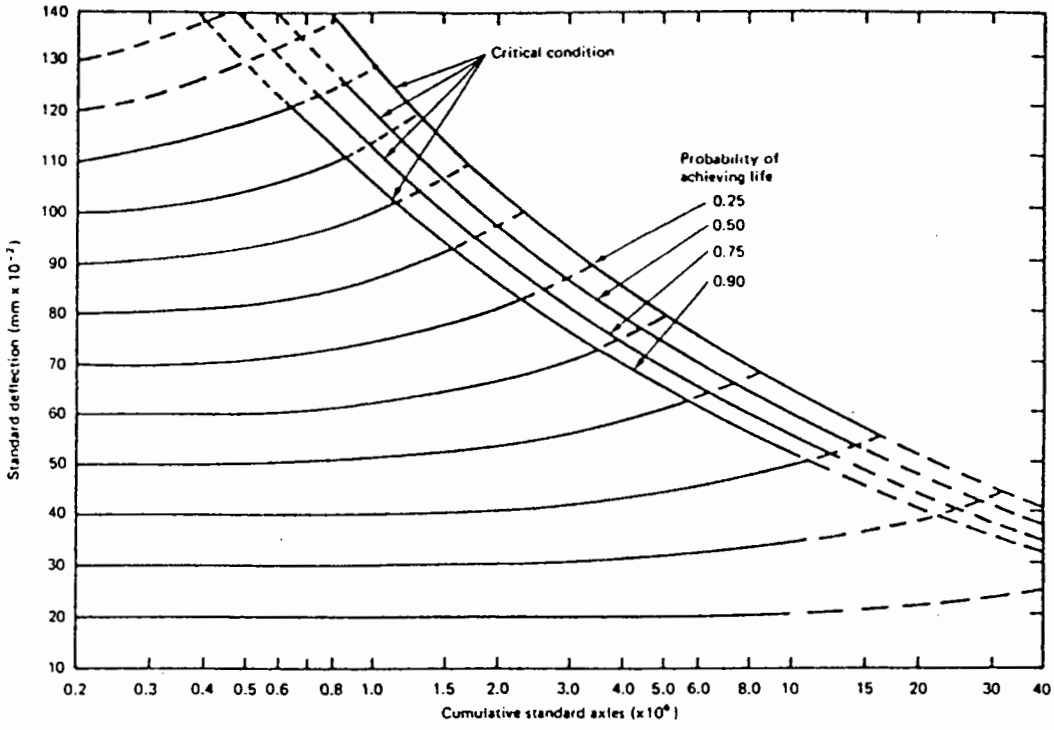

(a) Relationship between deflection and life

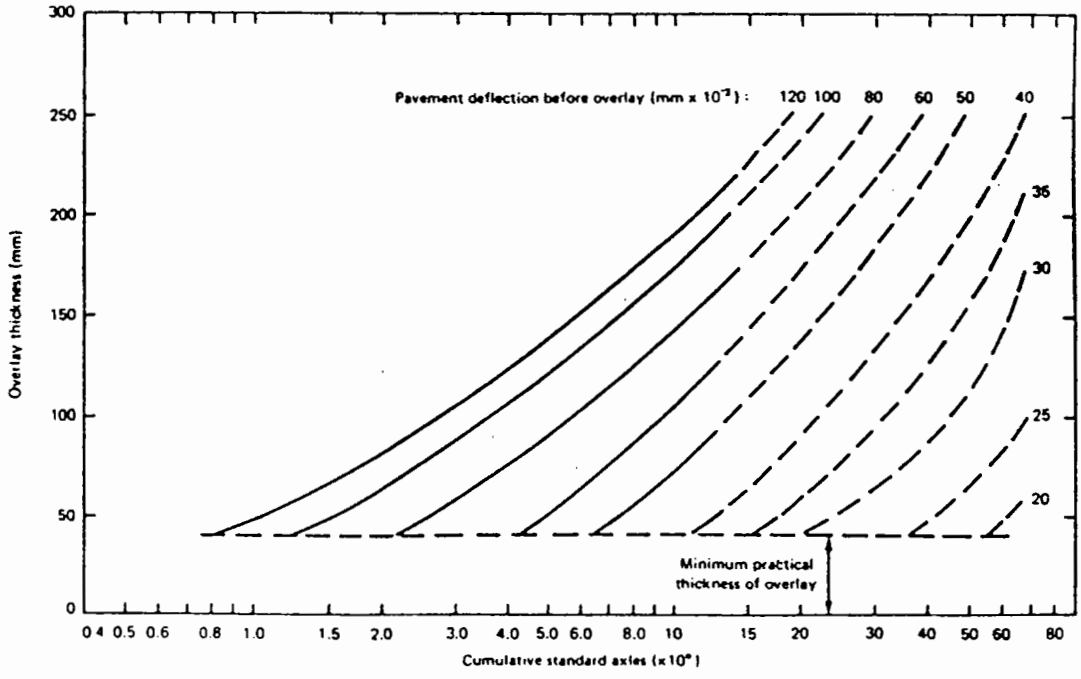

(b) Overlay design chart

Fig 1.2 Design charts from LR 833

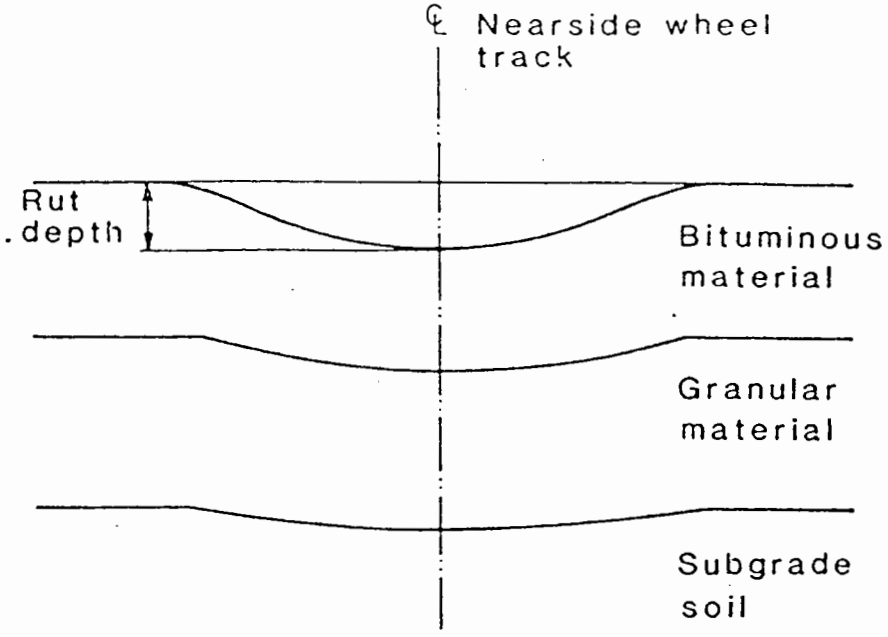

(a) Permanent deformation

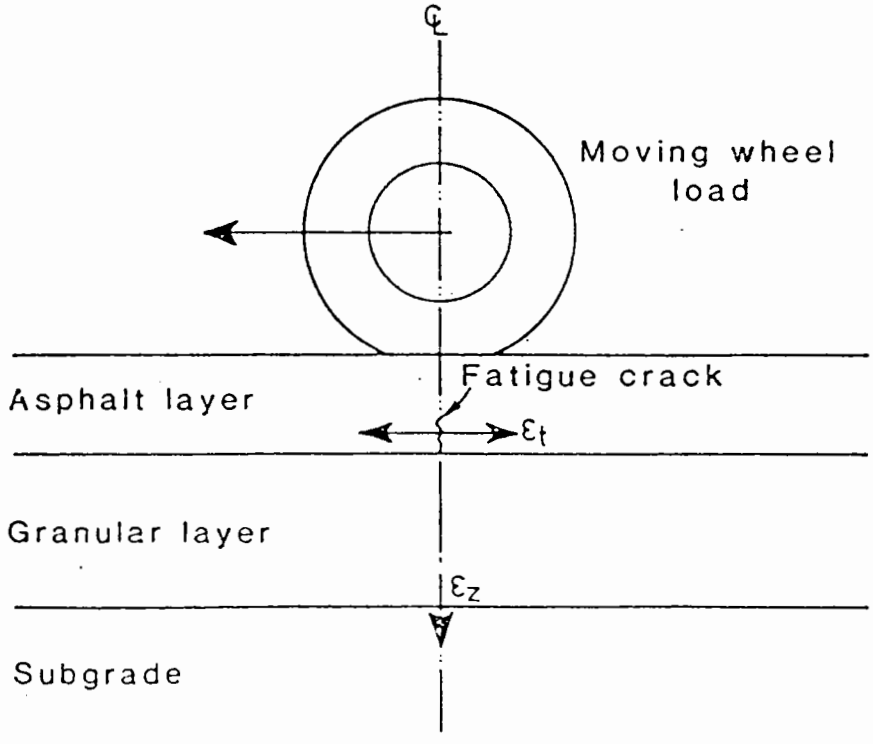

(b) Fatigue cracking and critical strains

Fig. 1.3 Failure modes and critical strains in asphalt pavements. (After Brown and Brunton 1984)

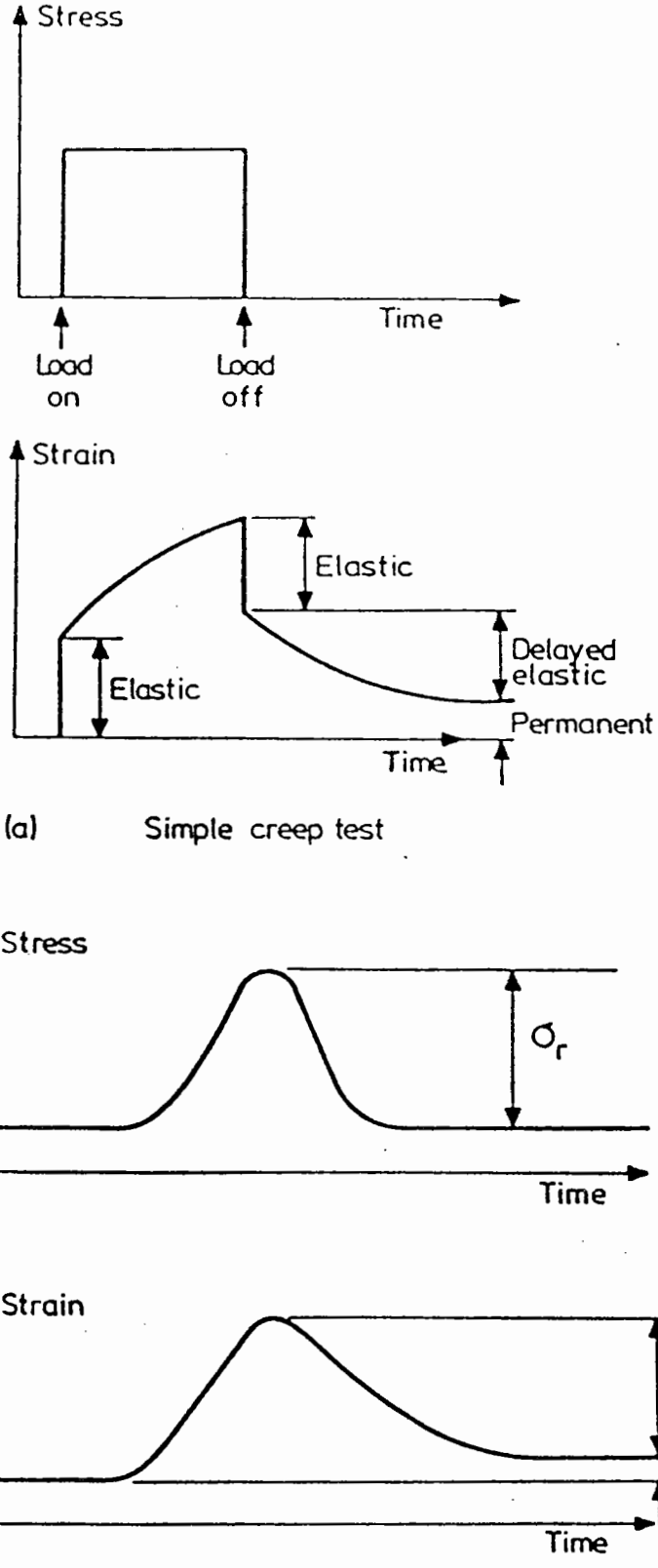

Fig. 1.4 Visco elastic response of bituminous material

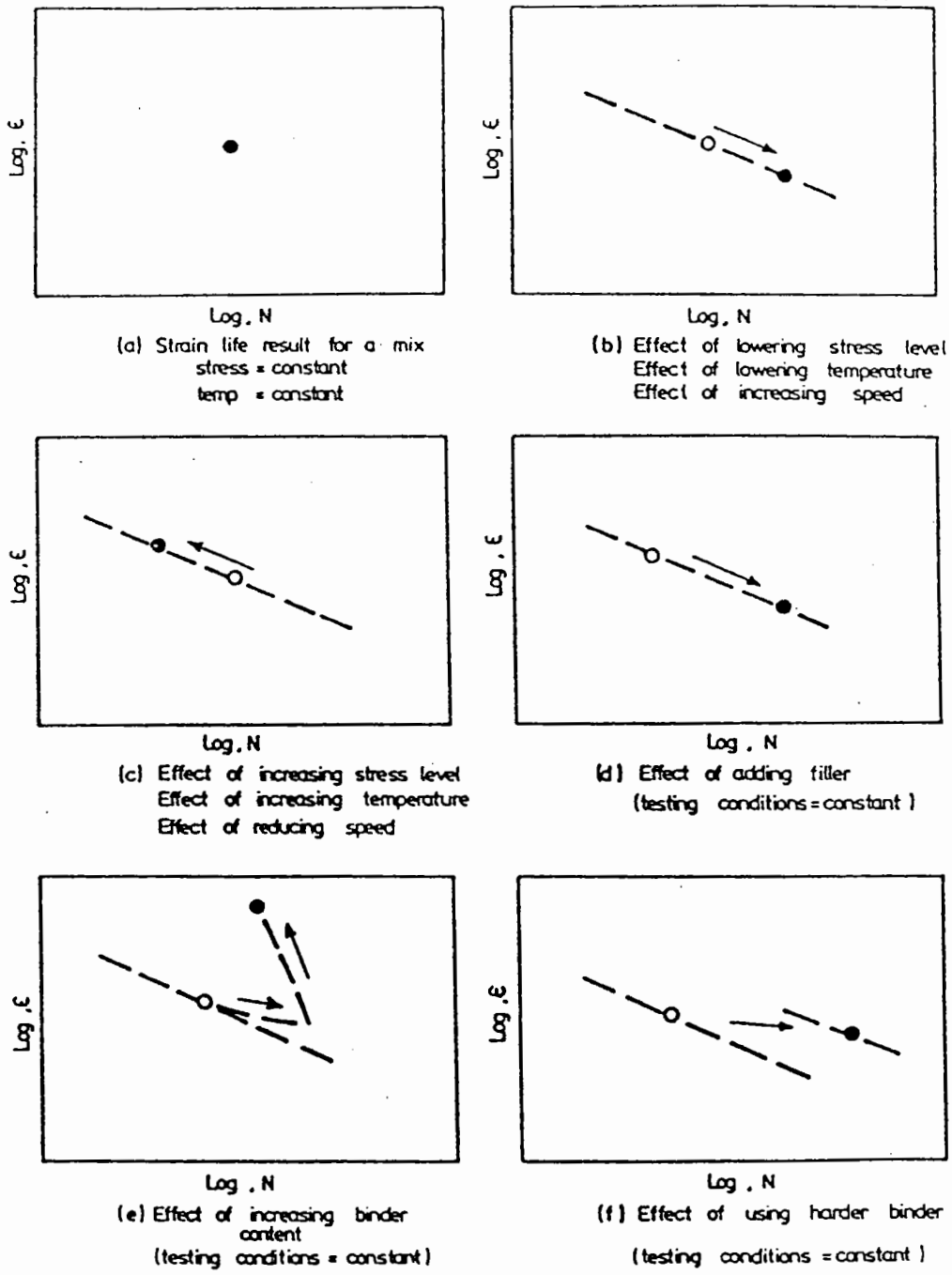

Fig. 1.5 Effect of test and mix variables on strain life relationship.(After Pell)

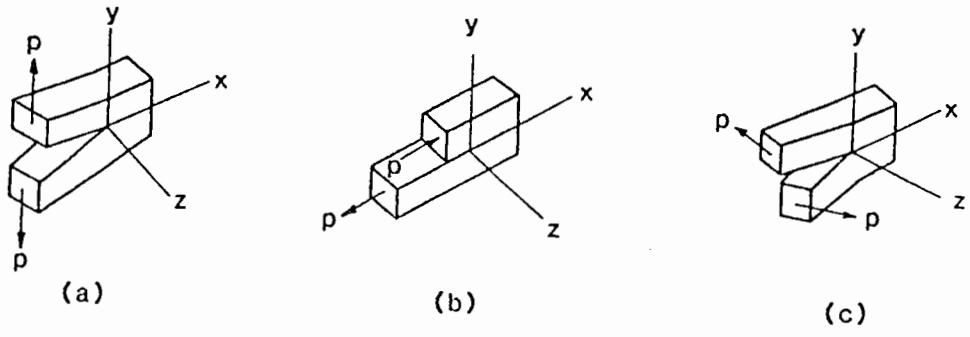

Fig 1.6 Cracking modes

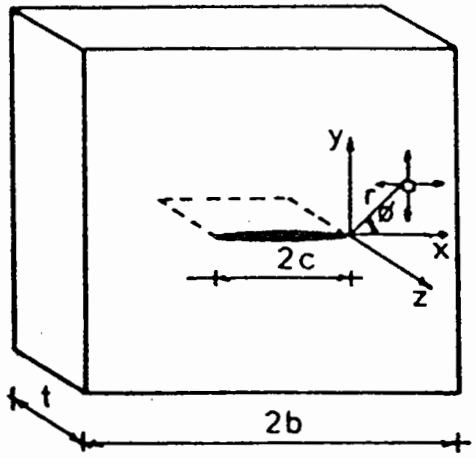

Fig 1.7 Coordinate system

2 INNOVATIVE METHODS FOR IMPROVED PAVEMENT DESIGN

2.1 INTRODUCTION

Efforts are constantly being made to improve the quality of pavements in order to decrease the frequency and cost of maintenance. This may take the form of improved bituminous materials, or alternatively solutions to specific problems such as reflection cracking.

Recent developments in bituminous mix design have resulted in the publication of new specifications for bituminous materials and improved mix design methods. Apart from improving mix design practice the properties of bituminous materials may be altered by the inclusion of various additives, such as polymers or rubber. These additives may enhance the temperature susceptibility and deformation characteristics of bitumen. Fibres, such as cotton or asbestos, may be added to bituminous material to give increased fatigue lives and improved resistance to permanent deformation.

Some alternatives are presented herein for the inhibition of reflection cracking. In addition to changing bituminous mix properties to reduce the rate of crack propagation, a strong tensile element may be provided over cracks likely to reflect through an overlay.

2.2 MODIFIED AND REINFORCED BITUMINOUS MIXES

2.2.1 Improved mix design

Current mix design methods are constantly being updated to cope with the greater demands being made on bituminous materials. Pavements are subjected to increasing volumes of traffic and

increasing axle loads, creating more wear on pavements. In the UK bituminous mixes have in the past been designed by a recipe method set out in the appropriate standards (BS 594 1973, BS 4987 1973), and little account was taken of specific aggregate properties or design situations.

The most common surfacing material is Hot Rolled Asphalt (H.R.A.), which is a gap graded material rich in bitumen and therefore highly impermeable. This mix is however susceptible to permanent deformation due to its high binder content and the nature of the grading.

A new specification has been published (BS 594, 1985) which puts forward a total mix design method for H.R.A. wearing courses. Although the aggregate grading remains unaltered, the optimum binder content may be obtained by the Marshall method of mix design,(The Asphalt Institute, 1984).

The materials most likely to resist permanent deformation are those in which the aggregate is continuously graded. Particle to particle content in the mix plays a dominant role in resisting deformation. The specification for these types of mix are currently being up-dated, although no change in the aggregate grading is expected. Alterations may take the form of closer control of laying and mixing temperatures to achieve the correct level of compaction.

Currently in the U.K., only heavy duty pavements are designed by the Marshall method. Both the aggregate grading and binder content are adjusted to give a durable and stiff mix. Total mix design gives greater flexibility to a designer so that account may be taken of aggregate sources and available aggregate gradings.

Research has been undertaken at Nottingham (Brown, Cooper and Pooley, 1985, Brown and Cooper 1984) in order that gap graded mixes currently in use may be modified by reducing the binder content and

increasing the filler content to maintain a low air void content. This has the effect of increasing the resistance of the mix to pavement deformation. The fatigue life of continously graded mixes may be improved by using either a lower penetration grade bitumen or designing the grading to be more dense, ie. to have a lower air void content.

2.2.2 Fibre reinforced asphalt

Investigations have been conducted into the possibility of reinforcing bituminous mixes with fibres. The hope is, that by introducing a tensile element into the bituminous mix, greater stability and resistance to cracking may be found. Many different types of fibres have been used including cotton, although natural fibres are prone to degradation (Bushing et al 1970). More recent research has concentrated on products such as high strength polymer fibres, asbestos fibres, glass fibres and steel fibres. Steel fibres (Gottschall 1985) have been used with reasonable success in both laboratory and full scale trials. Approximately 1.5% by mass of steel fibre is introduced to a conventional mix at the mixing plant, and compacted on site in the usual manner. Metal corrosion is neverthless a long term problem.

Glass fibres are a more common form of reinforcement; randomly oriented glass fibres were used recently with some success, (Montague 1985), to stabilise thin bituminous surfacing on rural pavements, although it has been reported that such reinforcement increased the susceptibility of a bituminous mix to cracking under laboratory conditions (Bushing 1968).

Asbestos fibre may be added at approximately 4% by mass to a hot mix (Marais 1979). Higher resistance to permanent deformation is claimed, with thinner overlays possible for the same structural performance.

2.2.3 Polymer additives to bitumen

It is generally accepted that polymers are added to bitumen in order to achieve an improvement in the mechanical properties of bitumen or of bituminous mixes, and an improvement in the temperature susceptibility of mixes, (Poroni 1985). Consequently various polymers are produced which can be added to bitumen, at between 3% to 6% by mass, to achieve this improvement in performance. If the polymer content becomes too high, say greater than 6%, the bitumen becomes viscous and unworkable. Polymers increase the elasticity and penetration index of a bitumen, which is a measure of the sensitivity of mix stability to temperature. These additives are therefore particularly attractive where high temperatures are expected. It is claimed that polymer modified bitumens are also less prone to attack from oil spillages, and can be used where this is a particular problem.

Waste plastics have also been recycled into asphalt (Nievelt 1978) with virtually the same effect as specialised polymer additives. Increased stability results, and therefore increased resistance to permanent deformation.

Polymer modified surface dressings are also available (Marvillet 1978) for use in cases of severe loadings where normal surface dressing might be inadequate. Positive results have been obtained to date and many proprietary brands are available.

2.3 EXISTING METHODS FOR INHIBITING REFLECTION CRACKING

Various solutions to the problems of reflection cracking have been investigated and some of the alternatives are outlined below.

2.3.1 Current design practice

Current design methods pay little attention to the particular problem of reflection cracking which may lead to the premature failure of a pavement. Existing solutions involve increasing the thickness of an overlay, thus increasing the time taken for a crack to reflect through. This does little to prevent the cause of reflection cracking, and because of this over-thick layer the pavement is structurally over designed. Thicker overlays do however insulate underlying pavements, and to a certain extent reduce diurnal thermal movements.

It is recommended that for major trunk roads subject to reflection cracking from underlying cracked layers, a wearing course of medium stone content (40%) be used (Croney 1977). Experience has shown that where high stone content asphalt wearing courses (over 50%) are used, cracks in underlying layers are reflected through a 100mm surfacing in about 5 years. With a 30-40% stone content in the wearing course this period is extended to more than 10 years. The thickness of surfacing in excess of 100mm, recommended in Road Note 29, (Road Research Laboratory 1970) for heavily trafficked roads, is intended to prevent thermal cracks in the roadbase being reflected through the surfacing within a period of about 15 years, by which stage an overlay would normally be required to restore the riding quality and skid resistance of the pavement.

2.3.2. Rubberised Asphalt Interlayers

The use of rubber to modify the properties of bitumen dates back to 1929 when tests were conducted on bitumen with a 1.5% to 4% latex rubber content (Coetzee, 1979). The resulting mix did not prove entirely satisfactory; not enough rubber was added to take full advantage of its properties of flexibility, elasticity and improved

temperature susceptibility. It is these characteristics which give a "rubberised asphalt" the ability to absorb vertical and horizontal strains expected above a crack tip, without itself cracking.

It was not until the early 1960's that rubberised asphalts became viable, with the addition of 25% ground vulcanised tyre rubber (MacDonald 1982). Rubber particles passing the 1.18mm sieve and retained on 600 m sieve were usually added to high penetration bitumen, the final mixture was tough, rubbery and elastic at room temperature.

Several methods of pavement construction have been examined using this material. Two such are shown on Fig. 2.1 (a) and (b) (Coetzee 1979, Neilsen 1984, Paterson 1984).

(a) The rubberised asphalt is sandwiched between two normal asphalt mixes with aggregate embedded in it to carry the vertical load. This is known as a Stress Absorbing Membrane Interlayer (SAMI). In some construction methods an open textured asphalt mix may be used as a wearing course to lend more flexibility to the pavement. The actual rubberised bitumen layer may be up to 10mm thick.

(b) The rubberised asphalt may be used as a thin (10-13mm) surface dressing. This is known as a Stress Absorbing Membrane (SAM). The additional benefit of this membrane includes waterproofing and the ability to remould and heal when damaged.

Both these treatments were found to be very successful in preventing reflection cracking, especially over badly fatigue cracked asphalt pavements. When using a SAMI, although some cracks reflect through, the rubberised asphalt often remains intact, preventing the ingress of water. It has been noted (Scherocman 1979), however that rubberised asphalt will not bridge wide shrinkage cracks in the original pavement.

Experiments have been carried out in the U.K. by TRRL (Szatkowski 1970) using rolled asphalt modified by the addition of small amounts of latex rubber. Favourable conclusions were drawn on the ability of the modified asphalts to control reflection cracking. The rubber content made it possible to increase the binder content above the recommended maximum percentage thus increasing the flexibility of such materials, giving a further advantage in crack prevention.

It would seem that rubberised asphalt increases the life, and decreases the maintenance costs, when used over badly fatigued pavements,and generally reduces the incidence of reflection cracking. These modified bitumens act like a rubber carpet, not strengthening the pavement, or restraining the movement, but absorbing concentrated movements.

2.3.2. Recycling

Recycling has become an increasingly important topic in pavement rehabilitation and reconstruction, due to escalating costs and availability of virgin aggregates and bitumens. The basic principle involves reworking the material in an existing pavement, and if necessary, adding rejuvenating agents and/or aggregate. Recycling, unless complete reconstruction is considered, does little to eliminate the problem of reflection cracking.

There are three main types of recycling (Epps 1980)

(a) Surface recycling. This process involves reworking to a depth of less than 25mm, by heater-planer, heater scarifier, hot milling, cold planing or cold milling devices. This operation is a continuous single pass, multi step operation, that may involve the use of new materials, including aggregate and bitumen modifiers. It has been suggested (Jones 1979) that it is often necessary to lay a

surface course over a recycled pavement, to improve the riding quality and skid resistence.

(b) In Place Surface and Base recycling.

This method consists of scarifying the surface (or base) of an asphalt pavement to a depth greater than 25mm. The pavement layers are then usually pulverised insitu, when new aggregate is added to achieve the designed gradation, and stabilizing agents such as bitumen, bitumen emulsion, portland cement, lime or other chemical rejuvenating agents added. The pavement materials are replaced and are reshaped to proper crown and slope and compacted (Mosey 1979, Kandhal 1984).

(c) Off site, central plant recycling.

In this type of construction the existing pavement layers are ripped or scarified and removed from the roadway. The materials are then crushed or pulverised and a mix design analysis conducted on the resulting blend. New aggregate and bitumen, with or without a rejuvenating agent, is added to the recycled mix, in the mixing plant. The resulting hot mixture is then placed and compacted on a roadway using conventional methods and equipment. (Beterson 1979, Servas 1984).

2.3.4. Geotextiles

There are at present, a large variety of fabrics available for use in pavement engineering, specifically intended to reduce the incidence of cracking in overlays. The majority of fabrics available are made from synthetic polymers of five groups, polypropylene, polyethylene, polyester, polyamide (Nylon) or vinyls (including P.V.C.).

Properties vary between polymers although in general polyamides have significantly greater strength. The fabrics may be produced by

several methods including the needle-punched process, the spun-bonded process, the woven process, and combinations thereof. Needle punching normally produces a thick fleecy fabric of low density, whereas fabric produced by weaving of threads, filaments or tapes, produces more usually a tighter thinner fabric with a higher mechanical strength (Ruddock 1983).

The use of fabrics to retard reflection and fatigue cracking, usually in overlays, has been widely documented.

Laboratory studies (Murray 1982, Smith 1982, Majidzadeh 1982), suggest that fabrics do reduce the severity and propagation rate of cracks. The majority of these studies have used asphalt beams, reinforced with fabric, on rubber supports; or at least some form of asphalt beam subjected to tension along its underside. In almost every case an improvement on actual life of a beam was realised when a fabric was used. The effect of fabric thickness with regard to bitumen uptake has been investigated (Smith 1982, Murray 1982) with the conclusion that thicker fabrics adsorbed more bitumen, and are on the whole more impermeable to water.

The action of a fabric in resisting crack growth is dependent on several parameters; its modulus of elasticity, susceptibility to shrinkage at high temperatures, and thickness and ability to absorb bitumen. Fleecy fabrics which absorb a lot of bitumen can act as relieving layers, in a mechism similar to that of a SAMI. Less absorbent fabrics with a higher modulus, would tend to limit horizontal movement in the overlay strain at the crack tip and delocalising the strain by debonding.

A large number of full scale trials have been initiated to investigate the applications of fabric in overlay design. (Hugo 1982, Gulden 1982, McGhee 1975, Way 1980, Dykes 1980, Eaton 1980, Mullen 1980) Fabrics may either be laid continuously over a badly

cracked area, or in strips over particular cracks. The normal method of construction, is to roll the material directly onto the existing pavement, after the application of a tack coat. and occassionally to lay a thin levelling course to ensure a smooth working surface. A variation of this form of construction involves placing sand or lime immediately over the crack to prevent bonding between the overlay and the old surface. Fabric is normally then nailed into position, and a further application of tack coat applied.

It was observed that wrinkles or discontinuities in fabrics may initiate cracking in an overlay (Button 1982), and care should be taken during the installation of any fabric to ensure minimum distortion.

It can be concluded that fabrics do not have a reinforcing effect when included in a flexible pavement, and that although horizontal strains are relieved under certain conditions, relative vertical movements at a crack tip remain unaffected by the presence of a fabric. Results from full scale trials in the extreme climate of Greenland, (Eaton 1980) show that large thermal movements at joints in slabs, causing reflective cracks, cannot be effectively controlled using fabrics. Trials in temperate or warm climates has shown that fabrics do have a beneficial effect in reducing both the severity and incidence of cracking in overlays. Including a fabric in an overlay has the additional benefit of acting as a water barrier, preventing the ensuing deterioration of the subgrade or underlying layers.

In general the literature suggests that fabrics should be adopted with the philosophy that they will act as a water proofing membrane and extend the useful life of an overlay. Fabrics should not be introduced with the intention of reducing overlay thickness or as a structural part of the pavement. Reflection cracking may be

reduced to a more tolerable level provided it is not caused by severe differential vertical movement.

2.3.5 Open Graded Bituminous Mixes

Open graded mixes are used occasionally in North America as "crack relief layers" over badly jointed or cracked pavement (Hensley, 1980). The mix can have a maximum aggregate size of 75mm, a void content of 20% to 30%, and a binder content between 1.5% and 3%. Construction involves placing at least 100mm of the open graded mix on to a badly cracked pavement, and paving over this with a large aggregate size base course and a normal wearing course.

The large interconnecting voids in the crack relief layer are intended to dissipate the concentrated strains at crack tips or joints and therefore prevent the propagation of cracks through to the asphalt overlay.

A similar idea, although perhaps only of cosmetic value, is the use of an open graded friction course on the surface of the pavement (Way 1980). Although the propagation or number of reflection cracks may not significantly be reduced, it is less apparent due to the texture of the pavement surface.

2.3.6 Wire Mesh Reinforcing

Many attempts have been made to reinforce pavements with either expanded metal mesh, or welded wire fabric. An extensive study at the Massachusetts Institute of Technology in the late 1950s (Horn 1956, Bicher et al 1956, Foley et al 1957) investigated both theoretical and practical aspects of reinforcing. In laboratory tests, they examined the movement and strain in wire mesh during loading over a joint. After field trials (Tons et al 1960) concluded

that,

"if horizontal joint movement is between 0.04" to 0.1" (1mm to 2.5mm), cracking may occur but can be prevented by narrow strip reinforcement. If the maximum yearly joint expansion is over 0.1", a continuous wire/fabric reinforcement appears a better solution".

Trials in Florida in 1959 (Smith et al 1959) using continuous wire mesh beneath an overlay at a heavily trafficked intersection, significantly reduced permanent deformation. It was emphasised that if mesh was to be used successfully it must lie flat as problems were encountered during paving.

In 1960 (Brownridge 1964) trials were carried out in both Northern Ontario, which experiences extreme winters, and Southern Ontario. In Southern Ontario the reinforcing mesh substantially reduced the incidence of reflection cracking for the first five years of service, while in Northern Ontario the mesh was not effective in controlling cracking.

Work carried out in the UK by TRRL, in the early 1950's, (Haywood 1955, Croney 1962) using mainly small mesh size expanded metal, concluded that cracking due to relative vertical movement could be delayed.

Spongy areas at the surface of the pavement gave a common problem and subsequently had to be removed. These areas were caused by the distortion of the metal during paving. The most effective way of preventing this was by means of a heavy metal sled, which was dragged over the mesh underneath the paver. The recommended minimum cover to metal mesh is about 75mm, as thinner layers are likely to crack, due to the movement of the reinforcing during paving.

2.3.7. Treatment of Concrete Pavements

Many problems exist when rehabilitating a failing concrete

pavement, especially if a flexible overlay is considered. The relative vertical movement across joints between concrete slabs caused by reflection cracking increases progressively with age, leading to premature failures in asphalt overlays. Water infiltrating the subgrade though slab joints can weaken the support, and corrode dowell bars, decreasing the load transfer across joints.

Thermal movement is a particular problem. Diurnal variations in temperature cause individual slabs to curl, due to temperature gradients through the slab, and this increases the movement at joints under trafficking. Seasonal variations in temperature cause the slabs to expand and contract, also creating severe reflection cracking problems, although this is more prevalent in geographical areas which experience a Continental climate. Seasonal movement of this type can be very large at any joint, and most methods of reflection crack control in these instances are inadequate. Concrete pavements may be rehabilited by several methods:

(1) Degradation of the concrete layer.

One option is the complete disintegration of the existing concrete structure. The pavement may be broken using heavy drop weights, and the rubble used as an extra granular subbase. This solves the problem of reflection cracking by elimating any areas of stress concentration. This option was adopted at Canvey Island (Pooley 1984) in an early full scale trial using polymer grids in asphalt. This alternative is not always feasible when construction level is a problem, i.e. bridge clearance or kerb heights.

(2) Vacuum grouting

It is possible to reduce the relative vertical movement at slab joints by vacuum grouting which fills in voids underneath the joint and creates a firm foundation to seat each slab, (Department of Transport 1980) The process involves applying a vacuum to holes

drilled through the slabs at either side of the joint. Grouting material is then sucked into the voids beneath the slab. Although the process will reduce vertical movements across joints it will not affect the thermal movements, and should be used only in conjunction with other preventative methods of reflection cracking control.

2.4 DISCUSSION

Polymer grid reinforced pavements are a combination of some of these inovative construction techniques. The two which are most relevant are wire mesh and fabric reinforced pavements.

The polymer grid has a stiffness similar to that of wire mesh, and the interlock mechanisms of reinforcement is similar. The polymer grid is not however susceptible to corrosion. The installation techniques of both wire mesh and fabrics are also relevant to polymer grid reinforced pavements.

These studies therefore give useful background information on the likely behaviour of polymer grid reinforced pavements and an indication of some of the development problems.

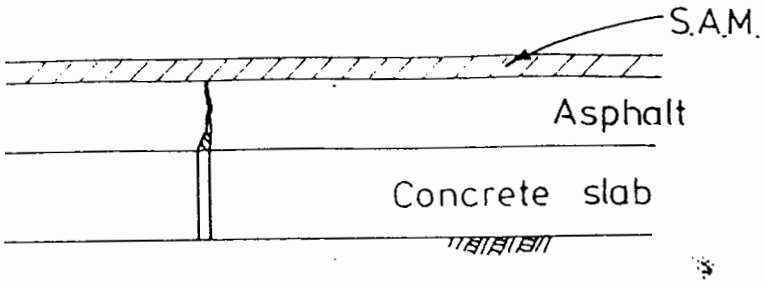

(a) S.A.M.

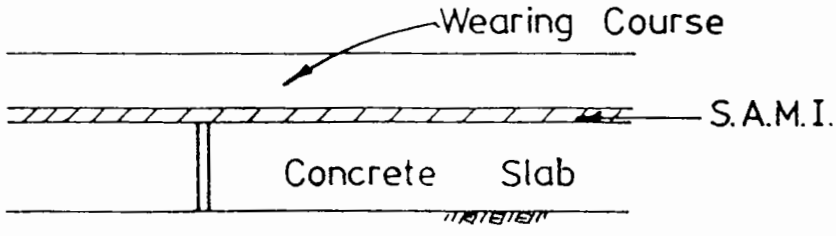

(b) S.A.M.I.

Fig 2.1 Stress absorbing membrane & interlayer

3 ADDITIONAL INVESTIGATIONS INTO POLYMER GRID REINFORCEMENT OF PAVEMENTS

3.1 INTRODUCTION

Several other research programmes have investigated the feasibility of using polymer grids to improve the performance of pavements.

In both the United States of America and Canada, laboratory studies and full scale trials have been undertaken. The results from the full scale trials are not yet available but have shown that the grid can be installed on site adequately.

The phenomenon of reflection cracking has been investigated using a simulator at the Texas Transportation Institute (Kennephol et al, 1984), and analytical procedures used to predict cracking are being developed. The effect of reinforcement on cracking has also been investigated.

The feasibility of including the grid in unbound pavements has also been studied and this is briefly reported.

3.2 GRID INSTALLATION PROCEDURES

Several methods of grid installation have been investigated. The present installation technique involves placing the grid on a surface free of major potholes and in a straight line. The end of the grid which is supplied in 50m rolls, is anchored to the surface by nailing through a thin metal strip. Once the roll or rolls (joints may easily be made) have been positioned correctly, a tension of about 6kN over the 2m width is applied using a site vehicle, and the other end anchored. The grid is then held in position on the surface by application of a surface dressing. The preferable binder

is penetration grade bitumen at 1.13 litres/m^2 but emulsions or cut-backs can be used, though they take longer to cure and this may delay the subsequent paving operation. Stone chippings of 10mm nominal size are spread at 5.4 kg/m^2 and rolled in to the hot bitumen with a pneumatic tyred roller. After cooling, the excess chippings are swept off the pavement surface and asphalt paving can proceed. The chipped surface may also be trafficked temporarily if necessary.

This installation procedure was developed to ensure that the grid did not move about under either delivery lorries or the asphalt paving machine. A consequence of this procedure is that the grid may only be placed at an interface between two asphalt lifts, or at the bottom of an asphalt layer. These locations are quite compatible with the uses of the grid for minimising permanent deformation and cracking respectively. The tensile properties of the grid are mobilised by interlock between the aggregate in the asphalt mix and the grid openings and the chippings used in the surface dressing operation facilitate this.

A further advantage of the technique is that the grid is given some thermal protection from the possible application of excessively hot asphalt during paving.

Alternative unsuccessful solutions were investigated at Nottingham (Brown et al 1985), which involved pushing the grid into a loose, hot asphalt mix. A similar construction method was available for pushing steel reinforcement into concrete pavements but the technology proved unsuccessful with asphalt. The grid was pushed into the asphalt with a variety of devices which included a modified drum roller with discs welded to the front drum. Large voids and uncompacted asphalt around the grid, coupled with uneven pressure on the grid made the method highly unsatisfactory.

3.3 OTHER LABORATORY STUDIES OF POLYMER GRIDS IN ASPHALT

A test programme was carried out at the University of Waterloo, Canada and at the Royal Military College at Kingston, Ontario, on the behaviour of asphalt pavements reinforced with "Tensar" AR1 (Hass 1983, Abdelhalim 1983, Abdelhalim et al 1983). The main testing programme was carried out using cyclic plate loading tests on experimental pavement sections, constructed in a test pit which measured 9.4m x 2.4m x 2.0m deep. In total five series of tests were performed. In each case the pit was divided into two, one half being reinforced, with the grid at the bottom of the slab, the other half unreinforced. The layer thicknesses and subgrade conditions were varied in the manner shown by Table 3.1. The test temperature was 23^{o}C, and a 40kN load was applied by a 300mm diameter stiff plate, at a frequency of 10Hz. Fig. 3.1 shows some typical results for test series 1, in which the asphalt construction was 150mm thick. Under the same conditions the reinforced pavement performed better than the unreinforced one. Amongst the parameters measured under an applied monotonic load were the maximum deflection, angle of curvature (a parameter combining the surface deflection and radius of curvature), and the permanent deformation. The angle of curvature is used as a parameter because it gives some indication of the structural strength of the upper layers in a pavement, whereas central deflection alone is most strongly influenced by the subgrade stiffness. In the particular example shown in Fig. 3.1, it can be seen that the reinforced structure has carried between 2.5 to 10 times the number of load applications before the same angle of curvature was realised.

The reinforced slab also required an additional 50,000 cycles to achieve the same magnitude of permanent deformation at the conclusion of the test. For a critical rut depth of 20mm the

Table 3-1 Test conditions for laboratory investigations at Waterloo

Asphalt Thickness (mm)	Subgrade Conditions	Comments
115	Dry	Reinforced and Unreinforced
150	Dry and Saturated	Reinforced and Unreinforced
165	Dry	Reinforced and Unreinforced
200	Saturated	Reinforced and Unreinforced
200	Dry	Reinforced
250	Dry and Saturated	Unreinforced

reinforced pavement carried 8.5×10^3 load applications, approximately 1.5 times that of the unreinforced section of the same thickness (150mm).

The conclusions drawn from this research were:

(a) that a substantial saving in the thickness of asphalt could be achieved,

(b) up to double the number of load repetitions for the same damage,

(c) prevention or minimization of fatigue cracking in the asphalt layer,

by including a polymer grid in the structure.

A further test programme was carried out at the Texas Transportation Institute on the effect of including polymer grids in asphalt overlays prone to reflection cracking (Kennepohl et al 1984). An "overlay tester" was developed (Germann et al 1979), which simulated the thermal movements at a joint in a pavement beneath an asphalt overlay. Cracks were induced in asphalt slabs by casting them over two metal plates which could move relative to one another in the horizontal plane. The crack length was monitored as each test progressed. The slabs were either unreinforced or reinforced within the asphalt layer.

It was shown that by including the grid, the resistance to cracking of an asphalt slab could be improved. Data from this series of tests was used to develop a theoretical method for predicting the life of either a reinforced or unreinforced overlay with respect to reflection cracking, based on fracture mechanics principles (see 1.3.3).

Using this model it was shown that the resistance to cracking of an asphalt could be further increased by providing reinforcement with a higher stiffness or a larger cross-sectional area. This was not

however substantiated by experimental data.

3.4 STUDIES OF POLYMER GRIDS IN PAVEMENT FOUNDATIONS

Extensive research was carried out at Oxford University (Milligan et al 1984) using polymer grids as reinforcement in pavements constructed of unbound granular material. These tests were carried out in the laboratory at one quarter scale.

The experimental arrangement is shown in Fig 3.2. A layer of granular material, the gradation of which was scaled accordingly, was compacted onto a soft saturated clay. A monotonic load was applied to the sample through a rigid footing. The arrangement was constructed in a box, Fig 3.2, with rigid perspex sides, plane strain conditions were assumed. The clear perspex sides enabled the developement of failure planes to be observed during testing. Failure was defined as load at which displacement started to increase rapidily. Comparative data was obtained by testing unreinforced samples and samples reinforced at the granular/clay interface.

The results showed that failure loads in reinforced constructions were typically 40% higher than in unreinforced constructions. It was noted however that failure was less easy to define for reinforced constructions as the load continued to increase steadily with displacement. The behaviour of reinforced and unreinforced constructions did not differ appreciably until displacements of approximatly 5mm were reached (i.e. 20mm in full scale). As the displacement of the footing increased so to did the benefit of including the grid. It is important to note that any benefit from including the grid may not be realized until large displacements have already occured. This may be more acceptable in unbound pavements where large surface ruts are not uncommon.

It is apparent that the load carrying ability of a geogrid in unbound pavements does not come into play until the level of strain in the plane of the grid becomes significant. The mechanisms of reinforcement are not identical in bound and unbound layers, although this study does illustrate that large deformations can be controled by including the grid within a pavement.

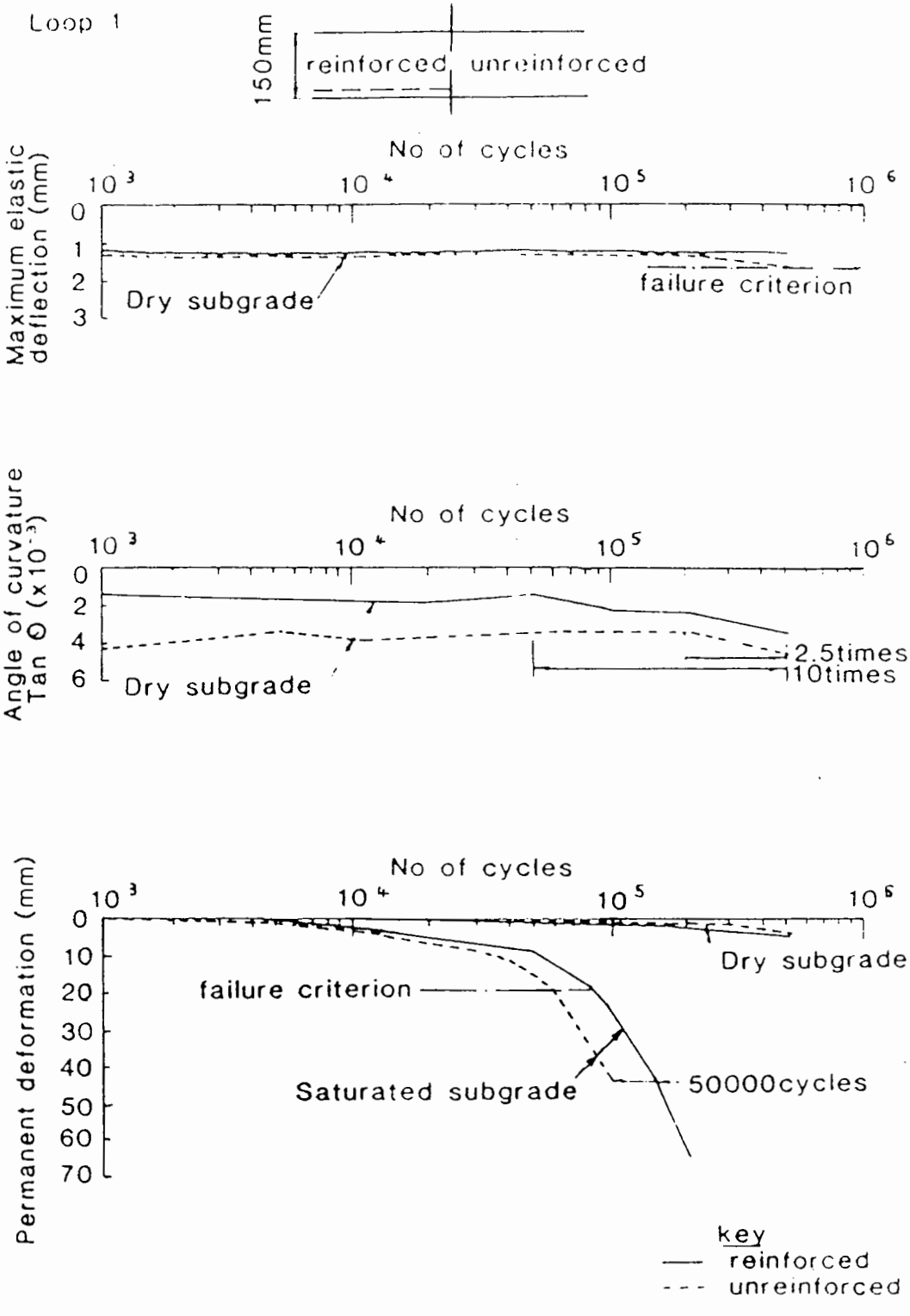

Fig 3.1 Typical results from test loop 1

(After Haas)

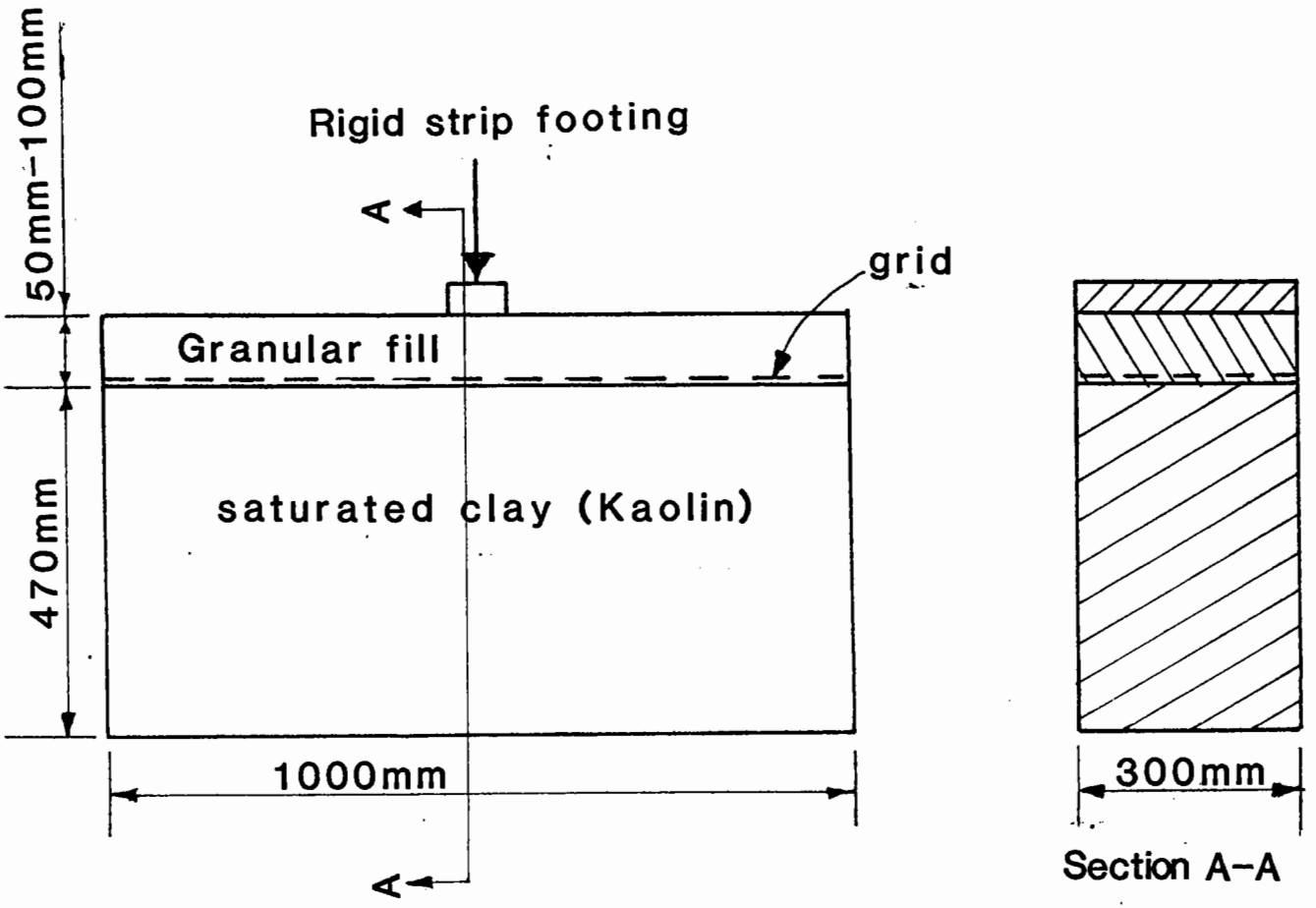

Fig 3.2 Apparatus used to test reinforced unbound material

(After Milligan et al)

4 THE POLYMER GRID

4.1 INTRODUCTION

The polymer grids used throughout this project were manufactured by Netlon Ltd. The polymer used was polypropylene and was protected from ultra violet light by the addition of carbon black. The polymer is inert to all chemicals naturally found in soils and has no solvents at room temperature, neither is the polymer subject to biological attack.

During the manufacturing process the polymer is biaxially orientated so as to align the molecules, the degree of orientation being quantified by the draw ratio, ie. the "stretched" length divided by the original length. As the draw ratio increase so too does the strength and stifness of the grid (Ward 1984). The strength of a particular polymer is also enhanced by increasing the crosslinking between chains of molecules in any one polymer. Normal draw ratios for the grid are approximately six.

Two basic types of grid have been used during the course of this research. The prototype grid was designated "Tensar SS3," and was replaced with a heat set material "Tensar AR1". "Tensar AR1" has been used throughout. The heat set process reduced the susceptibility of the polymer grid to shrinkage at elevated temperatures.

Typical dimensions of the "Tensar" AR1 grid are shown in Fig. 4.1. These measurements are the average values of twenty readings, taken at various locations, in a production roll of grid. The grid nomenclature is also shown on Fig. 4.1. The transverse direction ie. across the roll, is the direction of maximum orientation and is sometimes referred to as the primary direction. The longitudinal or

secondary direction, is the direction of least orientation, and hence has a marginally lower stiffness.

The grid is visco-elastic by nature and extensive research at Strathclyde University (McGowan et al 1984) on the long term behaviour of the grid has resulted in the development of isochronous plots which show the viscous behaviour of the grid when subjected to a steady load, over periods of time up to 20 years. This information is important when considering applications of the grid in reinforced soil structures. Here the grid is expected to withstand a load over a long period of time. From the isochronous plots it is possible to specify a safe load under which the grid will not fracture or deform unduly during the design life of the struture.

This information is less important in its application to pavement reinforcement. The grid in this situation is not required to resist a steady load but, rather to reinforce in two ways. In the long term the grid is required to prevent the plastic deformation of a pavement and bituminous materials which are much more susceptible to flow than the polymer grid. Secondly the grid is required to resist imposed traffic loads. Since the load pulse is short a high resilient modulus is realised in the grid.

The laboratory tests were designed therefore with pavement applications in mind. The elastic stiffness of the grid was found under various conditions of loading relevant to pavement engineering and the effect of temperature on the mechanical properties was also investigated. This is important because the grid can experience a severe thermal regime during paving. Two situations were examined where the grid subjected to elevated temperatures while fully and semi restrained. The fully restrained situation simulated the condition where the grid was bonded to a pavement, while the semi restrained situation simulated the grid placed in a loose mix.

4.2 MECHANICAL PROPERTIES

The virgin elastic stiffness of the grid was established for the polymer grid in the testing facility developed at Nottingham University. Unless otherwise stated, any viscous effects during testing have been ignored.

4.2.1. Experimental arrangement

An Instron servo controlled hydraulic 100kN testing machine, Fig. 4.2, was available, which had a linear actuator of 100mm stroke (Appendix A). The upper moveable crosshead could be locked to give a maximum spacing between the clamps of 800mm. The clamps, supplied by "Netlon Ltd", were designed to grip the grid and adapted to fit the hydraulic jaws of the Instron, Fig 4.3. The clamps were centrally attached with pins to short flat bars, held vertically in the hydraulic jaws. A grid specimen was then slid into the clamps, which were designed to locate a row of ribs of the specimen into a slot. The slot tapered down to the open end of the clamps, which were wide enough to just trap the ribs when the clamps were screwed together.

A temperature control cabinet was erected around the Instron and was fitted with a fan heater and a cooler. This enabled the temperature of a specimen in the Instron, to be maintained between $5^{o}C$ and $55^{o}C \pm 1^{o}C$.

Test specimens were taken from production rolls of polymer grid, and were cut from the centre and edges of each roll to eliminate the variability of material properties from one position to another. A sample of polymer grid in the Instron, ready to test, is shown in Fig. 4.4.

4.2.2. Stiffness testing

Stiffness testing was conducted on the polymer grid in the

transverse direction using a loading frequency of 1Hz, at various levels of peak to peak strain. The test temperature was $20^{o}C \pm 1^{o}C$. The peak to peak load was recorded from the digital panel meter on the Instron, which was fitted with a "peak catcher". Using a 10kN load cell, the load could be resolved to within 0.01kN. The peak to peak displacement was recorded using the output from the linear variable differential transformer (L.V.D.T.) which controlled the displacement of the actuator. This was also displayed on the digital panel meter of the Instron, a peak catcher recording the maximum and minimum values. The L.V.D.T. could resolve to 0.05mm. The gauge length of each specimen was measured before testing and was taken as the distance between the centres of extreme nodes, as shown on Fig. 4.5.

Fig. 4.6(a) taken from a chart recorder, illustrates a typical response of the grid during stiffness testing. Data of this type was used to plot Fig. 4.6(b) from which the elastic stiffness was calculated.

Seven samples were tested, each approximately 430mm long (transverse direction) by 380mm wide (longitudinal direction). The stiffness was calculated by dividing the peak to peak load by the peak to peak strain. An average value of 0.9 MN/m was observed in the transverse direction, which is the stiffest. This corresponds to a modulus of 12.9 GPa if the minimum cross sectional area of a transverse rib ($3.28mm^2$) is used to calculate stresses.

4.2.3. Ultimate strength tests

Tests were conducted on the grid to obtain values for the ultimate breaking strength of the grid. The test procedure was standard for all specimens and was conducted in the Instron. The reference condition for controlled strain rate testing to failure was

2% strain/min at $20^{o}C \pm 1^{o}C$. The clamping arrangement was identical to that used in the stiffness tests.

Seven samples were tested in the transverse direction, the average failure strength was 26kN/m and the range between 24.2kN/m and 27.6kN/m. The average value of 26kN/m corresponds to a tensile strength of 0.37 GPa if the minimum cross sectional area of a transverse rib is used to calculate the stress. Fig 4.7 illustrates the strain/load response recorded during a test to failure. In this case a brittle failure occured although this was not always the case. The strain at failure varied between 8% and 11%. Rupture did not normally occur at the section of the grid with the smallest cross-sectional area. This section is in fact the strongest part of the grid structure as the molecules have the highest degree of orientation. Rupture occurred through the nodes, ie. the intersection of the nodes where, due to the production process, the degree of orientation is a minimum.

4.2.4 Effect of temperature on elastic stiffness.

The Instron servo hydraulic testing machine was equipped with a temperature controlled cabinet, and the temperature of the grid could therefore be varied easily and stiffness tests undertaken.

The stiffness was measured at a frequency of 1Hz for various levels of mean strain up to 1%, and was calculated by dividing the peak to peak load per metre by the peak to peak strain as previouly. Fig. 4.8 shows the variation of stiffness with temperature for the grid. A separate sample was tested in each direction (i.e. in the tranverse and longitudinal direction). A temperature rise of $40^{o}C$ decreased the stiffness of the grid by approximately 50%. The index curve shown in Fig. 4.8 is parallel to the best fit curve for the longitudinal data. It passes through the index stiffness, 0.9MN/m,

at 20°C. As only one sample was tested at different temperatures, the index stiffness can be assumed to be the average stiffness if a large sample of grids had been tested.

Fig. 4.8 also includes a curve showing the variation of stiffness with temperature for a typical asphalt mix. The mix properties and boundary conditions from the calculated stiffnesses are shown in Table 4.1. The stiffness was calculated using the Shell procedure with the computer program PONOS (De Bats, 1972). Although the stiffness of the grid does decreases with temperature, the stiffness of a typical mix decreases much more rapidly with increasing temperature. The modular ratio, therefore, between the grid and asphalt will increase with increasing temperature, realizing greater reinforcing potential at higher temperatures.

4.2.5 Frequency effects on elastic stiffness

The stiffness of the polymer grid was monitored over a range of frequencies (1Hz to 30Hz) within the practical capabilities of the Instron testing machine. The stiffness was calculated in the usual manner, with at least five readings taken for each frequency at different mean levels of strain. Three specimens were tested, all in the transverse direction, at a test temperature of 22°C $\pm$ 1°C. The sample size was approximately 500mm long (transverse direction) by 430mm. As in previous testing the digital panel meter on the Instron machine was used to record the load and strain.

Table 4.2 shows the values of stiffnesses calculated at each frequency for all three specimens. There is little effect due to frequency except for a slight drop in stiffness below 6Hz. A possibility exists that this may have been due to a failure of the panel meter on the Instron to record accurately at high frequencies. This has not however been investigated further.

Table 4.1 Mix details and boundary conditions for typical Dense Bitumen Macadam

Mix Details			
Mix type	Binder Content (%)	Void Content (%)	Bitumen Penetration
Dense Bitumen Macadam Road Base	3.5	10	100

Boundary Conditions	
Thickness of layer (mm)	Traffic Speed km/hr
100	150

Table 4.2 Stiffness variation of "Tensar" AR1 with frequency at 22° ± 1°C (transverse direction).

Frequency Hz	Stiffness MN/m		
	Specimen No		
	1	2	3
1	0.9	0.9	0.9
2	1.0	1.0	0.9
3	0.9	1.1	0.9
4	1.0	1.2	1.0
5	1.0	1.2	1.0
6	1.0	1.1	1.1
7	1.0	1.1	1.0
8	1.0	1.1	1.1
9	1.0	1.1	1.1
10	1.0	1.1	1.1
15	-	1.1	1.0
20	1.0	1.1	1.1
25	-	1.1	1.1
30	1.0	0.9	1.0

4.2.6 Fatigue characteristics

Testing has been carried out to investigate the effect of a large number of load applications on the stiffness of the grid. Owing to the difficulty in continuous testing in the Instron hydraulic testing equipment, (due to pressure failure in the oil supply), few samples were tested for over 0.5 million cycles without a rest period. The limitations of the testing equipment also meant that the tests were performed in strain control and not load control. Load relaxation therefore occurred during each test. The temperature control cabinet placed around the specimen enabled the temperature of the grid to be maintained to within $\pm 1^{o}C$.

All tests were conducted on the grid in the transverse direction. The specimens were held in position in a manner identical to that used for the stiffness testing. Each sample was 430mm wide (in the longitudinal direction) and 600mm long (in the transverse direction). The load was applied at a frequency of 6Hz, chosen because it was easily within the capabilities of the testing machine. Three specimens are reported herein. They are numbered 1, 4 and 5. Other specimens which were tested are not reported here because of frequent breakdown of the Instron during testing.

Specimens 1 and 4 had an applied mean tensile strain of 5% and cyclic tensile strain amplitude of 0.4%. Specimen 1 was tested at ambient temperature without any form of temperature control, while Specimen 4 was maintained at $41^{o}C$. Specimen 5 had a mean tensile strain of 2% and a cyclic strain amplitude of 0.08% and was maintained at a temperature of $20^{o}C$.

Figs. 4.9 to 4.11 illustrate the results, showing the maximum and minimum loads recorded during each test, and the load relaxation. Throughout each test, although load relaxation occurred, the cyclic load amplitude remained constant, indicating that the elastic

stiffness also remained constant.

Rest periods of approximately one hour duration occurred during the testing of both Specimens 4 and 5. The grid exhibited a "memory" after these events and load relaxation occurred more quickly until the virgin curve of load relaxation against number of cycles was rejoined. (see Figs. 4.10 and 4.11)

The temperature during testing of Specimen 1 was not controlled and Fig. 4.9 shows how, as the test progressed, the temperature of the grid increased by 6.0^{o}C from 23.5^{o}C to 29.5^{o}C. Table 4.3 shows the values of stiffness calculated from the peak to peak levels of load and strain, and the temperature of the grid, as the test progressed. The rise in temperature brought about a decrease in stiffness of 0.1MN/m. This is similar to that which can be estimated from the relationship between stiffness and temperature derived for the grid in Fig. 4.8.

The mean load relaxation for each test is shown in Fig. 4.12. In Specimens 1 and 4, all the test parameters were identical, except temperature. The temperature of specimen 4 was held at 41^{o}C, while the temperature of Specimen 1 varied from 23.5^{o}C to 29.5^{o}C. Due to the higher temperature the mean load and cyclic load amplitudes were less for specimen 4, and load relaxation therefore occurred at a slightly lower rate compared to Specimen 1.

Specimen 5 differed from Specimen 1 by having a much smaller mean load and cyclic load amplitude, and load relaxation again occured at a much slower rate.

The fatigue data shows that the elastic stiffness of the polymer grid does not vary after a large number of load repetitions. The material is, however, prone to creep or alternatively load relaxation. To what extent this may be a problem "in situ" has yet to be investigated, although laboratory tests to date have not shown

Table 4.3 Temperature and Stiffness estimated for specimen 1 during testing

No of load cycles	Stiffness (MN/m)	Temperature of grid (^{o}C)
0	0.97	23.5
600	0.97	23.9
1000	0.97	23.9
$2x10^3$	0.96	24.1
$5x10^3$	0.96	24.4
$10x10^3$	0.94	24.6
$20x10^3$	0.95	25.1
$53x10^3$	0.93	26.3
$100x10^3$	0.90	27.3
$398x10^3$	0.87	29.6

this to be a problem.

The rate of load relaxation, as expected, was seen to be a function of applied mean tensile load and cyclic load amplitude. At higher mean levels of load, and larger cyclic load amplitudes, relaxation occured at a quicker rate.

4.3 TEMPERATURE EFFECTS ON SEMI-RESTRAINED GRIDS

High temperatures during paving were considered a major concern when including polymer grids in asphalt. It had been noted (Brown and Brodrick 1982), that when polymer grids were subjected to elevated temperatures shrinkage occurred, accompanied by a reduction in stiffness. The degree to which shrinkage occurred was dependent on several factors, including the temperature and exposure time to elevated temperatures, and the degree of restraint offered to the grid while at elevated temperatures. It has been observed that "Young's Modulus" of polymers produced by tensile drawing, is related to the draw ratio and increases steadily with increasing draw ratio" (Ward 1984).

A test was sought that would be typical of the thermal regime and degree of restraint offered to the grid in a hot loose asphalt mix, but would be convenient to conduct in the laboratory with repeatable results.

Three tests were conducted on the prototype grid "Tensar SS3" and predate the production of the heat set "ARI". It is expected that "AR1" will be less susceptible to high temperatures.

4.3.1 Heat treatment procedures

A variety of experimental arrangements were used to expose the grid to elevated temperatures, each producing a different restraining

effect and thermal regime. The tests are described as follows.

(1) Asphalt: This procedure consisted of laying hot asphalt over the grid, which was placed in a wooden mould. The asphalt was compacted using a vibrating plate. This was considered to give a true representation of the in situ conditions, but proved inconvenient and difficult to control. The asphalt often left the grid in a state which made subsequent testing difficult.

(2) Bakelite: In this series of tests the grid was clamped between sheets of bakelite. The "sandwich" was either placed in a preheated oven or heated from room temperature gradually.

(3) Sand: Sand was used to apply heat to the grid in two ways. One method was to pour the hot sand directly onto the grid in a mould, while the other involved heating the sample in sand from room temperature.

(4) Clay: A more unusual method of restraining the grid was examined by "cooking" it in baked clay. Soft clay was compacted around the grid and allowed to harden. After loading with a surcharge the complete package was heated in an oven.

(5) Oil: An oil bath was raised to the desired temperature, and a sample of grid dropped in. The oil offered no restraint to the grid.

4.3.2 Shrinkage and stiffness effects

The resultant magnitude of shrinkage strain, against the maximum exposure temperature for the various treatments is shown in Fig. 4.13. Under semi-restrained conditions the grid shrinks, and for any one treatment, the degree of shrinkage increases with an increase in exposure temperature or time. Where no restraint was offered to the grid i.e. in the oil bath, the grid reverted almost to its original, unstretched dimensions, developing a shrinkage strain of

almost 70% at 180°C. (Fig. 4.14)

The stiffness of each of the grid specimens was measured by the methods described in section 4.2, before and after heating. Fig. 4.15 presents the data showing the ratio of stiffness after heating ($S_{a.h}$) divided by stiffness before heating ($S_{b.h}$). A decrease in stiffness is evident as the magnitude of shrinkage increases. At low magnitudes of shrinkage the stiffness before and after heating are similar, with one exception where the grid was fully restrained in clay.

4.4 EFFECT OF TEMPERATURE ON FULLY RESTRAINED GRID

It has been established that when the polymer grid, an orientated polymer, is subjected to elevated temperatures for an extended period of time, it will soften and if unrestrained, shrink. When used on site in a flexible pavement according to the procedure outlined in Chapter 2, the grid is anchored at either end, and effectively bonded to the underlying pavement with the "chip seal" layer. It is in effect therefore, fully restrained, and shrinkage is prevented. Forces are therefore set up in the grid as it is heated during paving, and these forces were monitored in the laboratory.

The effect of this thermal regime on the stiffness of the grid was investigated. This testing was undertaken in the usual manner. "Tensar SS3" grid was used in all the tests on this section and it is anticipated that the heat set grid "ARI" would be influenced rather less than is indicated by the results.

4.4.1. Restraining force measurements

The apparatus,shown in Fig. 4.16, was used to fully restrain the

grid during heating, while monitoring the tension built up in grid. Test samples measured 7 ribs wide in the longitudinal direction, and 6 ribs long in the transverse direction. The restraining force was measured in the transverse direction i.e. the direction of maximum orientation. Strips of plywood were used to clamp the specimen in position. One end was attached to a rigid base and the other attached to a temperature compensated load cell, via a threaded bar, which allowed a slight pretension to be applied to the grid before testing. Samples were placed in a preheated oven for various lengths of time, removed, and then allowed to cool to ambient temperatures. The temperature was recorded continuously using a thermocouple taped to the surface of the grid. Hard copies of both outputs (load and temperature) were traced on a pen recorder driven at a known constant speed.

Two typical results are illustrated in Fig. 4.13 which shows the restraining force varying with the temperature of the grid. The full set of data from these tests are included in Appendix B. A slight pretension was applied to each specimen to take up any slack in the grid and immediately on placing the specimen in the preheated oven, this preload relaxed before the restraint force increased to a maximum value. This maximum value was usually reached within 2 hours of the test commencing. After removal from the oven, the load relaxed somewhat but still retained a certain degree of tension. Table 4.4 shows the maximum restraining force attained during heating and the length of time each specimen was held in the oven. A correlation was found, Fig. 4.18, between the maximum restraining force and maximum temperature of the grid in the oven. As the temperature at which the grid was restrained increased, so too did the force required to prevent it from shrinking. This shrinkage force was observed to reach an upper plateau limit of around 0.9kN/m

Table 4.4 Test description and properties of SS3

Sample No.	Max Temp. (°C)	Max Restraining load (kN/m)	Time in oven (Hrs.min)	Stiffness after heating (MN/m)	Peak load at failure (kN/m)
1	130	.22	0.40		
2	150	.83	2.25		
3	130	.65	5.30		
4	140	.63	1.20		
5	150	.70	21.10	.65	-
6	142	.87	2.15	.94	27.3
7	132	.86	1.10	1.06	28.6
8	133	.69	2.00	.82	31.6
9	133	.82	"	1.02	30.0
10	125	.46	"	.96	28.7
11	107	.32	"	.98	30.3
12	100	.18	"	1.09	29.6
13	95	.05	"	.99	29.5
14	105	.09	"	.93	27.3
15	20	-	0	1.00	-
16	20	-	0	.95	29.0
17	20	-	0	.99	27,6

at temperatures of 135°C and above. The Vicat softening point of polypropylene is 148°C and this corresponds reasonably well with the critical temperature above which no increase in restraining force was measured.

4.4.2 Stiffness measurements

The elastic stiffness of each specimen was measured after heating, in the usual manner, and the results are shown in Table 4.4. Samples 15, 16, and 17 which were not heated were control tests. These results show that the stiffness of the grid, if not allowed to shrink during heating, does not differ significantly from that of the unheated material. In a pavement therefore the grid would be expected to have the same stiffness as the virgin grid, even after paving. Comparing these results to Fig. 4.15, at zero shrinkage, the ratio of stiffness before heating to after heating was 1.

4.5 CONCLUSIONS

The tests conducted on the grid were primarily to discover the index properties and to devise suitable laboratory testing procedures. Consequently, stiffness and failure tests have been developed. For the current heat set material the average stiffness in the transverse direction was 0.9MN/m and the average ultimate strength 26kN/m.

The ambient temperature has an effect on the stiffness of the grid, and it was noted that an increase in temperature of 40°C reduced the stiffness of the grid by 50%. The grid was however, less temperature susceptible than bituminous material and consequently can still act positively as a reinforcing element at elevated temperatures. The grid was not susceptible to fatigue, although load

relaxation does occur, neither was the stiffness of the grid affected by the frequency of testing.

In semi-restrained conditions the grid will shrink if exposed to elevated temperatures and if no restraint is offered during heating will revert virtually to its original dimensions. It was found that the shrinkage strain was directly related to a reduction in stiffness. It would be more normal for the grid to be fully restrained during paving. Investigating this situation in the laboratory it was shown that forces are set up in the grid during heating which are not fully dissipated on cooling. These forces may act as a prestress in the pavement and could be beneficial to the pavement performance. Furthermore, it was discovered that the stiffness of the grid did not alter after heating when fully restrained.

The mechanical properties of the grid are not significantly affected by paving temperatures which will be kept to a minimum in situ as the grid is positioned on a cold surface. The chip seal normally used during instalation will further reduce the temperature by acting as a insulating layer. In the event of the temperature of the grid rising above 140^{o}C, excessive restraining forces may lead to distortion of the grid, but this situation is unlikely in practice.

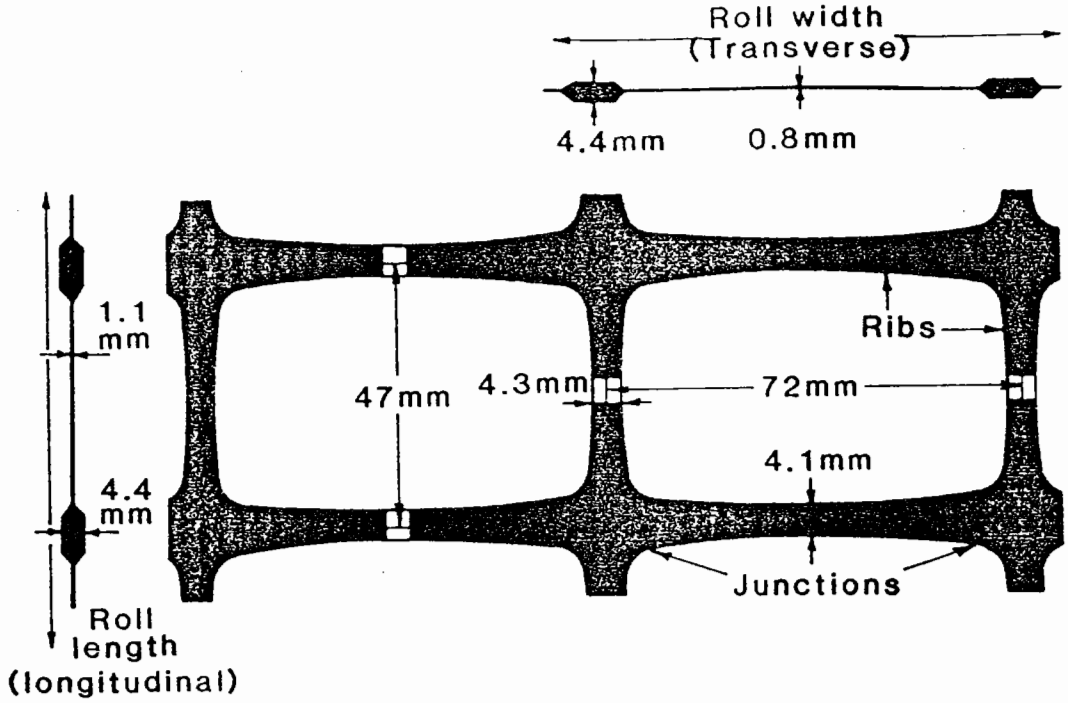

Fig. 4.1 Dimensions of polymer grid "AR1"

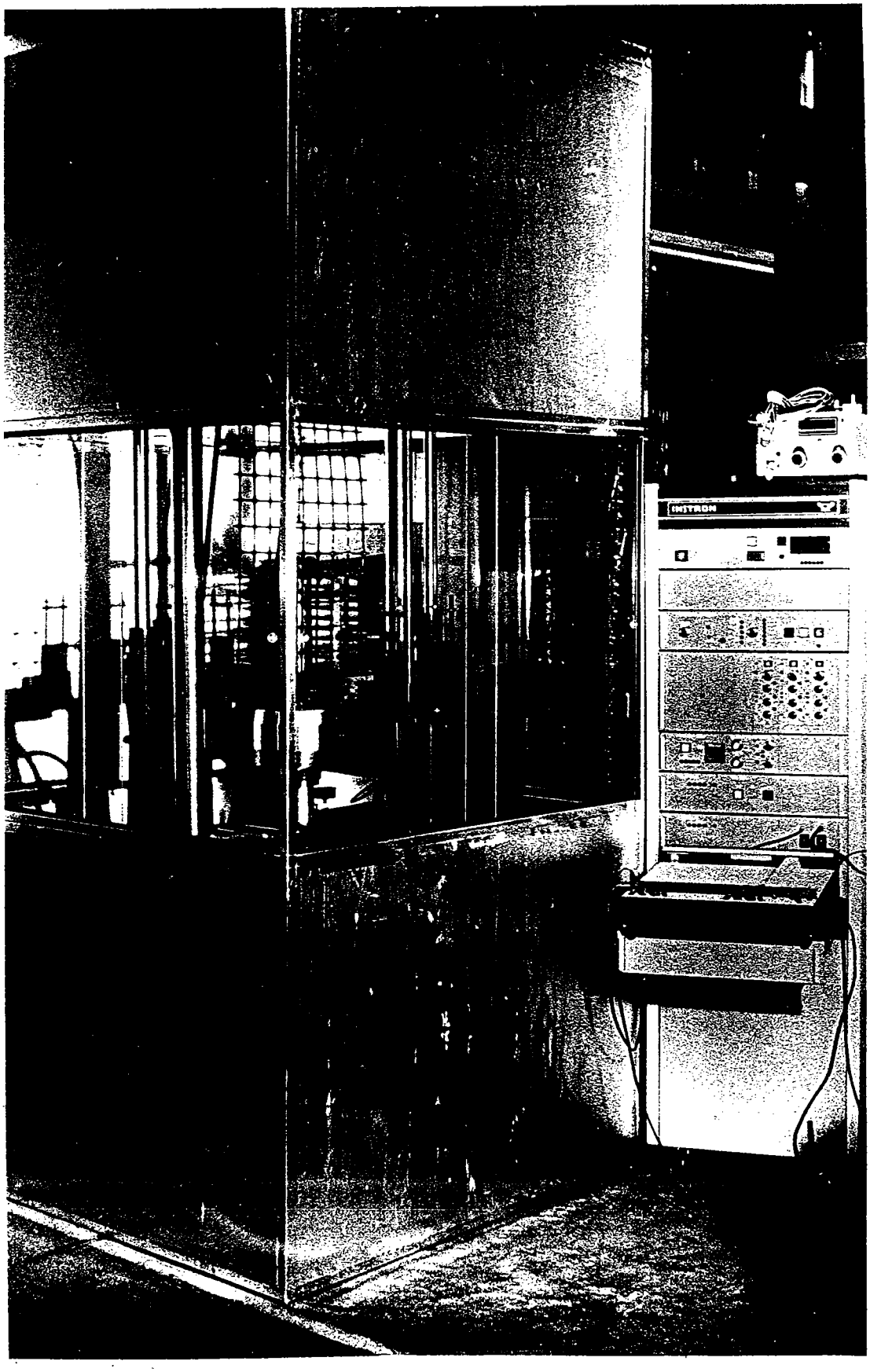

Fig. 4.2 Instron testing facility

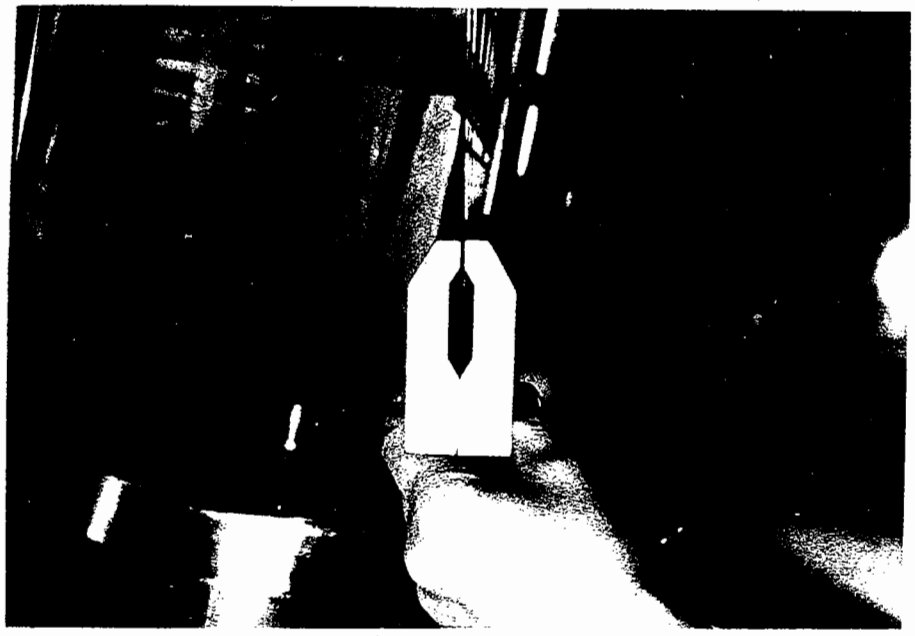

Fig. 4.3 clamps for polymer grid

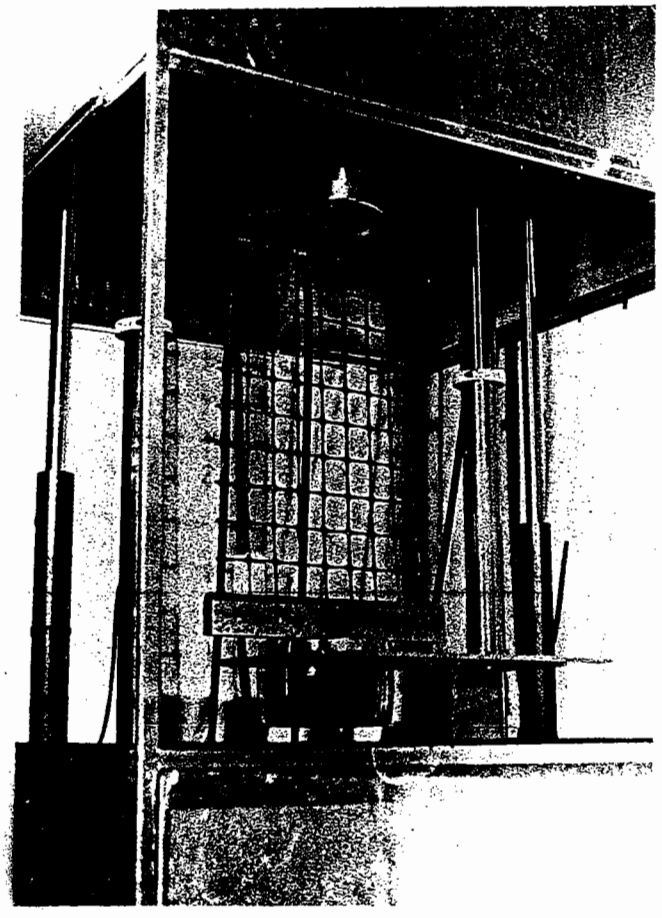

Fig. 4.4 Grid in testing facility

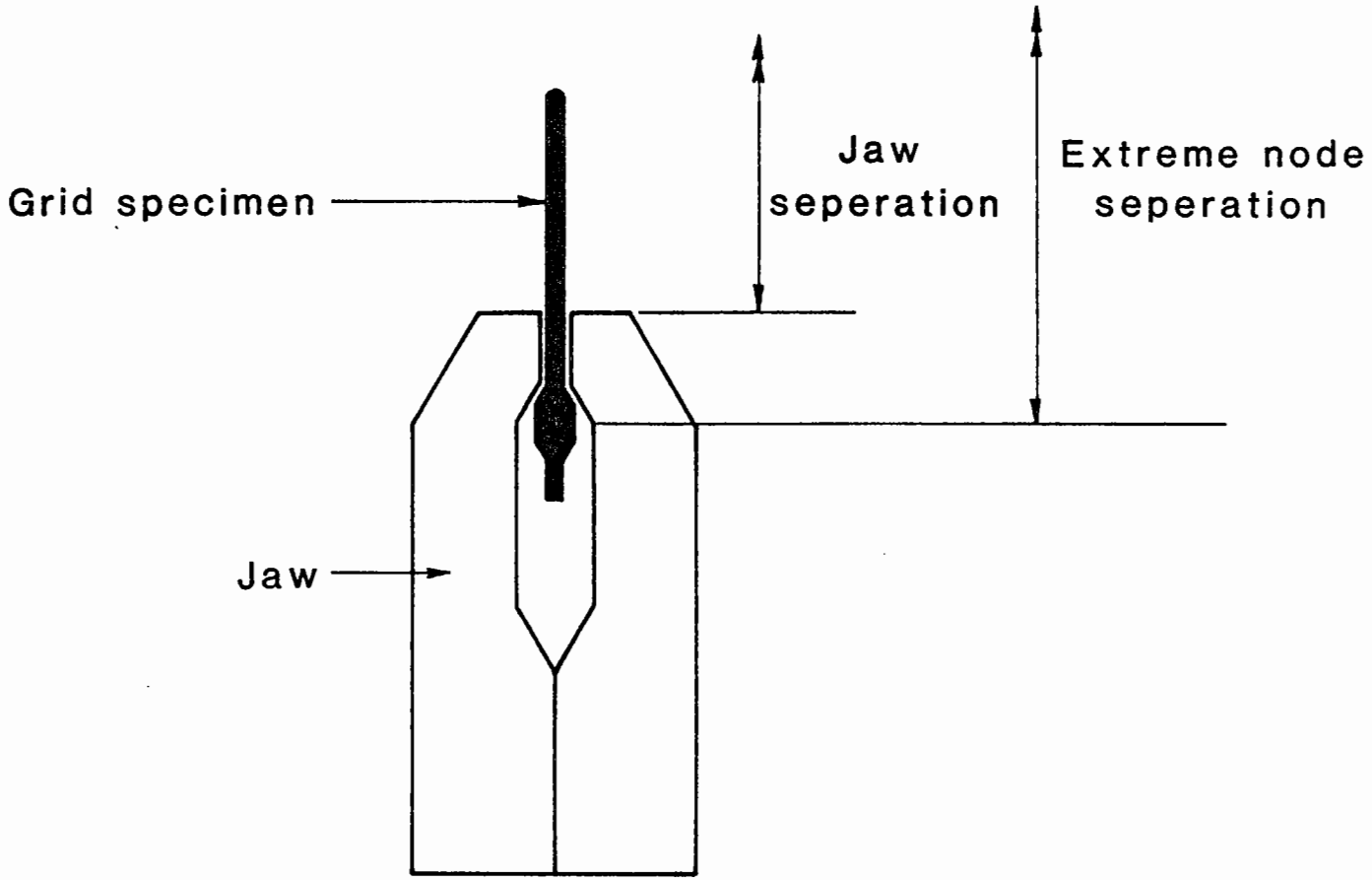

Fig. 4.5 Possible Gauge Lengths in Stiffness Testing

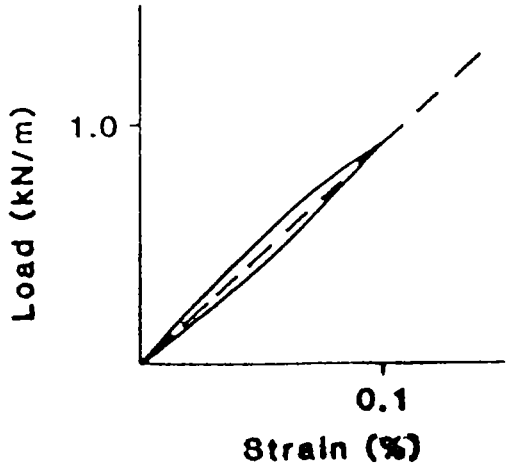

(a) Typical response of grid under cyclic loading

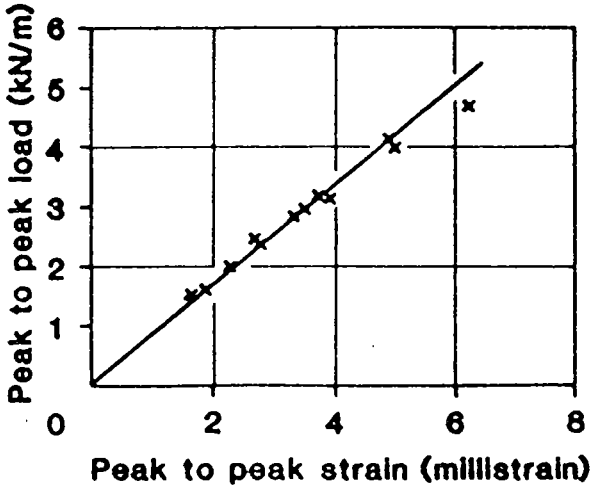

(b) Peak to peak load against peak to peak strain

Fig. 4.6 Data from stiffness testing on polymer grid

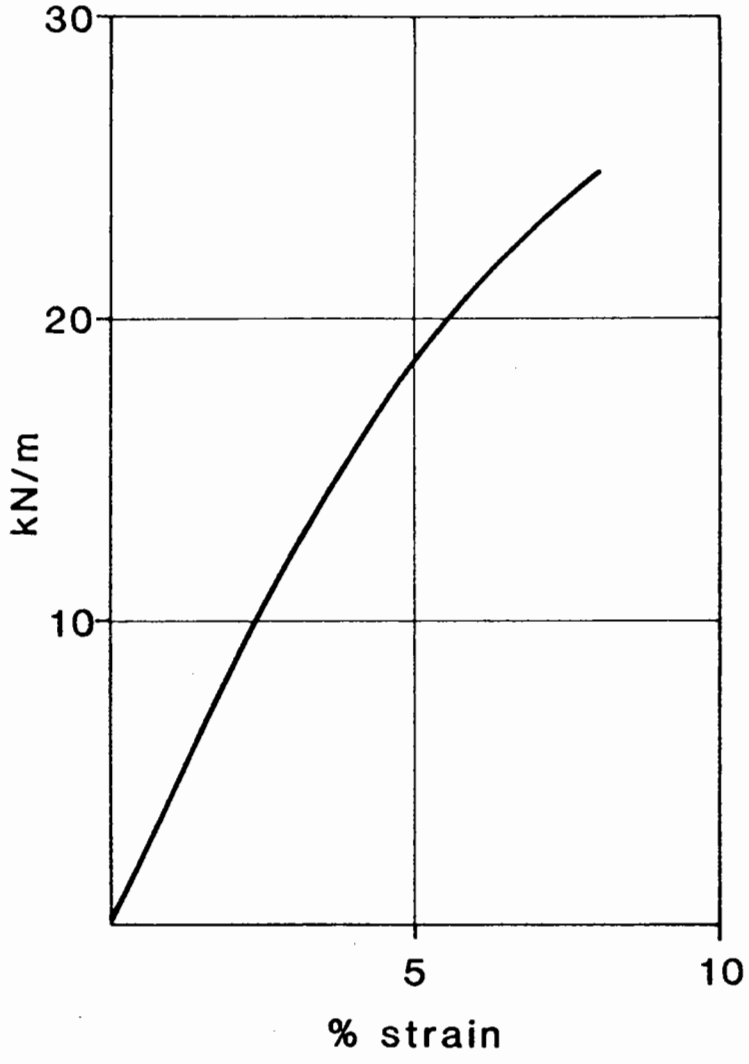

Strain rate - 2% strain/min
Temperature - 20°C ± 1°C

Fig. 4.7 Typical Controlled Strain Rate Test to Failure of Tensar AR1

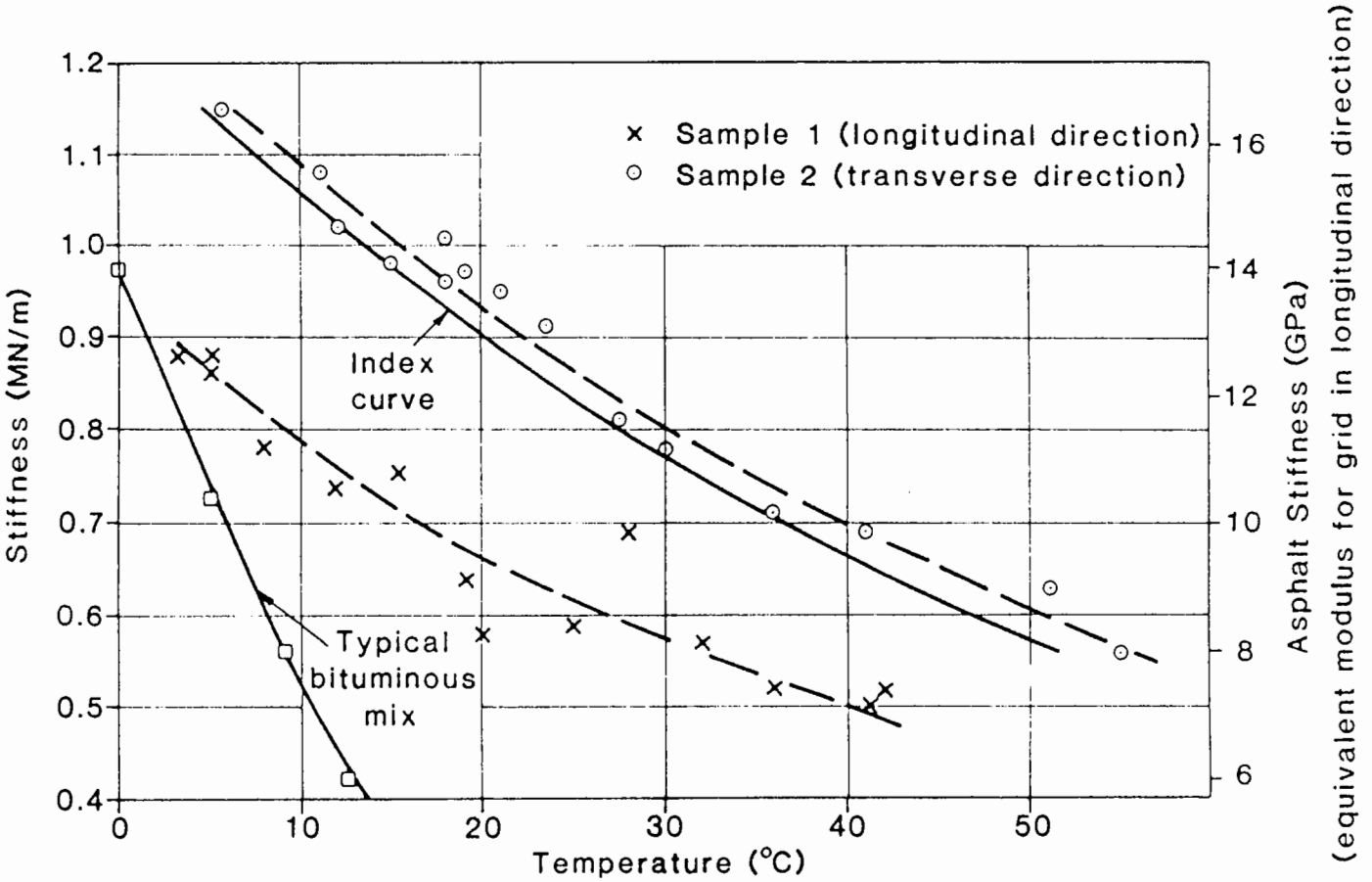

Fig. 4.8 Variation of stiffness with temperature for Tensar AR1 and a typical bituminous mix

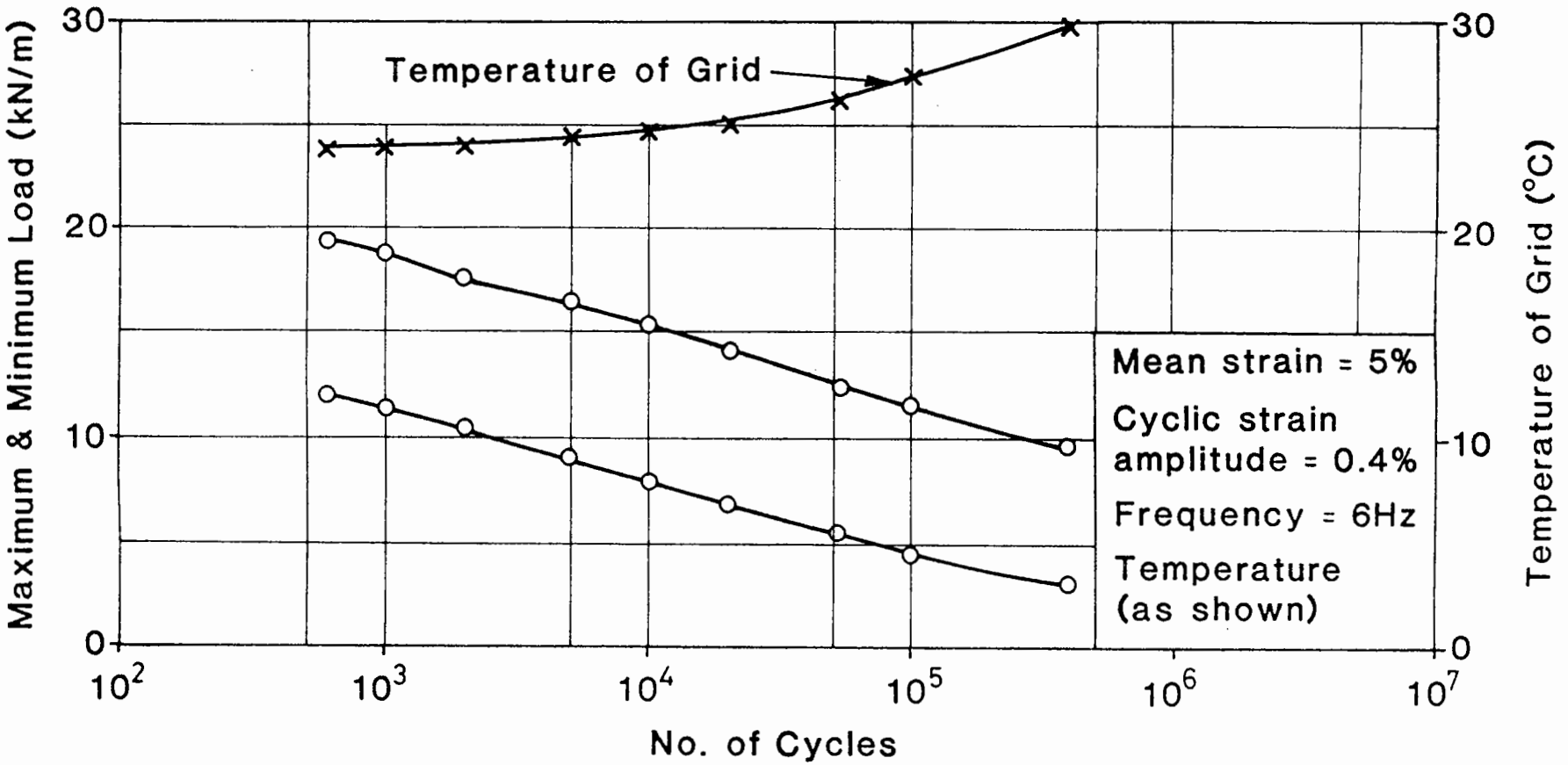

Fig. 4.9 Load Relaxation of Specimen No. 1

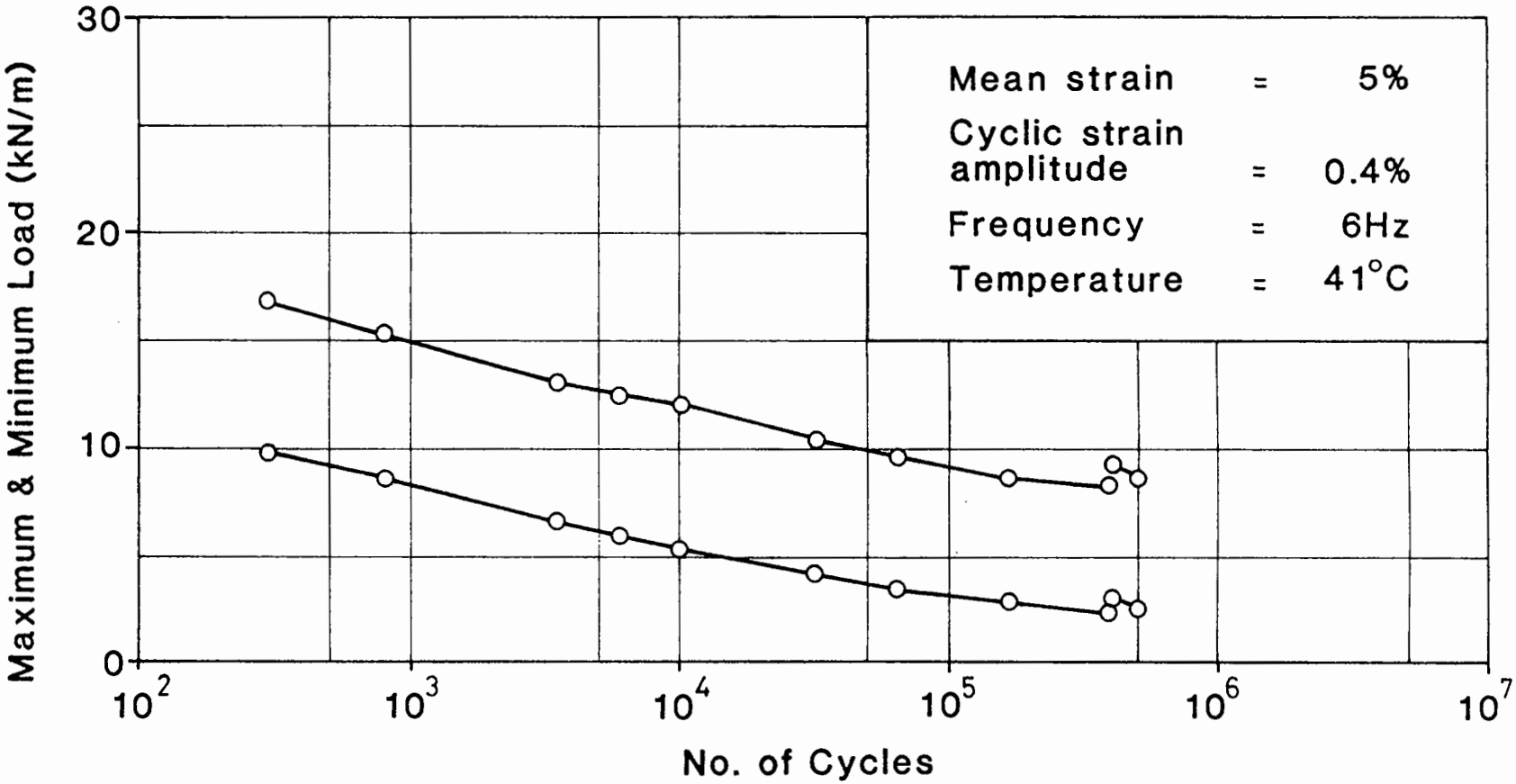

Fig. 4.10 Load Relaxation of Specimen No. 4

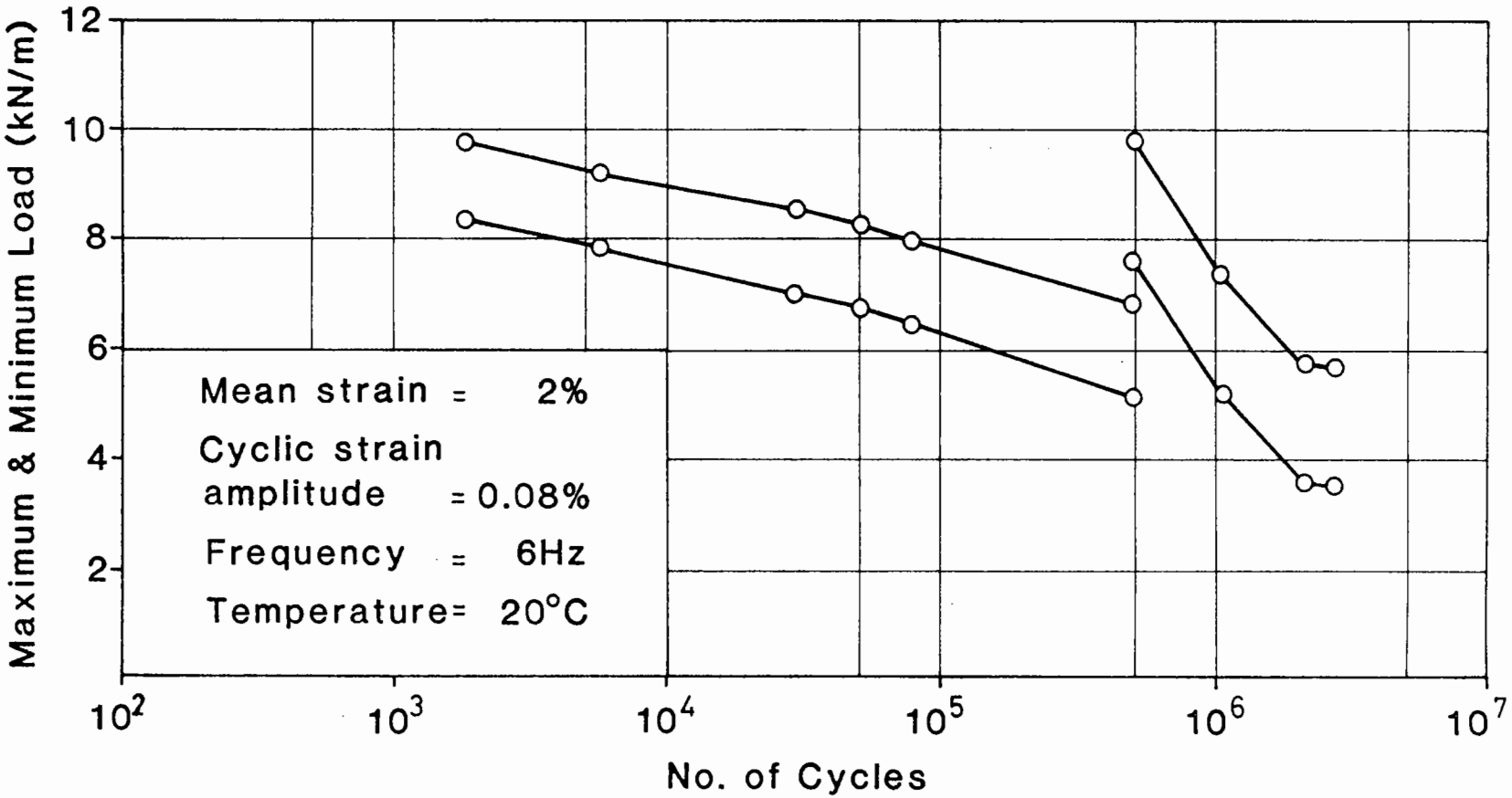

Fig. 4.11 Load Relaxation of Specimen No. 5

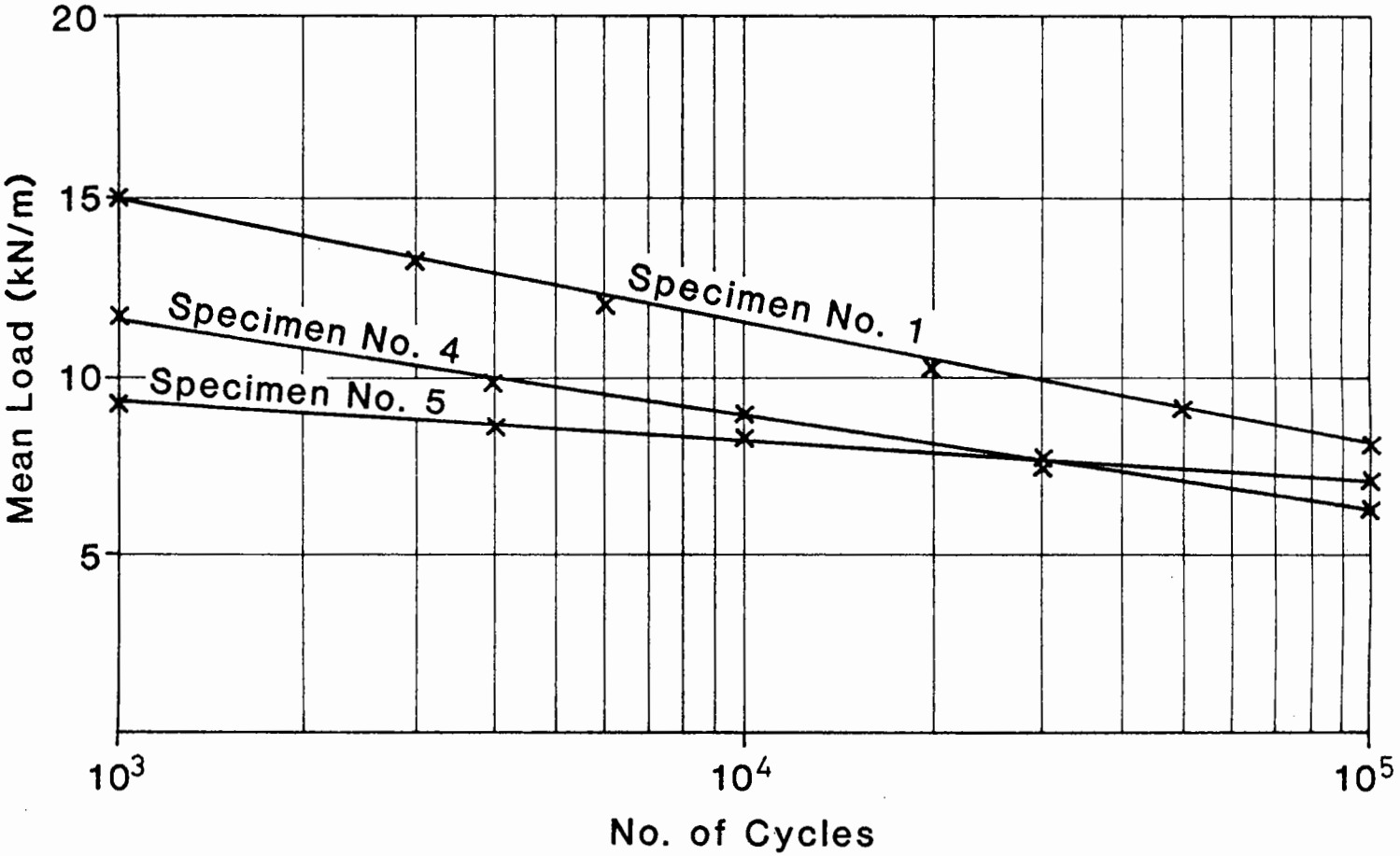

Fig. 4.12 Mean Load Relaxation During Fatigue Tests

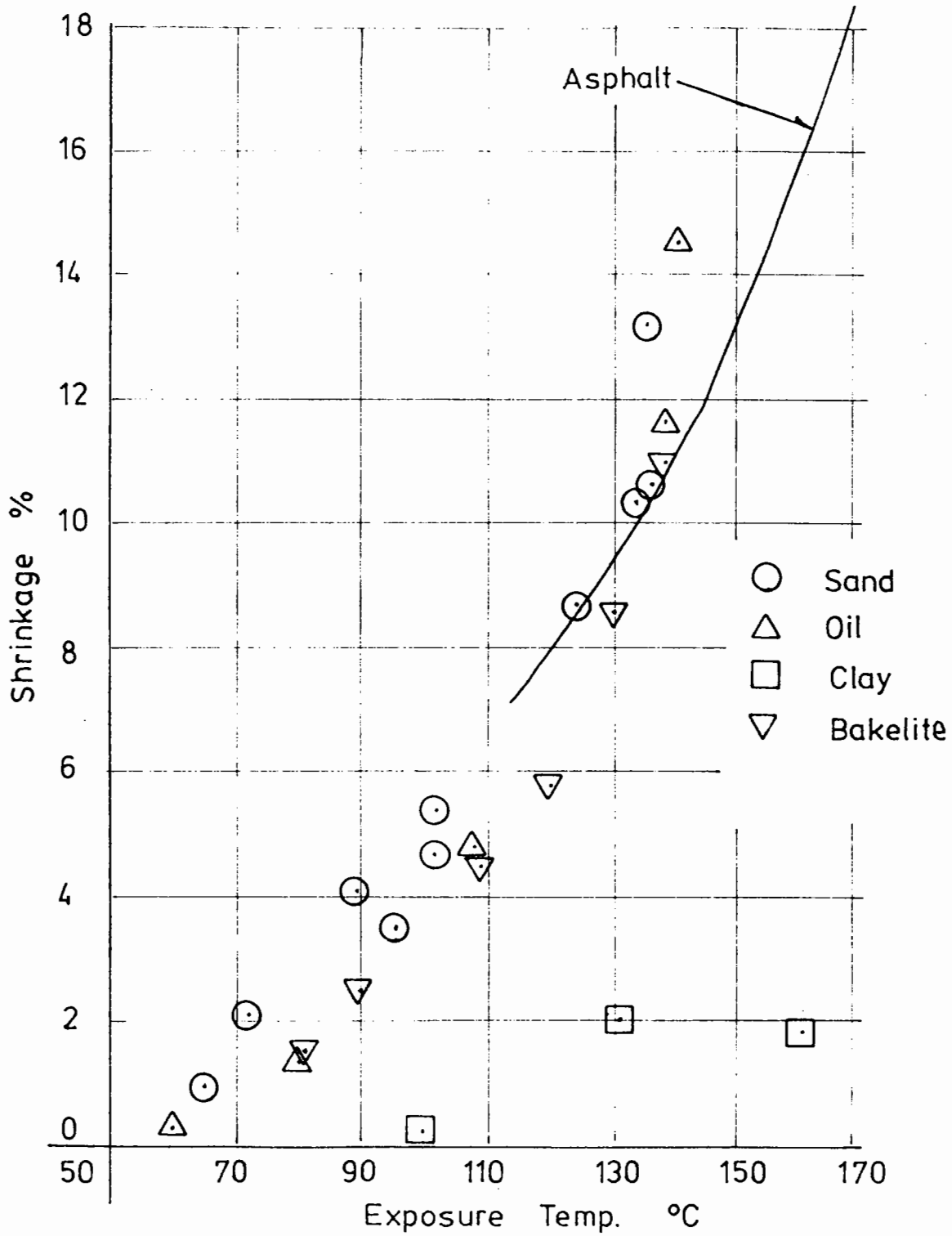

Fig. 4.13 Shrinkage on heating

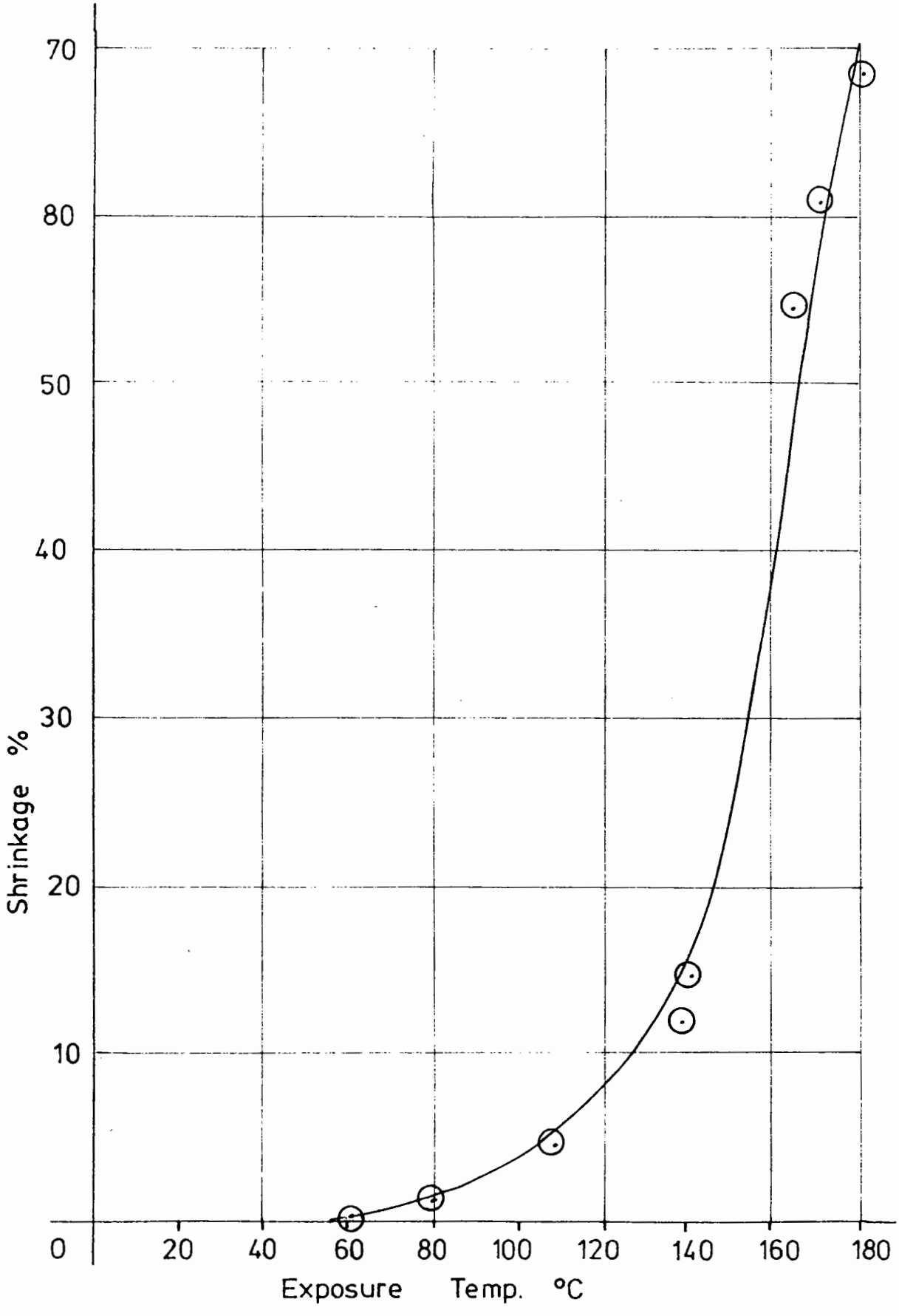

Fig. 4.14 Tensar (AR1) in oil

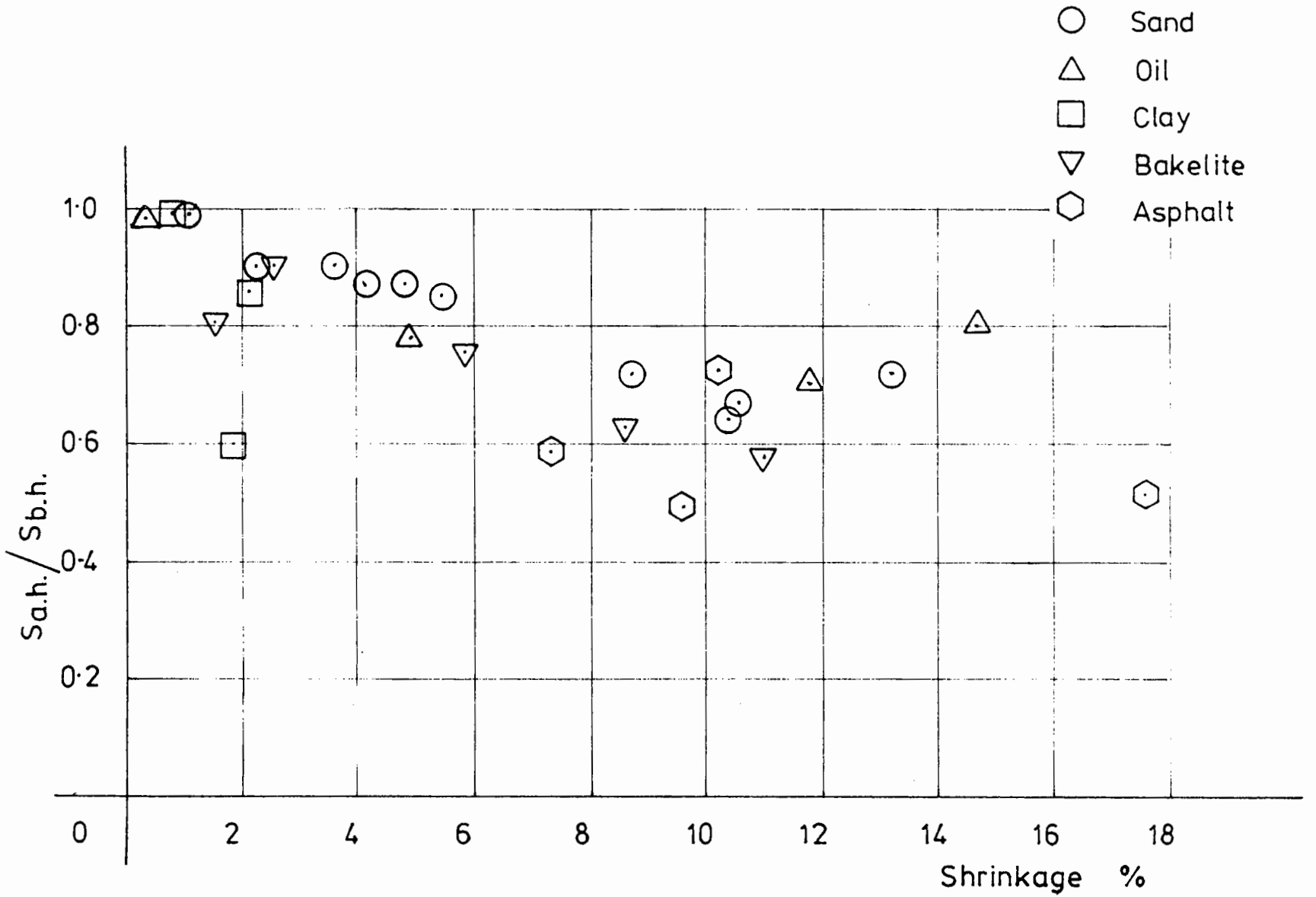

Fig. 4.15 Stiffness change,on heating ,as a function of shrinkage

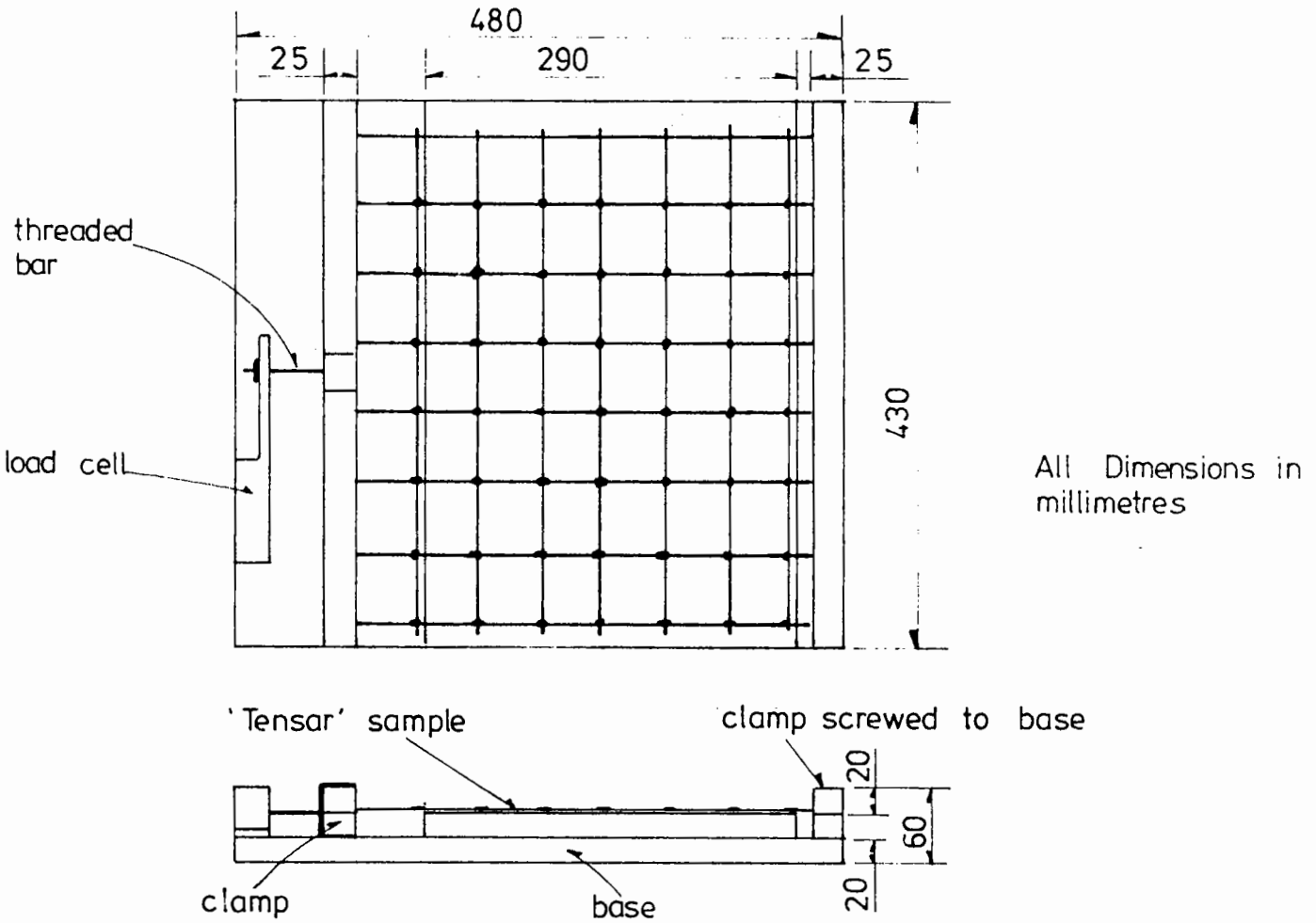

Fig. 4.16 Apparatus to measure shrinkage force

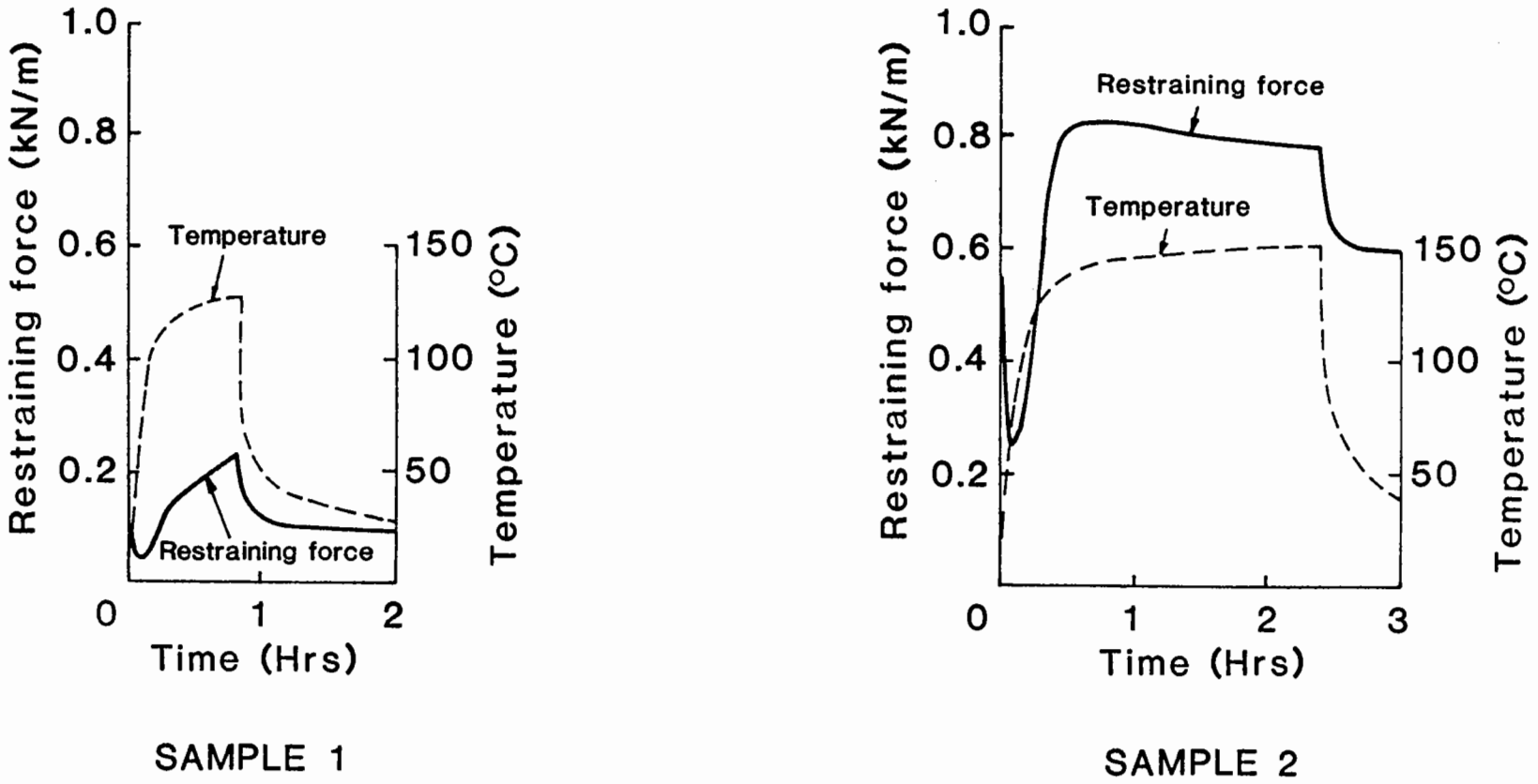

Fig. 4.17 Restraining Force With Temperature Changes in SS3

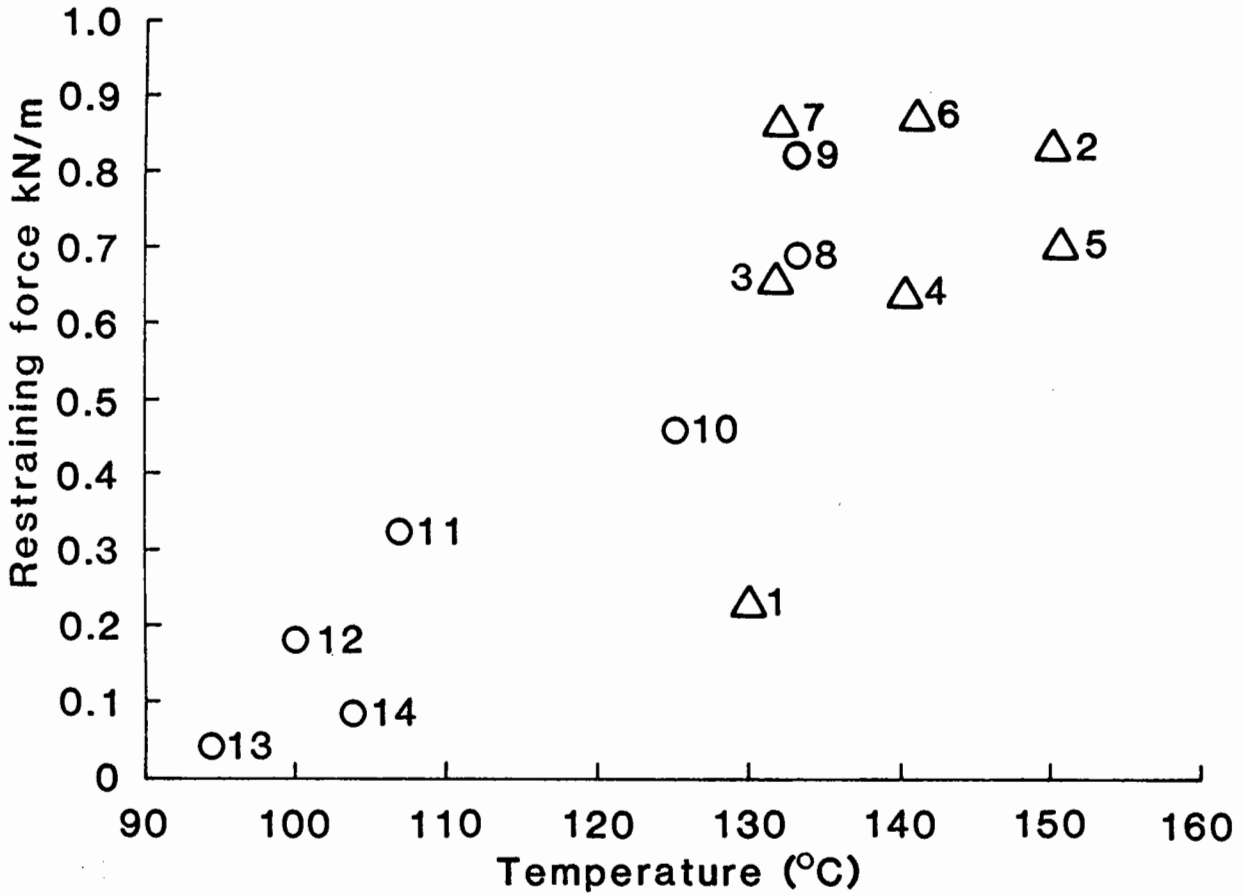

Fig. 4.18 Maximum Restraining Force Against Temperature for SS3

5 REFLECTION CRACKING INVESTIGATION

5.1 INTRODUCTION

A principal cause of premature failure in flexible overlays is reflection cracking. Two laboratory tests were developed to simulate this phenomenon, and to study the effect of including a polymer grid in the overlay.

The first test was developed so that a large number of specimens could be tested quickly and any benefit of including the grid could be readily observed. Asphalt beams, resting on an elastic foundation, were subjected to cyclic loading. A crack was induced in the beams, and the time taken for cracks to propagate in unreinforced and reinforced beams was compared.

The second test was more representative of traffic loading. Asphalt slabs resting on an elastic support, with a stress concentration beneath, were subjected to a load from a rolling wheel in the Slab Testing Facility (S.T.F.). A comparison of the behaviour of reinforced and unreinforced slabs was then made.

The slow opening and closing of concrete joints in an overlayed pavement, caused by diurnal or seasonal variations in temperature are another major cause of reflection cracking. A testing rig was developed at Nottingham to simulate this movement, but owing to lack of time no test results were obtained. A full description of the testing rig is given in Appendix C.

5.2 TESTS ON BEAMS

Because of the simple arrangement of this test the more complicated stress regime at the crack tip which occurs during a load pulse caused by traffic loading could not be simulated. Despite this

limitation the test produced useful data in showing the benefit of including the grid in an asphalt layer.

5.2.1 Experimental arrangement

The tests were conducted on asphalt beams which measured 525mm x 150mm x approximately 100mm deep. The general experimental arrangement is shown in Fig.5.1. The beams were cast onto two high quality plywood sheets 18mm thick, with a 10mm gap between to act as a crack initiator.

This gap simulated an existing crack or joint in a pavement to be overlayed. The spacing was held constant during sample preparation by using a 10mm aluminium spacer which was removed before testing. Carborundum paper was glued to the surfaces of the plywood sheets, and this created a roughened surface to which the asphalt could adhere.

Each test beam rested on a rubber support 25mm thick. A Shore durometer was used to test the resilience of the rubber. A Shore value of 35 was obtained (ASTM ,1980). The Shore durometer measured the force required to push a needle of known dimensions into the surface of a rubber sheet. The rubber provided a resilient support, simulative of the response encountered in a pavement, and allowed the asphalt beam to flex under the applied cyclic load.

Fig. 5.2 shows, schematically, how the horizontal movement across the crack was recorded. An L.V.D.T. with a resolution of 5 microns was held in position by plastic studs glued to the plywood. (During testing no strain was measured in the plywood. This was checked by using a demec gauge between pips glued to each of the plywood sheets). The plastic studs were 70mm apart and since no strain was recorded in the plywood, the movement monitored by the L.V.D.T. was therefore the relative movement between the sheets of

plywood, i.e. across the 10mm gap. This gave an indication of the level of strain level in the asphalt at the onset of testing.

Crack length was monitored visually as the vertical distance from the base of the asphalt layer. The sides of each beam were painted white to facilitate this observation. An average value of crack length was calculated from measurements at each side of the beam throughout the test.

A general view of the experimental arrangement is shown in Fig. 5.3, the beam is set up in the Instron hydraulic testing machine.

5.2.2 Beam preparation

The asphalt mixes were prepared in the laboratory. The total weight of each beam was 16kg and four batches each of 4kg had to be prepared due to the limited capacity of the mixing facilities. The target grading curve for each bituminous mix type was achieved by weighing out individual bin sizes of aggregates which had been pre-sieved. The aggregate was heated to 140^{o}C in an oven, the desired amount of bitumen, also preheated to 140^{o}C, was added to the aggregate in a mixer which was kept at 140^{o}C by an oil jacket. Each 4kg tray of mix was returned to the oven after mixing and all four trays were kept in the oven for 30 minutes to ensure the mix was at the same temperature in each tray.

Beams 1 to 14R, (the beams are numbered in Table 5.1, the appendix R denotes a reinforced beam), were compacted in a steel braced wooden mould which was not preheated before compaction. They were compacted using a static pressure of 1300kPa, provided by a hydraulic ram acting on a rigid steel plate over the mix.

The remaining beams, 15 to 25, were compacted into a preheated rigid steel mould. Compaction was achieved using a Kango hammer with a flat metal sheet (125mm x 125mm x 20mm thick) welded to the bottom

Table 5.1 Asphalt beam descriptions (continued)

Test Series	Beam Number	Asphalt mix type and void content	Type of reinforcement	Position of reinforcement
A	1	H.R.A. 10%	unreinforced	-
	2	"	"	-
	3	"	"	-
	4R	"	Tensar SS3	Base of asphalt
	5R	"	"	"
	6R	"	"	"
	7R	"	"	25mm up from base
	8R	"	"	"
	9R	"	"	"
	10R	"	"	"
	11R	"	"	50mm up from base
	12R	"	"	"
	13R	"	"	"
	14R	"	"	"

Table 5.1 cont. Asphalt beam descriptions

Test Series	Beam Number	Asphalt mix type and void content	Type of reinforcement	Position of reinforcement
B	15*	A.C. 8.5%	unreinforced	-
	16*	"	"	-
	17R**	"	Tensar AR1	base of asphalt layer
	18R**	"	"	"
C	19	H.R.A. 3.2%	unreinforced	-
	20	"	"	-
	21R	"	ICI grid	base of asphalt
	22R	"	"	"
D	23	Asphapol	-	-
	24	"	-	-
	25	"	-	-

* 'chip seal' layer only at base of asphalt

** grid installed using the 'chip seal' method

of a chisel attachment. This more efficient, dynamic form of compaction, meant that these beams had a considerably lower void content than the beams compacted in the previous manner. A smooth surface finish was achieved on these beams by placing a neatly fitting piece of wood onto the top of the mix and vibrating this with the Kango hammer.

The beams were allowed to cool overnight before the mould was removed and the sides painted with a white emulsion.

5.2.3 Test conditions

All the beams were tested under identical conditions of applied stress, frequency of loading, temperature and with the same support conditions.

A sinusoidal load was applied to the specimen through a rubber loading platen (200mm x 150mm) at a frequency of 5Hz. This corresponds to a vehicle speed of approximately 30km/hr (Brown and Brunton 1984(b)). The load was cycled between 1.3 kN and 8.3kN. (For control reasons it was not possible to cycle the load from zero to a peak load). This produced a minimum and maximum contact stress of 43kPa and 275kPa. The load was monitored using the internal load cell of the Instron testing machine and the result displayed on a digital panel meter.

The temperature was held constant at $20^{o}C \pm 1^{o}C$ in the temperature control cabinet erected around the Instron.

5.2.4 Beam and reinforcement details

In all, 25 beams of various mix type and reinforcement detail were tested, the description are summarised in Table 5.1. Four distinct series of tests were conducted: A, B, C and D, each series with either a different mix type or reinforcement detail.

(1) Series A

Beams 1 to 14R were constructed of a typical Hot Rolled Asphalt (H.R.A.), wearing course, designed to BS594, schedule 1A. (BS594, 1973). The mix details are given in Table 5.2. Due to the poor method of compaction the beams had a high air void content, an average of 10%.

The void content of each mix was calculated using the equations shown in Appendix D. The volume of each sample can be obtained by weighing it in air and water.

Series A predates the advent of the "chip seal" method of installation "Tensar SS3" grids were used as the reinforcing element.

The grid was located at three different positions in these asphalt beams, at the base of the asphalt layer, 25mm up from the base, and 50mm up from the base. The width of the beam (150mm) accommodated a layer of grid having three transverse ribs as reinforcement, hence the maximum stiffness was available across the crack.

In the beams 4R,5R and 6R the grid was positioned at the base of the asphalt layer and was set into the roughened plywood surface in the mould prior to the placement and compaction of asphalt. In those beams which had reinforcement within the depth of the beam, 7R to 14R, asphalt was placed and compacted in the mould to the required depth prior to the positioning of the grid, which was then inserted and the remaining asphalt compacted on top.

(2) Series B

Beams 15 to 18R were constructed from a continuously graded asphaltic concrete, the details of which are given in Table 5.3. The average void content in this case was 8.9%.

In tests 17R and 18R the grid was installed on top of the

Table 5.2 Hot rolled asphalt wearing course: typical mix detail.

Schedule 1A BS594

Sieve Size (mm)	% Passing	
20	100	granite
14	82	
10	77	
5	65	
2.360	58	sand
0.600	56	
0.212	31	
0.075	9	filler
Dust	0	

Specific gravity of granite aggregate 2.81
Specific gravity of sand 2.65
Specific gravity of filler 2.82
7.9% of 50 pen bitumen

Table 5.3 Details of asphaltic concrete

Sieve Size (mm)	% Passing
12	100
10	87
5	62
2.36	40
1.18	27
.600	18
.300	12
.150	7
.75	4
Dust	0

14mm granite aggregate
Specific gravity of aggregate 2.81
5.5% of 100 pen bitumen.

roughened plywood sheets using the "chip seal" method. The chip seal was also applied to the plywood sheets in the unreinforced beams, 15 and 16, to eliminate any beneficial effects it may have had, and isolate the effect of the grid. The preheated 100pen bitumen used in the "chip seal method" of installation was applied from a hot can, fitted with a spreader bar. The bitumen was then quickly hand dressed with 6.3mm granite chippings. After the bitumen had cooled the excess chippings were removed using a suction device.

(3) Series C

The bituminous mix in this instance was in similar to the H.R.A. wearing course used in Series A, except that due to the greater compactive effort imparted during construction an average lower void content of 3.2% was obtained.

The reinforcing element used in beams 21R and 22R was an open meshed, woven grid with metal fibres interwoven into the fabric. The resilient modulus of the grid was 1.23 KN/m. The tests were conducted at a mean strain up to 1%, a cyclic strain of approximately 0.3% and temperature of $24^{o}C \pm 1^{o}C$. The ultimate strength of the grid was 8.7 kN/m, at a strain rate of 2% strain/min and temperature of $24^{o}C \pm 1^{o}C$.

The grid was positioned at the base of the asphalt layer.

(4) Series D

Beams 23 to 25 were constructed from an Asphapol cushion course. This is a polymer modified asphalt which comprises of mineral fillers, polymer additives and bitumen. The modified bitumen is produced with the intention of inhibiting or delaying cracking in bituminous overlays over joints or cracks. No reinforcement was included in these beams. The air void content was estimated to be less than 1%.

5.2.5 Results

5.2.5.1 Series A

Fig. 5.4 shows the average crack lengths plotted against the number of load cycles for the three unreinforced beams 1 to 3 and the beams reinforced at the base of the asphalt layer, 4R to 5R. While, in the unreinforced case, cracks propagated to a depth of over 70mm within approximately 200,000 cycles, no cracking was evident in any of the three reinforced beams, which were tested up to a maximum of 218,000 cycles. This dramatic effect is illustrated visually on Fig. 5.5. A severe crack can be seen, through the unreinforced beam Fig. 5.5(a), with a crack width at the base of 2mm - 3mm, whereas no cracking is visible in the reinforced beam Fig. 5.5(b).

Figs. 5.6 and 5.7 show how cracking developed in those H.R.A. beams reinforced 25mm and 50mm from the base of the asphalt layer, respectively. Surprisingly, in this case the beams reinforced at mid depth (50mm) inhibited cracking to a slightly greater extent that those beams reinforced 25mm from the base. Fig. 5.8 represents visually two typical beams from each of these tests. It is significant to note the reduction in the severity of crack when compared to an unreinforced beam Fig. 5.5 (a). A tendency for these hairline cracks to heal after testing, this was noticed and this was not apparent in unreinforced beams.

The results from all of these tests are brought together in Fig. 5.9, which shows the propagation of cracks for unreinforced beams, beams reinforced within the asphalt layer, and beams unreinforced at the base of the asphalt layer. The best fit line drawn through the data in Fig. 5.9 shows that hairline cracking in beams reinforced within the asphalt layer took three times as long to propagate as those that were unreinforced.

5.2.5.2 Series B

Fig 5.10 presents the average crack length against number of load cycles for beams 15 to 18R, i.e. the asphaltic concrete beams. Again those beams reinforced at the base of the asphalt layer (17R and 18R) showed no signs of cracking up to 1,000,000 repetitions of load cycles, while beams 15 and 16 cracked to a depth of approximately 80mm after 720,000 cycles and 415,000 cycles respectively. Fig. 5.11 shows photographs taken of a typical beam for each case, at the end of testing.

5.2.5.2 Series C

Fig. 5.12 presents the crack length versus number of cycles for beams 19 to 22R. These beams were constructed from a well compacted H.R.A. wearing course, and beams 21R and 22R were reinforced with the low modulus ICI grid at the base of the asphalt layer. The grid inhibited crack growth in the asphalt beams although cracks did propagate up to a depth of 20mm after 500,000 load cycles, unlike those beams reinforced with Tensar grid at the base, which showed no sign of cracking. The unreinforced beams 19 and 20 cracked to a maximum depth of 44mm after 500,000 cycles.

The lower void content in these unreinforced beams compared to beams 1,2,3 also a H.R.A. wearing course, show how this affects cracking. Reducing the void content reduced the mix susceptibility to cracking. (Compare Fig. 5.12 with 5.4)

5.2.5.4 Series D

Beams 23,24 and 25 were constructed of asphapol, a polymer modified bitumen. After 500,000 load cycles they cracked to a depth of approximately 26mm, Fig 5.13. This is an improvement over the normal H.R.A. wearing course, Fig. 5.12. which at the same number of cycles had cracked to 44mm.

5.2.6 Measurement of horizontal movement across gap

The horizontal movement across the 10mm gap in the plywood sheets was recorded during loading for beams 1 to 14R, Series A, using the method illustrated in Fig 5.2. The results are presented in Fig. 5.14. A distinction is made between beams reinforced at various positions within the layer. Initially, at the start of testing, this resilient movement across the gap was approximately the same for each beam, 45μm. Assuming this movement was transmitted to the asphalt immediately over the 10mm crack, and also assuming no debonding between the asphalt and the carborundum paper, a repeated strain of approximately 0.45% would have developed in the asphalt. At this extremely high level of strain the asphalt would crack after several load applications.

5.2.7 Discussion on beam tests

To inhibit or reduce the propagation of reflection cracks in an asphalt overlay the overlay must be capable of either absorbing the high levels of strain or reducing the strain by debonding from the underlying layer, thereby increasing the gauge length over which the movement must be taken up. During testing it was noticed that some debonding occured in those beams reinforced at the base of the asphalt layer with the polymer grid. This coupled with the strong tensile element of the grid at the base of the asphalt, prevented any concentrated values of strain from occuring above the gap.

The grid also prevented any build up of permanent strain in the asphalt beams. This can be seen from the cracks which developed in beams reinforced with the asphalt layer Fig. 5.8, compared to the crack severity of unreinforced beams, shown in Figs 5.5(a). The crack width at the base of the unreinforced beams was between 2-3mm.

From extensive research on the fatigue life of bituminous

materials at Nottingham (Pell and Cooper 1984, Cooper and Pell 1974, Brown and Brunton (b) 1984) predictive methods have been produced based on the material properties of each mix. If the level of tensile strain at the base of an asphalt layer, and the type and volume of binder used is known, the fatigue life of an asphalt pavement may be predicted from either the Nomograph or equations shown on Fig. 5.15.

The H.R.A. wearing course used in test series A had a binder volume of 16.6% and an initial softening point of 53.6^{o}C. As the level of tensile strain decreases the fatigue life increases in general. In the reflection crack beam test the level of strain may have been reduced by debonding. (i.e. the initial movement across the plywood gap may have been distributed over 10mm or a greater length). Fig. 5.16 shows the effect of increasing the gauge length over which this opening and closing movement must be taken up. The theoretical increase in the number of cycles to failure increases significantly as the debonded length increases. This serves to illustrate the principle that debonding over the crack would increase the time taken for a crack to reflect through an overlay.

5.3 TESTS ON SLABS

A rolling wheel moving over a pavement which is partially cracked induces a complicated stress pulse at the crack tip or joint as shown in Fig. 5.17. As the wheel approaches the joint, maximum differential movement occurs across the slab generating high shearing stresses above it. As the wheel passes directly over the joint maximum tensile stress occurs over the crack tip. Under certain loading conditions it may be possible for compressive forces to exist above the crack tip.

This stress regime was duplicated in the laboratory by using the

Slab Testing Facility (S.T.F.), a detailed description of which is included in Appendix E. Fig 5.18 shows the S.T.F. in operation.

These tests were an extension of the reflection cracking tests carried out on asphalt beams. The tests on the beams could not simulate the shearing stress exhibited over the crack tip as the wheel approached the joint and hence the S.T.F. represents a considerable improvement.

Three pairs of slabs were tested, each pair included one reinforced with "Tensar" AR1 and one unreinforced. Two types of bituminous mix were used, a typical hot rolled asphalt (H.R.A.) wearing course in pair 1 and 2 and an asphaltic concrete in slab 3. The appendix R denotes a reinforced slab.

5.3.1 Experimental arrangement

The experimental arrangement enabled a wheel to be moved over an asphalt slab at a known load and speed. The asphalt slabs were cast on to a pair of plywood boards with a 10mm gap between them which acted as a crack initiator. This arrangement rested on a rubber base on a steel pallet. Fig. 5.19 shows the arrangement.

The resilient support was provided by a 25mm thick layer of shot blasted rubber which had a Shore hardness of 35. Some care had to be taken to achieve a uniform resilient response across the pallet as earlier tests had shown that high flexibility produced increased deformation in the slab.

The box section, provided at either end of the rubber support, was only included in the latter two pairs of slabs tested. Fig. 5.20 shows the effect of including the box section on the behaviour of the slab. The first slab pair tested cracked from the top down due to a hogging moment produced as the wheel moved on to the slab surface. As a consequence, the reinforcement which was positioned at the base

of the slab, could play little part in inhibiting the crack growth. The box section provided for the other slabs tested meant that hogging was prevented and the slab could only bend to give tension on the bottom face.

The wheel speed over the slab was 3 km/hr in all tests. The wheel load was maintained at 2.8kN for pair 1/1R and 2/2R but was increased to 4kN for the thicker pair, 3/3R. Due to uneveness of the slab surface and a slow response of the load feedback in the system, the load profile, although identical for each pass, was not constant over the slab. The plan of the slab shown in Fig. 5.21 shows the position of measurements taken during the test. The rut profile was measured relative to a cross beam which stood independent of the slab, (Fig. 5.21(b)) at three different positions. Permanent deformation across the plywood gap was recorded by glueing two Demec pips to the plywood at each side of the gap. Transverse deformation of the slab surface was recorded using Demec pips glued to the surface of the slab. Cracking was monitored visually throughout the test and failure was easily identified when the slab cracked completely or "hinged".

5.3.2 Slab preparation and details

The slab pairs were cast into a rectangular box section mould Fig. 5.22, and compacted together so as to obtain identical mix properties and thicknesses. Following delivery of the hot asphalt, it was manually placed in a steel mould using shovels and rakes, Fig. 5.23. The construction detail of a slab is shown in Fig. 5.24.

In the reinforced slab, the grid was bonded to the plywood base with a chip seal layer. A chip seal layer was also included in the unreinforced slab so as to isolate the effect of the grid. The grid bonded easily to the plywood and few problems were encountered during

this process. The 100 pen bitumen was spread with a metal watering can which had a spreader bar attached to the spout. This ensured an even spread of bitumen.

The grid was orientated with the longitudinal direction across the gap. A small vibrating roller was used to compact the mix. Initial passes were without vibration. On cooling, the mould was removed and the slabs separated using a Kango hammer. Each individual slab was 1.22m long and 0.86m wide. The two plywood sheets onto which the slabs were cast were held in position during construction by screwing them to a plywood base. The 10mm gap between sheets, was filled with a rectangular steel bar to prevent ingress of asphalt during laying and compaction. The metal bar was removed from slab pair 1/1R during testing but was not removed from slab pairs 2/2R and 3/3R as it caused unnecessary disturbance to the slab and had no effect on cracking when left in place.

When slabs were ready to test, the plywood base was removed, and the slabs together with the plywood "crack initiator" base, were then placed onto the rubber support on the steel pallet.

Slab pairs 1/1R and 2/2R were made using a typical hot rolled asphalt wearing course. The mix was cored and analysed after testing and details are shown in Table 5.4. Slabs 1/1R were 40-50mm thick and Slab 2/2R 50-60mm thick.

Slab pair 3/3R was constructed of a continuously graded asphaltic concrete, the details of which are given in Table 5.5. The thickness of this slab varied between 95mm and 105mm.

5.3.3 Results

Due to the unusual loading conditions (i.e. hogging moments induced) in Slab pair 1/1R, cracking was initiated at the surface of the slab, and since the grid was at the base of the layer it was of

Table 5.4 Details of hot rolled asphalt wearing course

Sieve Size (mm)	% Passing
14	100
10	85
5	70
2	67
.600	65
.212	28
.075	10
Dust	0

Binder content 7.4% (50 pen)
Void content 5%

Table 5.5 Details of asphaltic concrete used in slab and pavement test facility

Sieve Size (mm)	% Passing
20	100
14	99
10	82
5	56
2	29
0.600	12
0.212	6
0.075	3
Dust	0

Binder content 5.0% (100 pen)
Void content 7.8%

limited value in inhibiting cracking. Table 5.6 describes the development of cracking in the slab. Despite the positioning of the grid, an increase in the number of passes to failure was realised. For the unreinforced case, cracking began at 2,000 passes and failure occured at 15,000 passes. The failure condition was recognised by the onset of hinging in the slab, (when the slab was cracked through a hinge formed over the crack). In the reinforced case, (Slab 1R), cracking was not observed until 20,000 passes and failure did not occur until 40,000, a prolongation in life of 2.6 times.

The progress of cracking in slab pair 2/2R is summarised in Table 5.7. Cracking was first noticed in the uninreinforced slab at 15,000 passes and failure was judged to have occurred by 30,000 passes. No cracking was visible after 100,000 passes, so testing was discontinued at this point.

Cracking was first noticed in the unreinforced slab 3 at 25,000 passes and the slab had cracked completely by 40,000 passes as shown in Table 5.8. In the reinforced slab 3R, no cracking was visible at 100,000 passes when the testing was discontinued.

The rut depth was monitored throughout the testing on all the slabs and no significant difference was noticed between reinforced and unreinforced slabs. The magnitude of deformation was however small, a maximum of 5mm in slab 3, but it appeared that the grid had little or no effect when positioned at the base of the asphalt layer. Transverse deformation across the rut was monitored by Demec pips glued to the surface of the asphalt. No significant difference between reinforced and unreinforced slabs was observed, the deformation being in the order of 2-3mm for both reinforced and unreinforced slabs at the end of testing. The permanent deformation as monitored by the Demec pips glued to the plywood either side of the 10mm gap is shown in Fig 5.25. In every case the plywood moved

Table 5.6 Summary of cracking from slab pair 1,1R

No of passes	Slab 1	Slab 1R (reinforced)
2,000	Faint cracks on surface in wheel path	No cracks
4,500	Faint cracks extending totally across slab	" "
13,000	Severely cracked across top	" "
15,000	Slab cracked completely, hinging occuring	" "
20,000		Faint cracks on surface
27,000		Cracks extended across slab
40,000		Slab cracked completely - hinging occuring

Table 5.7 Summary of cracking data from slab pair 2, 2R

No of passes	Slab 2	Slab 2R (reinforced)
15,000	Faint cracks at edge of slab	
20,000	Cracks rising from gap visible at edges of beam	
25,000	Faint cracks on surface of slab in wheel path	
30,000	Obvious cracks through slab, hinging occuring	
100,000		No visible cracking

Table 5.8 Summary of cracking data from slab pair 3, 3R

No of passes	Slab 3	Slab 3R (reinforced)
25,000	Cracks rising from gap visible at edges of beam	
35,000	Faint cracks on top surface of slab across centre	
40,000	Cracked completely, hinging occuring	
100,000		No visible cracking

apart during testing a significant amount in the unreinforced slabs compared to the reinforced slabs. The grid had the effect therefore of controlling permanent strain at the crack during testing.

5.3.4 Discussion

In each test, the potential of the polymer grid to inhibit cracking through an asphalt layer has been observed. Although the grid was positioned away from the surface of crack initiation in slab pair 1/1R the number of passes to failure was significantly increased in the reinforced case.

In slab pairs 2/2R and 3/3R the reinforcement did not allow cracking to initiate. In both the reinforced slabs debonding was noticed between the surface of the plywood and the asphalt layer, allowing movement of the plywood but controlling the tensile strain in the asphalt layer. The length over which the debonding took place was difficult to estimate but may have been about 50mm either side of the gap. If this was the case the average level of transient strain experienced in the asphalt over the joint would be reduced by a factor of about eleven, i.e. transient deformation would be acting over 110mm as opposed to 10mm.

It was observed that cracking was initiated in each of the unreinforced slabs at approximately the same magnitude of permanent deformation across the 10mm gap. For slabs 1, 2, and 3 cracking was first noticed at 2,000, 15,000 and 25,000 respectively, when the level of permanent deformation in each case was between 1.0mm and 1.25mm. (See Fig 5.25.) The permanent deformation did not reach this level in any of the reinforced slabs. Under traffic loading in a pavement having cracks or joints in an underlying base, the development of longitudinal permanent deformation is less likely to occur. Although the mechanism of crack growth may be different, the

debonding effect of the grid at either side of the joint will still inhibit cracking and maintain the integrity of the asphalt layer.

Longer term deformations due to opening and closing of the joint are likely because of temperature variations in the underlying pavement. In this case, the grid should again be beneficial in holding the asphalt layer together, either through aiding debonding over the joint, or reinforcing the asphalt by reducing the extent of movement of the underlying pavement.

Permanent deformation of the asphalt noticed by monitoring the rut profile and transverse movement, was not significantly affected by the inclusion of the grid. The grid was positioned at the base of the layer immediately on top of the rigid, non deformable, plywood. Permanent strains which caused rutting must have taken place nearer the surface of the slab, as shown in Fig. 5.26, and the grid would, therefore, have had little influence.

5.4 CONCLUSIONS

The most salient feature of the complete series of reflection cracking tests conducted on beams was the ability of the polymer grid to prevent completely the propagation of cracks through the asphalt when positioned at the base of asphalt layer. This was the case in all of those beams reinforced with "Tensar" grid. Debonding was noticed at the asphalt/plywood interface and this coupled with the strong tensile element prevented any cracks forming, or any permanent deformation at this interface which would cause crack growth.

When the grid was included within the asphalt layer the severity of crack was greatly reduced as the grid again inhibited permanent deformation. Those beams reinforced within the asphalt layer had on average a three fold increase in life compared to the unreinforced beams.

The denser mixes (i.e. high binder volume) were more resistant to cracking, as expected. The well compacted H.R.A. wearing course in test series C cracked to a lesser extent than the H.R.A. wearing course in test series A.

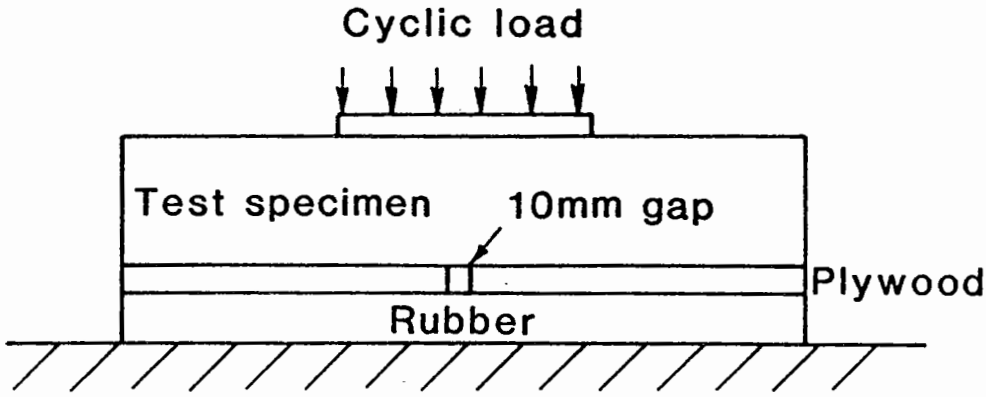

Fig. 5.1 General Experimental Arrangement of Reflection Cracking Test

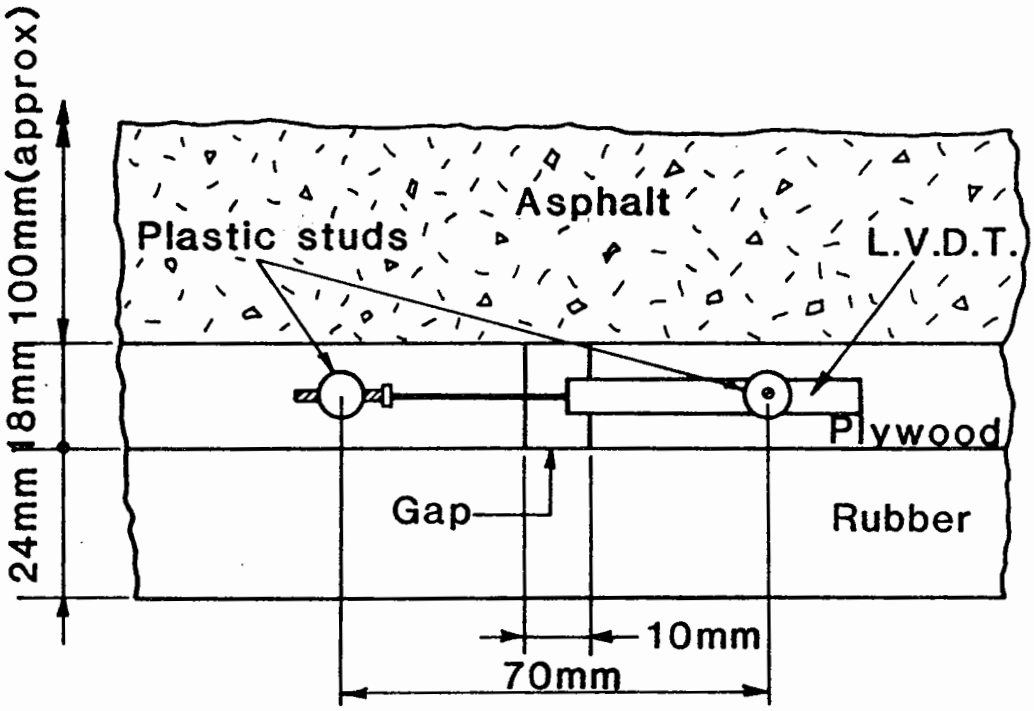

Fig. 5.2 Detail of Crack Initiator

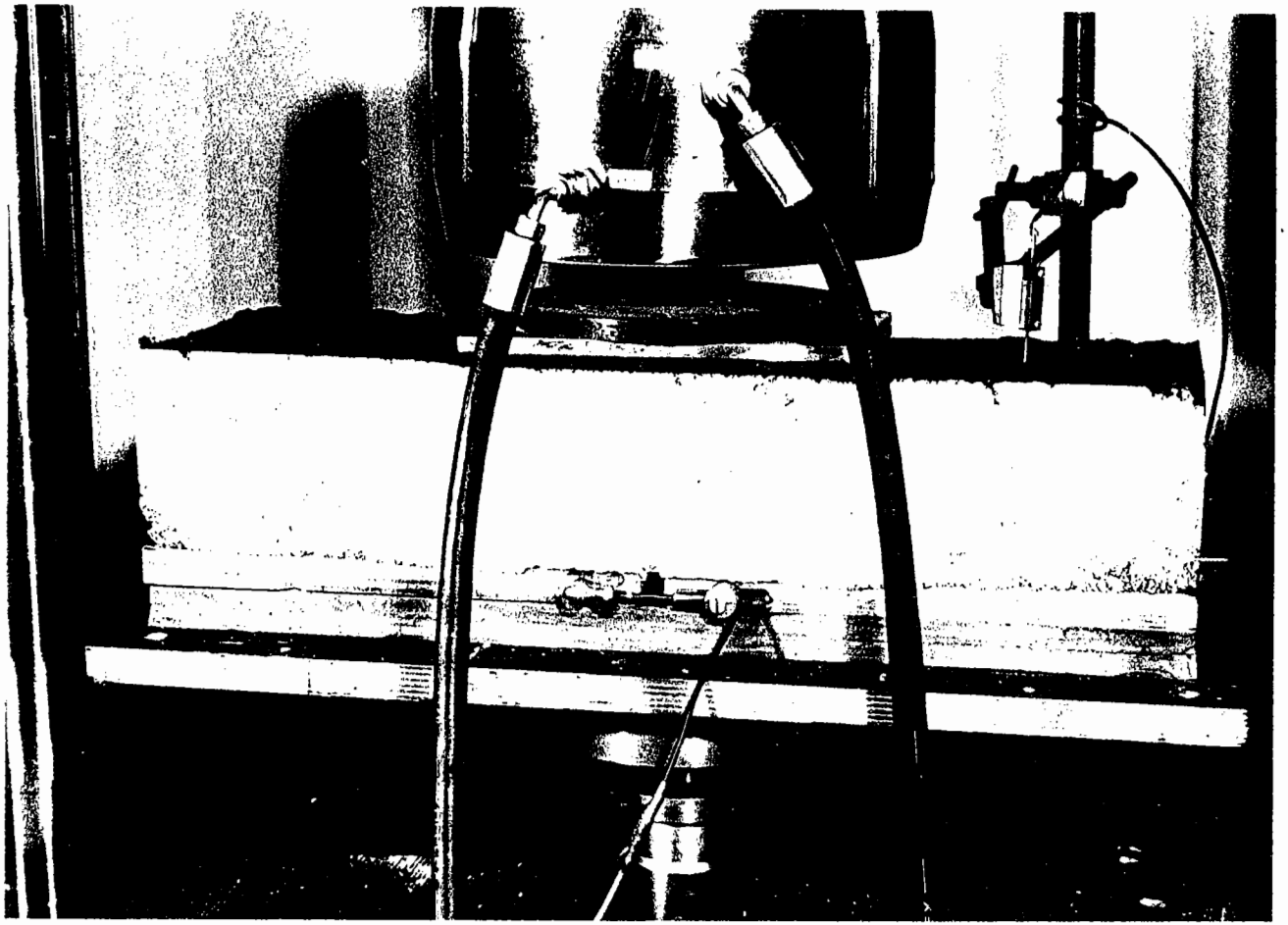

Fig 5.3 A general view of the reflection cracking beam test

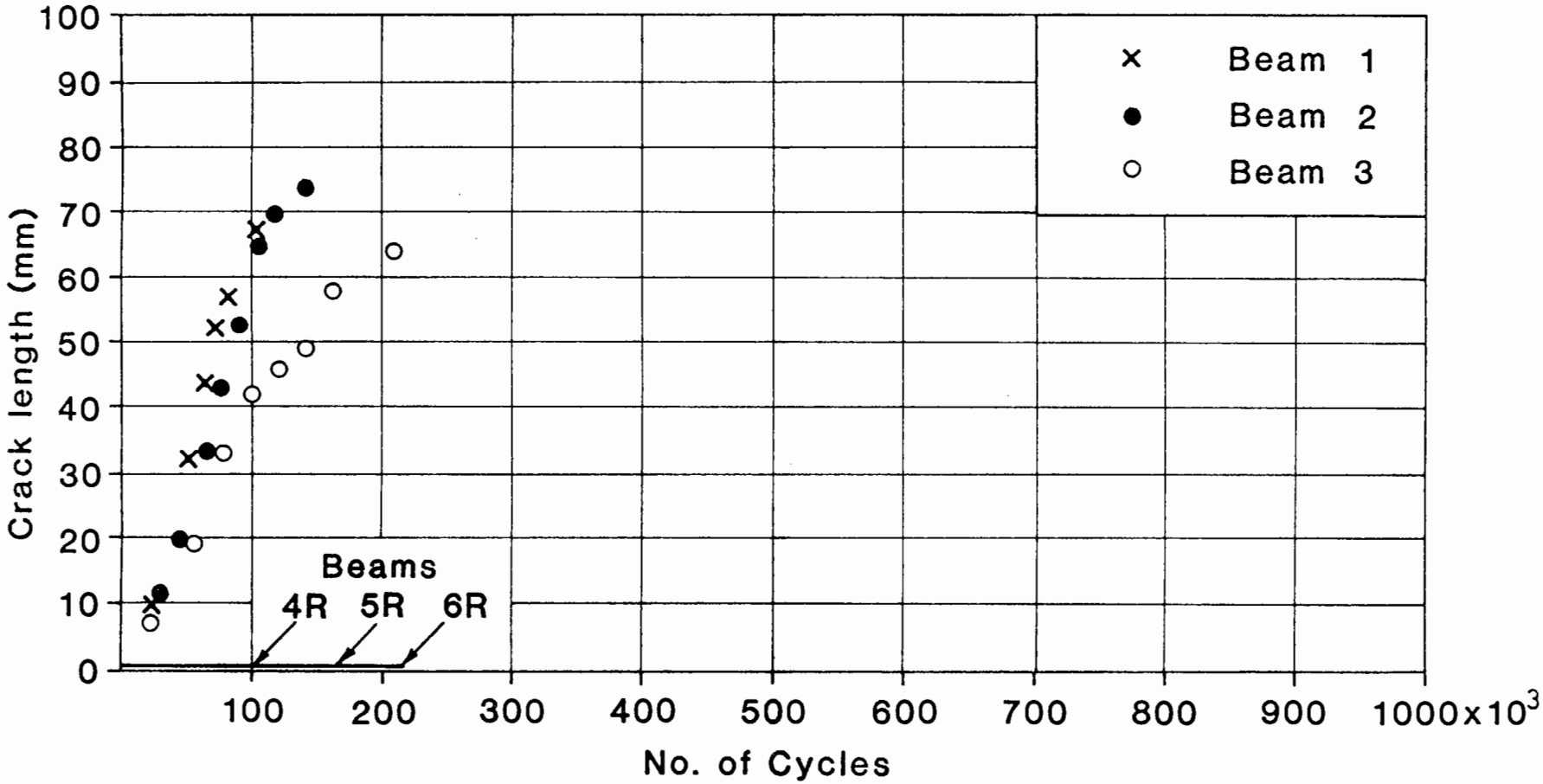

Fig. 5.4 Crack lengths for Unreinforced Beams and Beams Reinforced at Base of Asphalt Layer(H.R.A.)

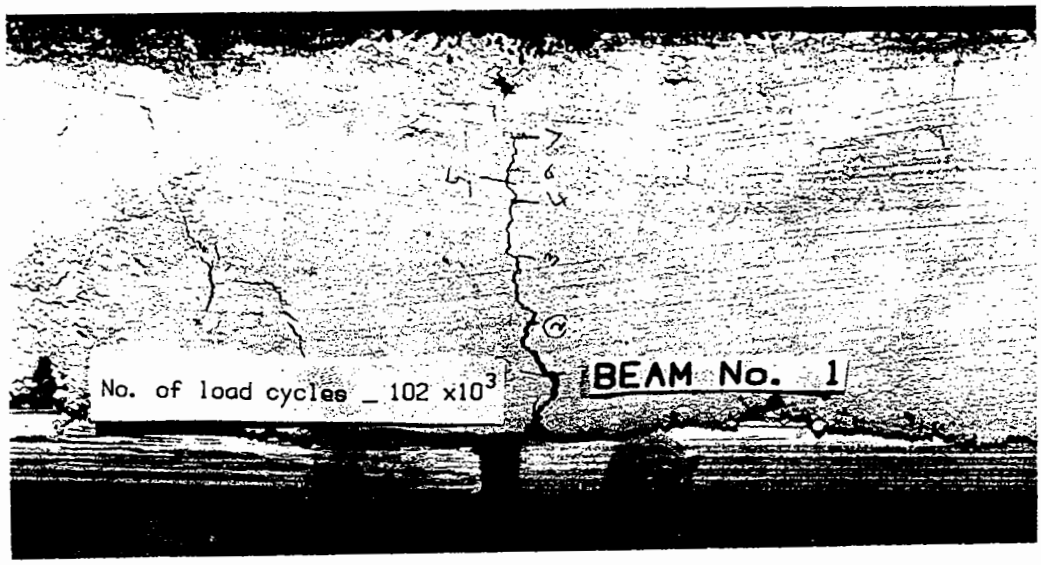

(a) unreinforced

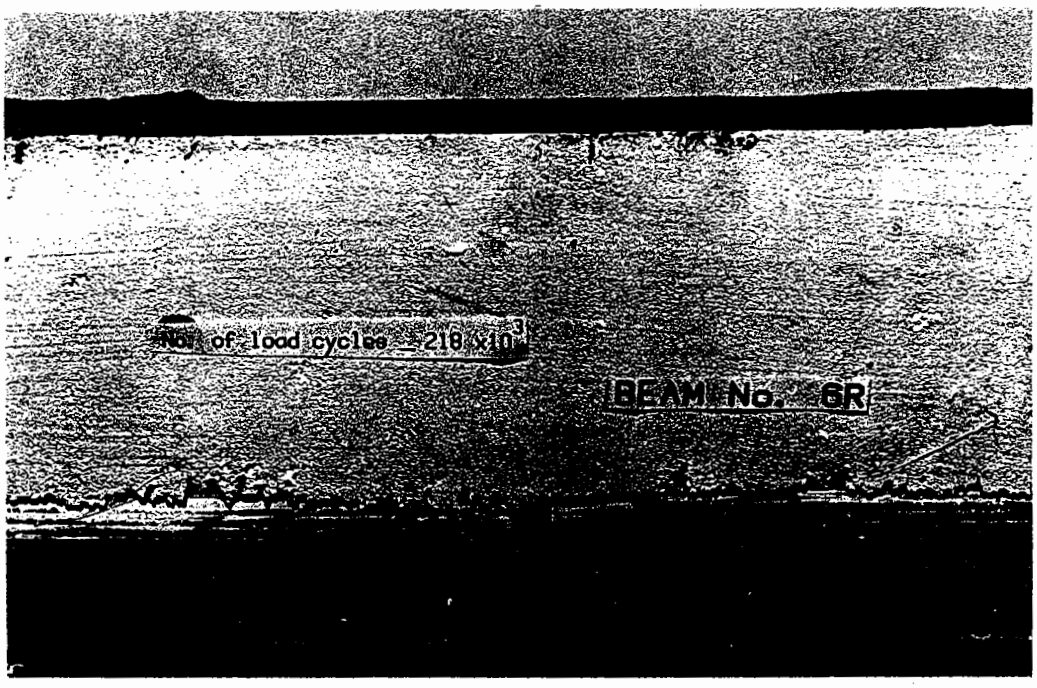

(b) reinforced at base of asphalt layer

Fig 5.5 H.R.A. beams reinforced & unreinforced

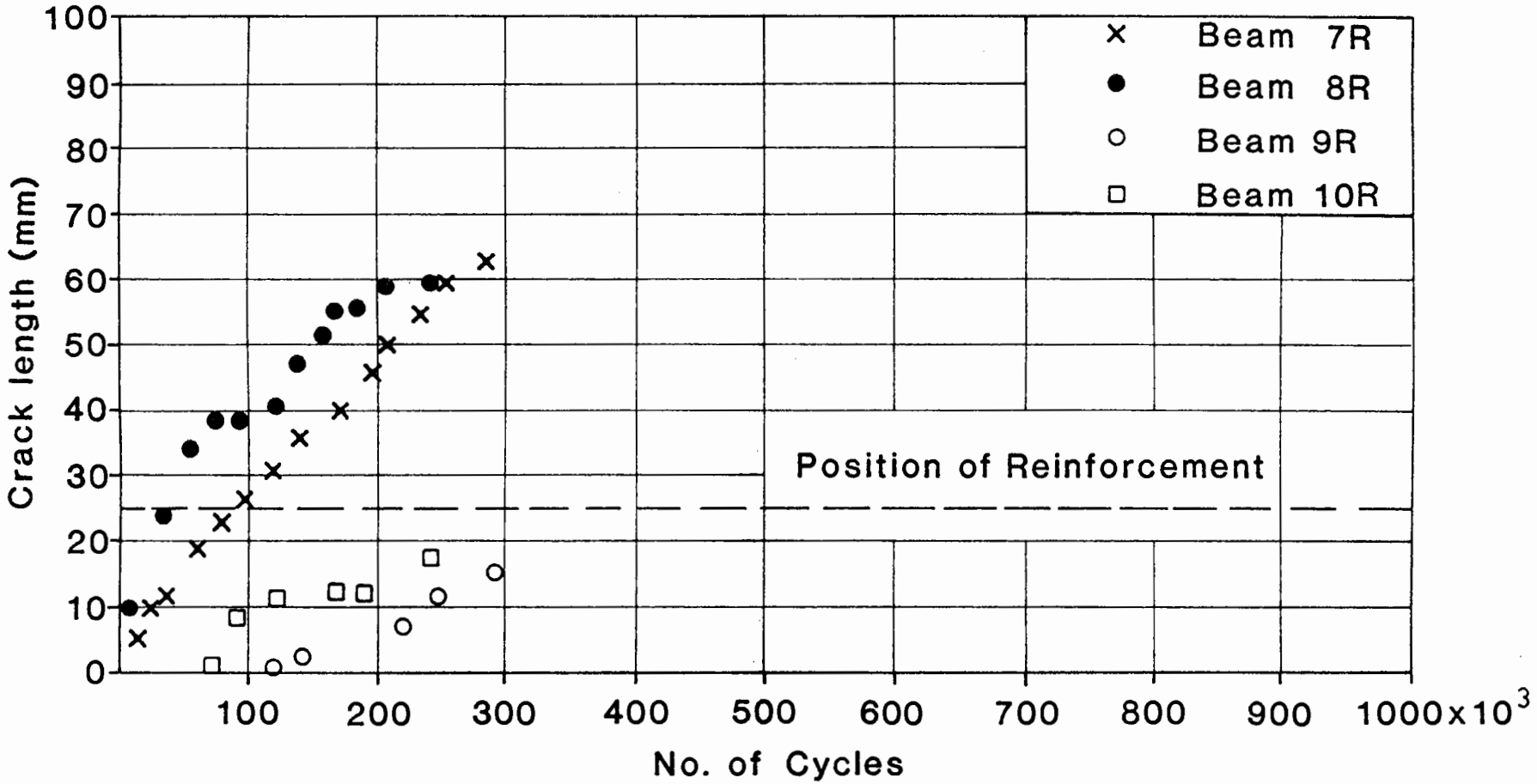

Fig. 5.6 Crack length for Beams Reinforced 25mm from Asphalt Base (H.R.A.)

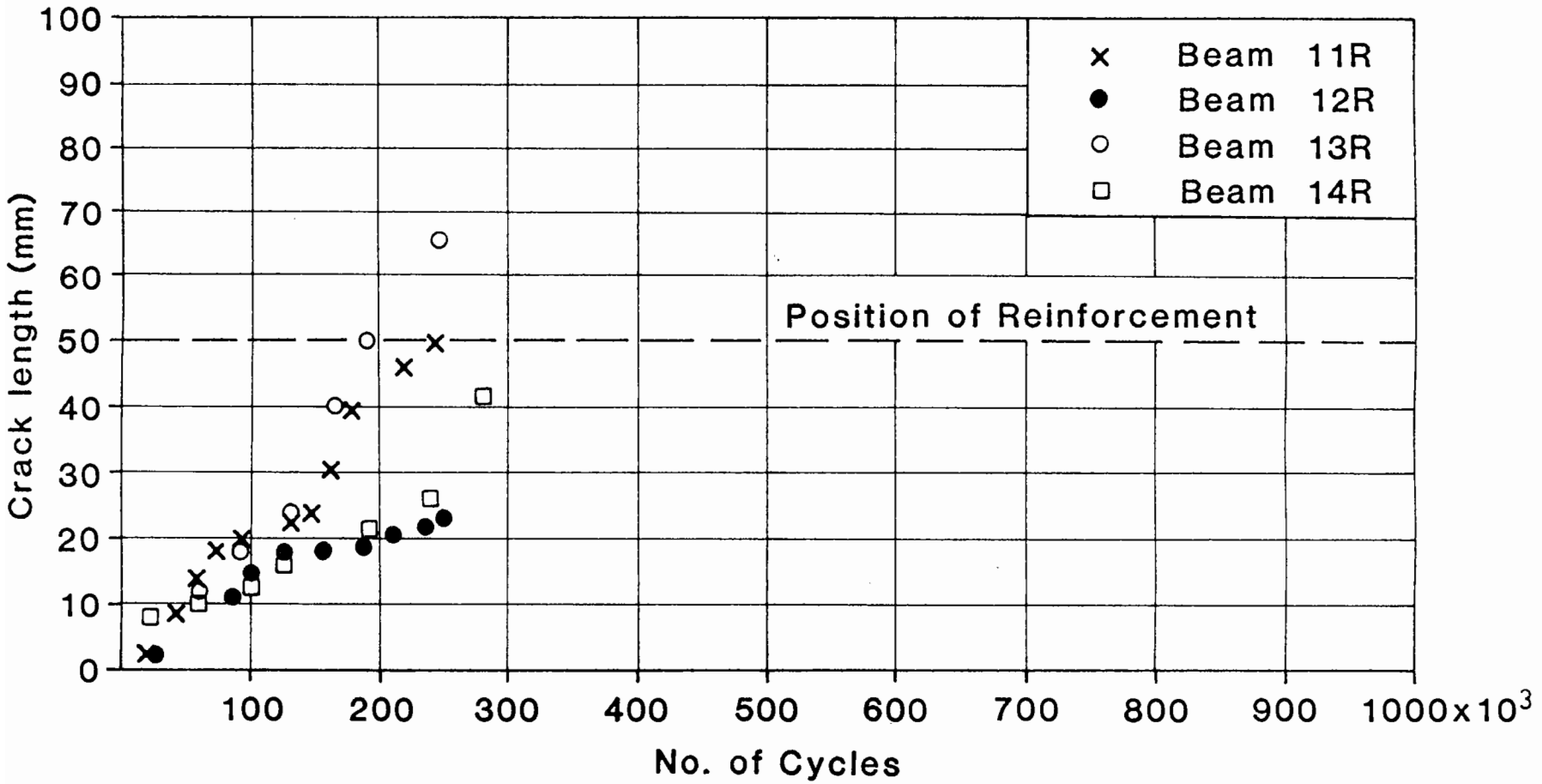

Fig. 5.7 Crack Lengths for Beams Reinforced 50mm from Asphalt Base (H.R.A.)

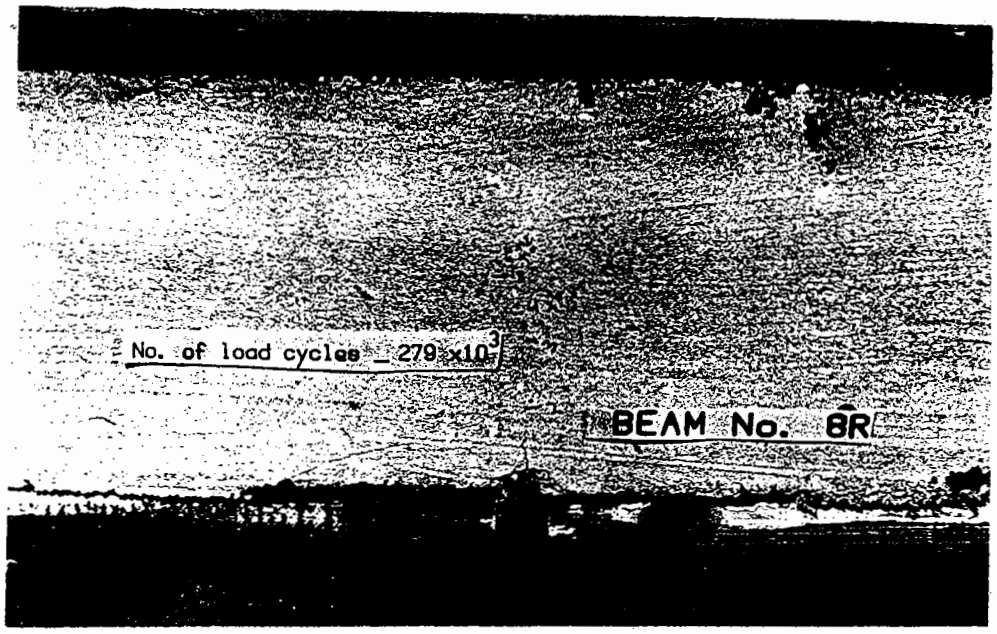

(a) reinforced 25mm from base of asphalt

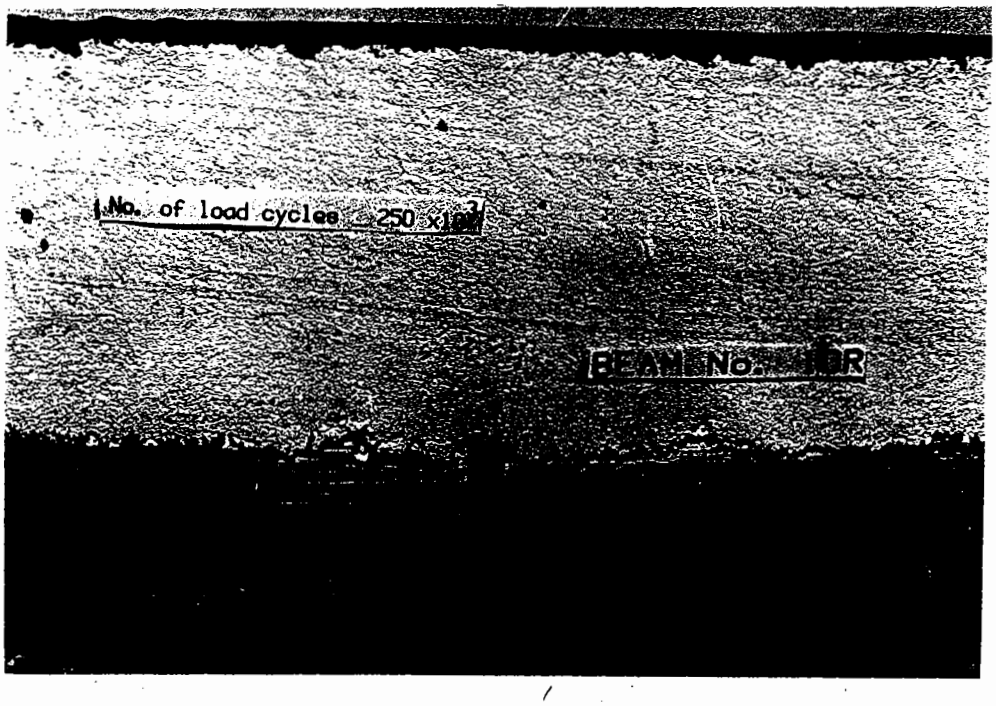

(b) reinforced 50mm from base of asphalt

Fig 5.8 Reinforced H.R.A. beams

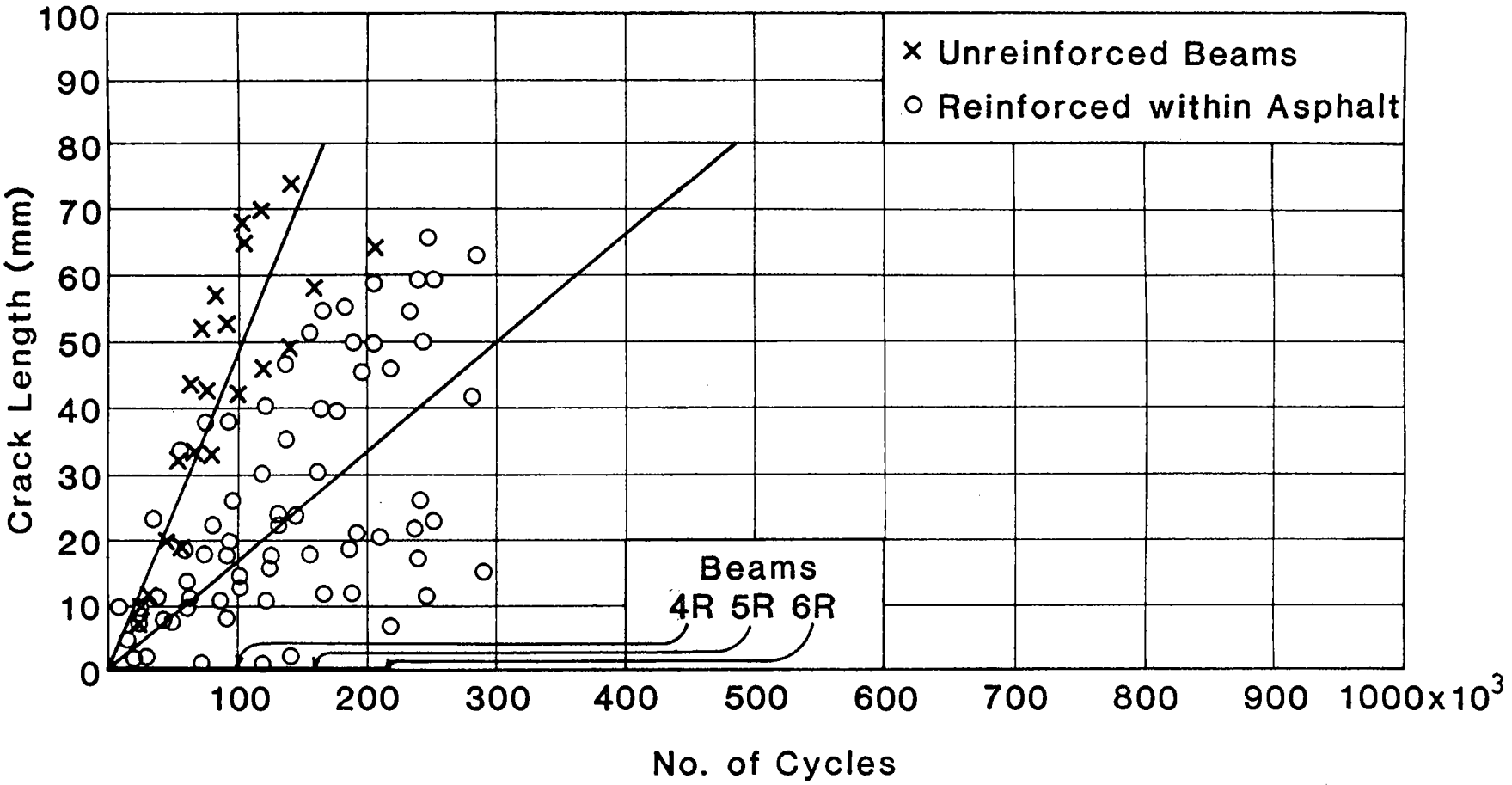

Fig. 5.9 Crack Lengths for H.R.A. Beams 1 to 14R

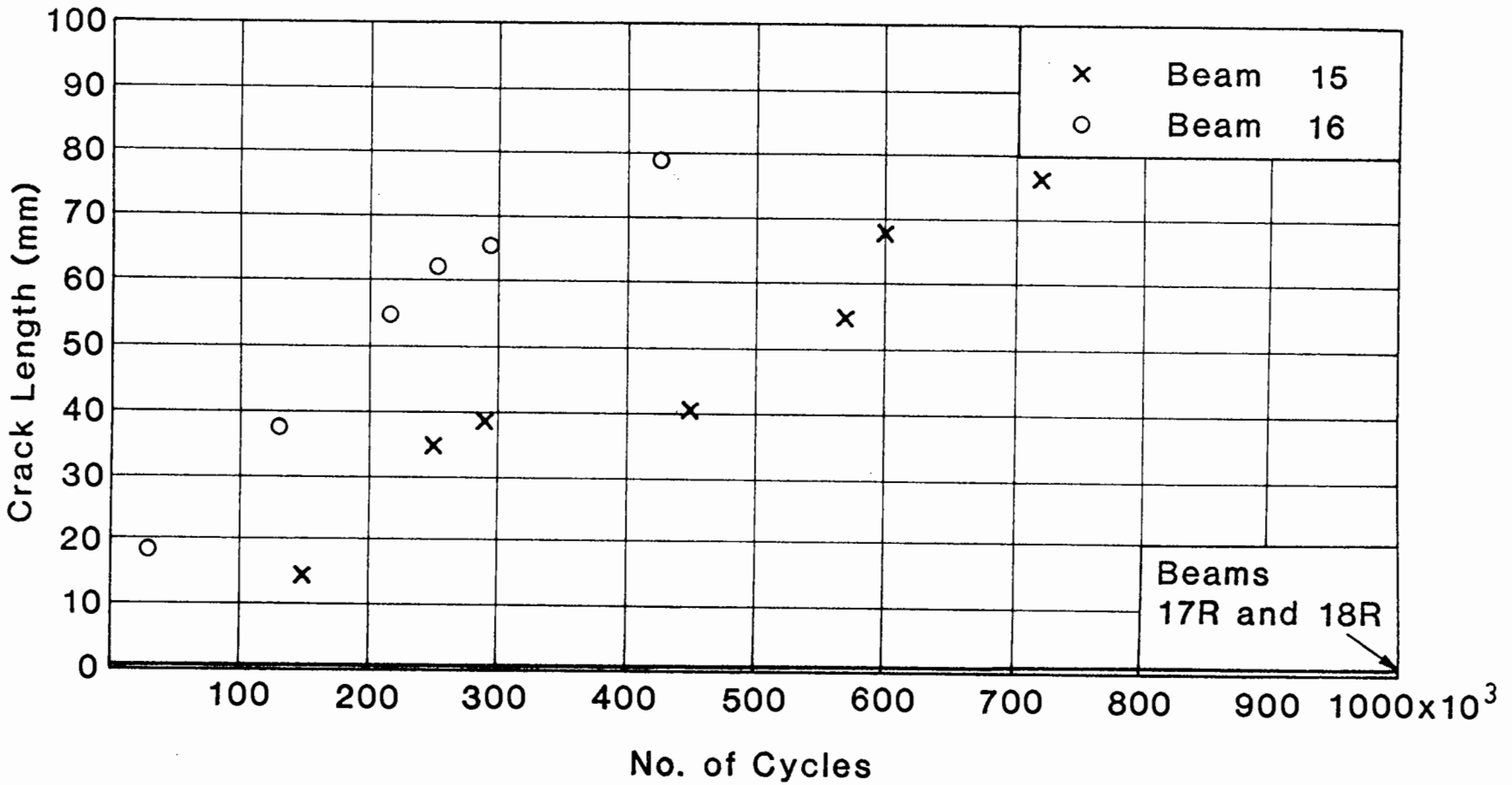

Fig.5.10 Crack Lengths for Unreinforced Beams and Beams Reinforced at Base of Asphalt Layer (A.C.)

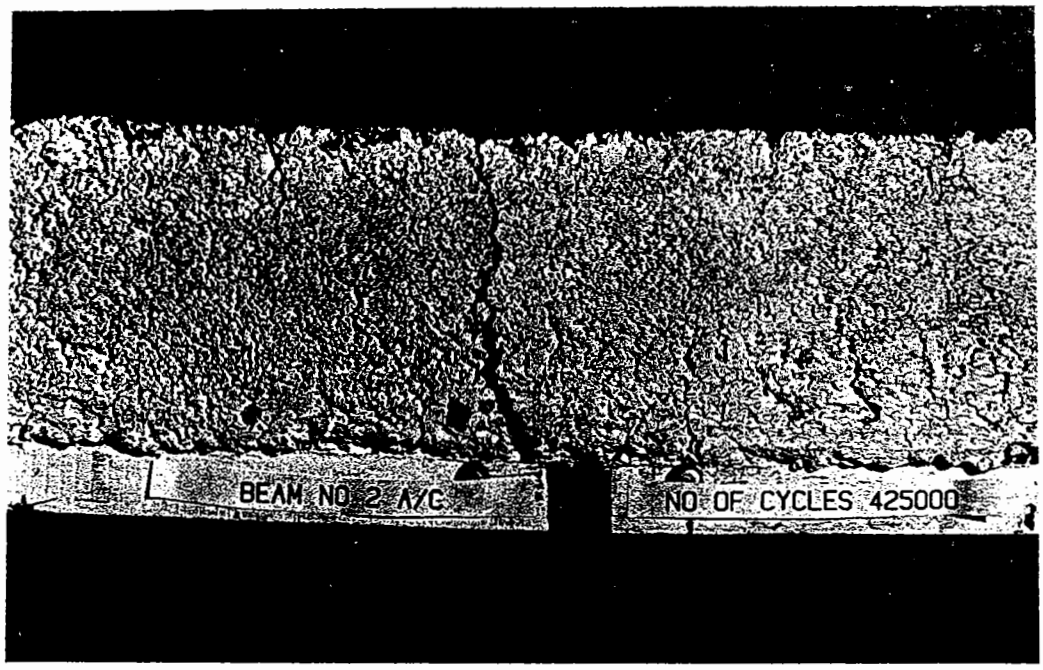

(a) unreinforced

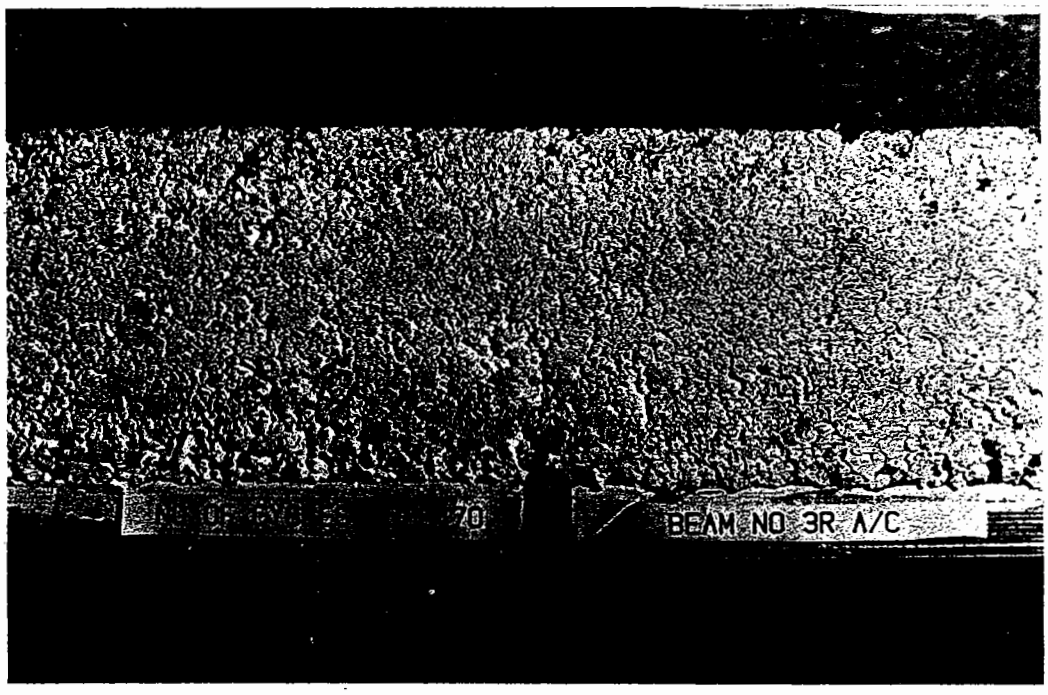

(b) reinforced at base of asphalt layer

Fig 5.11 Asphaltic concrete beams, reinforced & unreinforced

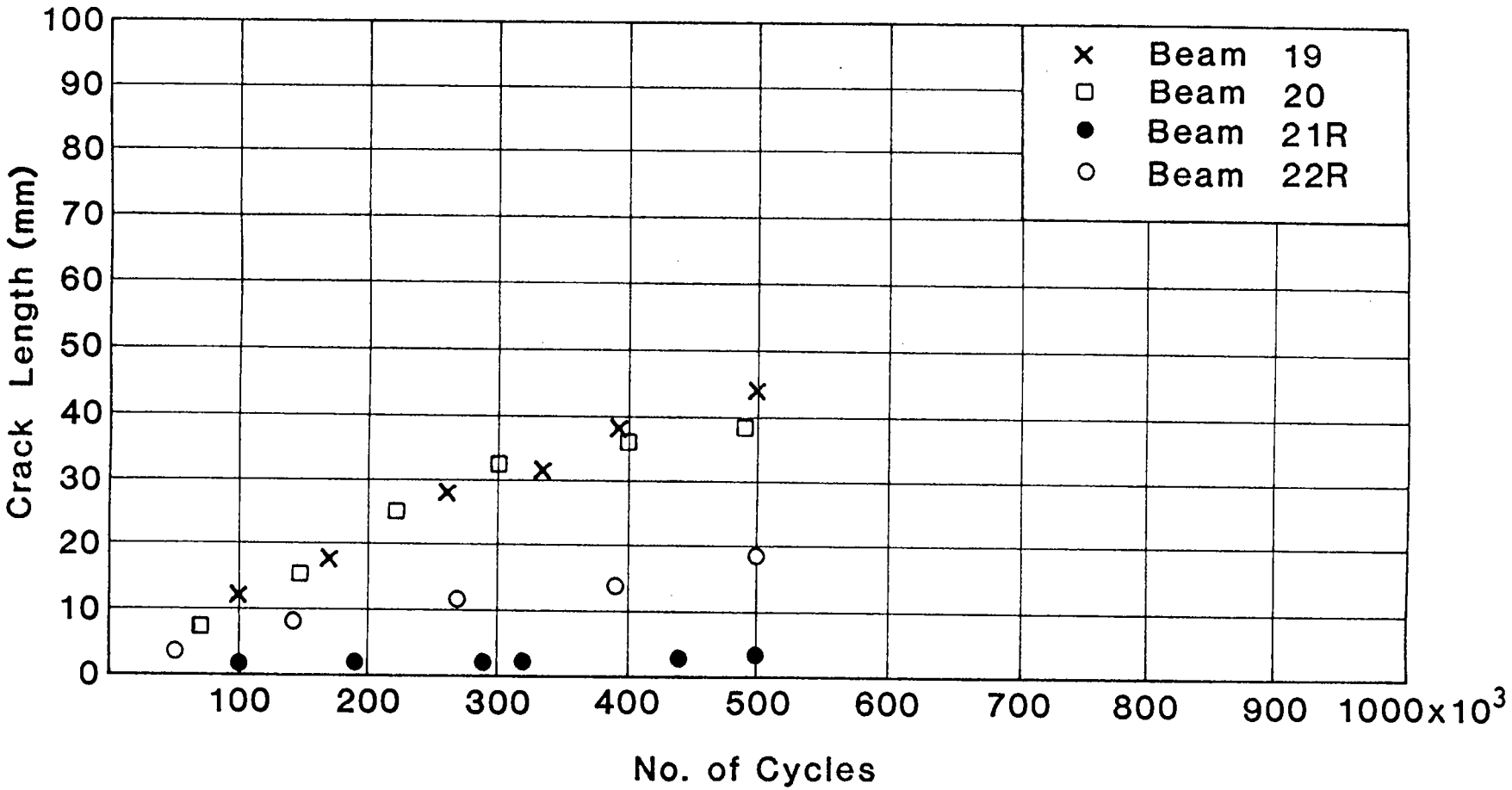

Fig. 5.12 Crack Lengths for Unreinforced Beams and Beam Reinforced with ICI Grid at Base (H.R.A.)

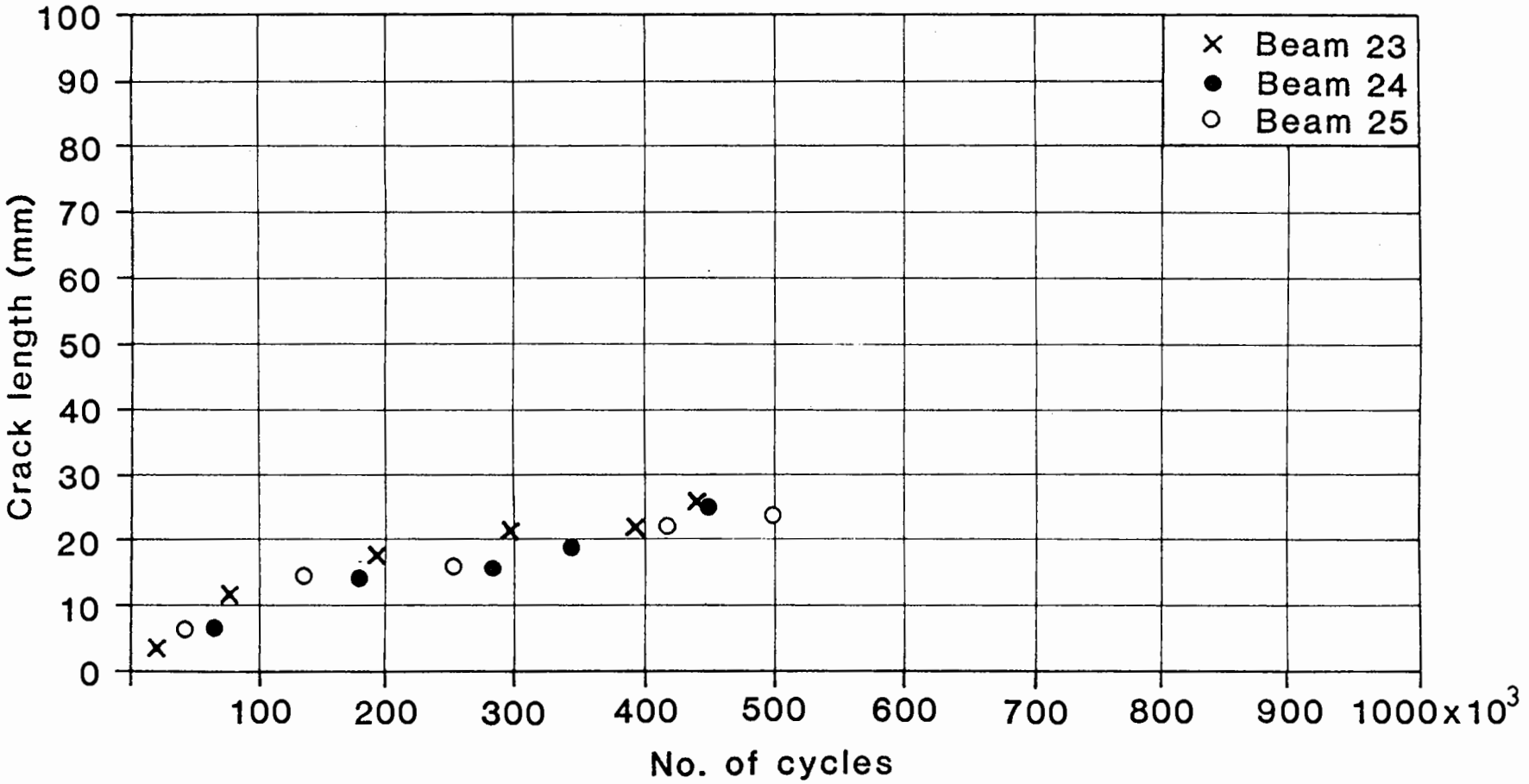

Fig. 5.13 Crack Lengths for Asphapol Cushion Course Beams

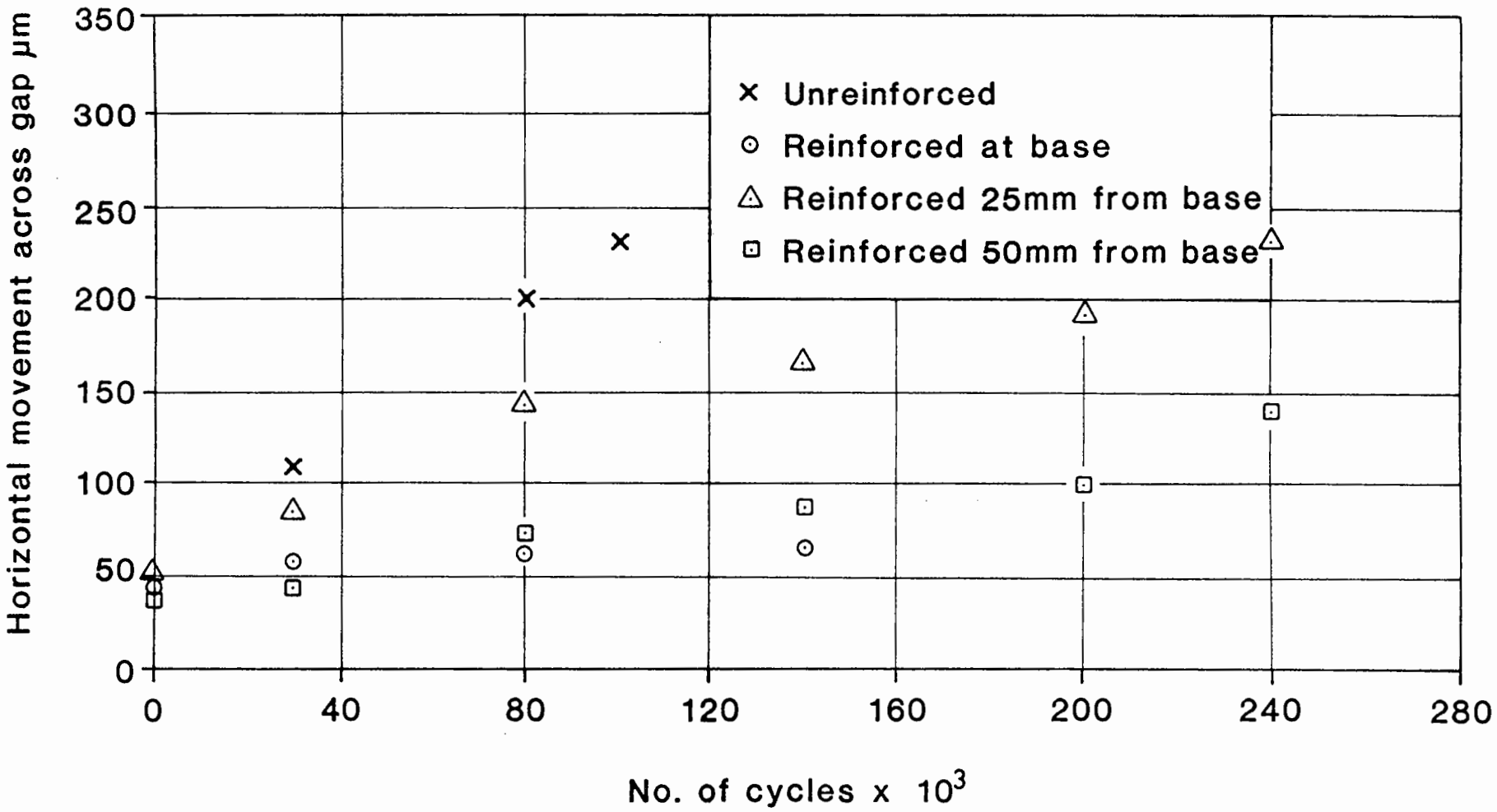

Fig. 5.14 Average Horizontal Movement Across Crack for Beams in Test Series A

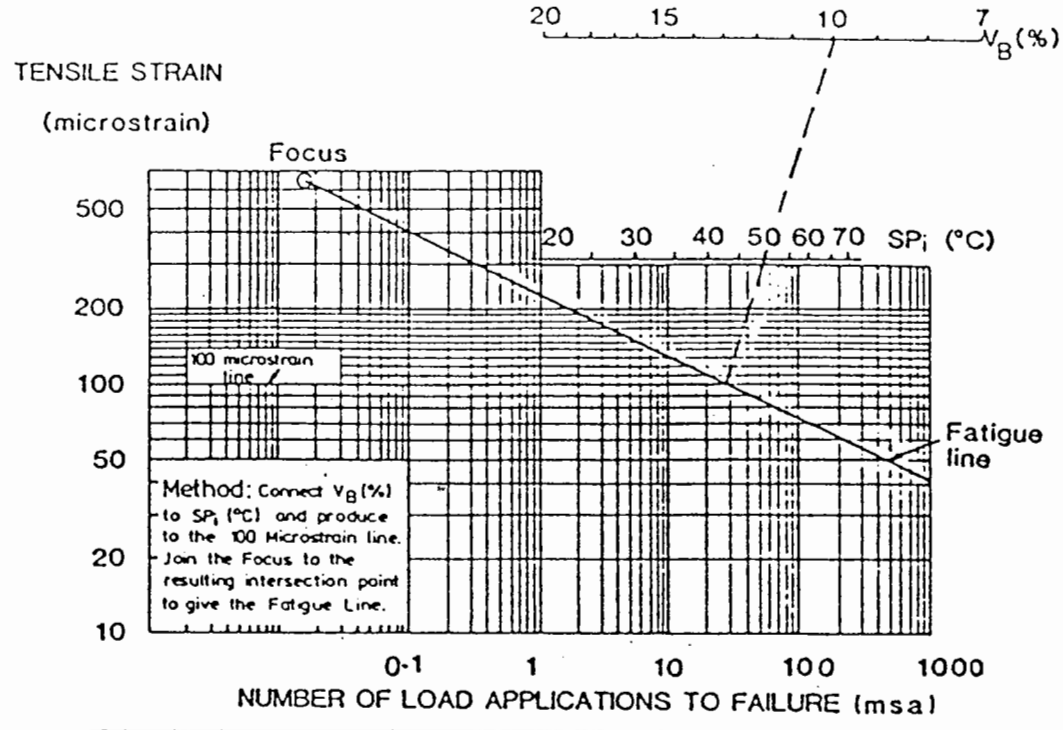

$$\log \varepsilon_t = \frac{14.39 \log V_B + 24.2 \log SP_i - 46.06 - \log N}{5.13 \log V_B + 8.63 \log SP_i - 15.8}$$

$$\log N = 15.8 \log \varepsilon_t - 46.06 - (5.13 \log \varepsilon_t - 14.39) \log V_B - (8.63 \log \varepsilon_t - 24.2) \log SP_i$$

Fig. 5.15 Nomograph for the Determination of Fatigue Strength (Derived from Cooper and Pell)

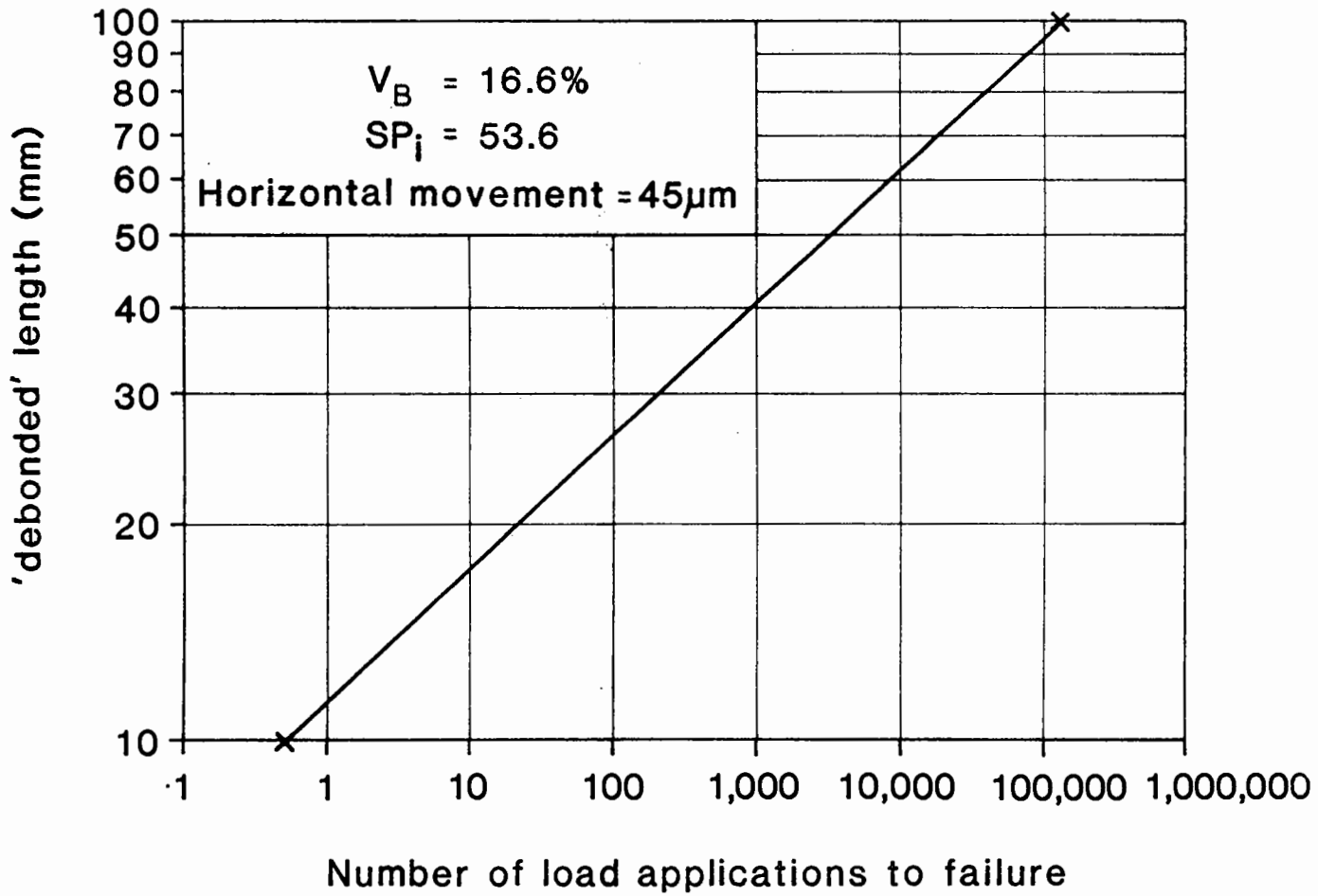

Fig. 5.16 Theoretical Fatigue Life for H.R.A.

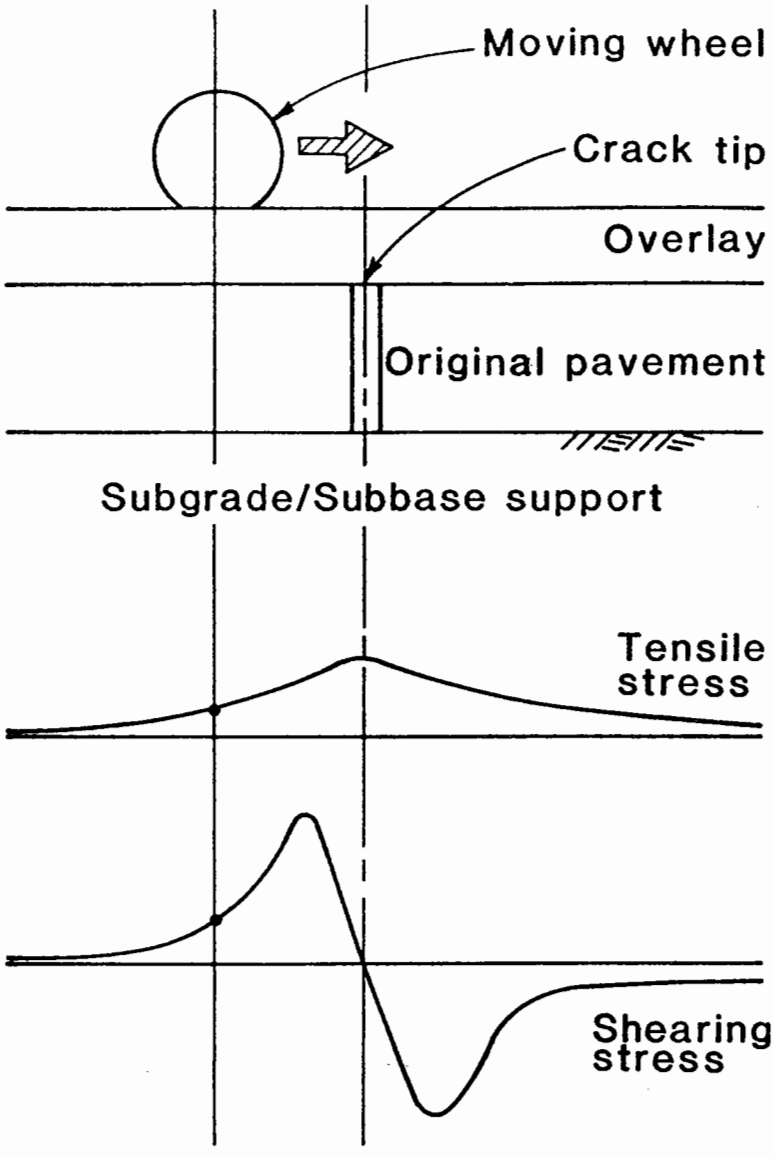

Fig. 5.17 Stresses Induced at Crack Tip Due to a Moving Wheel Load

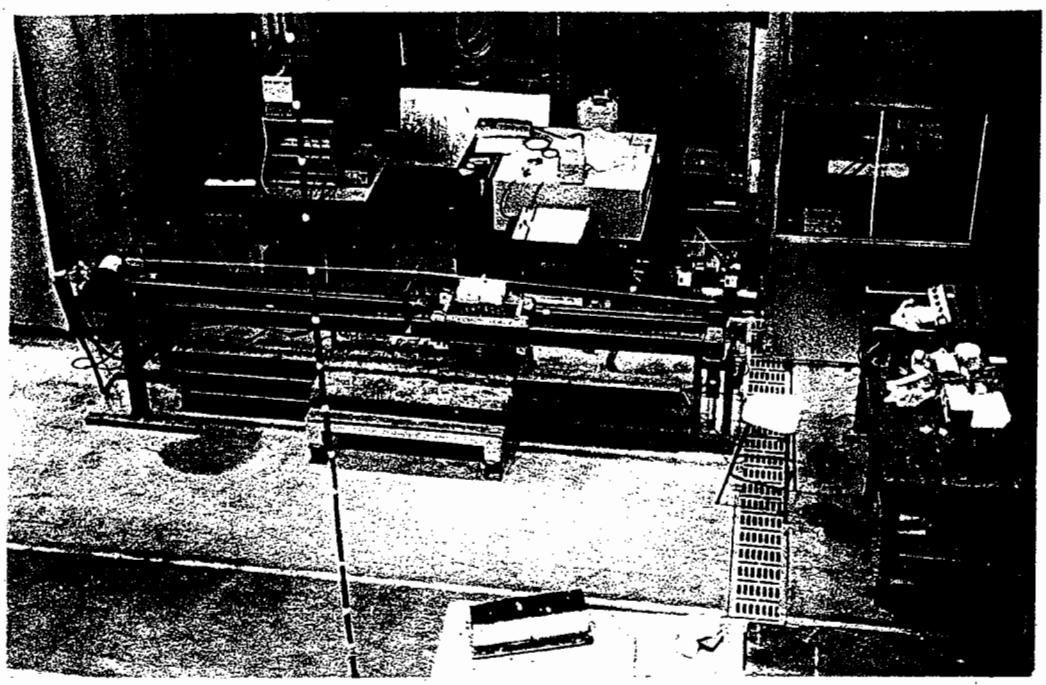

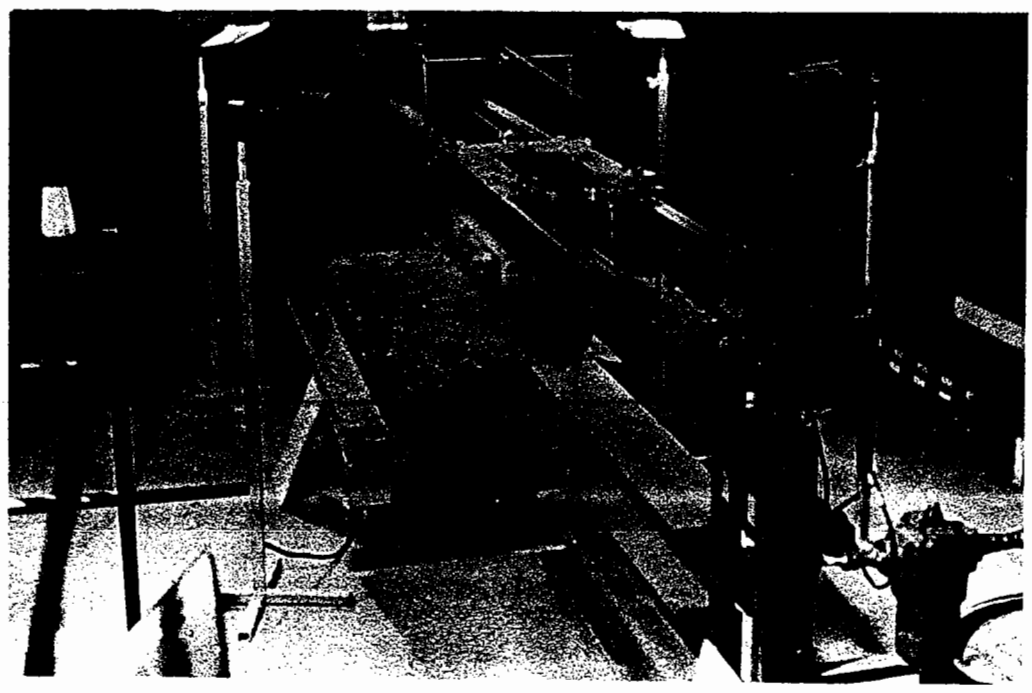

Fig 5.18 Views of the slab testing facility

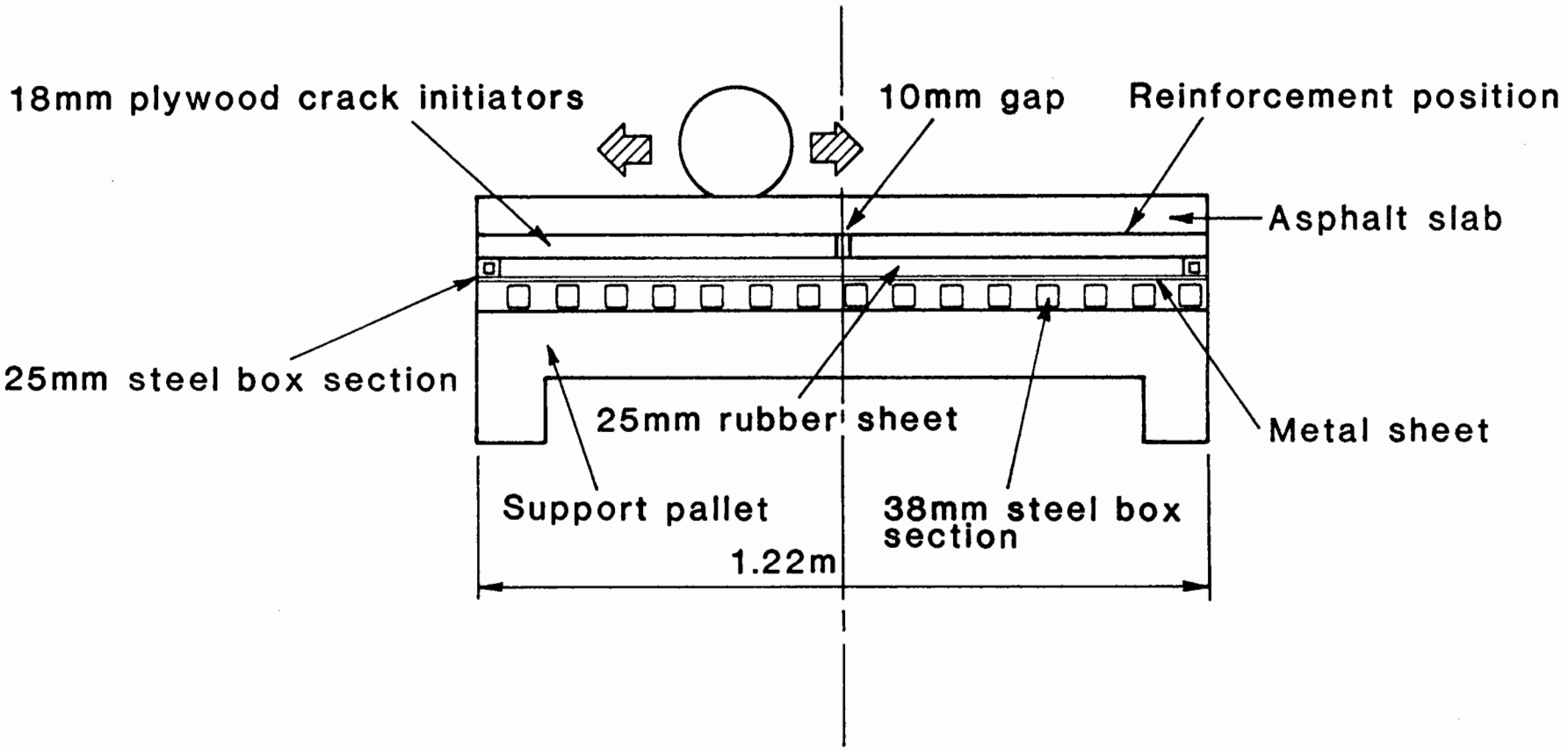

Fig. 5.19 General Experimental Arrangement for Reflection Cracking Test in the Slab Testing Facility

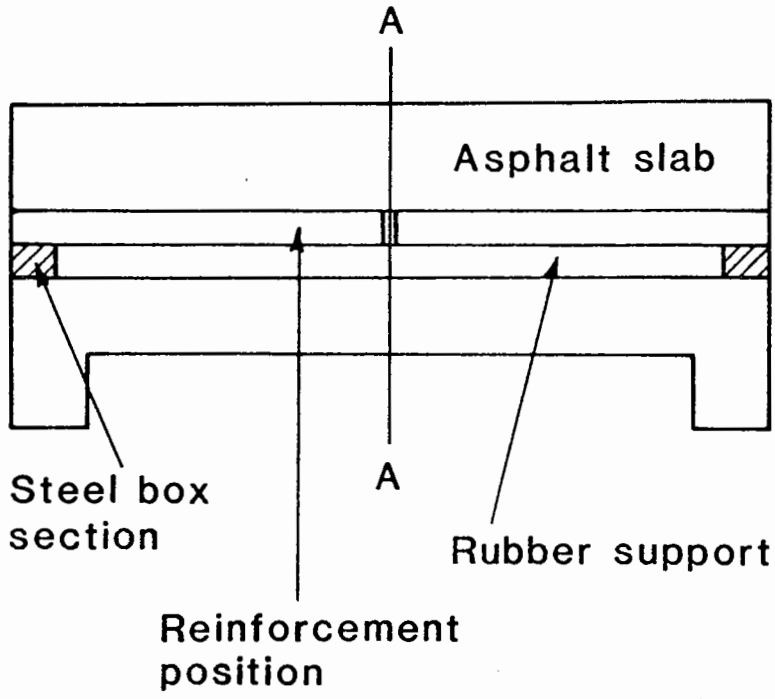

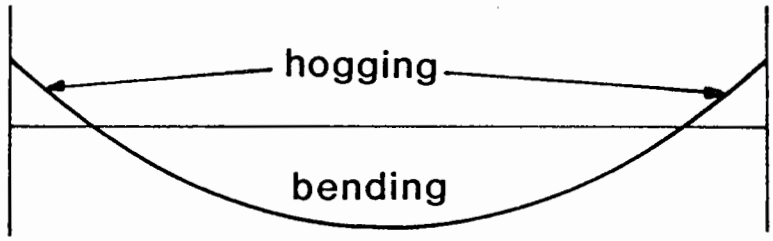

(a) No box section

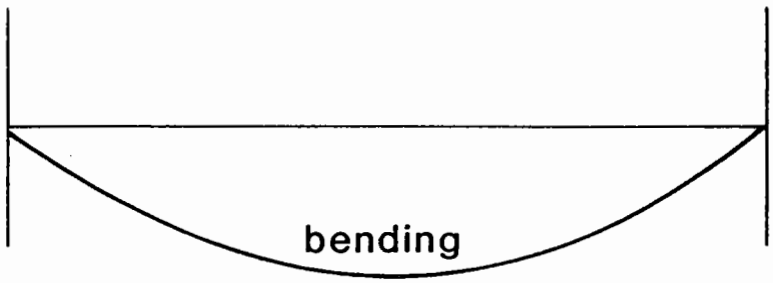

(b) Box section included

Fig. 5.20 Influence lines for Bending Moment on Asphalt Slab at A-A

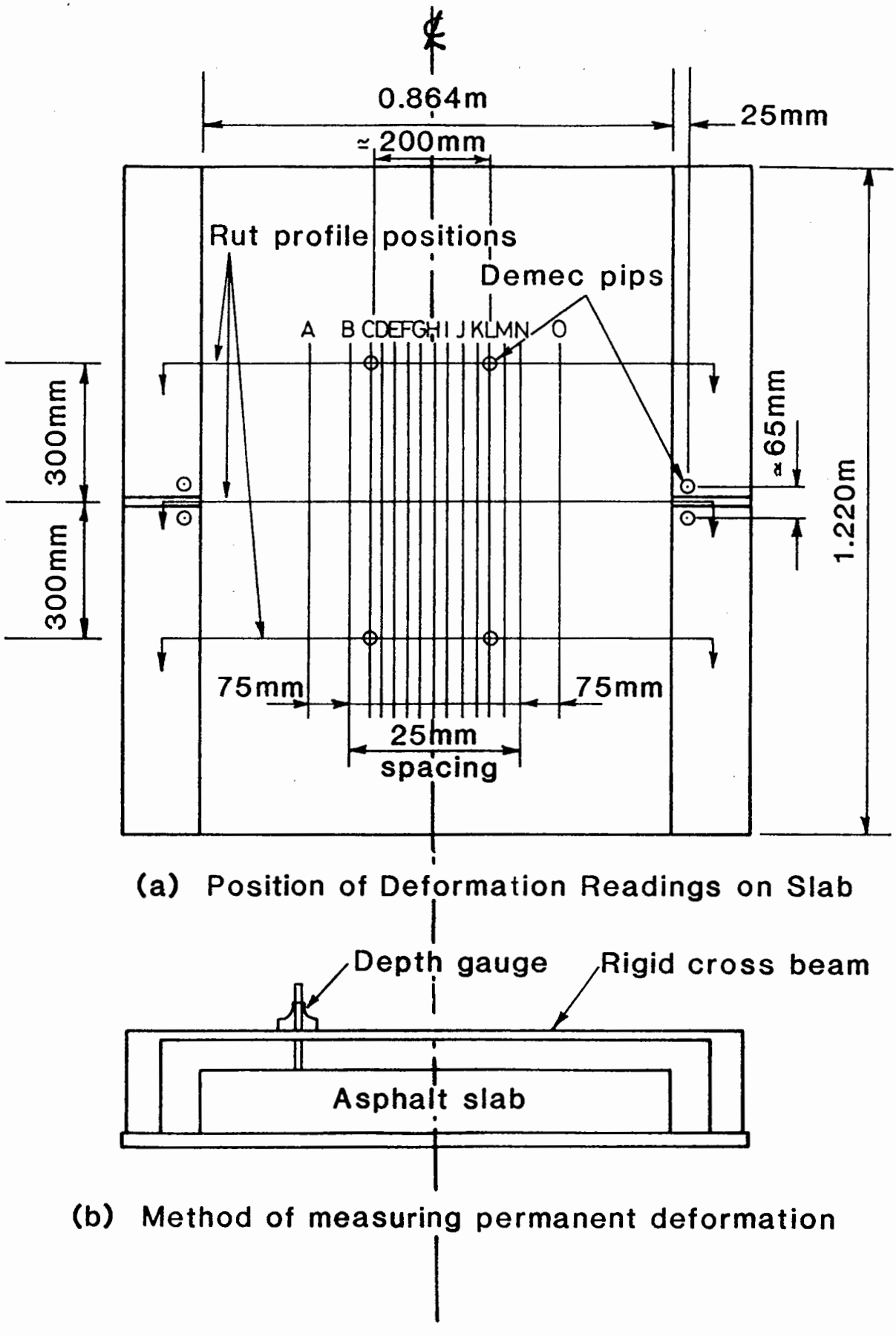

Fig. 5.21 Description of Slab Monitoring System

Fig. 5.22 Steel mould for slabs

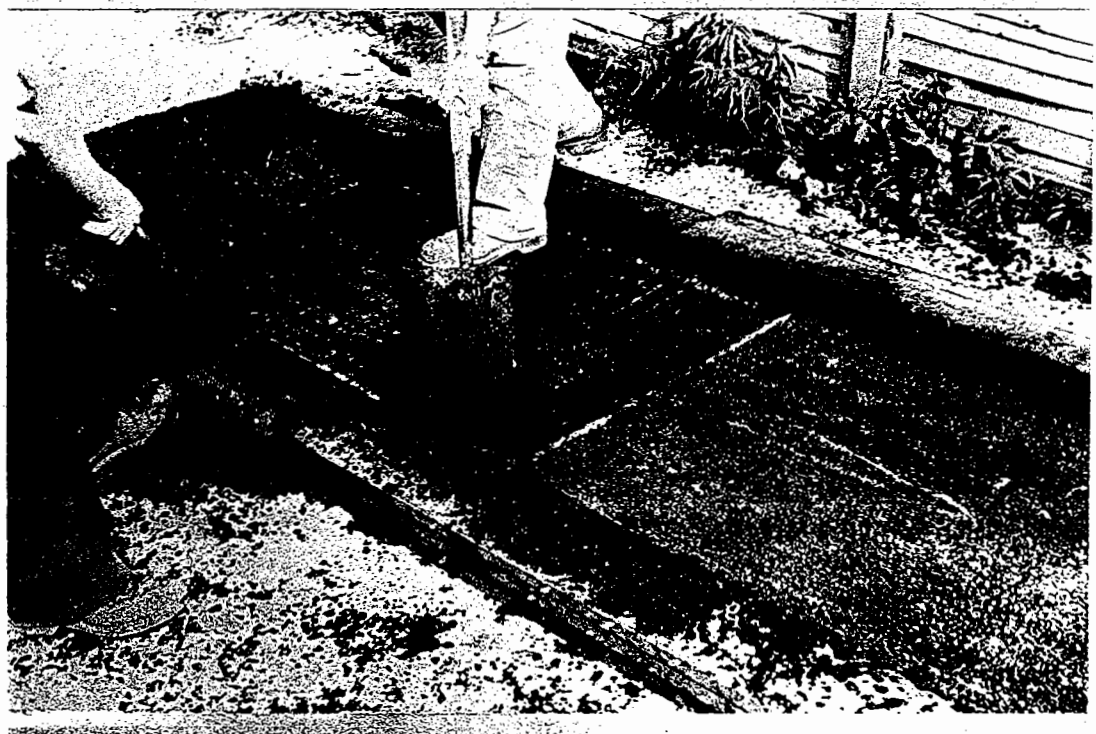

Fig. 5.23 Construction of slabs

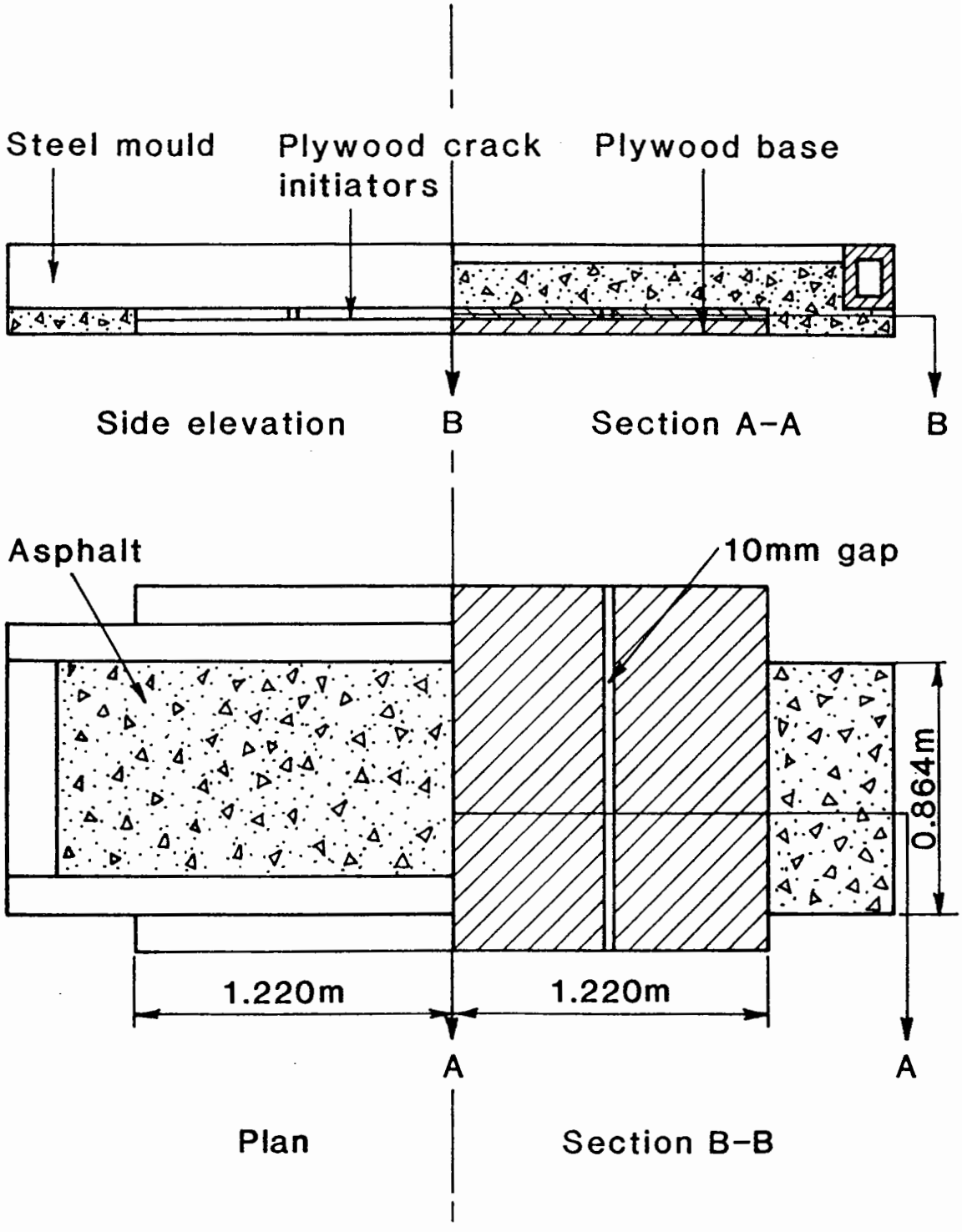

Fig. 5.24 Details of Asphalt Slabs in Reflection Cracking Tests

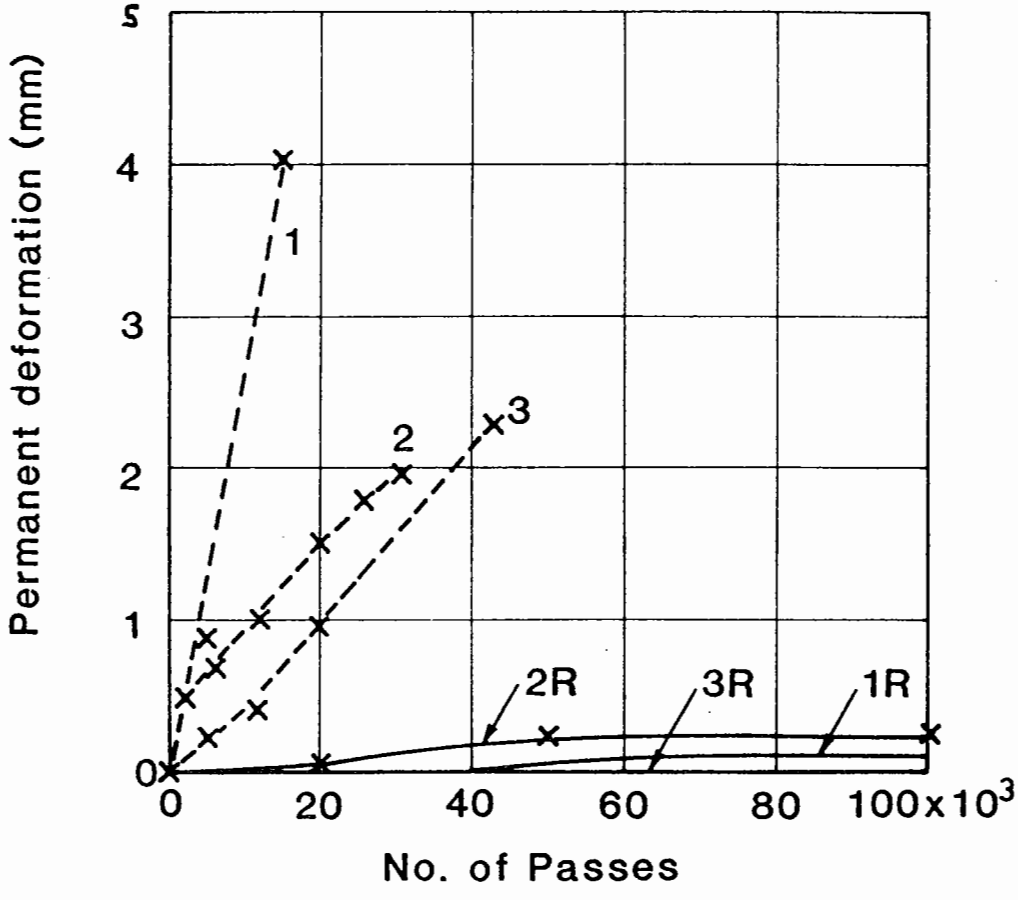

Fig. 5.25 Permanent Deformation Across 10mm Gap

6 PERMANENT DEFORMATION INVESTIGATION

6.1 INTRODUCTION

Extensive testing was undertaken to evaluate the potential of a high strength polymer grid in reducing the severity of permanent deformation in asphalt mixes. To this end pairs of bituminous slabs, reinforced and unreinforced, otherwise of similar composition, were tested under a rolling wheel load in both the Pavement test facility (P.T.F.) and the slab testing facility (S.T.F.).

The P.T.F. (Brown and Brodrick 1981(a)) at Nottingham enables full scale pavements to be tested under controlled laboratory conditions. The facility is able to apply wheel loads up to 10kN at speeds up to 10km/hr. The temperature of the pavement can be maintained within the range $5^{o}C$ to $35^{o}C$.

In total 13 pairs of slabs were tested under various wheel loads and varying bituminous mix type. Slab 1 was subdivided into Slab 1 and Slab 1R, (the appendix R denoting that reinforcement was included), as were the other slabs.

All the tests predate the development of the "chip seal" technique (Section 3.2), now used to install the grid and therefore this procedure was not used. The tests also predate the introduction of "Tensar" AR1, and "Tensar" SS3 was used throughout except for one case where a prototype large aperture grid was used.

The testing was already underway in the P.T.F. at the beginning of this project and has been reported previously (Brown and Brodrick 1982), but it was felt that for completeness all the experimental data should be presented here.

The bituminous mixes investigated were a hot rolled asphalt (H.R.A.), a wearing course, a base course and modified base course,

and a dense bitumen macadam (D.B.M.) base.

Direct comparison of the deformation rates of each slab is not possible as slabs 1/1R to 8/8R, 9/9R to 10/10R, and 11/11R to 13/13R were all conducted at different wheel loads and therefore contact stresses, and in two different pieces of apparatus.

During each test the development of pavement deformation was monitored on the surface of each slab.

6.2 SLAB AND REINFORCEMENT DETAILS

The general technique developed for preparing pairs of reinforced and unreinforced slabs has been described elsewhere (Section 5.3.1.) and only some of the details were different in this case.

6.2.1 Slab preparation

The steel framework used as a mould, was placed over the 18mm thick plywood bases, (Fig. 5.22) which had lengths of steel angle secured to each end. After construction the steel angle allowed the slab to be broken into two halves one of which was reinforced. The surface of the plywood was not treated in any way.

The hot asphalt was delivered by lorry from a local quarry and was manually placed in the moulds using shovels and rakes. Two construction methods were used:-

(a) Construction method 1

In this case the asphalt was placed and compacted in one lift. Reinforcement, included in one half of the mould, was placed on the loose mix at the desired depth and the remaining mix was then laid before compaction.

(b) Construction method 2

This method involved compacting the slabs in two lifts with the

grid sandwiched between the two layers. The grid was therefore always at a distinct interface within the slab. During construction the grid was held in position by placing small amounts of loose mix at each corner.

Table 6.1 numbers all the slabs from 1/1R to 13/13R and gives details of which type of construction method was used. In each reinforced slab the grid was orientated so that the transverse ribs were across the width of the slab, i.e. orthogonal to the direction of wheel travel.

After the mix had cooled, the steel mould was removed and the slabs separated by breaking through to the steel angles. The angles were sufficiently below the surface of the mix to prevent any interference with the wheel or rut development.

6.2.2 Slab description and mix details

A full description of each slab showing material type, and air void content, construction method, thickness and position of reinforcement is given in Table 6.1.

The large aperture grid referred to in Slab 12R was a prototype manufactured by Netlon Ltd. This grid was produced using the same polymer and by the same manufacturing process as "Tensar" SS3 or AR1, but had larger physical dimensions. The aperture size in this case was approximately 103mm x 103mm and had a lower stiffness than "Tensar" SS3 or AR1 due to the lower draw ratios in manufacture, although this was not investigated in detail. All the other slabs were reinforced with "Tensar" SS3.

Several types of bituminous mix were used in preparing the slabs, the aggregate gradings of which are shown in Fig. 6.1. The H.R.A. wearing course complied with BS 594. Schedule 1A, with 30% coarse aggregate, maximum size 14mm and 7.9% of 50 pen bitumen. The

Table 6.1 Summary of Slab descriptions (continued)

Slab No.	Material	Construction Method**	Slab thickness (mm)	Ratio of grid depth to slab thickness	Initial void content (%)
1	Hot rolled asphalt wearing course	1	89		7.8
1R			86	0.71	9.1
2			85		4.7
2R			86	0.77	6.1
3			93		5.1
3R			93	0.54	7.4
4			77		6.9
4R			78	0.47	4.6
5		2	104		2.4
5R			104	0.49	2.8
6			105		2.0
6R			103	0.63	3.4
7	Dense Bitumen Macadam		87		8.7
7R			87	0.40	9.7
8			89		8.9
8R			89	0.69	8.7

Table 6.1 Summary of Slab descriptions (continuation)

Slab No.	Material	Construction Method**	Slab thickness (mm)	Ratio of grid depth to slab thickness	Initial void content (%)
9	Hot rolled asphalt base course	1	107		1·9
9R			108	0.53	2.5
10			110		2.0
10R			108	0.50	2.5
11	Hot rolled asphalt base course (modified)		80		2.9
11R			80	0.50	4.6
12	Hot rolled asphalt wearing course	2	80		4.7
12R*			80	0.51	4.0
13			80		3.9
13R			80	0.50	4.9

* Large aperture grid
** 1 - Compacted in one lift (i.e. grid, if included, compacted within loose mix)
2 - Compacted in two lifts (i.e. grid, if included, positioned at a distinct interface)

H.R.A. base course complied with BS 594 Table 6 and had 65% coarse aggregate maximum size 28mm and 5.7% of 50 pen bitumen. The grading curve of the modified H.R.A. base course was altered to give an increased resistance to permanent deformation but in other respects was the same as a normal HRA base course. The D.B.M. complied to BS 4987 Section 2.3.4 and was a wearing course mix with 14mm nominal maximum aggregate size, binder content 5% of 100 pen bitumen.

The initial air void content of each slab is recorded in Table 6.1. Generally higher levels of density were achieved when the slabs were compacted in two lifts, construction method 2. In this case each individual layer was subjected to the same compactive effort as the thicker single layer used in construction method 1.

6.3 EXPERIMENTAL ARRANGEMENT

6.3.1 In the pavement test facility

The wheel load was applied to slabs 1/1R through to slabs 10/10R in the P.T.F. The existing clay subgrade was sealed by laying concrete over a polythene membrane. This provided a base on which to construct a reinforced resilient support for the slabs. Fig. 6.2 shows the arrangement with steel I section beams sandwiched between four phenolic film faced plywood sheets, normally used for concrete shuttering. This type of plywood was found to have a suitable resilience so that the platform for slabs reasonably reproduced the type of support which asphalt might experience in the field. Half the platform was used for testing a pair of slabs while the other half supported the next pair which would then be at the correct temperature for testing since the P.T.F. is housed in a temperature controlled room. Side restraint was added to the slabs in the form of aluminium angles screwed to the plywood base.

6.3.2 In the slab testing facility

Slabs 11/11R through to 13/13R were tested in the S.T.F. which has been described in detail elsewhere (Appendix E). Each slab supported by its plywood base, was positioned on a steel pallet centrally located under the wheel path of the S.T.F. Four thermostatically controlled floodlights were directed at the upper surface of the slab. Heat was conducted through each slab until a minimum temperature gradient with depth was obtained ($31^{o}C$ to $29^{o}C$).

6.3.3. Methods of permanent deformation measurement

A grid was marked on each slab with road paint to facilitate successive measurements of the transvers profile at the same locations while deformation developed. Positions, over the central 600mm of each slab, were chosen with the spacing as shown in Fig. 6.3. The deformation was recorded manually at each point on the grid from a fixed beam set across the slab. The average of the readings at Positions 1, 2 and 3 was used to determine the permanent deformation profile across the slab.

The deformation recorded in the tests conducted in the P.T.F. were measured using a displacement transducer which was fixed relative to the slab base at either side of it. An average of three readings was also used to determine permanent deformation. Measurements were taken before loading and then after 1000, 2000, 5000, 10,000, 20,000, 30,000 and 50,000 passes.

6.3.4. Test conditions

All the tests were conducted at a temperature of $30^{o}C \pm 1^{o}C$. Table 6.2 shows the test conditions for each slab. Slabs 1/1R through to 8/8R were tested in the P.T.F. A contact area of radius

Table 6.2 Test conditions for slabs

Slab No.	Wheel load (kN)	Contact stress (kPa)	Wheel speed (km/hr)
1,1R	8.3	415	8
2,2R	"	"	"
3,3R	"	"	"
4,4R	"	"	"
5,5R	"	"	"
6,6R	"	"	"
7,7R	"	"	"
8,8R	"	"	"
9,9R	5.0	250	"
10,10R	"	"	"
11,11R	"	440	3
12,12R	"	"	"
13,13R	"	"	"

80mm was assumed by measuring the thread pattern on the pavement surface. This gave an approximate contact pressure of 415kPa.

Slabs 9/9R and 10/10R were also tested in the P.T.F. although at a lower wheel load of 5kN. This gave a contact pressure of approximately 250kPa.

The remaining slabs 11/11R through to 13/13R were tested in the S.T.F. The wheel load was 5kN and wheel speed 3km/hr. In this facility the tyre has smaller dimensions and therefore not as great a contact area. The tyre contact area, although elliptical, approximated to a circle of radius 60mm and gave an estimated contact pressure of 440 kPa.

6.4 RESULTS

6.4.1. Degree of compaction and the effect of reinforcement

The initial void contents of each slab was given in Table 6.1. It is apparent, comparing the H.R.A. wearing course slabs 1/1R to 8/8R, that those specimens constructed using method 2 (i.e. compacted in two layers) had a lower void content than those slabs constructed using method 1, an average of 2.7% compared with 6.5% respectively. The D.B.M. wearing course had an average void content of 9.0% which as expected was higher than the H.R.A. because of the lower binder content and smaller percentage of fine aggregate and filler.

The general, the grid has had an effect on the state of compaction of each slab. In slab pair 3/3R the unreinforced slab had a void content of 5.1% whereas the reinforced slab had a void content of 7.4%, a 2.3% increase. Only in slab pairs 4/4R, 8/8R and 12/12R were the void contents comparable. The grid therefore hinders compaction, and to achieve the same density, reinforced asphalt requires a greater compactive effort.

6.4.2. Development of permanent deformation

In all the slab pairs tested the deformation in the reinforced slabs was less than that in the unreinforced slabs. The value of permanent deformation at the end of testing for reinforced and unreinforced slabs is presented in Table 6.3, the average value of which, for all the slabs was 0.46, i.e. the deformation has been reduced by approximately one half.

The build up of deformation for each slab is illustrated in figs. 6.4 to 6.8. These results represent the amount of vertical permanent deformation along the centre line of the wheel track and are an average of three readings.

The D.B.M. used in slabs 7/7R and 8/8R has deformed the more than the other slabs tested. D.B.M. is regarded usually as a deformation resistant material, and the poor resistance here may be due to the high penetration grade bitumen used when compared to the other mixes (100 pen compared to 50 pen) and the high initial air void content. At the high testing temperature ($30^{o}C$) 100 pen bitumen has a significantly lower stiffness and viscosity than 50 pen bitumen. Hence under the same loading conditions, larger deformation increments per wheel pass occur for the softer material.

The modified H.R.A. basecourse slabs 11/11R, showed a significant increase in resistance to permanent deformation when compared to the standard H.R.A. wearing course. Slabs 12/12R and 13/13R, and were tested to 70,000 passes and, slabs 12R and 13/13R were tested to 50,000 passes. Severe fatigue cracking occurred in the unreinforced slab, 12, and the test was curtailed at 36,000 passes. Fig. 6.9 illustrates slab 12, and 12R, (slab 12R was reinforced with the large aperture grid). The rut depth in the unreinforced and reinforced slab was 17.3mm and 6.3mm respectively. The underside of the unreinforced slab was badly cracked and

Table 6.3 Permanent deformation at the end of testing

Slab No.	Material	Average vertical deformation (mm)		Ratio Reinforced deformation / Unreinforced deformation
		Unreinforced	Reinforced	
1,1R	HRA	12.4	7.5	0.60
2,2R	W/C	7.1	4.1	0.51
3,3R		10.4	3.1	0.30
4,4R		9.1	3.1	0.34
5,5R		14.7	10.0	0.68
6,6R		15.7	12.2	0.78
7,7R*	DBM	28.3	7.3	0.26
8,8R*	W/C	18.8	5.3	0.26
9,9R	HRA	7.5	3.4	0.45
10,10R	B/C	5.5	3.6	0.65
11,11R**	HRA B/C mod	6.0	2.9	0.48
12,12R***	HRA	17.3	6.3	0.36
13,13R	W/C	22.5	5.5	0.24
				Av.0.46

* taken at 30,000 passes
** taken at 70,000 passes
*** taken at 36,000 passes

deteriorated, as shown in Fig 6.9(b).

During the test programme it was apparent that failure occurred at an earlier stage in the unreinforced slabs, and in some cases (i.e. slabs 7, 8, 12, 13) complete deterioration was imminent. This was never the case in the reinforced slabs, where the integrity of the slab was always maintained to the end of testing.

Figs. 6.10 to 6.14 show the average profile across the slabs (measured at 50,000 passes unless otherwise stated). It is clear that both vertical permanent deformation and lateral flow of the asphalt has been reduced by the reinforcement. Examining slab pair 5/5R, Fig. 6.11, the width of the rut is less in the reinforced case, and the shoulders either side are more pronounced. This is confirmed by the results plotted in Fig. 6.15, which shows the typical development of transverse permanent deformation in slabs 12/12R and 13/13R. This was measured by Demec pips glued either side of the rut, at a spacing of 200mm. The movement of apshalt away from the rut was significantly greater in the unreinforced slabs (14mm) compared with the reinforced slab (2-3mm).

Table 6.4 shows the equivalent number of load applications that were required to deform the unreinforced slabs by the same amount as the reinforced slabs at the end of each test. The ratio of number of load applications in the reinforced slabs to that in the unreinforced slabs for this given rut depth is then presented. The minimum ratio was 3.9 times the maximum 30.0,and the average was 9.4. If the ratios in test 3/R, 4/R and 8/R are ignored, since they are significantly higher than the other tests, the average ratio was 5.3 which seems more realistic.

6.5 DISCUSSION

During construction of the slabs a disparity in density between

Table 6.4 Number of load applications for given rut depth

Slab No.	Permanent deformation (mm)	No. of load applications to given deformation		Ratio $\frac{\text{life (reinforced)}}{\text{life (unreinforced)}}$
		Unreinforced	Reinforced	
1,1R	7.5	11,200	50,000	4.5
2,2R	4.1	10,000	50,000	5.0
3.3R	3.1	3,500	50,000	14.3
4,4R	3.1	2,000	50,000	25.0
5,5R	10.0	10,600	50,000	4.7
6,6R	12.2	12,800	50,000	3.9
7,7R	7.3	3,900	30,000	7.7
8,8R	5.3	1,000	30,000	30.0
9,9R	3.4	10,800	50,000	4.6
10,10R	3.6	12,500	50,000	4.0
11,11R	2.9	8,400	70,000	8.3
12,12R	6.3	10,600	50,000	4.7
13,13R	5.5	9,000	50,000	5.5

Av.9.4

unreinforced and reinforced slabs was discovered, the grid in most cases hindering the compaction of the asphalt layer. This suggests that voids are created around the grid within the layer possibly caused by movement of the grid due to the severe thermal regime during paving. Although in general the void contents were higher in reinforced slabs, the resistance to permanent deformation was always greater. By increasing the compactive effort on reinforced slabs to achieve the same density as unreinforced slabs, greater reductions in permanent deformation might have been achieved.

The grid was shown to resist lateral flow in the asphalt layer. The slabs were cast on a rigid, non deformable plywood base, all deformation therefore occurred by either lateral flow of the asphalt or volumetric strain, and not deformation in the lower layers of the structure as may be the case in a pavement. The test conditions are, however, more representative of an asphalt overlay on a rigid pavement or a situation in which kerbs are not used and lateral restraint not provided. The tests illustrate the ability of the grid to reinforce asphalt by preventing of lateral flow on account of the effectiveness of the interlock mechanism.

6.6. CONCLUSIONS

In all the slabs tested the reinforced slab deformed significantly less than the unreinforced slab. The ratio of reinforced to unreinforced vertical deformation varied between 0.78 to 0.24 with an average ratio of 0.46.

In general as the severity of a particular test increased so too did the benefit of including the grid. The grid should be of most benefit in situations where current mix design practice is unable to control pavement deformation, because of either the severity of loading or high temperatures.

The factors drawn from Table 6.4 show an average increase in life of 5.3 can be achieved for reinforced slabs over reinforced slabs, for the same level of deformation. A conservative increase in life of 3 would be appropriate for reinforced slabs over unreinforced slabs, and has been used in Chapter Nine in the preliminary design guide for reinforced overlays.

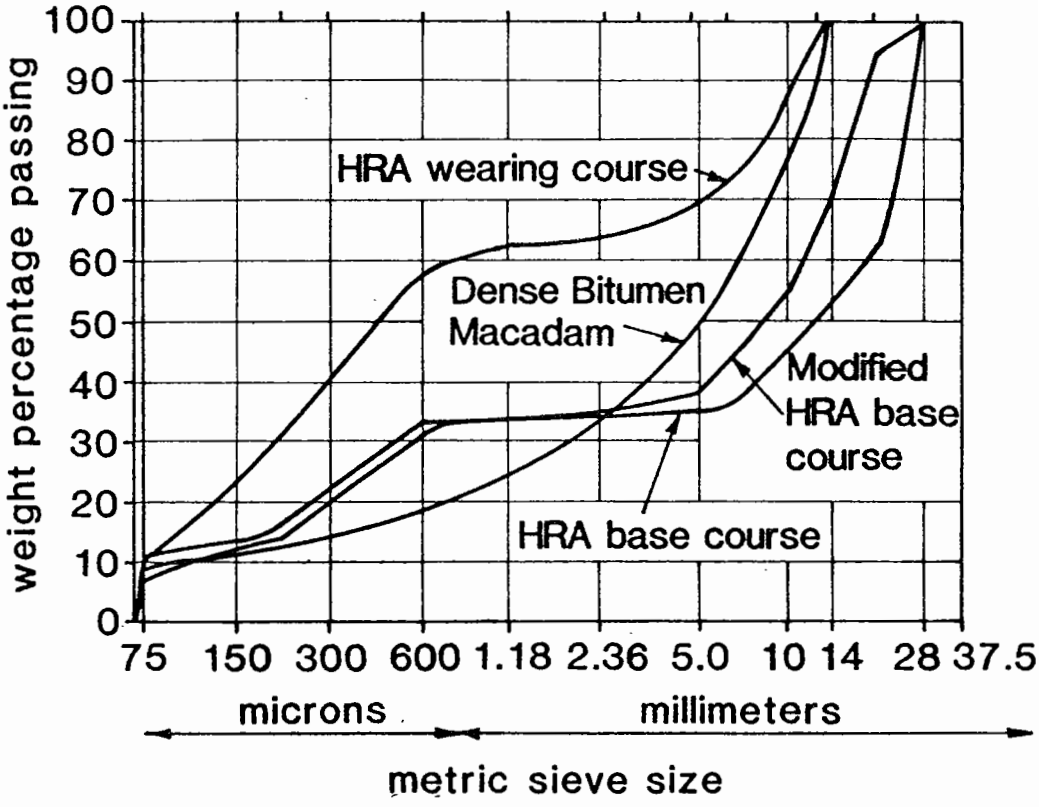

Fig. 6.1 Aggregate Grading for Slabs in Deformation Tests

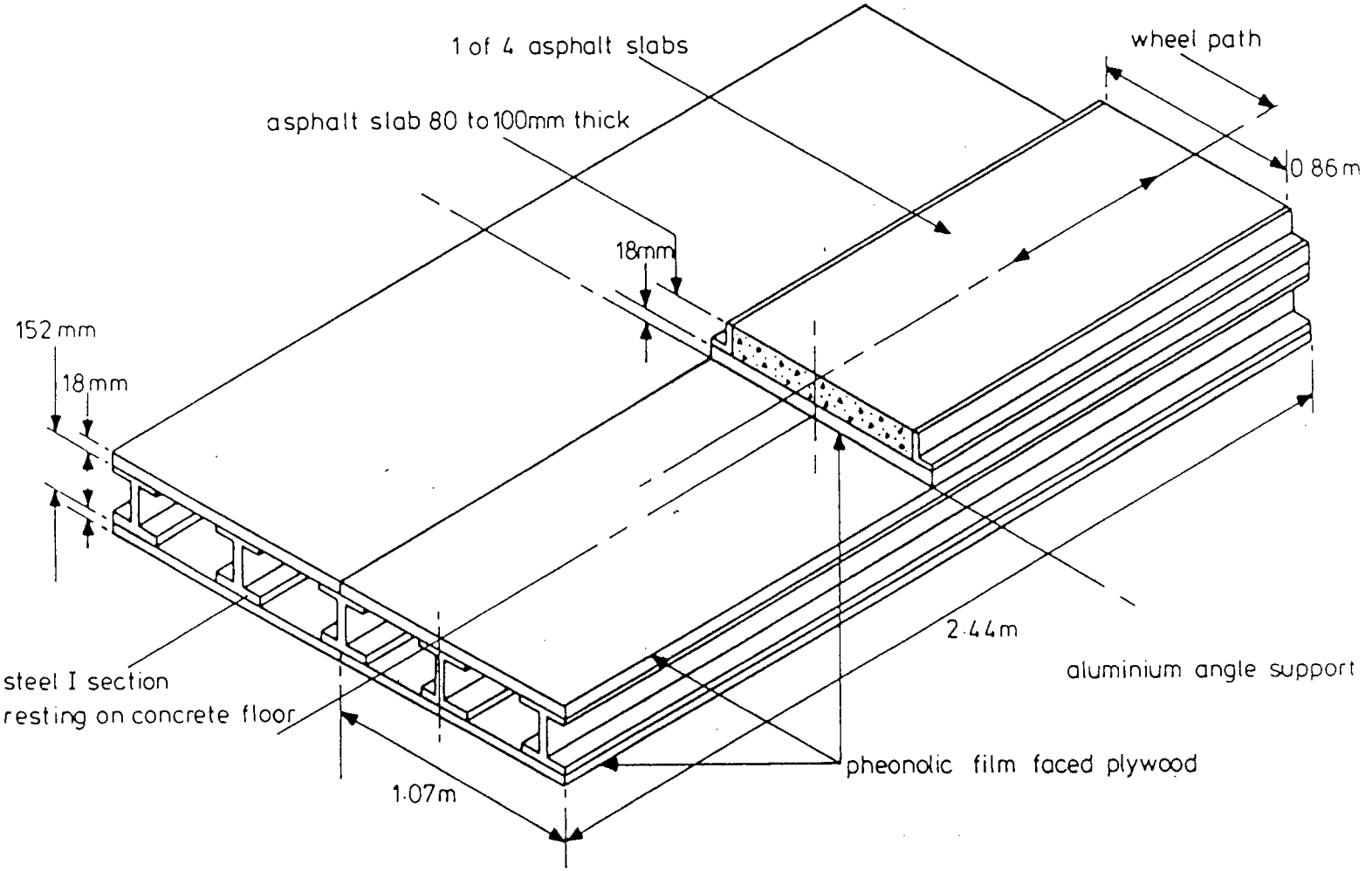

Fig. 6.2 Support arrangement for slab in the pavement test facility

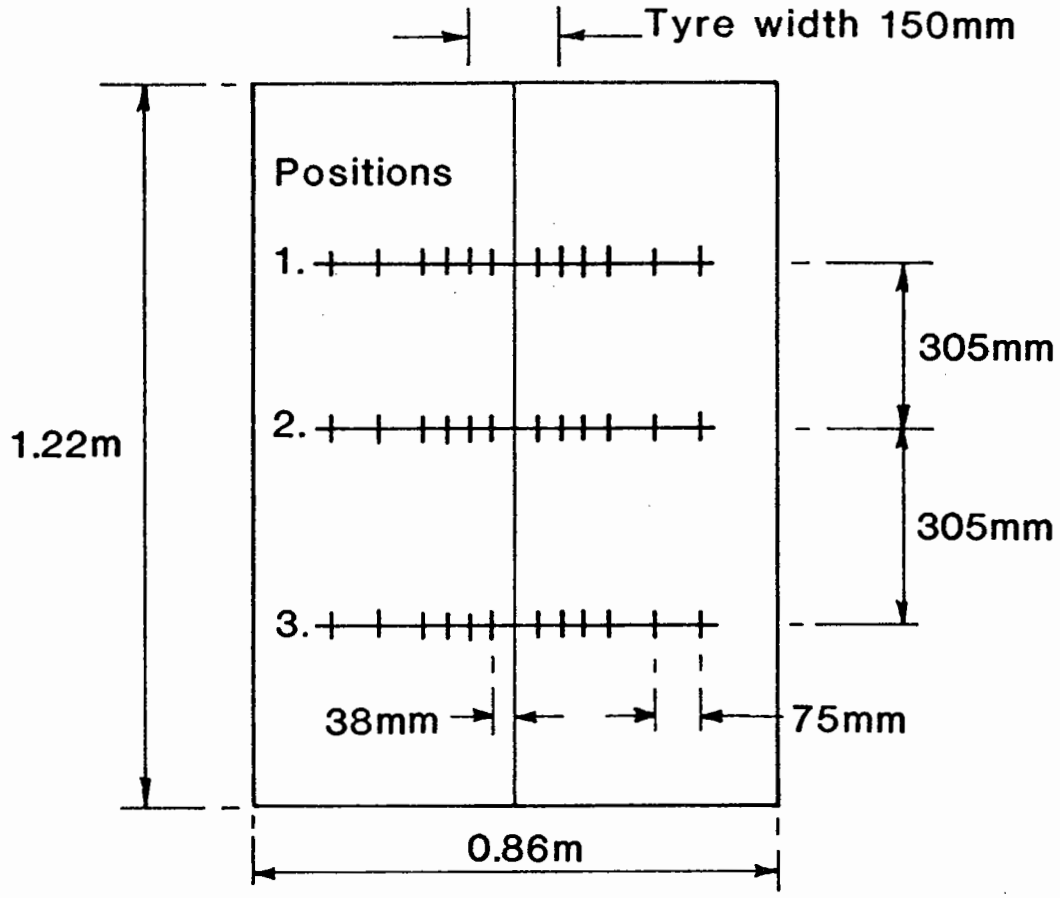

Fig. 6.3 Grid for profilometer measurements on slab

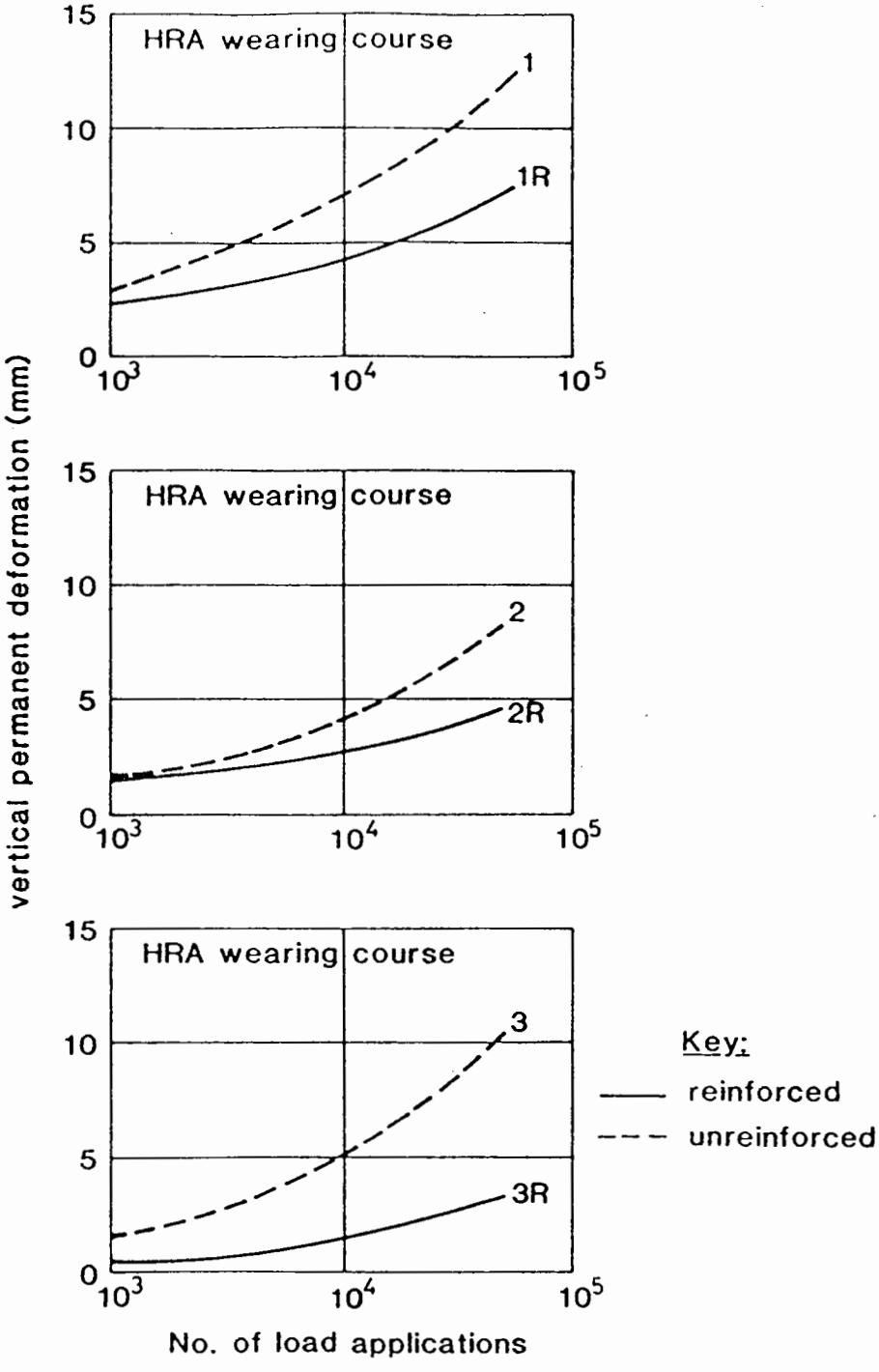

Fig. 6.4 Permanent deformation for slabs 1 to 3R

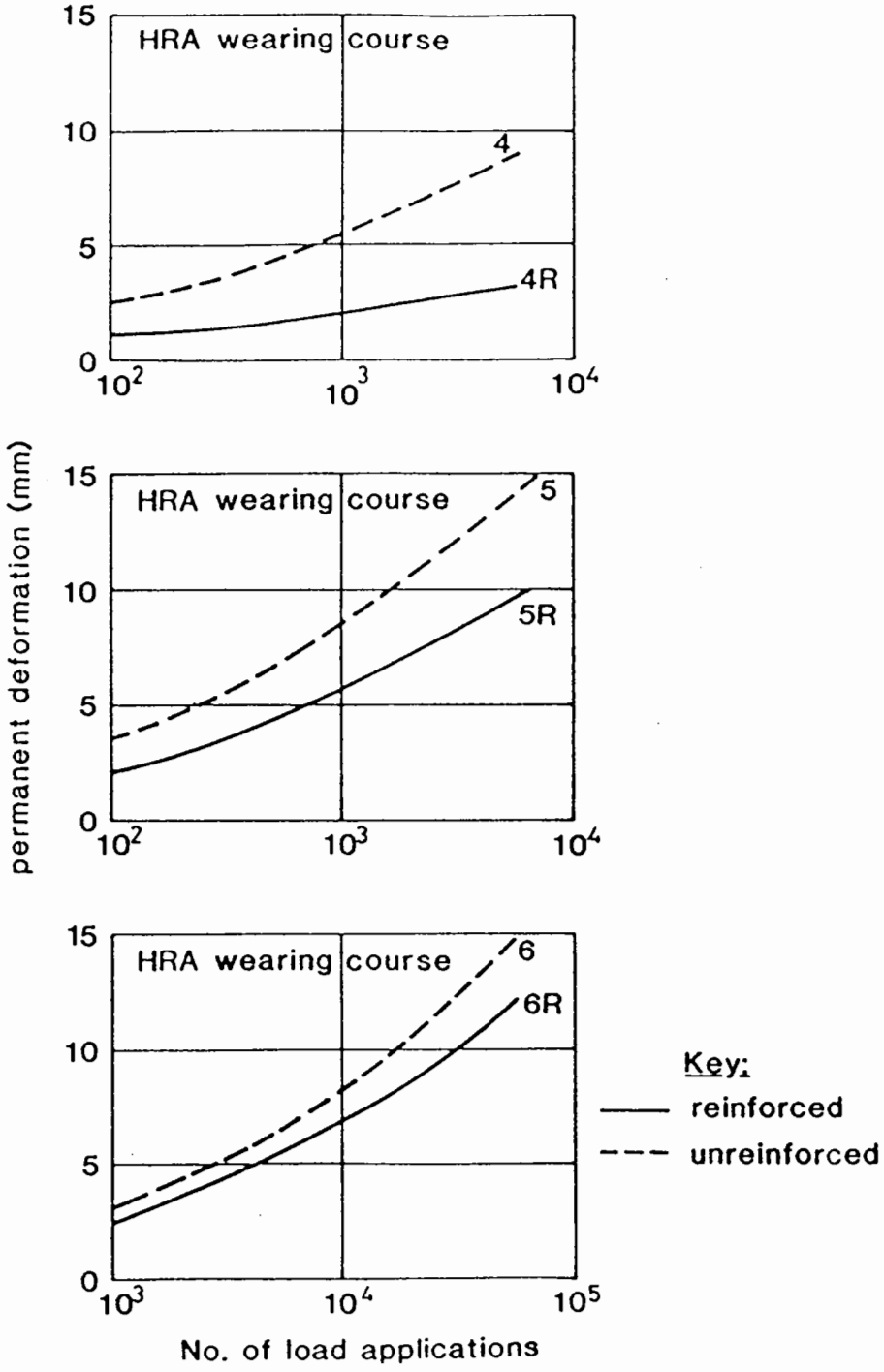

Fig. 6.5 permanent deformation for slabs 4 to 6R

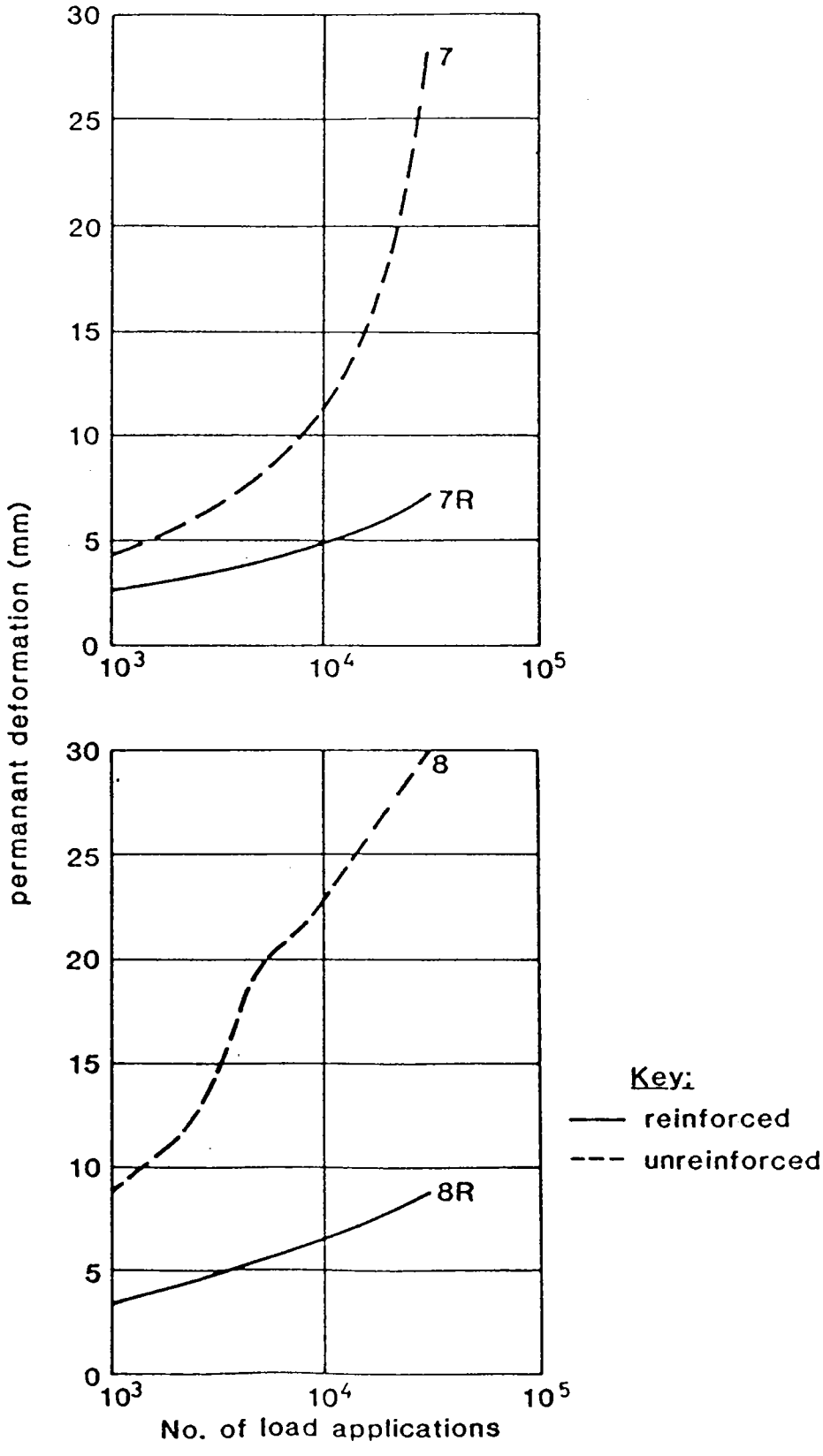

Fig. 6.6 Permanent deformation for slabs 7 to 8R

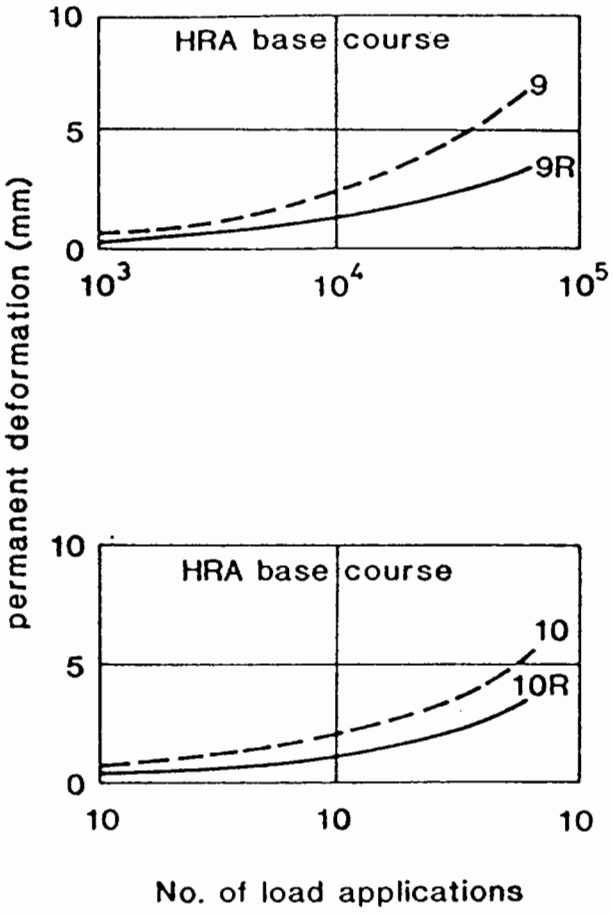

Fig. 6.7 Permanent Deformation for Slab 9 to 10R

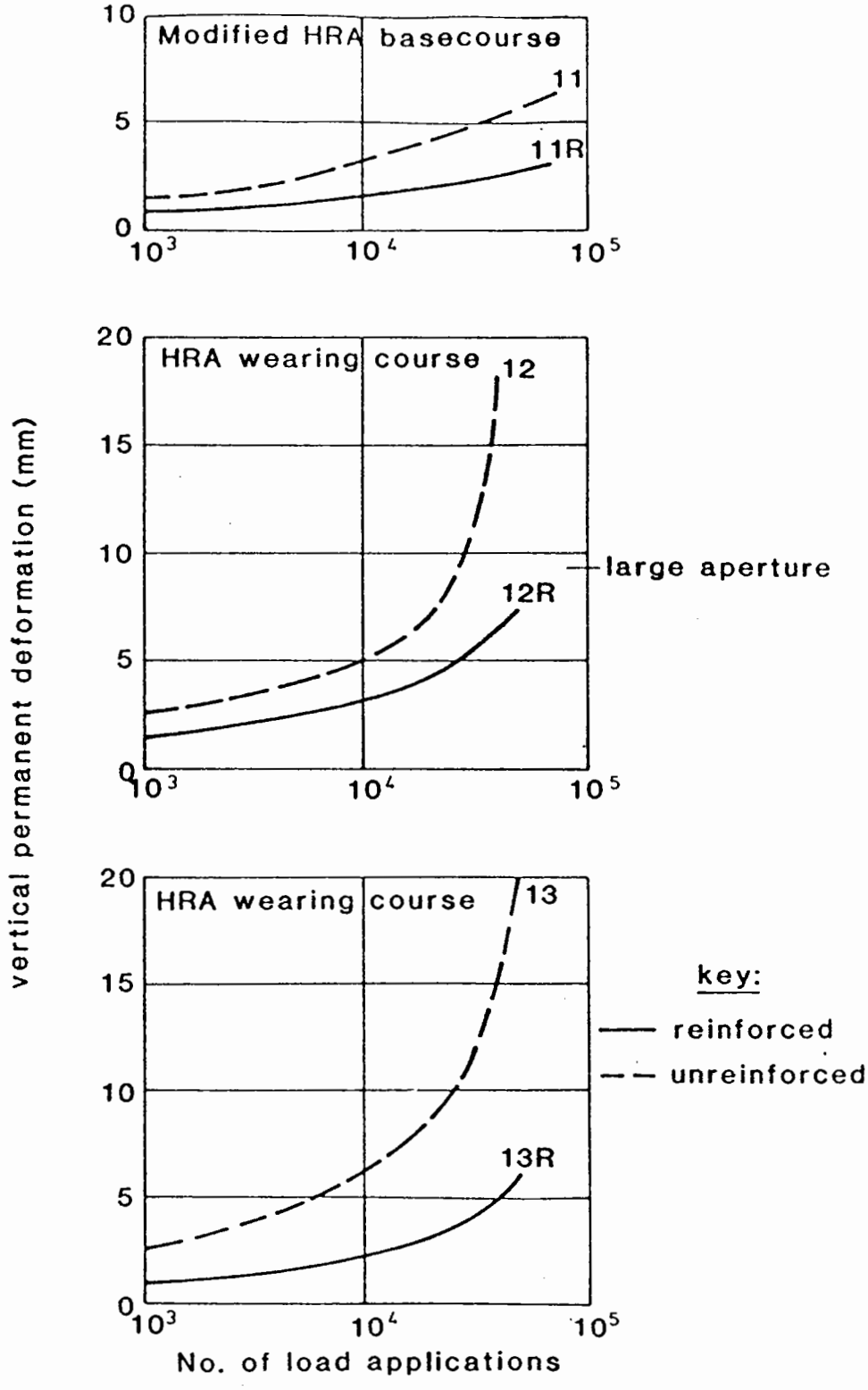

Fig. 6.8 Development of vertical permanent deformation for slabs 11 to 13R

(a) Rutting: unreinforced left, reinforced right

(b) Cracking: unreinforced left,reinforced right

Fig. 6.9 Comparison of reinforced and unreinforced slabs

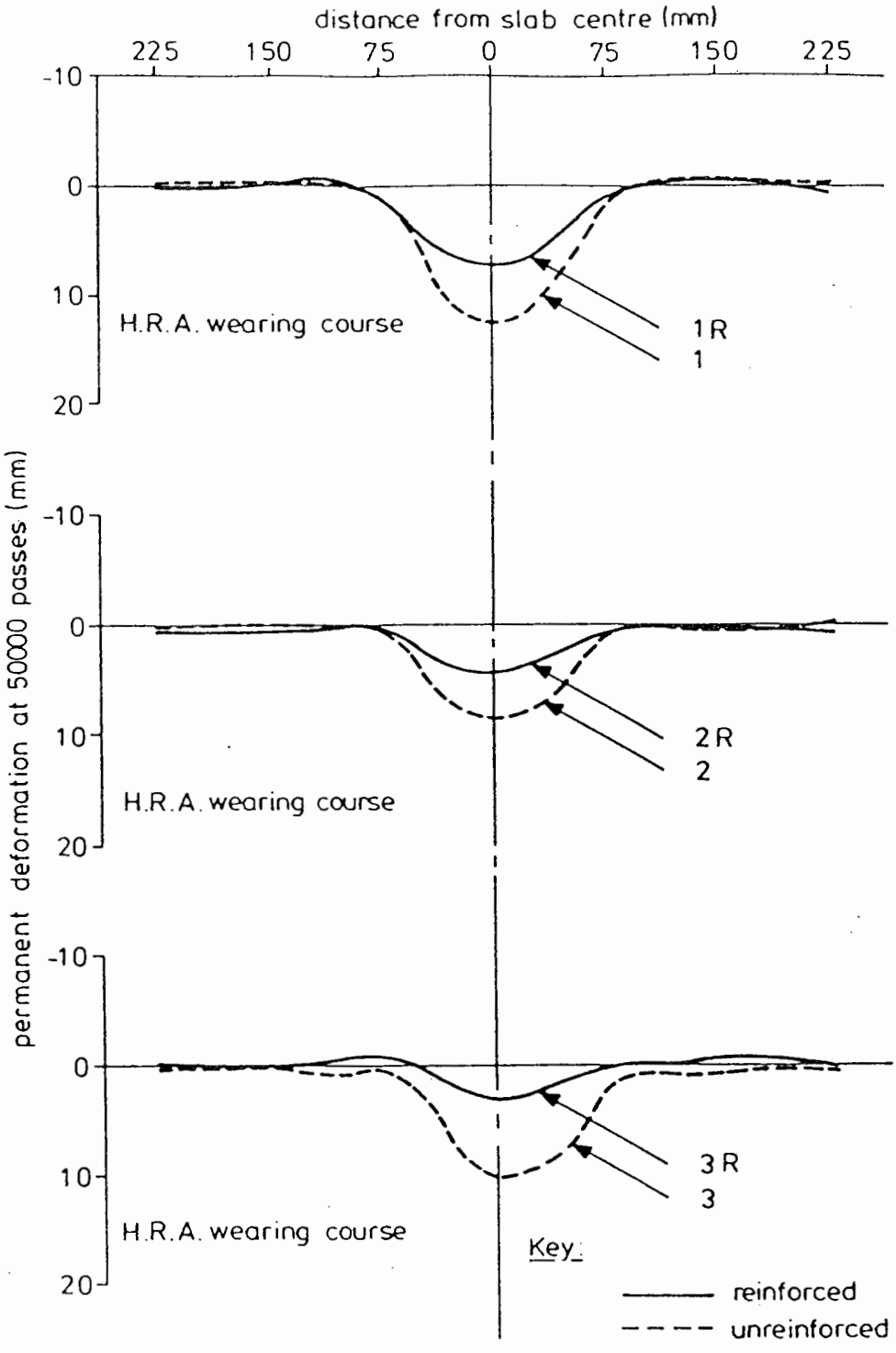

Fig. 6.10 Transverse profiles for slabs 1 to 3R at 50,000 passes

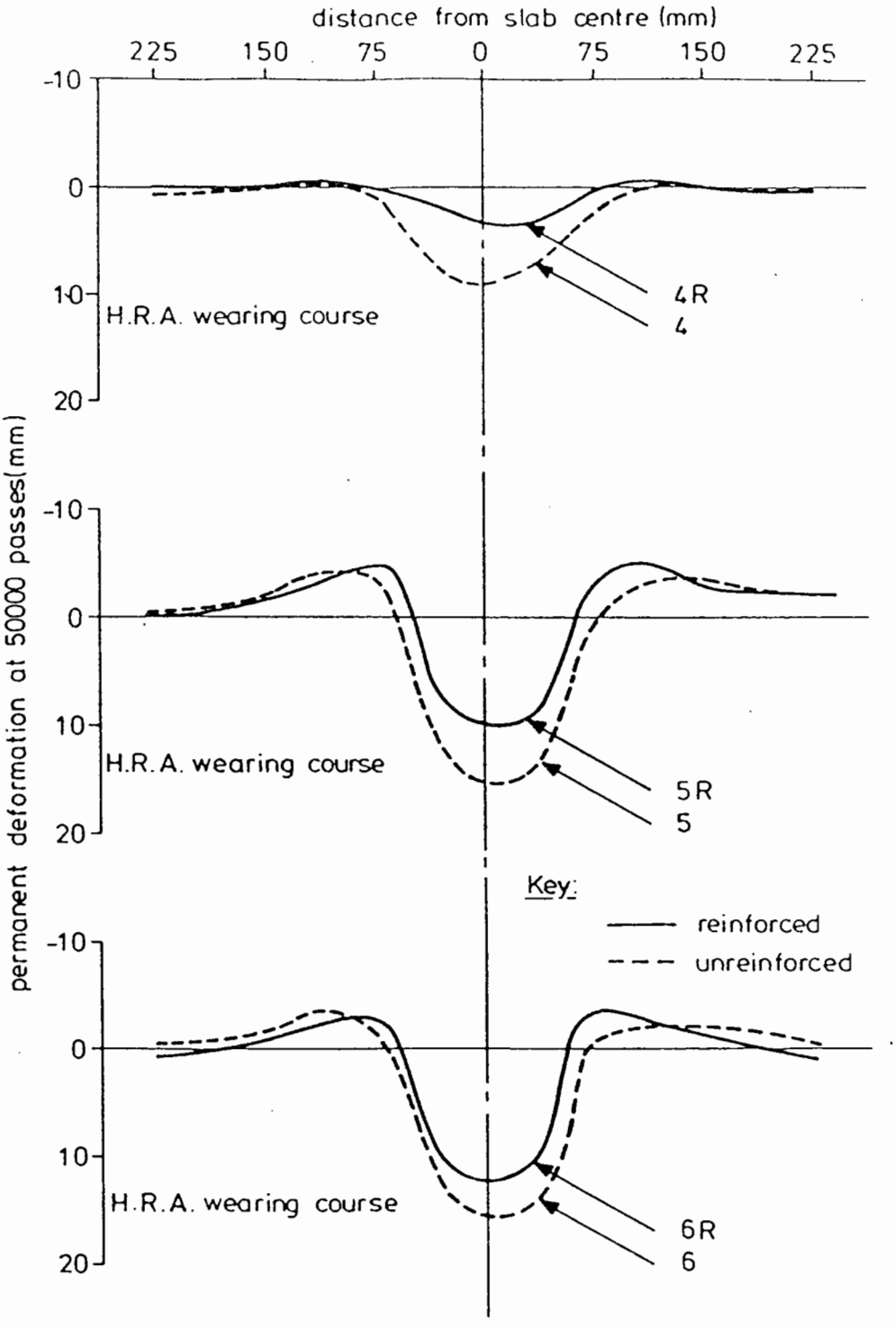

Fig. 6.11 Rut profile for slabs 4 so 6R at . 50,000 passes

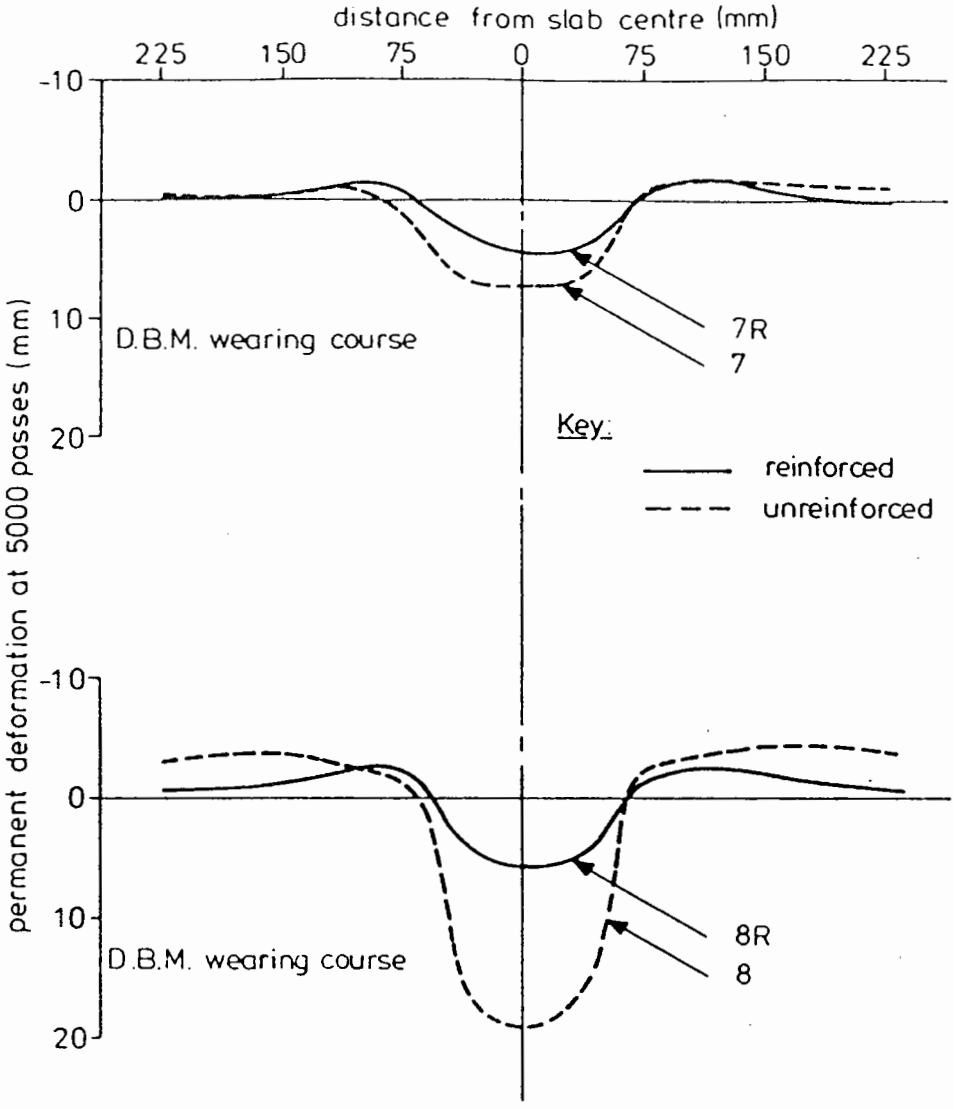

Note : these profiles were taken at 5000 passes as subsequent deformation was considered unrealistic.

Fig. 6.12 Rut profiles for slabs 7 to 8R at 5,000 passes

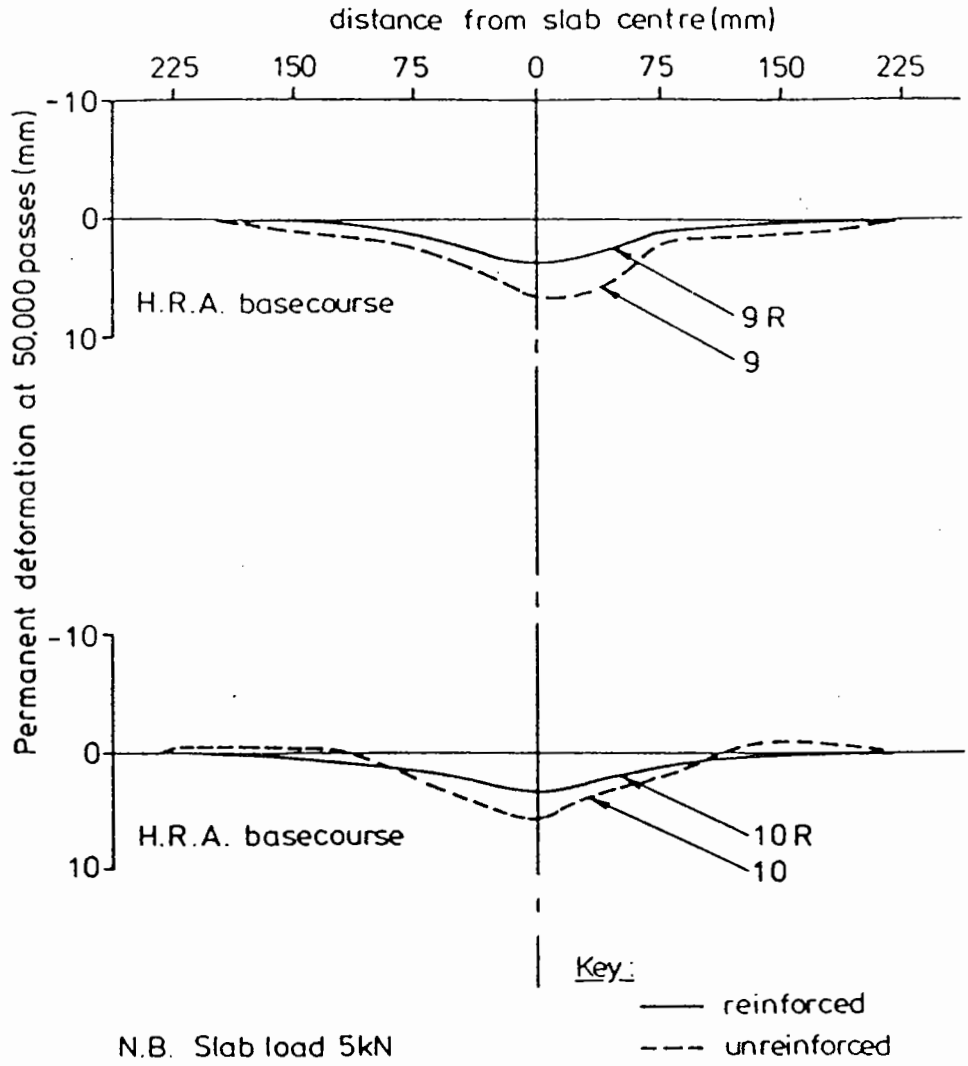

Fig. 6.13 Rut profiles for slabs 9 to 10R at 50,000 passes

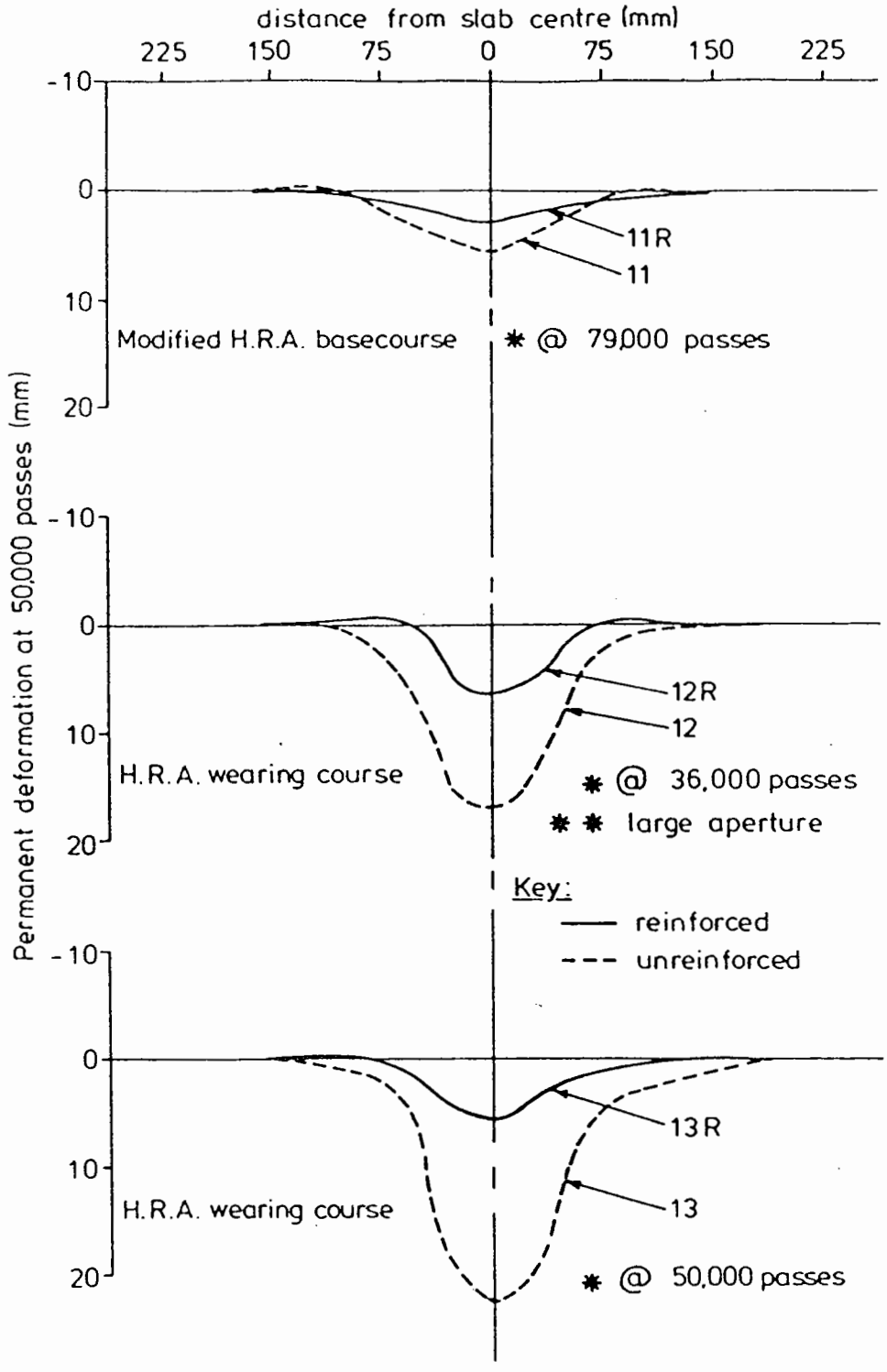

Fig. 6.14 Rut profiles for slabs 11 to 13R

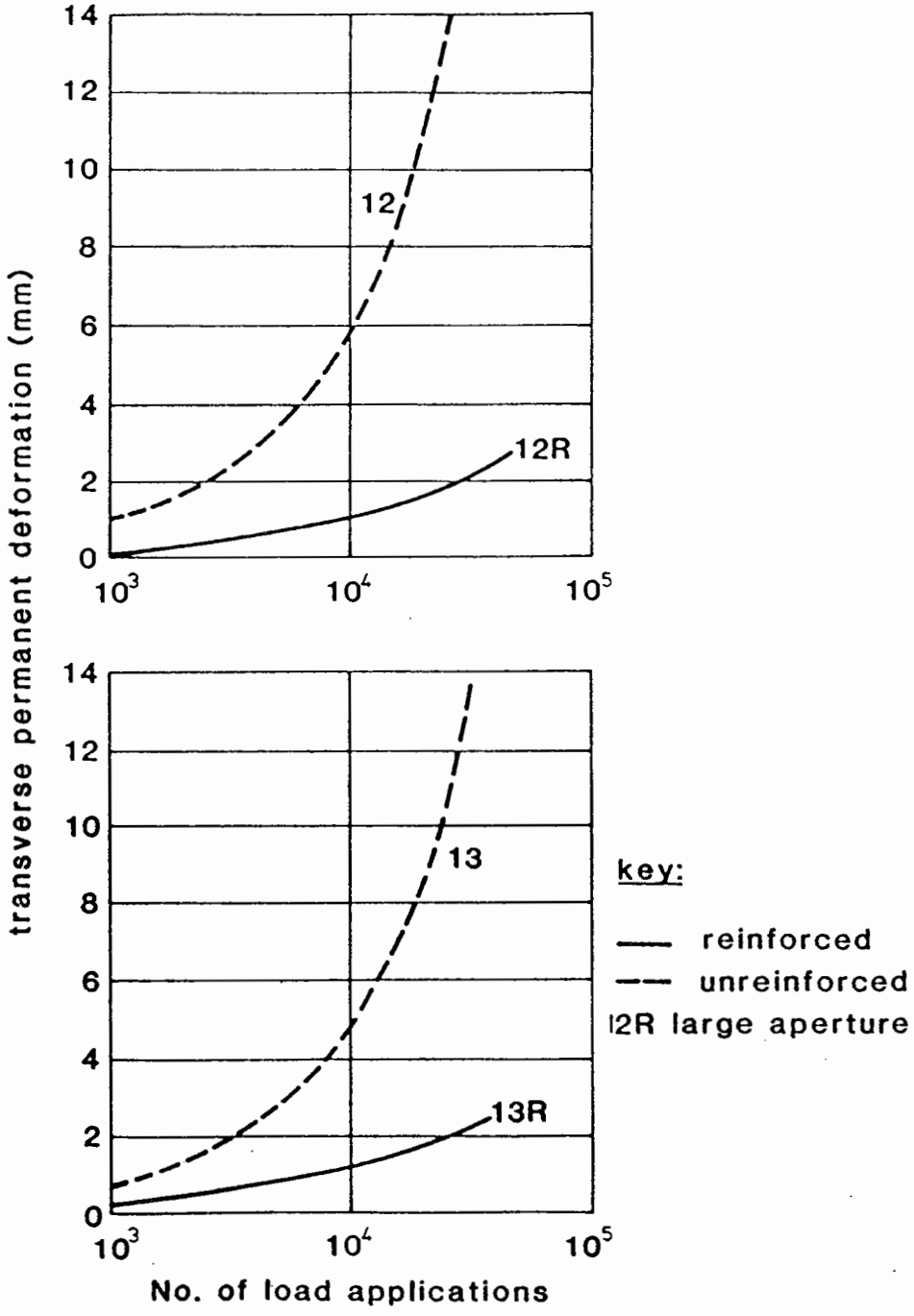

Fig. 6.15 Development of transverse permanent deformation

7. CONSTRUCTION IN THE PAVEMENT TEST FACILITY

7.1 INTRODUCTION

The Pavement Test Facility (P.T.F.) was used to study two pilot scale pavements. In each of the constructions the behaviour of an unreinforced section was compared to that of a reinforced section or sections.

The first pavement constructed was a full depth asphalt design. The pavement was divided into two halves, one half was reinforced with "Tensar" SS3 at the base of the asphalt layer, and the other half was unreinforced. The unreinforced half shall be referred to as P1, the reinforced half as P1BR (the appendix BR signifying Bottom Reinforcement). After testing was concluded on the full depth pavement it was overlayed with a wearing course. A second layer of grid was included at the interface of the overlay and the existing pavement on section PIBR.

The second pavement consisted of a thin aphaltic concrete layer on a foundation of low stiffness. This was subdivided into three sections. One section, P2, was unreinforced, and one section P2BR was reinforced with "Tensar" AR1 at the base of the asphalt layer and the third section, P2MR, was reinforced at the mid depth of the asphalt layer.

A Falling Weight Deflectometer (F.W.D.) (Bohn et al 1972), was used to determine the values of insitu stiffnesses of both the pavements. These results are discussed separately in Appendix F.

7.2 FULL DEPTH ASPHALT PAVEMENT

The work carried out in the P.T.F., investigated the performance of the pavement, first, the grid was placed between a clay subgrade

and a stiff asphalt base, and secondly when it was placed between the asphalt base and a wearing course. These locations were chosen as they represent practical levels for grid installations on site.

The first experiment was to study any increase in load spreading ability of the reinforced base, while the overlay trial was to study rutting resistance as an extension to earlier work on simple slabs. The previous philosophy of testing unreinforced and reinforced structures under the same test conditions was adopted to compare performance directly.

7.2.1 Pavement construction

The general construction of the pavement, and the location of instruments is shown in Fig. 7.1. The pavement consisted of 150mm of Dense Bitumen Macadam (D.B.M.) compacted directly onto the parent material in the pit which was a Keuper Marl. The dimensions of the concrete test pit in the P.T.F were 4.5m x 2.4m x 1.5m deep.

The pavement was divided into two sections of equal length (2.25m). One section (P1BR), was reinforced with the polymer grid at the base of the asphalt layer and one section (P1) remained unreinforced. The grid was held in position on the subgrade with hooks pushed into the clay.

The pavement was subsequently overlaid with 40mm of hot rolled asphalt (H.R.A.) wearing course. A layer of grid was included at the bottom of the wearing course in section P2BR. This was pinned to the existing pavement using road nails. The finished pavement is shown in Fig. 7.2 and the grid, fixed at one end with a metal bar, is illustrated in Fig. 7.3.

7.2.1.1 Subgrade Details

The liquid limit of the Keuper marl was 35% and the plastic limit 18%. The top 350mm of the Marl which had dried beyond the plastic limit, was removed and replaced with new material at a moisture content of between 18% and 19%. The C.B.R of undisturbed samples taken from this newly placed layer were between 3% and 4%.

7.2.1.2 Dense Bitumen Macadam Base

The D.B.M. base course was compacted in two lifts of 70mm using a single drum vibrating roller. The D.B.M. complied with BS 4987 Table 7. An analysis was conducted on cores taken from the pavement and the results are shown in Table 7.1. Uniaxial stiffness testing was conducted on cores, the results are again presented in Table 7.1. This was achieved by glueing end platens to asphalt cores approximately 150mm long and 100mm in diameter. The cores were subjected to a uniaxial load in a servo hydraulically controlled testing rig. The uniaxial load was monitored through a load cell incorparated into the testing rig, and the uniaxial strain recorded through two L.V.D.T.s attached to location pips glued to either side of the asphalt core.

7.2.1.3 Hot Rolled Asphalt Wearing Course

The H.R.A. wearing course was compacted in one 40mm lift using a single drum vibrating roller. This mix complied with BS 594 Schedule 1A. Samples of the mix were analysed and the results are presented in Table 7.1.

7.2.2 Instrumentation

The layout of instrumentation is shown in Fig. 7.1. Both reinforced and unreinforced sections were instrumented using

Table 7.1 Details of Bituminous Mix

1. Basecourse:

Specification: B.S. 4987 Table 9
Binder Content: 3.8%
Grading: continuous
Max. particle size: = 20mm

Average of measurements of 3 sets of cores after testing.

Position	Void Content %		Thickness (mm)		Stiffness at 10HZ (GPA)	
	Reinforced	Unreinforced	Reinforced	Unreinforced	Reinforced	Unreinforced
loaded area	2.5	2.0	122	122	6.0	6.3
unloaded area	4.6	3.6	141	142	5.7	10.0

2. Wearing course

Specification = B.S. 594 Schedule 1A
Binder content = 7.9%
Grading = Gap, 30% stone, 8.9% filler
Max particle size = 14mm

Note:- It is difficult to obtain satisfactory cores from a 40mm layer so analysis as with the basecourse was not carried out.

diaphragm pressure cells developed at Nottingham, and Bison soil strain coils (Brown et al 1981).

The diaphragm pressure cells were calibrated in clay and granular material by previous researchers, (Brown et al 1980) and a correction factor was produced for each material. The pressure cell underregisters in the clay and the factor applied to the recorded stress was 1.09. The factor for the subbase was 1.0.

A soil strain coil pair measures movement between two unattached coils on the electromagnetic inductance principle. Various sizes of coil are available and will measure movements over differing separations. The coils in this case were 25mm diameter and approximately 5mm thick. Each coil has several hundred copper windings, contained in an epoxy protective coating. One of the pair is activated by a constantly fluctuating current and this induces a signal in the passive coil, the magnitude of which is a function of the physical separation of the coils.

Three pressure cells were placed in each section, in the subgrade layer, 38mm below formation level. They were orientated so as to measure vertical transient stress. Two pairs of coaxially aligned strain coils were set into the subgrade in each section to measure vertical and lateral (radial) strain. The latter were offset from the centre line because of space limitations, but were directly under the wheel at regular intervals during the tests. Two pairs of strain coils, aligned in the coplaner manner, were placed at the subgrade/asphalt interface in each section in order to measure tensile strain at the bottom of the asphalt layer. They were covered with a fine asphalt mix, prior to paving, for protection.

A further two pairs of strain coils in each section were glued to the surface of the D.B.M. base, along the wheel track, after tests on the base were completed. The coils and cables were protected with

a fine H.R.A. mix before the overlay was added.

Permanent deformation was recorded at intervals during the test on the grid shown in Fig. 7.4(a). Deformation was recorded using a profilometer which consisted of an L.V.D.T. mounted on a beam which was maintained at a fixed height above the surface of the pavement.

7.2.3 Test conditions

The wheel loading was maintained at 8.3kN at a speed of 8km/hr throughout the test.

7.2.3.1 Tests on D.B.M. Base

The trafficking was carried out at four temperatures, 17^{o}C, 22^{o}C, 38^{o}C and 34^{o}C. There were approximately 10,000 passes of the wheel for each temperature. This total was applied to nine positions at 75mm centres as shown in Fig 7.4(b), and approximated to a normal distribution of load applications.

7.2.3.2. Tests on Overlay Construction

The tests were carried out at 28^{o}C and 35^{o}C until 50,000 and 91,000 passes respectively of the wheel had been completed. The transverse distribution of the wheel remained unaltered for these tests.

A final single track test, with the wheel only in the central location, was conducted for a further 10,000 passes at 35^{o}C.

7.2.4 Results

Results from the insitu measurements obtained during testing are presented separately for each temperature and for the base and overlay constructions. Surface permanent deformation was the major method of assessing the performance of the reinforced structure, this

was supplemented by the permanent and elastic strain readings from the strain coils, and the transient stresses from the pressure cells in the subgrade.

7.2.4.1 D.B.M. Base

7.2.4.1.1 Permanent deformation

Fig. 7.5 shows the build up of permanent deformation in the wheel track for each of the test temperatures. The results show a similar performance for both reinforced and unreinforced sections. Only at 34^{o}C, when the asphalt stiffness was reduced, and the magnitude of permanent deformation was greater, did any benefit become apparent from including the grid.

7.2.4.1.2 Permanent strain

The permanent strains recorded in the subgrade and asphalt at 10,000 passes for each test temperature is given in Table 7.2. The vertical strains shown was the average of two readings in each section. One pair of coils measuring radial strain in the subgrade reinforced section failed during the test at 34^{o}C, and only intermittent readings were obtained from one of the coils in the asphalt in the unreinforced section measuring radial strain. This may unbalance the results for the radial strains and the vertical subgrade strains are likely to be the most reliable.

The vertical permanent subgrade strains are of a similar order for the reinforced and unreinforced sections. At higher temperatures a lower proportion of the vertical permanent strain occured in the subgrade and a higher proportion occured in the asphalt layer.

7.2.4.1.3 Elastic Response

The elastic response was measured by the pressure cells and strain

Table 7.2 Permanent Strains at 10000 passes

(radial strains about subgrade/base interface)

Temp (°C)	Vert. subgrade strain (%)		radial subgrade strain (%)		radial asphalt strain (%)	
	Reinforced	-	Reinforced	-	Reinforced	-
17	0.48	0.12	-0.04	-0.04	-0.09	-0.04
22	0.93	1.21	-0.23	-0.24	-0.70	-0.40
28	0.50	0.49	-0.35	-0.36	-0.60	-0.41
34	0.32	0.28	0.00	-0.32	-0.28	-0.05

coils under the moving wheel load. Averages of the pressure cell and strain coil readings in the reinforced and unreinforced sections are given in Tables 7.3 and 7.4. Subgrade vertical stresses and strains in each section were almost identical, indicating that the grid did not increase the elastic stiffness of the asphalt.

Radial elastic strain readings (Table 7.4) were also similar for the reinforced and unreinforced sections, although less reliable. The soil strain coils, when placed close to the subgrade surface and directly under the hot asphalt mix, are vulnerable to the high local movements during laying and rolling. This may lead to faulty electrical connections to the coil, and may explain the occasional loss of signal.

An elastic analysis of the pavement structure as carried out by the F.W.D. is presented in Appendix F.

7.2.4.2 Overlay construction

7.2.4.2.1 Permanent deformation

When the wearing course overlay was added to the base, the accumulated surface deformation from the previous tests of over 16mm was eliminated. The ensueing deformation is shown in Fig. 7.6. The test temperature was 28^{o}C. Results are also shown for the 10000 passes at 35^{o}C, and for the single track test.

Slightly less deformation occurred in the reinforced section for the multitrack test but this trend was amplified considerably when single tracking was introduced.

The permanent strains for these tests, reported in Table 7.5, were recorded at 10,000 passes in order to be compatible with Table 7.2. The general trends are consistent with those in Table 7.2, for example the gradual decrease in vertical subgrade permanent strain as the test progressed and as the asphalt temperature increased.

Table 7.3 Subgrade Vertical Stress and Strain Pulse Values.

Temp (°C)	transient stress (kPa)		elastic strain (microstrain)	
	Reinforced	-	Reinforced	-
17	24	23	530	470
22	34	32	2900	2900
28	50	51	3400	2900
34	98	100	3700	3700

Table 7.4 Elastic Radial Strains.

Temp (°C)	elastic radial Top of subgrade (microstrain)		strain radial Bottom of base (microstrain)	
	Reinforced	-	Reinforced	-
17	-150	-150	-170	-140
22	-1000	-1000	-	-1500
28	-1500	-1300	-1900	-1700
34	-1800	-2600	-1800	-2300

Table 75 Permanent Strains at 10000 passes (Overlay) .

Temp (°C)	Vert. subgrade strain (%)		Radial Strain (%)					
			Top of subgrade		Bottom of base		Bottom of wearing course	
	Reinforced	-	Reinforced	-	Reinforced	-	Reinforced	-
28	0.10	0.07	-0.01	0.00	0.00	0.01	-0.07	-0.23
34	0.00	0.02	0.05	0.00	-0.07	-0.03	-0.08	0.32

Table 7.6 summarizes all the permanent strain data at the end of each test.

7.2.4.2.2 Elastic Response

The vertical transient stresses and elastic strains recorded are shown in Table 7.7. By comparing Table 7.7 to Table 7.3, it can be seen that the overlay reduced the magnitudes substantially. A similar trend can be seen for the subgrade and subgrade/basecourse interface radial strains, for example compare Table 7.8 with Table 7.3. Again transient stresses are almost identical for both the reinforced and unreinforced sections, although small reductions in the reinforced elastic strains were observed. This trend was reversed for the radial elastic strains at the wearing course-basecourse interface. Taken overall, the elastic response of the reinforced pavement was similar to that of the unreinforced structure.

7.2.5 Excavation of the pavement

In order to recover and examine the grid it was necessary to remove the asphalt layer which was approximately 180mm thick in total. It was decided to saw this out in blocks rather than use a pneumatic chisel (breaker) in order to reduce the dust hazard and to ease disposal. A problem did arise in that the saw blade only cut to a depth of 154mm but this was overcome by levering and rocking the sawn bocks until they separated.

Sawing also required the use of cooling water which drained away during this process but saturation of the clay surface was unavoidable. However, once the surface was exposed a clear imprint of the grid in the clay could be seen and the grid had to be forced

Table 7·6 Permanent Strain (%) at the completion of all tests.

	No of passes	Temp (°C)	ε_v subgrade		ε_r subgrade		ε_r basecourse		ε_r overlay	
			reinf.		reinf.		reinf.		reinf..	
Before overlay	16,000	17	0.64	0.26	-0.06	-0.04	-0.09	-0.04		
	10,000	22	0.93	1.21	-0.23	-0.24	-0.71	-0.4		
	20,000	28	0.60	0.62	-0.47	-0.52	-1.13	-0.65		
	100,000	34	0.33	0.28	0	-0.32	-0.39	-0.36		
with overlay	50,000	28	0.22	0.09	0	-0.06	0	0	-0.22	-0.63
	91,000	34	+0.15	0.18	+0.17	+0.05	-0.07	0	-0.69	-0.51

Table 7.7 Subgrade Vertical Stress and Strain Pulse Values (Overlay)

Temp (°C)	transient stress (kPa)		elastic strain (microstrain)	
	Reinforced	-	Reinforced	-
28	37	35	930	960
35	78	75	2400	2100

Table 7.8 Elastic Radial Strains (Overlay)

Temp (°C)	microstrain					
	Top of subgrade		bottom of basecourse		bottom of wearing course	
	Reinforced	-	Reinforced	-	Reinforced	-
28	-450	-520	-520	-530	-605	-554
35	-1100	-1200	-1200	-1300	-1263	-1070

off the asphalt base during separation of the blocks. A well defined impression of the grid was also left on the bottom of the asphalt. The asphalt blocks were a combination of the base and wearing course lifts and during levering with a long crowbar occasional separation occurred along the reinforced interface. The grid under these circumstances remained attached to the detached wearing course section. A similar separation was not seen for the unreinforced blocks which may have been indicative of a more satisfactory bond. Examination of the grid at both levels did not reveal any significant distortion in the aperture size or shape.

7.3 THIN ASPHALT CONCRETE PAVEMENT ON SOFT SUPPORT

Full scale trials and laboratory simulations (Milligan et al 1984) have shown that to make a positive contribution towards permanent deformation in a pavement constructed with reinforcing membranes located in the lower layers of a pavement, significant deformations must first occur. As deformation develops, the tensile strength of a geomembrane confines the construction materials and, hence, limits further strains. From the previous construction in the P.T.F. it was evident that unless high shear strains were developed no resultant benefit would be gained from including the grid.

Severe premature fatigue cracking usually occurs where a pavement structure is not sufficiently adequate to prevent high levels of tensile strain occuring at the base of the layer. In this situation a tensile element at the base of the asphalt layer may hold the base together, such that fatigue cracking should either take longer to propagate to the surface, or be less severe.

A pavement susceptible to high permanent and elastic

deformations was constructed in the P.T.F. to investigate these phenomena.

A thin asphaltic concrete pavement with a granular subbase was constructed over a very soft clay. By reinforcing the construction at two different positions, (sandwiched in the middle of the asphalt layer and at the base of the asphalt layer), and also constructing an unreinforced control section, the effect of the grid was observed. The three sections were constructed as part of the same pavement in the P.T.F., each section being 1.330m long. Each section was instrumented and vertical stresses and strains were recorded in the subgrade and subbase. Strain transducers also recorded radial strain at the bottom of the asphalt layer.

The bituminous mix used in the construction was designed to represent, as closely as possible, a typical asphaltic concrete, and was mixed at a local quarry. The grid used in the test was "Tensar" AR1.

An F.W.D. was available after testing was completed, and it was used to assess the insitu values of stiffness for the pavement in the manner developed for site use. The results are presented together with data from the previous pavement in Appendix F.

7.3.1 Pavement construction

The general construction of the pavement is shown in Fig. 7.7. The pavement consisted of 80mm of asphaltic concrete, 100mm of lightly compacted Type 1 subbase, and 50mm of soft Keuper marl. The parent material in the pit was also Keuper marl.

The pavement was divided into three sections of equal length (1.330m.), two sections were reinforced and one, control, remained unreinforced. Each section is described and refered to as follows:-

(a) Section P2 - This was the control section and was

unreinforced.

(b) Section P2MR - A layer of grid was included at mid-depth in the asphalt layer.

(c) Section P2BR - A layer of grid was included at the base of the asphalt layer.

7.3.1.1 Subgrade details

The surface of the marl had dried out and a hard crust had formed. This layer was removed and a C.B.R. of 8% was recorded before any further construction. The C.B.R. was measured using a hand operated proving ring penetrometer. This instrument records the maximum load required to push a cone of known dimensions into the soil, and was previously calibrated to convert this force into a C.B.R. value.

A 50 mm layer of soft clay was then lightly compacted onto the marl using a hand operated tamper The clay was delivered from a local brickworks and was extracted from the brick making process after the clay had been crushed and the moisture content increased, but before it had been extruded into brick form and allowed to dry. The clay, when first introduced into the pit, had a moisture content of between 25% and 27%, which gave it a very soft consistency. A small proportion of woodshavings were also present in the clay, having been added in the brickworks during remoulding.

Before any compaction was carried out on the clay, it was allowed to dry to a moisture content of between 21% and 22%. During this time, the parent material in the pit, (Keuper marl) softened considerably due to migration of water from the soft clay. This was discovered when placing the instrumentation in the subgrade at a later date.

The proving ring penetrometer was again used to evaluate the

C.B.R. of the soft clay, along the centre line of the pit (i.e. directly underneath the intended wheel track). Fig.7.7 shows the values of C.B.R. obtained for each section. Section P2, P2MR and P2BR had an average C.B.R. of 0.6%, 0.7% and 0.8% respectively.

7.3.1.2 Subbase details

The material used was a typical Type 1 granite subbase (Dept. of Transport 1976), supplied by a local quarry. The final layer thickness was 100mm and the maximum aggregate size 40mm. The material was placed in a loose state and lightly compacted with a hand pulled garden roller. Although this had no great effect on increasing the density of the subbase it produced a smooth surface on which the grid could easily be placed in Section P2BR, and onto which the asphalt could be laid.

A nuclear density meter was used to evaluate the insitu bulk density and moisture content of the material. Seven readings were taken at various positions over the pit and the average reading of bulk density was measured as 1480 kg/m^3. The minimum reading obtained from the nuclear density meter was 1346 kg/m^3 and the maximum 1523 kg/m^3. The nuclear density meter also estimated the average moisture content at 6.9% and the average dry density at 1384 kg/m^3.

An estimation of the bulk density for the subbase was obtained using a manual method. A box of known volume (300 x 300 x 250mm) was filled with the lighly compacted material, level with the top. Knowing both the weight of the box empty, and full, the weight of subbase was easily calculated. This weight divided by the known volume gave the bulk density, which was 1539 kg/m^3. (This was an average of three measurements). Although compaction for both cases, in the pit, and in the box, were not identical it was assumed they were similar enough for the comparative data to be useful.

The bulk densities obtained using the nuclear density meter and the manual method therefore agree to within 4% of each other.

7.3.1.3 Asphaltic concrete layer

The material used in the bound layer was a continuously graded asphaltic concrete. This material was designed using the "Marshall method" (The Asphalt Institute 1984) and mixed and delivered by a local quarry. A sample of the material, as delivered, was analysed in the laboratory and the grading curve achieved as shown in Fig. 7.8 with the mix details. The binder content was approximately 5% and the void content was 8.8%. The void content was measured from cores extracted from undisturbed areas of the pavement after testing.

The bound material was compacted in two 40mm layers using a single drum pedestrian controlled vibrating roller. The delivery temperature was 140^{o}C which was maintained throughout the construction period.

In section P2BR the grid was placed at the bottom of the asphalt layer and was installed several days before the delivery of the asphalt. The grid was loosely held down onto the subbase with some of the granular material and coated with a layer of 100 pen bitumen, poured from a watering can, adapted by attaching a spreader bar to the spout. 6.3 mm chippings were then spread on the hot bitumen. The "chip seal" technique of grid installation in this situation did not seem an efficient method of bonding the grid to the surface of the subbase. (The purpose of the "chip seal" technique is to prevent the grid distorting during paving under the action of the paving train of delivery lorries) The subbase presented an uneven surface on which to bond the grid and the chippings were too small. The rate of spread of chip seal on this particular asphalt was in excess of 3 litres/m^2 and of chipping 15kg/m^2 compared to the more usual 1.2

litres/m^2 and 5.4kg/m^2. It has subsequently decided that 10-14mm chippings would have been more suitable, as these would protrude far enough above the grid to prevent traffic from acting on it.

After compacting the first layer of asphalt, the grid was installed in section P2MR, again using the chip seal technique. Since the asphalt on which the grid was being placed was still hot the 100 pen. bitumen used in the chip seal did not cool as quickly as it might have under normal circumstances. The grid therefore had to be held flat on the ground while the bitumen hardened sufficiently. No difficulty was encountered compacting the top layer of asphalt on to the grid.

7.2.3 Temperature of grid and asphalt during and after construction

A number of thermocouples were attached to the grid, and at various depths in the pavement during construction. These thermocouples monitored the temperature of the grid and asphalt during and after paving.

The asphalt was delivered in an insulated lorry, covered by a tarpaulin which maintained the temperature of the asphalt at 140^{o}C. The asphalt was moved from the lorry to the pavement in wheel-barrows and had, therefore, cooled slightly before comming into contact with the grid.

Fig. 7.9(b) shows the positions of the five thermocouples used and the temperature decay recorded during paving. Thermocouples 1 and 2 were attached to the grid at the asphalt/sub-base interface with insulating tape. Thermocouple 3 was also at the asphalt/subbase interface although it was not attached to the grid. Thermocouples 4 and 5 were placed at the asphalt/asphalt interface with 4 taped to the grid in this position. When the first 40mm layer of asphalt was placed, the temperature of the grid at the asphalt/subbase interface

fell from 90^{o} to 50^{o} in less than one hour. When the second (top) layer of hot asphalt was placed, the temperature of the lower layer rose, along with the temperature of the grid in this layer until the temperatures throughout the depth of the pavement were similar. The temperature of the pavement, both at the mid-depth position and at the base, decayed at the same rate for approximately 18 hours until equilibrium with ambient temperature (20^{o}C) was reached.

7.3.3 Instrumentation

Each of the three sections, P2, P2MR and P2BR were instrumented using diaphram pressure cells and Bison soil strain coils. Strain transducers were also positioned at the base of the asphalt layer in two of the sections, P2 and P2MR. The general layout is show in Fig. 7.10. The strain coils were positioned in three locations: the top of the subbase, the top of the soft clay layer, and 100mm into the subgrade. Duplicate values of strain were measured in each section. Because of the large aggregate size in the subbase (40mm) the coils set in this material were protected by surrounding them with a fine dust, passing 212μm.This is shown in Fig. 7.11.

In addition to their sensitivity to axial separation, the output from strain coil pairs is also affected by rotation of one coil relative to the other.

The pressure cells were located in the subgrade at the base of the soft clay layer and in the middle of the subbase layer Fig. 7.10. The pressure cells placed in the subbase were also protected with a surround of fine material which was held in position around the pressure cell by a "cling film" bag, (Fig. 7.12). This protection prevents large aggregate particles pressing on the cell diaphram. All the pressure cells and strain coils in each section of the pavement were located along the centre line of the wheel path.

Strain transducers (type FTCII, manufactured by Dynatest, Denmark) were used in sections P2 and P2MR, and were located as shown in Fig. 7.10, 345mm from the centre line of the wheel track. The transducer is I shaped,Fig. 7.13, and consists of steel end bars joined by a strip of epoxy fibre glass material. The epoxy fibre glass strip is straingauged so that it is most sensitive to tension, or axial strain, and the sensitivity to bending is attenuated although not totally eliminated.

Fig. 7.14 shows the strain transducer during installation, located on a bed of bitumen over the subbase. The transducer was subsequently covered with the bituminous mix before paving so as to protect it.

Calibration of the transducer should, ideally, have been carried out by embedding the instrument in an asphalt specimen with a similar stiffness and mix composition to that in the P.T.F. and subjecting the specimen to a known strain. This method would have eliminated any effects of slippage of the transducer or perturbation of the mix. As time would not permit this more thorough calibration, strains were calculated using the given strain gauge factor (2.0) of the transducer. This enabled the strain to be directly calculated from the change in resistance of the strain gauge. The acquisition of this data was further simplified through the use of carrier amplifiers, which enabled the value of strain to be directly output after presetting the gain on the amplifier. A peak catcher in this system allowed the elastic strain pulse to be recorded for two consecutive passes of the wheel. For each strain transducer, this was then automatically printed each time the system was powered.

The surface profile of the pavement was recorded using a profilometer (Fig. 7.15) consisting of a linear potentiometer mounted on a roller carriage which was driven by an electric motor across the

pavement. The profile was then drawn automatically by a pen recorder using the analogue output of the linear potentiometer on the carriage, and the elastic motor.

7.3.4 Test conditions

The load exerted by the rolling wheel on the pavement was 9 kN and the internal tyre pressure was 550 kPa. From a previous investigation into the effect of wheel tread, tyre wall strength, tyre pressure and load the contact pressure acting on the pavement was estimated to be 500 kPa, giving a radius of contact area (assuming this to be circular) of 75.7mm. The load was kept constant over the three test sections although some variation did occur due to the uneveness in the longitudinal profile of the pavement. Fig. 7.16 shows a typical plot of the load profile along the pavement. A slight discrepancy in the outward and return passage of the wheel can be seen. Two load profiles are shown, one at 1500 passes and one at 7500 passes. The load has been kept within 0.5kN of the target (9kN).

The wheel moved at a constant speed of 7 km/hr. The temperature of the pavement was kept at a constant 20^{o}C throughout the testing. It was observed that during long continuous runs of the P.T.F., the temperature of the asphalt in the wheel track increased by up to 5^{o}C, due to the repeated loading of the wheel. This may have reduced the overall expected life of the pavement. As elastic strain and transient stress pulses were usually taken early in any continuous run of the P.T.F., the temperature of the pavement can be assumed to have been 20^{o}C.

The total number of passes aapplied to this pavement was 200,000. During the first 100,000 passes the transverse position of the wheel varied, as shown in Fig. 7.17 (the distribution in Fig 7.17

was repeated every thousand passes). For the second half of the test, the wheel only tracked along the centre of the previous lateral distribution. This increased the severity of the test due to the concentration of the wheel in one track.

7.3.5 Results

7.3.5.1 Permanent deformation in the pavement

The permanent strains in the subgrade and subbase were recorded using soil strain coils, the positions of which were shown in Fig. 7.10. Duplicate readings of strain were recorded in the subbase and subgrade for each section; only the average values are given here. Table 7.9 shows the final total permanent strain for each section of the pavement. The accumulation of strain with the number of wheel passes is shown in Fig. 7.18. In each section, the permanent strains in the granular subbase were considerably higher, possibly due to its lightly compacted state.

The development of permanent strain in both the subgrade and subbase was least in sections P2BR. No abrupt change in rate of strain can be seen in this section and the values of strain at 200,000 passes are significantly lower than in the other two Sections.

Although the strain at 200,000 passes in the granular layer of section P2MR is similar to that in section P2, for the latter a rapid increase in strain rate develops towards the end of the test (see Fig. 7.18 (a) and (b)). This is seen again in the values of strain in the subgrade where, although the strain in the clay of section P2MR is higher in the earlier part of the test, there is no rapid increase in strain rate, as in P2. The sharp increase in strain rates for P2 occurred at approximately 150,000 passes when the bituminous layer was observed to crack along the shoulders of the

Table 7.9 Permanent strain and deformation in the Pavement

Section		Av. gauge length (mm)	Av. final strain (%)	Δl (mm)	ΣΔl (mm)	Av. Rut depth (mm)	Ratio of $\frac{\Sigma\Delta l}{\text{Rut depth}}$
P2	subgrade	116.57	15.9	18.53	38.64	54.3	0.71
	subbase	108.14	18.6	20.11			
P2MR	subgrade	118.15	8.8	10.40	31.68	40.2	0.79
	subbase	111.98	19.0	21.28			
P2BR	subgrade	125.34	5.2	6.52	17.97	23.7	0.76
	subbase	105.08	10.9	11.45			

rut. Cracking was first noticed in the wheel track of sections P2 and P2MR at between 20,000 and 30,000 passes. At 200,000 passes, the test had to be stopped as section P2 was becoming so badly deformed. In this condition the movement of the wheel was hindered and a uniform load profile impossible to maintain.

The transverse surface profiles were recorded throughout the test and are shown on Figs. 7.19 to 7.21. Two profiles were taken in each section. The vertical exageration (the ratio of vertical to horizontal scale) is 10.6. The extent of the transverse wheel distribution for the first 100,000 passes is also shown. Between 100,000 and 200,000 single track loading along the centre line was adopted. The photographs on Fig. 7.22 show the surface deformation for each of the three sections. From the profiles and observations, it is apparent that failure occured in P2 by cracking and shearing of the edge of the rut until the wheel punched through the bituminous layer. Shoulders either side of the rut only formed on this section.

Fig. 7.23 shows the development of permanent deformation plotted as rut depth, against the number of passes of the wheel. Each line is the maximum average rut depth averaged for the two profiles in each section. This measurement, therefore, includes any shoulder formation either side of the rut. For a critical rut depth of 20mm, section P2BR showed an increase in life of 2.7 compared to section P2.

The unreinforced pavement showed a rapid increase in rate of deformation between 100,000 and 150,000 passes when severe cracking along the shoulder and failure occured. Section P2MR showed a steady increase in rut depth but with no obvious impending failure although cracking along the shoulder did occur at a relatively early stage, at between 20,000 and 30,000 passes, as did the unreinforced pavement. The action of the reinforcement in this case kept the bituminous

layer intact.

Section P2BR had the lowest rate of permanent deformation and showed no visual signs of distress on the surface of the pavement at the end of the test. As a percentage of the rut depth in the unreinforced section, the rut depth in section P2MR and P2BR were 74% and 44% respectively at 200,000 passes.

The average permanent deformation in the subbase and subgrade ($\Delta 1$) at the end of the test is shown in Table 7.9, as recorded by the strain coils embedded in these layers. For each section of the pavement the ratio of the total recorded deformation in the subgrade and subbase to rut depth as measured by the profilometer is presented. These were 0.71, 0.79 and 0.76 for sections P2, P2MR and P2BR respectively. The deformation occuring in the subbase and the top 125mm of the subgrade therefore accounts for approximately 75% of the deformation at the surface of the pavement. Deformation, other than that recorded by the strain coils might occur at a greater depth than 125mm into the subgrade.

7.3.5.2 Elastic response of the pavement

Elastic strain and transient stress pulses under the rolling wheel were measured in the subbase and subgrade The elastic strain was also measured at the base of the asphalt layer using the strain transducer.

The average gauge length over which the strain coils measure is 110mm and, hence, an average value of strain only over this depth can be estimated. The properties of the subgrade varied considerably over this gauge length, since the layer of soft clay was only 50mm deep. The properties of the subbase were consistent with depth, although a strain gradient can be expected. The transient stress pulse, measured with the pressure cell, was, on the other hand,

recorded at a unique depth within the pavement. Typical recordings of strain pulses in the subgrade and subbase are shown in Fig. 7.24. Both the delayed and immediately recoverable (elastic) responses are illustrated.

The measured values of elastic strain in the subbase and subgrade for each section are presented in Table 7.10. (The instrumentation was not capable of recording strains greater than 8000$\mu\varepsilon$ and, where values obviously exceeded this, 8000$\mu\varepsilon$ is shown as the minimum value). Note should be taken of the values of C.B.R. obtained on the soft clay and shown in Fig. 7.1. For P2, P2MR and P2BR these were 0.7%, 0.6%, 0.8% respectively. The relative values of initial strain recorded in the subgrade reflect the C.B.R.'s, i.e. the highest value of strain was recorded in section P2MR (6142$\mu\varepsilon$) where the C.B.R. was lowest (0.6%).

As expected, the strains are higher in the top of the subgrade than in the subbase. Initially Section P2MR had the highest values of vertical strain and, therefore, the weakest foundation. (Some slight variability in the support conditions over the pavement area were unavoidable).

As the test progressed so too did the magnitude of resilient vertical strain, especially in Sections P2 and P2MR. The elastic subgrade strains exceeded 8000$\mu\varepsilon$ after 50,000 and 34,000 passes in Sections P2 and P2MR respectively and, by the end of testing, the elastic strains in the subbase were approaching or exceeding 8000$\mu\varepsilon$.

Section P2BR behaved in a different manner. The elastic strains in the subgrade and subbase increased only very slightly as the test progressed. The final elastic strains at the end of testing in the subgrade and subbase were 4490$\mu\varepsilon$ and 1577$\mu\varepsilon$ respectively compared to the initial values of 4117$\mu\varepsilon$ and 1452$\mu\varepsilon$.

Elastic radial strain at the base of the asphalt layer was

Table 7.10 Vertical elastic strain in the pavement and radial strain at the base of the asphalt layer ($\mu\varepsilon$)

No. of Passes	P2			P2MR			P2BR	
	εv	εv	εr	εv	εv	εr	εv	εv
	Subgrade	Subbase	asphalt	subgrade	subbase	asphalt	subgrade	subbase
1,000	4657	1058	270	6142	2012	370	4117	1452
4,000	5580	1245	270	6525	2344	370	4792	1452
7,000	6030	1411	-	7650	2573	-	4995	1577
14,000	6412	1763	-	7087	3112	-	4567	1577
20,000	6075	1900	-	6750	3112	-	5175	1618
28,000	6637	2261	350	6862	3693	450	5422	1826
34,000	6950	2241	410	>8000	3527	470	4860	1577
50,000	>8000	2100	440	>8000	3672	540	4455	1473
53,000	>8000	3200	400	>8000	3000	-	5195	2075
100,000	>8000	3500	410	>8000	4600	430	4410	2946
200,000	>8000	7500	180	>8000	>8000	100	4490	1599

measured only in Sections P2 and P2MR at a radial distance of 345mm from the centre of the wheel track, and values are shown in Table 7.10. (The strains measured were compressive. The sense of this strain was validated by analysing this structure theoretically using BISTRO (Peutz et al, 1968) - a linear layer elastic analysis, see Fig 7.25.) Compressive strains are evident away from the loaded area. The strains were initially higher in Section P2MR than in P2 (370$\mu\varepsilon$ compared to 270$\mu\varepsilon$), and increased as the test progressed. The strains in both sections reduced substantially from 410$\mu\varepsilon$ to 180$\mu\varepsilon$ in Section P2 and from 430$\mu\varepsilon$ to 100$\mu\varepsilon$ in Section P2MR, between 100,000 and 200,000 passes.

The stresses measured in the subgrade and subbase are presented in Table 7.11. As expected, higher stress levels were measured in the subbase. The pressure cell in the subbase of Section P2 failed after 20,000 passes. The initial magnitude of stresses in the subgrade were between 31kPa and 38kPa and increased slightly as the test progressed, to between 36kPa and 45kPa in all sections. The stress pulses measured in the subbase were more variable, intially 53kPa, 218kPa and 191kPa in Section P2, P2MR and P2BR respectively. The grid, when included at the base of the asphalt layer has therefore prevented any large increase in the magnitudes of vertical elastic strain in both the subgrade and subbase during the course of the test. This suggests that section P2BR pavement has still the same load carrying capacity as it had at the beginning of testing, and therefore the integrity of the asphalt layer has been maintained, with little or no fatigue cracking.

No significant difference between the vertical strains in the subgrade and subbase were noticed between sections P2 and P2MR. In this position the grid has had little effect on the propagation of cracks in the asphalt layer and consequently on the stiffness of the

Table 7-11 Vertical transient stress pulses in the subgrade and subbase (kPa)

No. of Passes	P2		P2MR		P2BR	
	σv Subgrade	σv Subbase	σv Subgrade	σv Subbase	σv Subgrade	σv Subbase
1,000	31	53	38	218	37	191
4,000	31	86	52	205	37	205
7,000	31	99	52	237	39	205
14,000	31	92	52	269	41	198
20,000	31	152	49	266	41	224
28,000	37	-	52	224	41	198
34,000	28	-	52	192	39	198
50,000	31	-	34	192	47	205
53,000	23	-	26	77	34	165
100,000	26	-	112	61	69	304
200,000	36	-	45	115	41	270

asphalt.

7.4 DISCUSSION AND CONCLUSIONS

In the full depth asphalt pavement the grid did not significantly improve the deformation resistance of a relatively stiff and deep bituminous layer when placed at the bottom of this layer on a subgrade of 3% to 4% C.B.R. There was some evidence of improved performance in the reinforced section when the base temperature was 34^{o}C. The loading positions were distributed over a 300mm width and deformations did not exceed 4mm for any single test.

A slight reduction in deformation was obtained when the grid was placed at the bottom of the 40mm overlay which was constructed from a more deformable mix.

The largest reduction in permanent deformation was obtained when the overlaid pavement was subjected to single track loading.

The grid did not cause any increase in the elastic stiffness of the reinforced layer so that transient stresses and strains were the same in reinforced and unreinforced structures.

Excavation of the pavement showed that the presence of the grid may reduce the strength of the interface between any overlay and its base. The excavation procedure did, however, impose quite severe conditions and more reliable data on this subject is reported in Chapter Eight.

The pavement constructed on a soft support has highlighted the importance of placing the grid in the correct position within a structure to obtain the maximum benefit. The pavement was constructed on a soft support, liable to large elastic and plastic deformations. The asphaltic concrete layer was therefore susceptible to cracking and rutting. Little benefit was realized initially by placing the grid in the middle of the asphalt layer, and

not until the pavement was severely cracked and rutted did the grid begin to inhibit any further deterioration.

When the grid was positioned at the base of the asphalt layer, a significant reduction in permanent deformation and increase in fatigue life was achieved. No cracking was noticed in this section at the conclusion of testing. The maximum tensile strains in a pavement are at the bottom of the asphalt layer, and consequently, with the grid in this position, the development of permanent strain was to a large extent prevented.

The increase in life for the section reinforced at the base of the asphalt layer, over the unreinforced section, was by factors approximately 3 and 10 for permanent deformation and fatigue cracking respectively. This agrees well with data produced from previous testing (Brunton and Brown 1984).

The grid was not affected by the temperature of the asphalt during paving. The grid temperature was monitered during paving and although the delivery temperature of the asphalt was 140^{o}C, the temperature of the grid did not rise above 110^{o}C, due to the cooling effect of the underlying layers, and the insulation of the "chip seal" layer.

The elastic and permanent strains developed during this test are significantly greater than those that might be expected in a heavy duty pavement. The results obtained should therefore only be applied to thin flexible pavements subjected to high loads or constructed on a weak foundation.

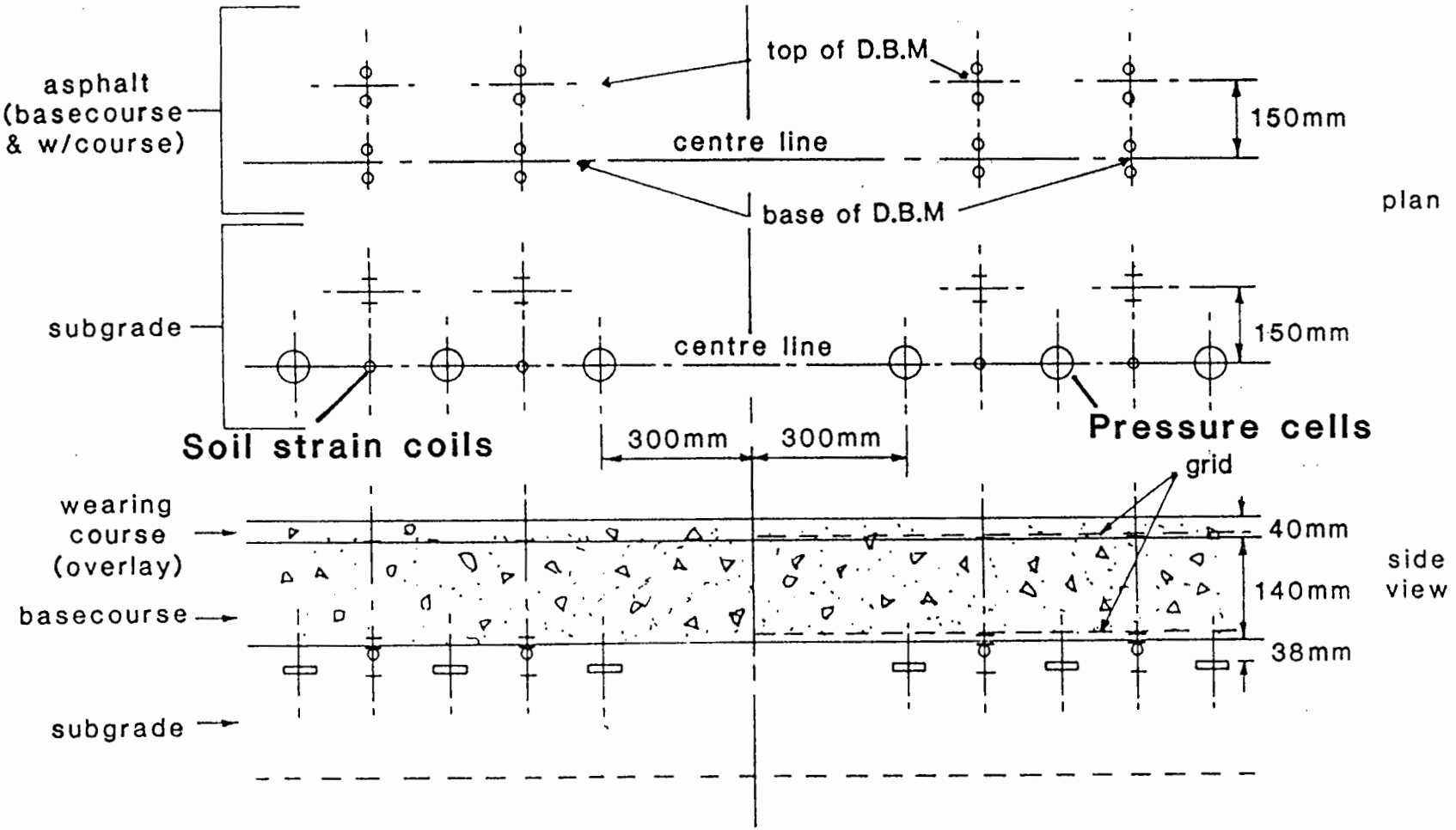

Fig 7.1 Pavement P1 Structure and location of instruments

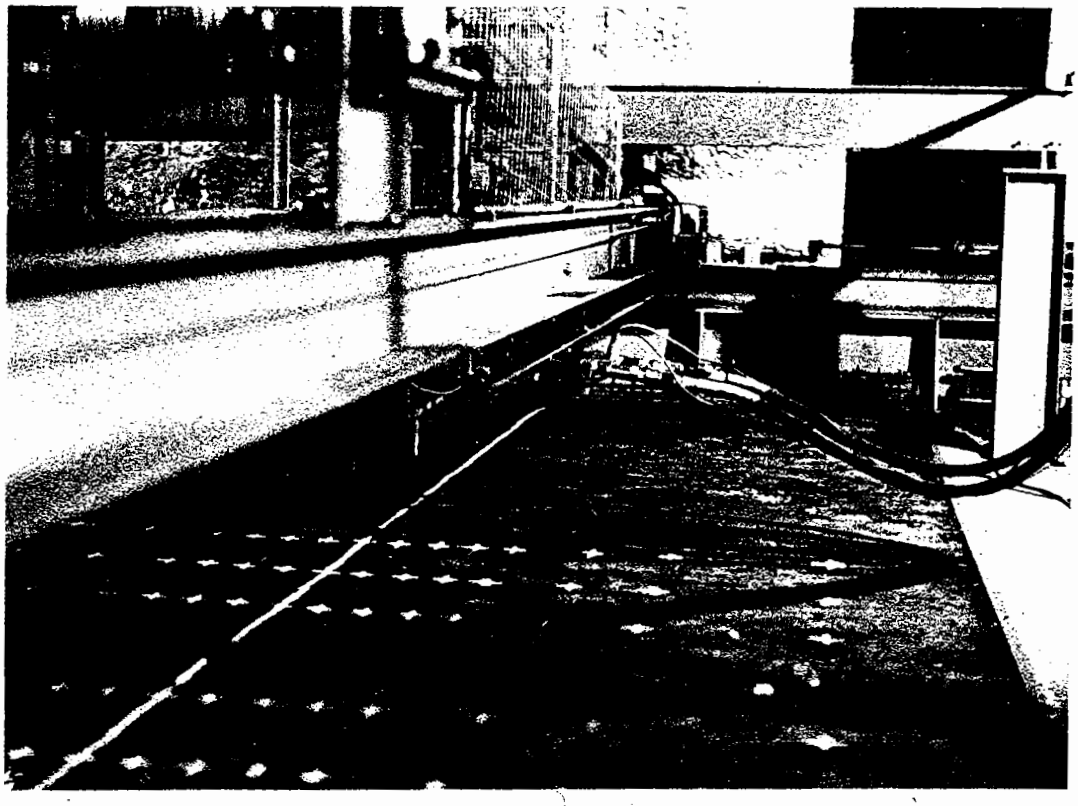

Fig. 7.2 The pavement test facility

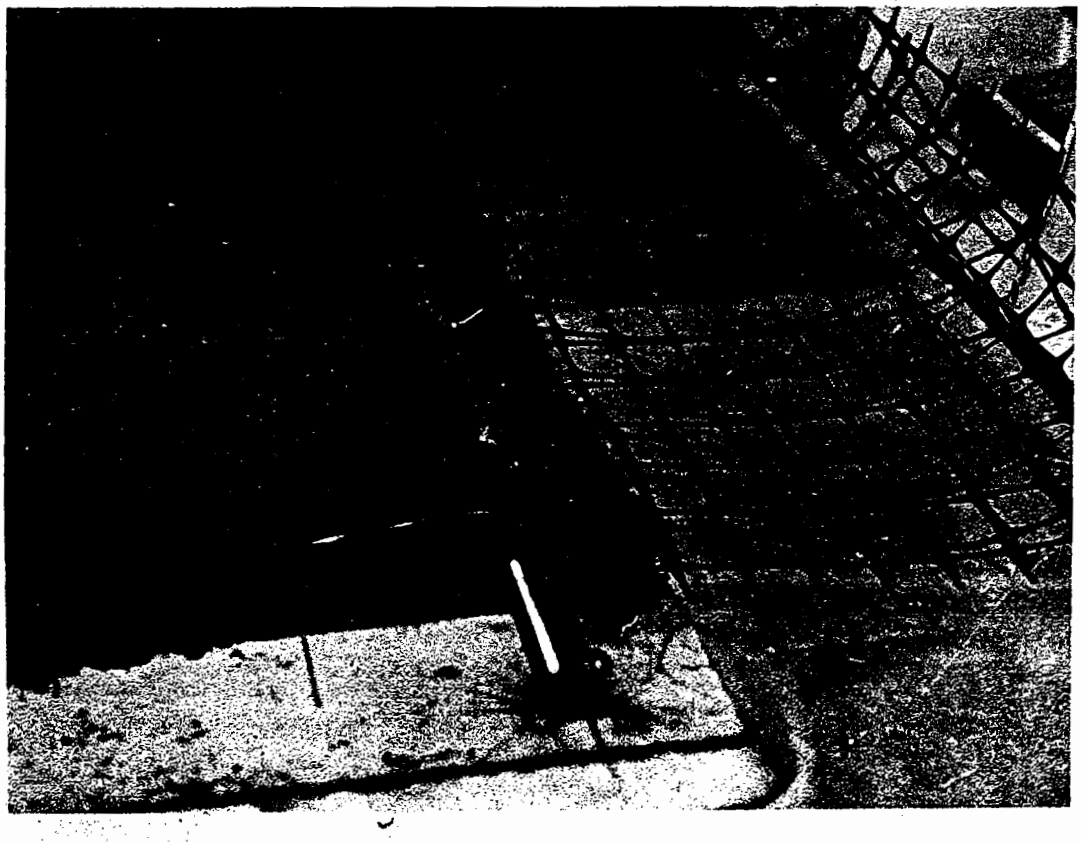

Fig. 7.3 Grid anchored with a reinforcing bar

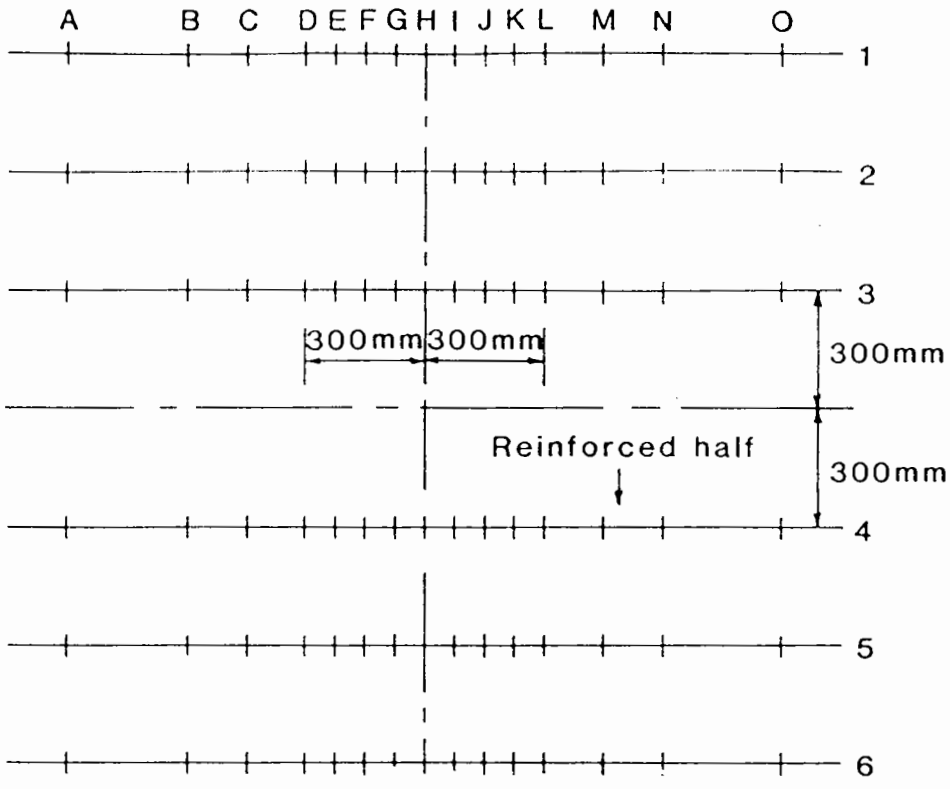

(a) Profilometer grid

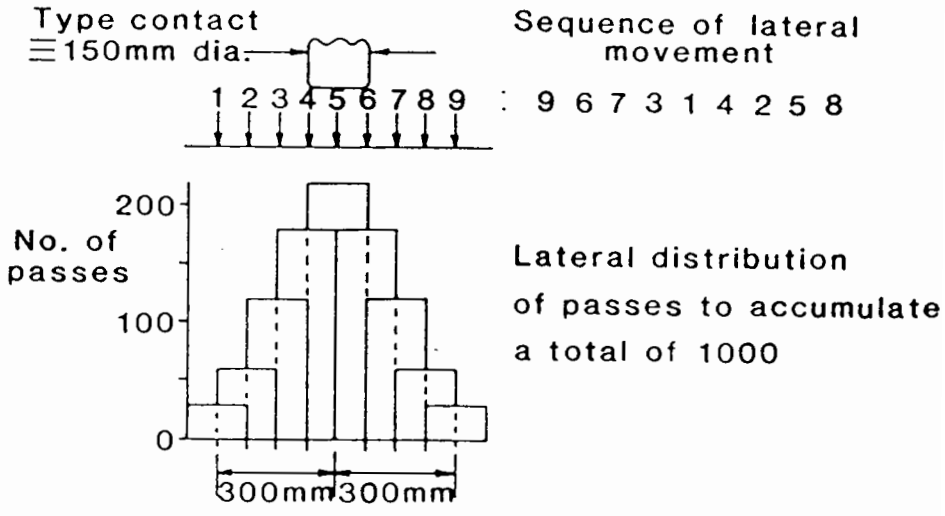

(b) Loading profile

Fig. 7.4 Profilometer grid and loading profile

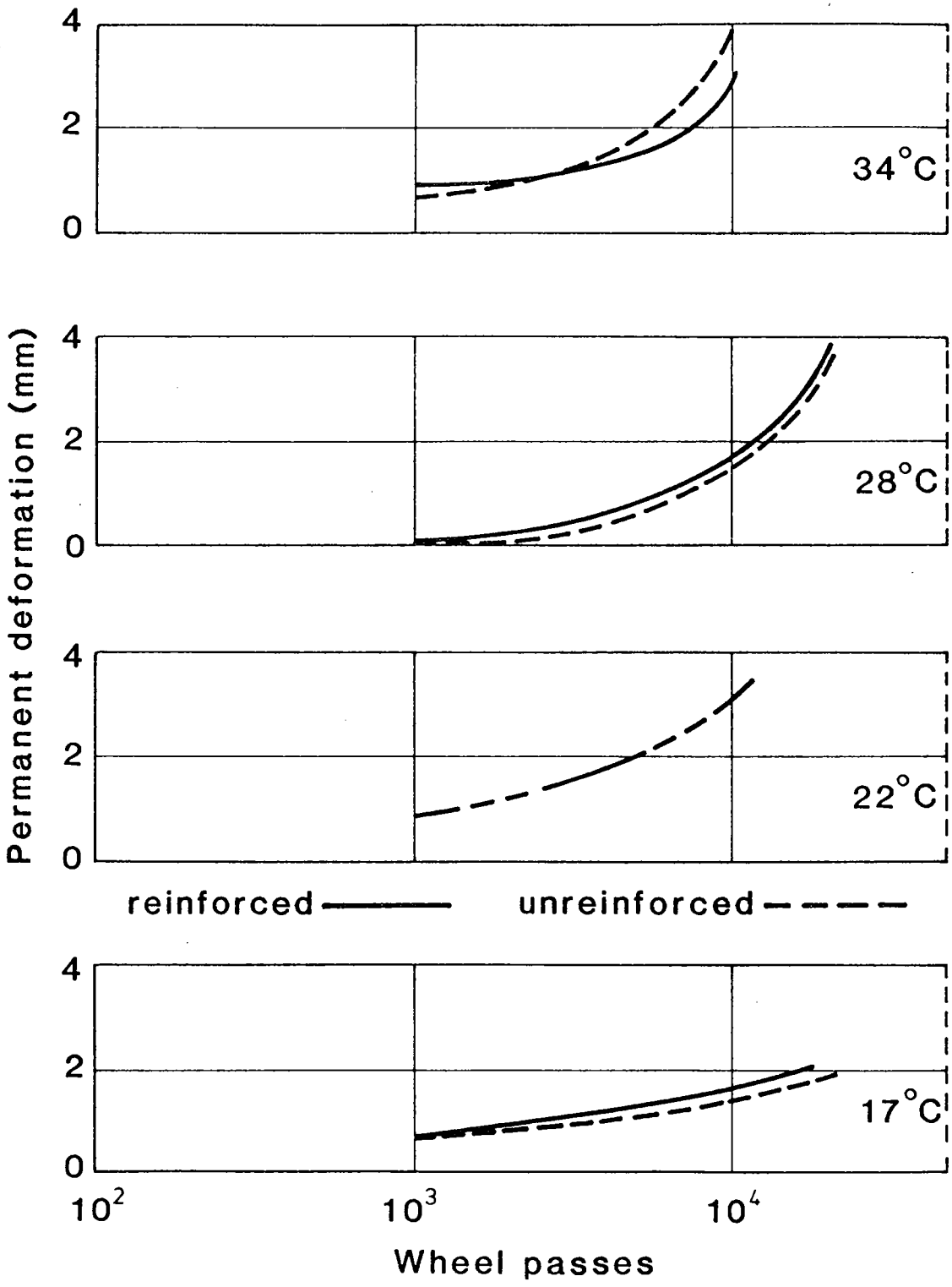

Fig. 7.5 Build up of deformation D.B.M. basecourse

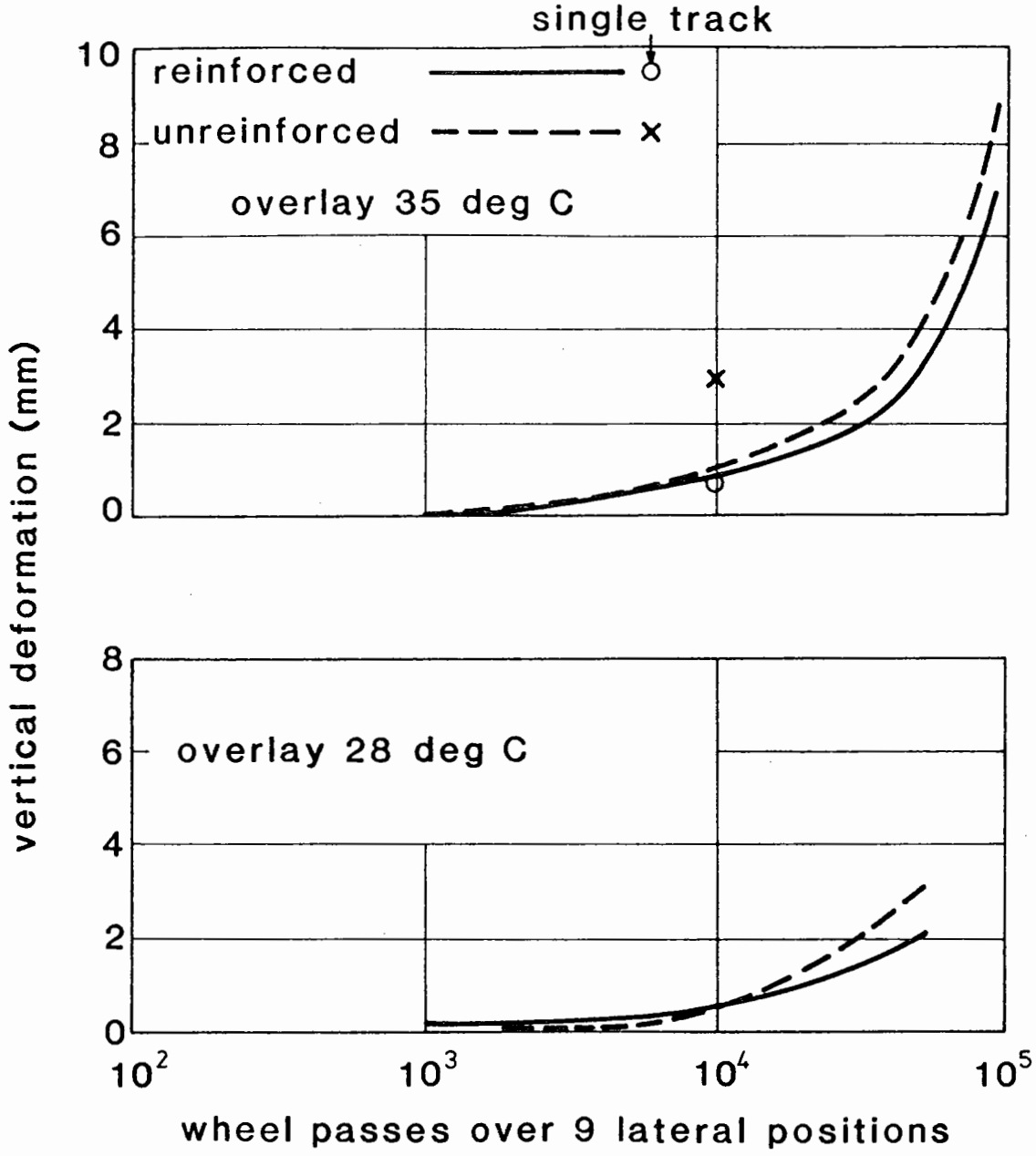

Fig. 7.6 Pavement central deformation

Overlayed construction

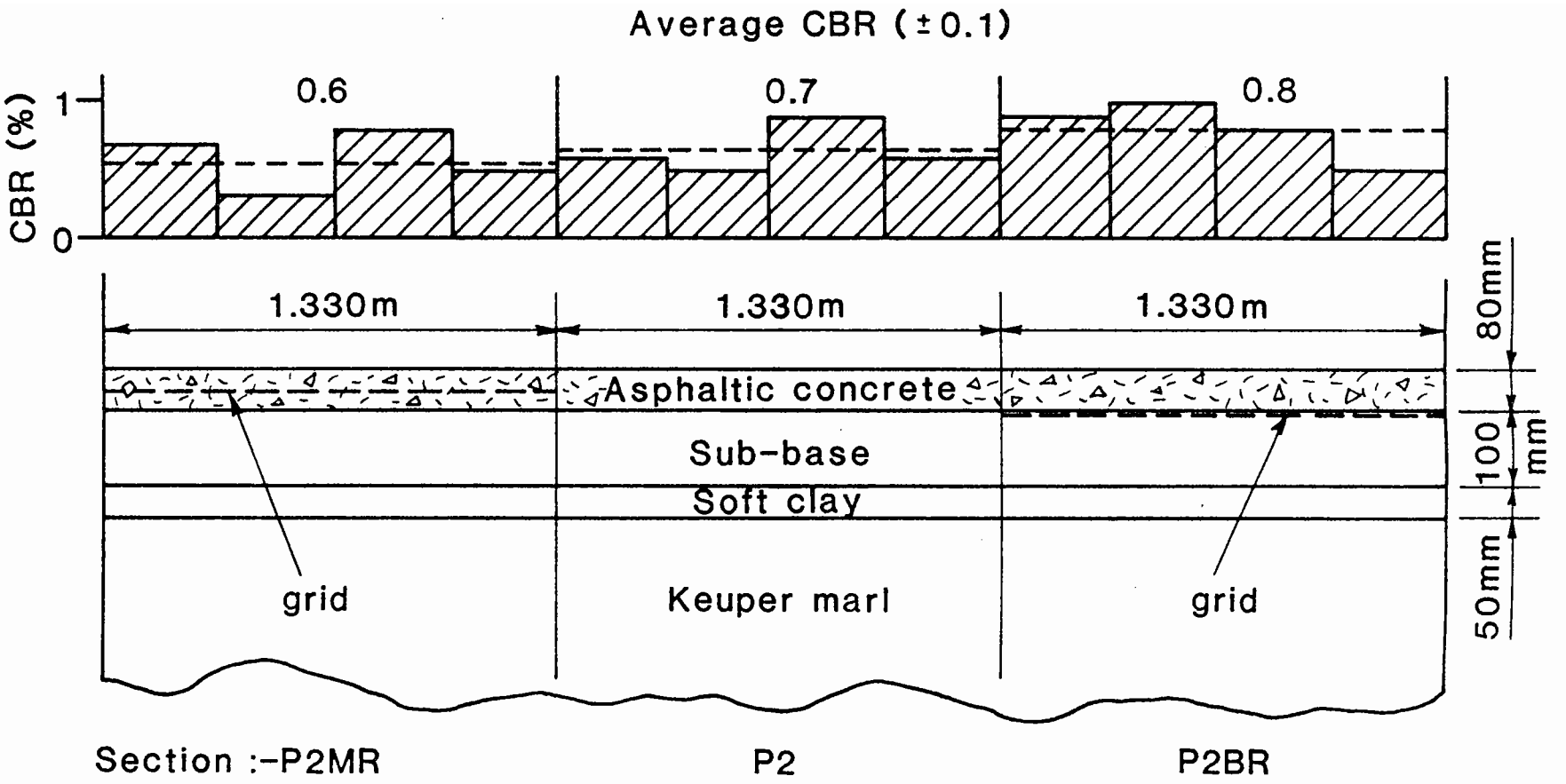

Fig. 7.7 General Experimental Arrangement in Pavement Test Facility and CBR Values of Soft Clay Layer

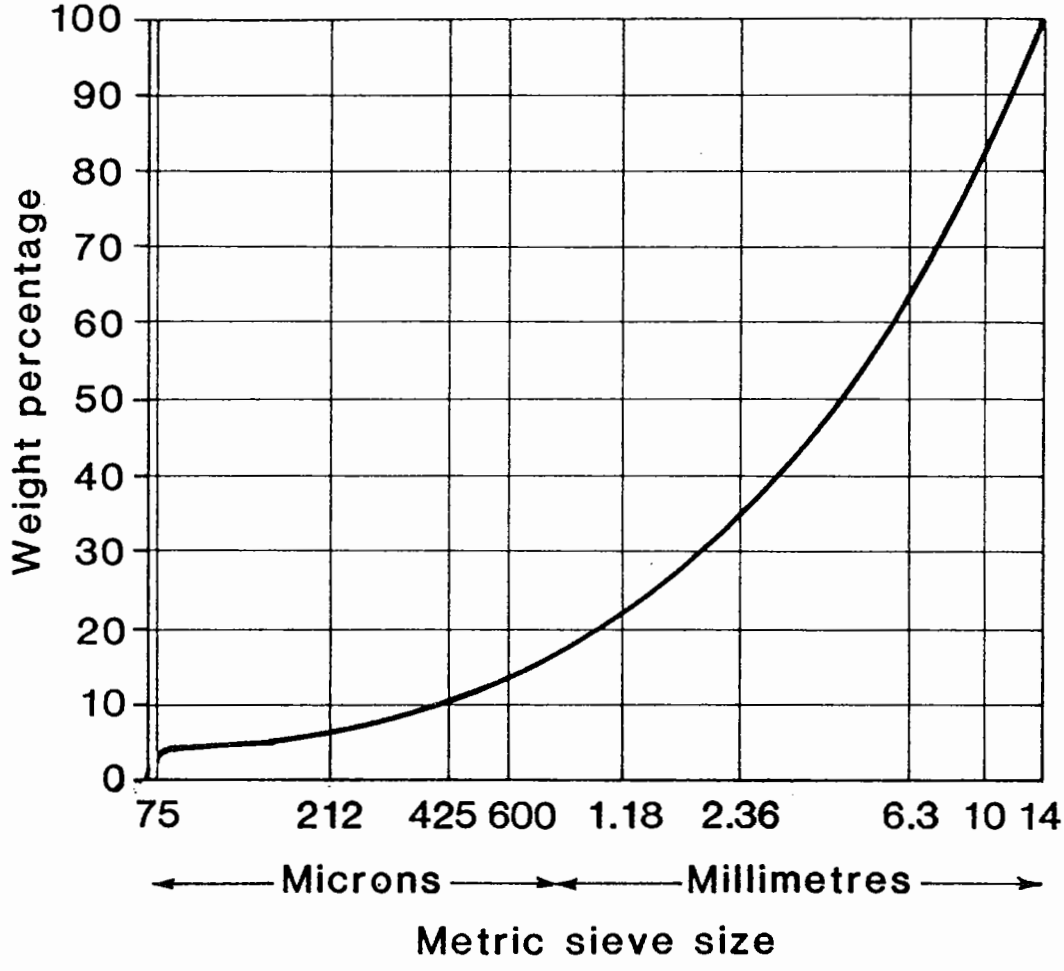

Binder content 5.0% (100pen)

Void content 8.8%

Fig. 7.8 Details of Asphaltic Concrete used in P.T.F.

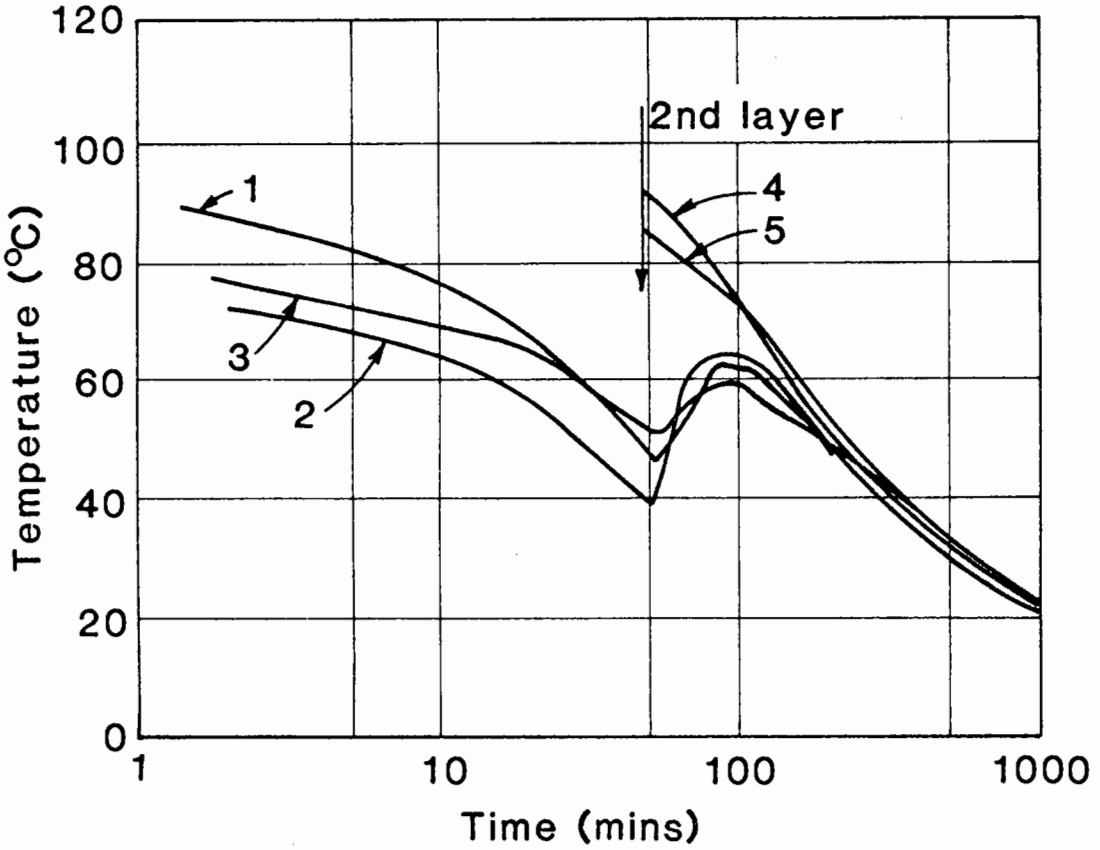

(a) Temperature decay in pavement

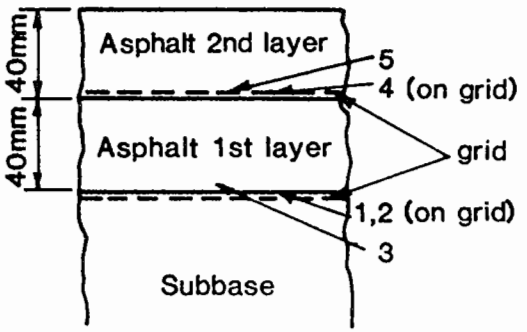

(b) Position of thermocouples

Fig. 7.9 Temperature Decay in Pavement During Construction

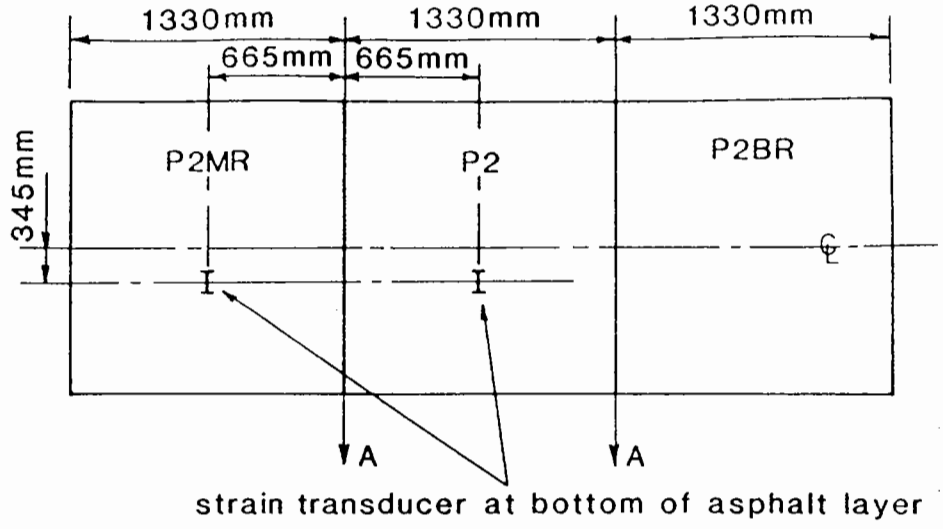

(a) Plan of pavement P2 and strain transducer position

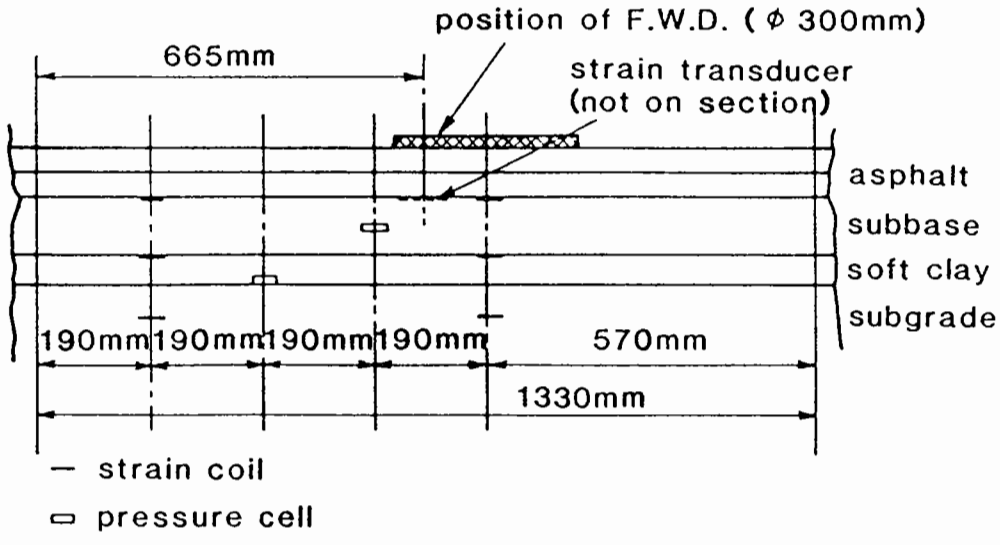

(b) Section A–A, strain coil and pressure cell positions

Fig. 7.10 Detail of instrumentation on pavement P2 for a typical section

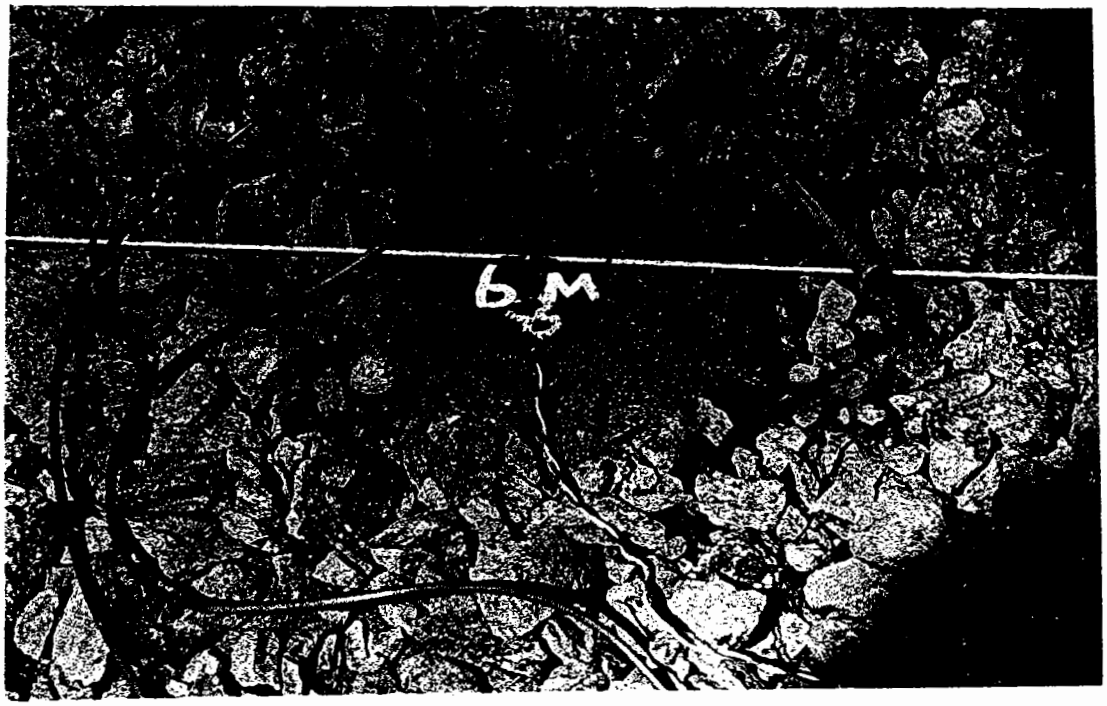

Fig. 7.11 Soil strain coils in subbase

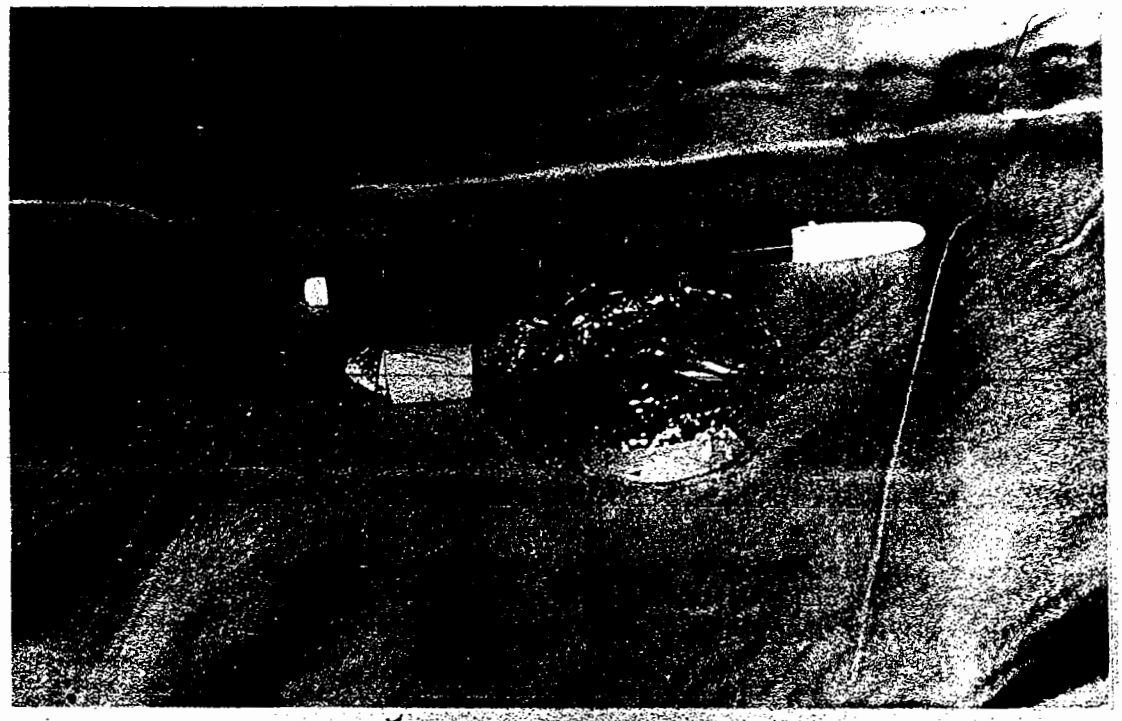

Fig. 7.12 Diaphragm pressure cell in protective sheath

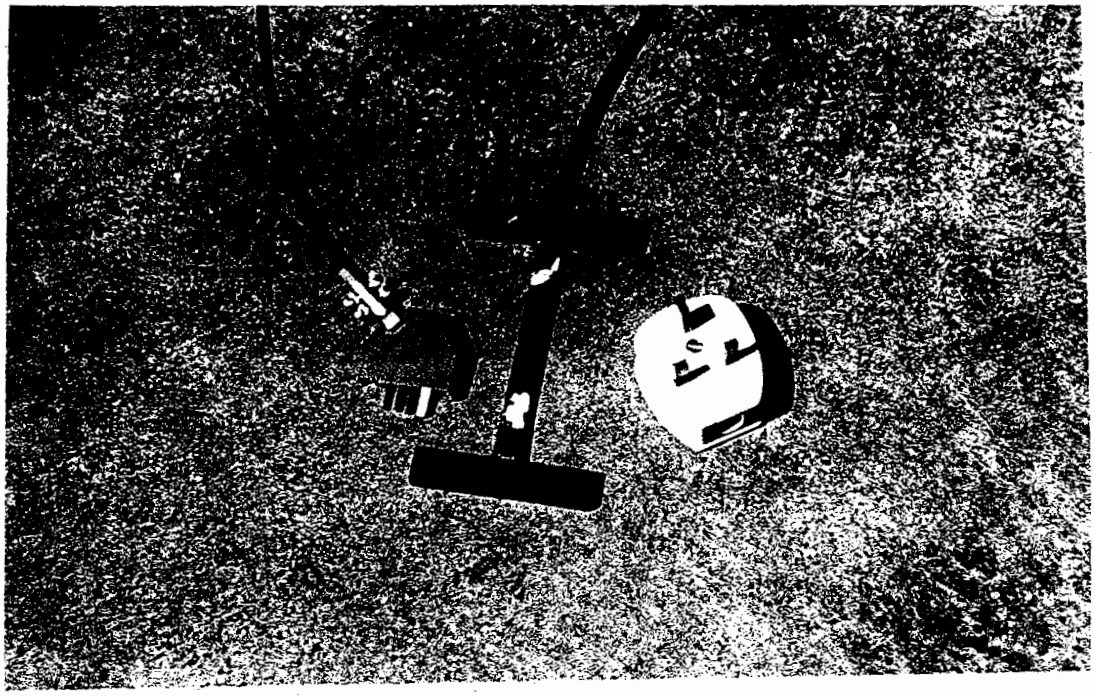

Fig. 7.13 Strain transducers (FTCII)

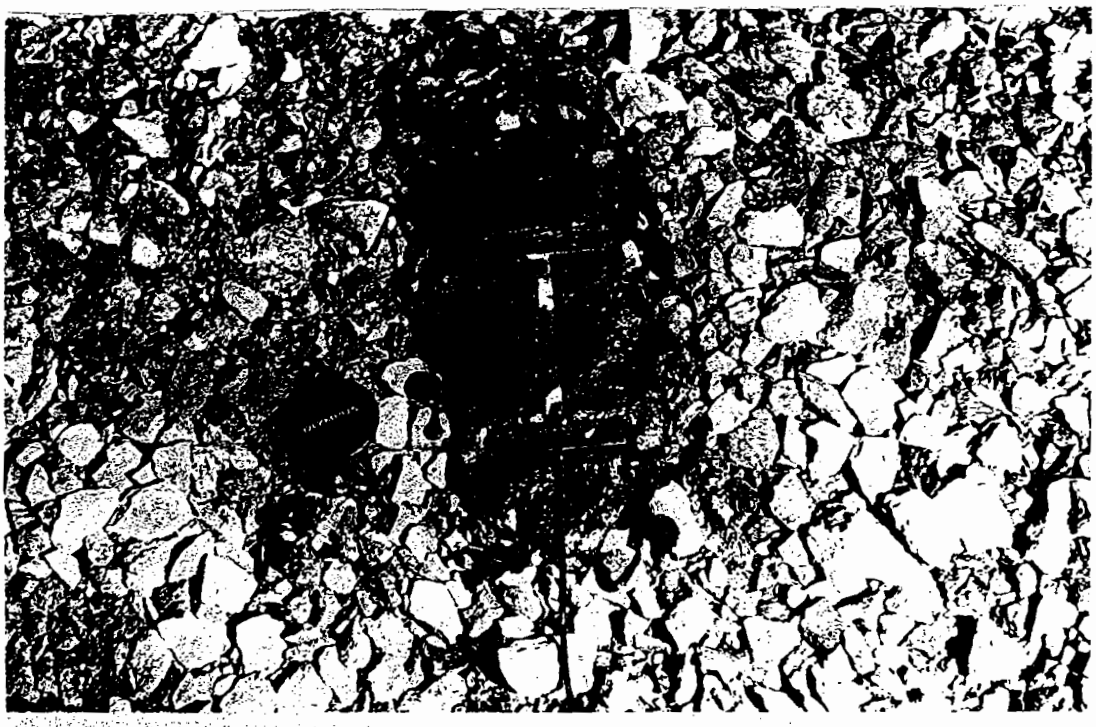

Fig. 7.14 Strain transducers in bed of mastic

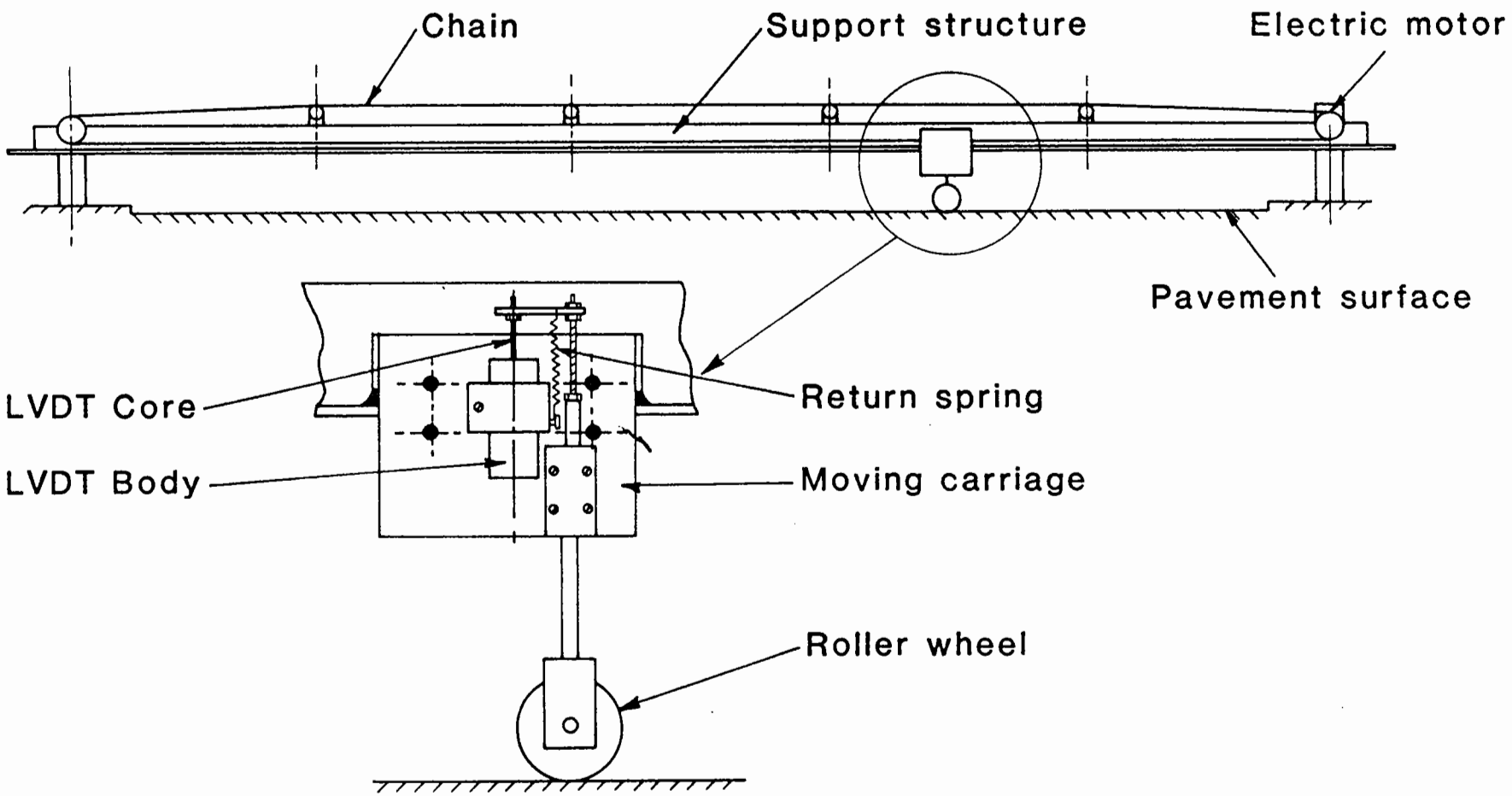

Fig. 7.15 Profilometer used for transverse profiles on pavement.

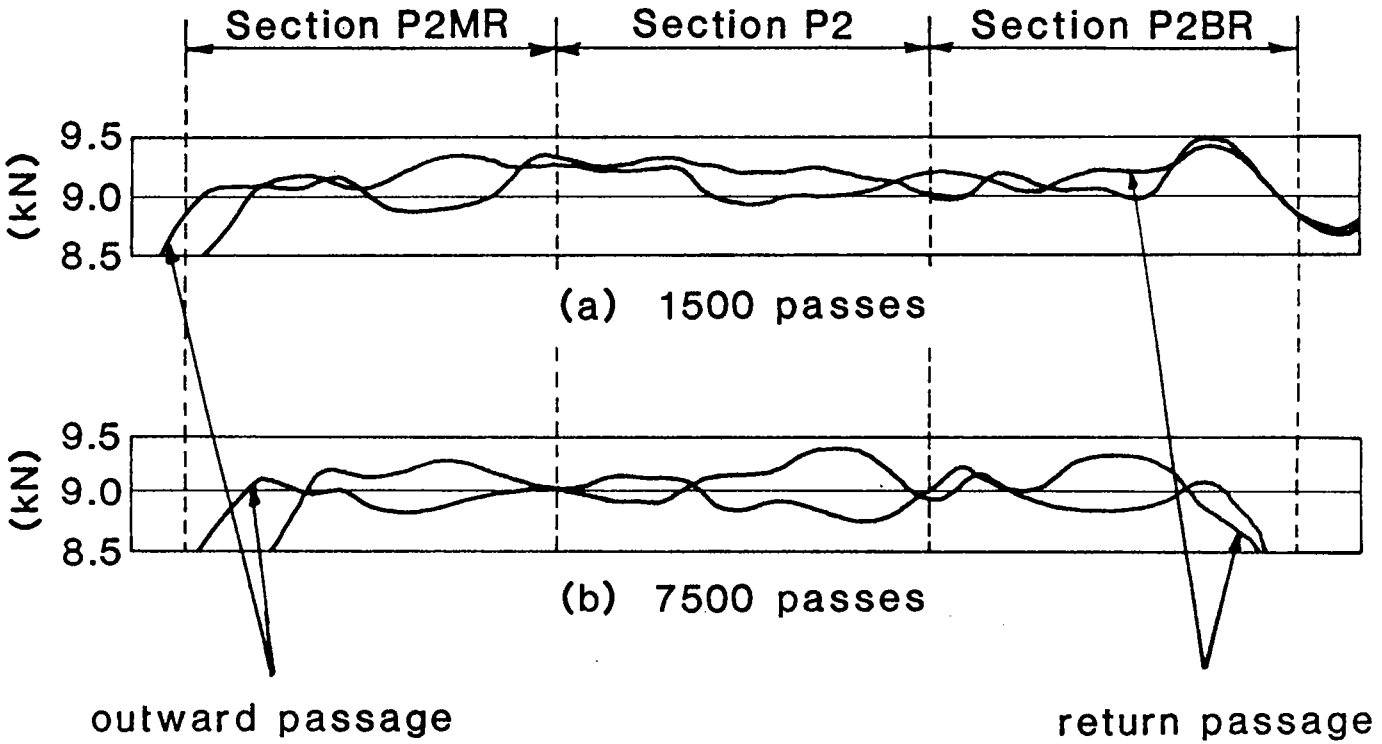

Fig. 7.16 Longitudinal Load Profile

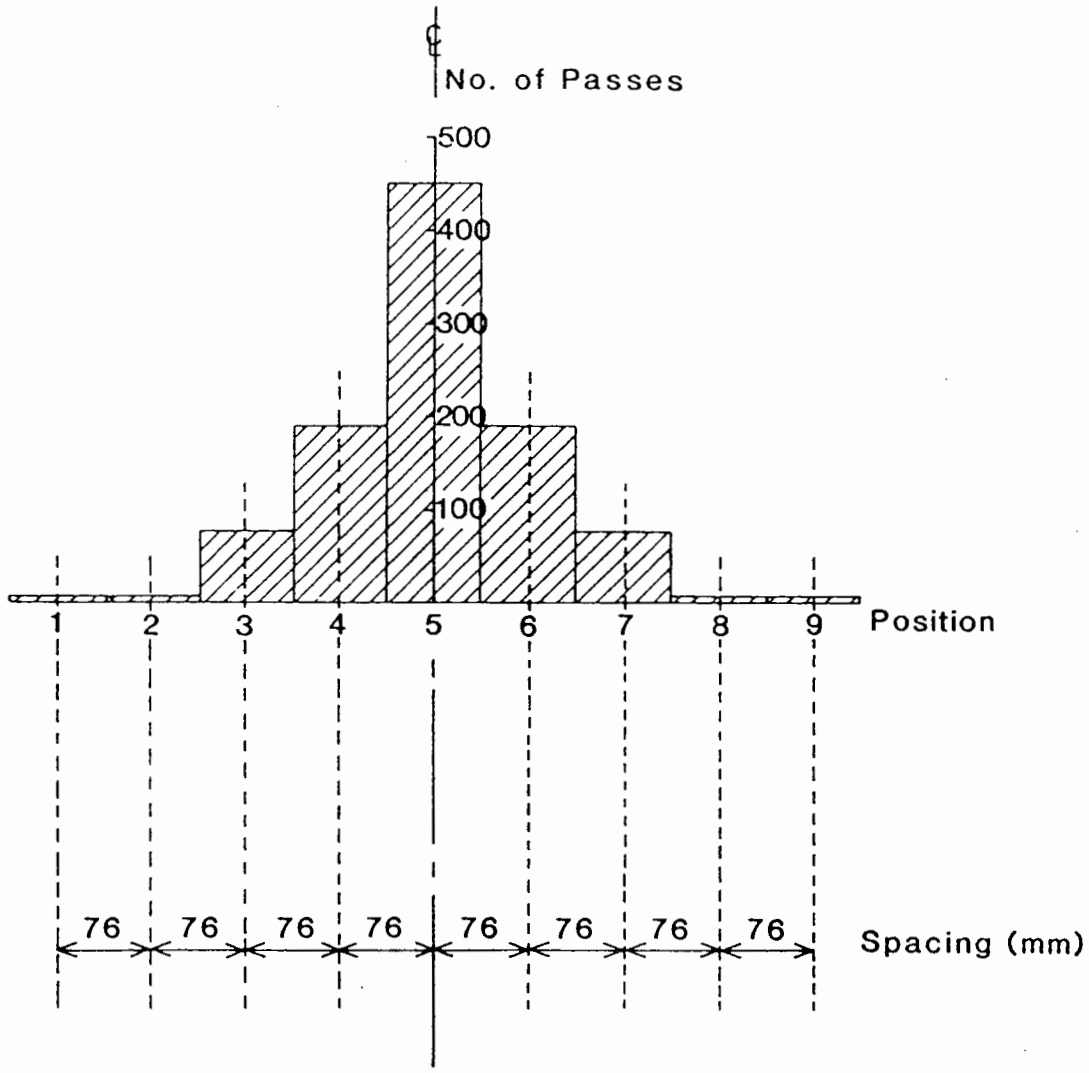

Fig. 7.17 Transverse wheel distribution and spacing for 1000 passes

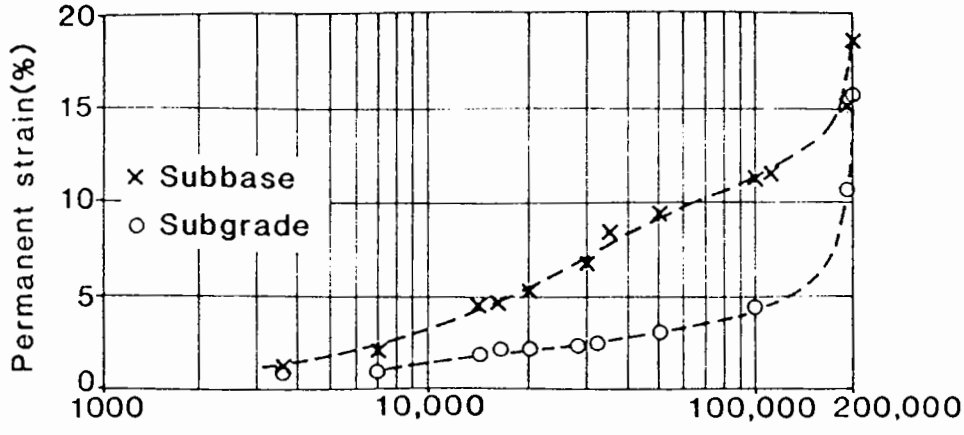

(a) Section P2

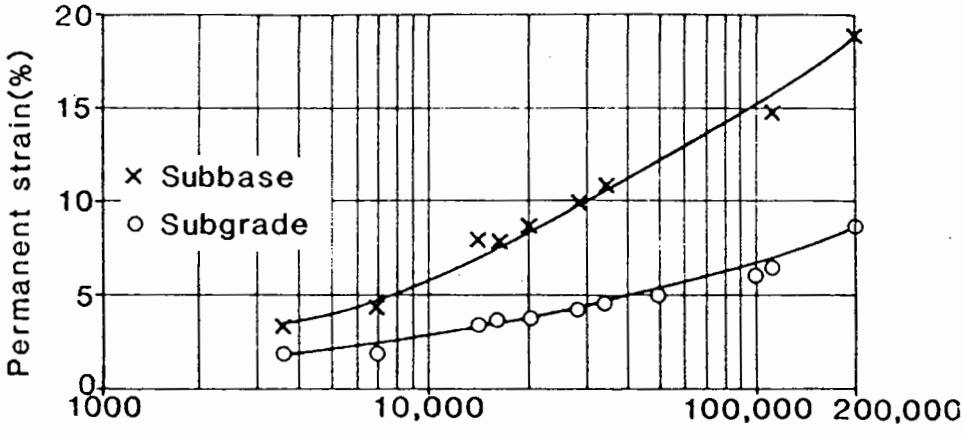

(b) Section P2MR

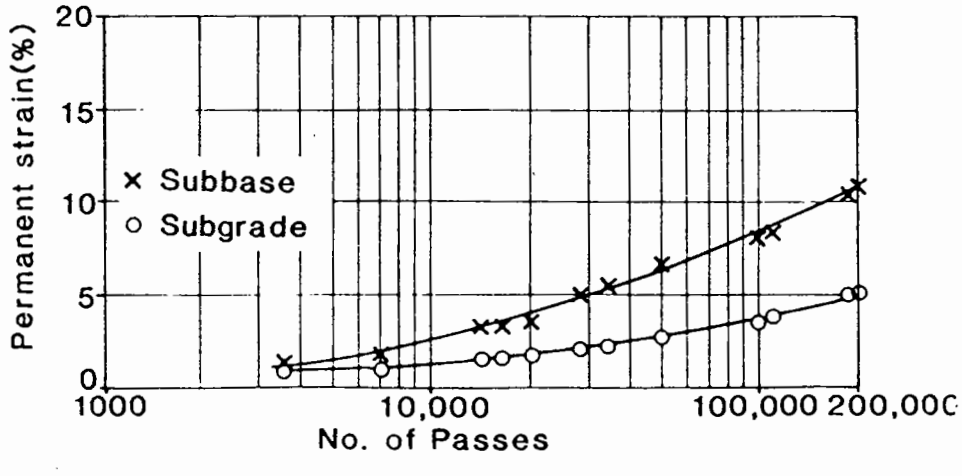

(c) Section P2BR

Fig. 7.18 Permanent Strain in Pavement P2

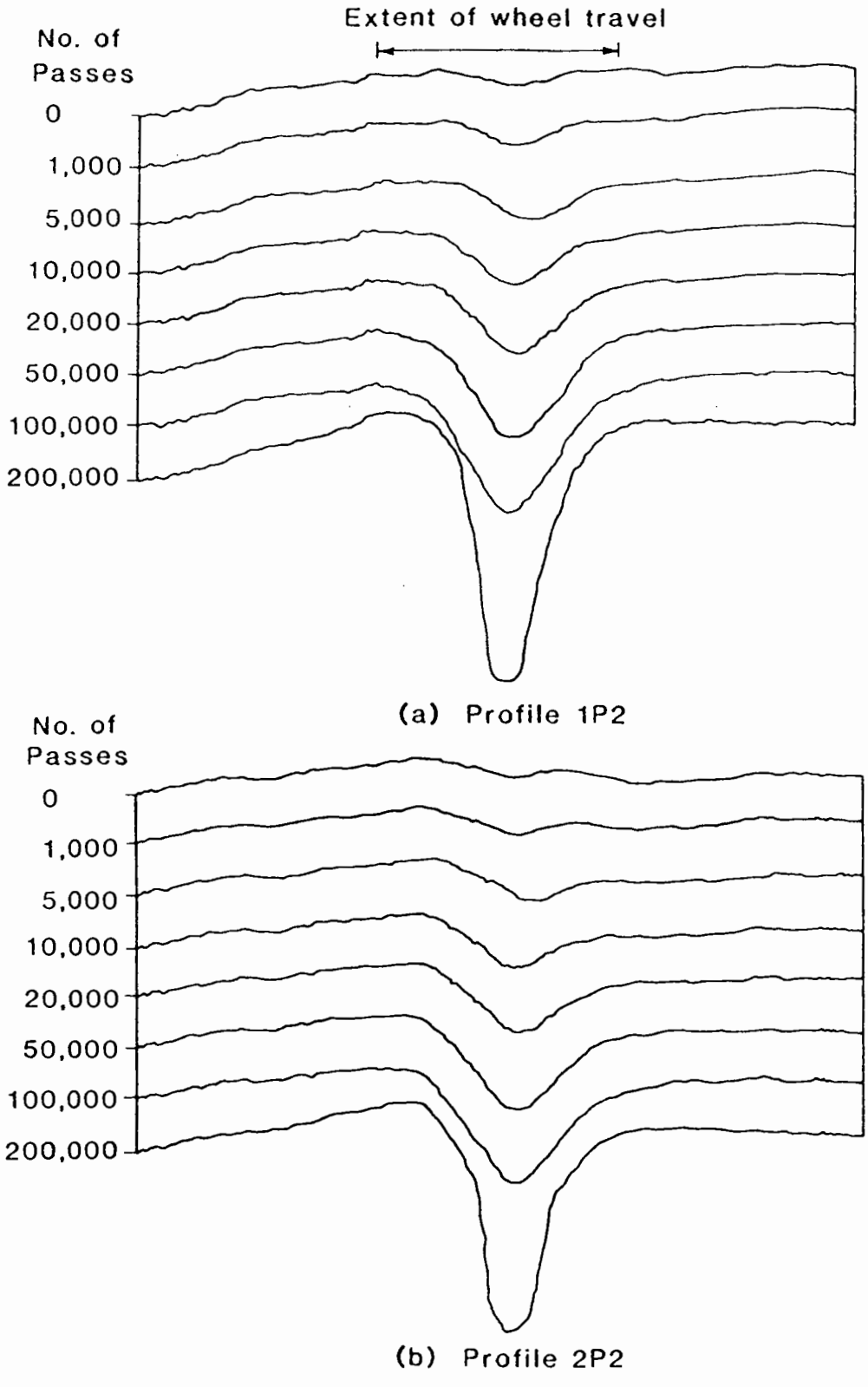

Fig. 7.19 Rut Profiles for Section P2

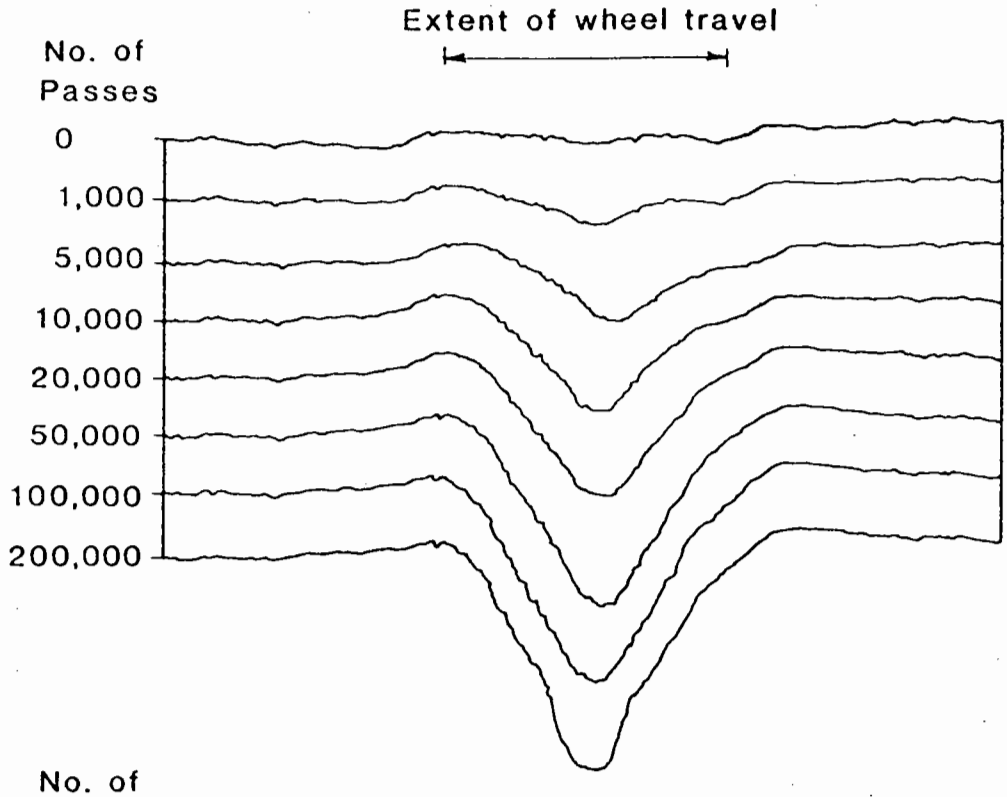

(a) Profile 1P2MR

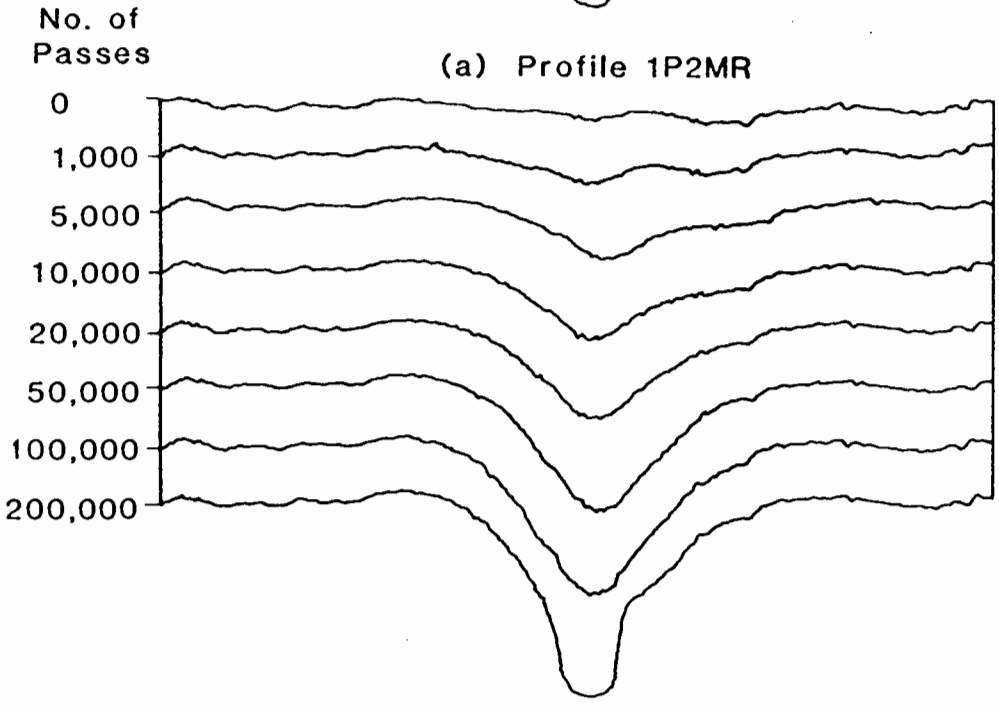

(b) Profile 2P2MR

Fig.7.20 Rut Profiles for Section P2MR

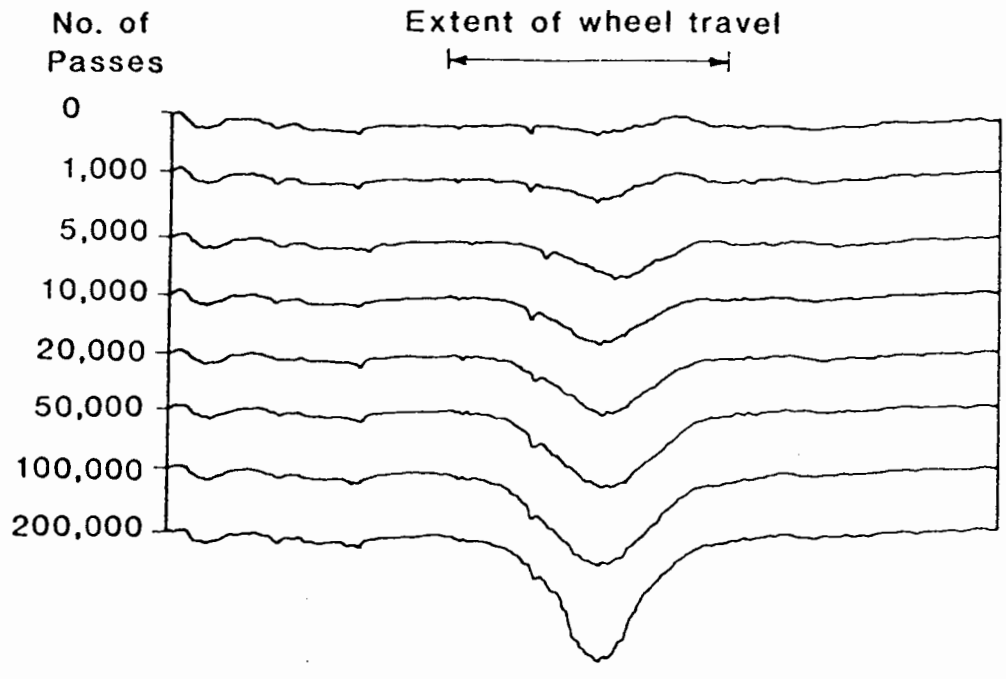

(a) Profile 1P2BR

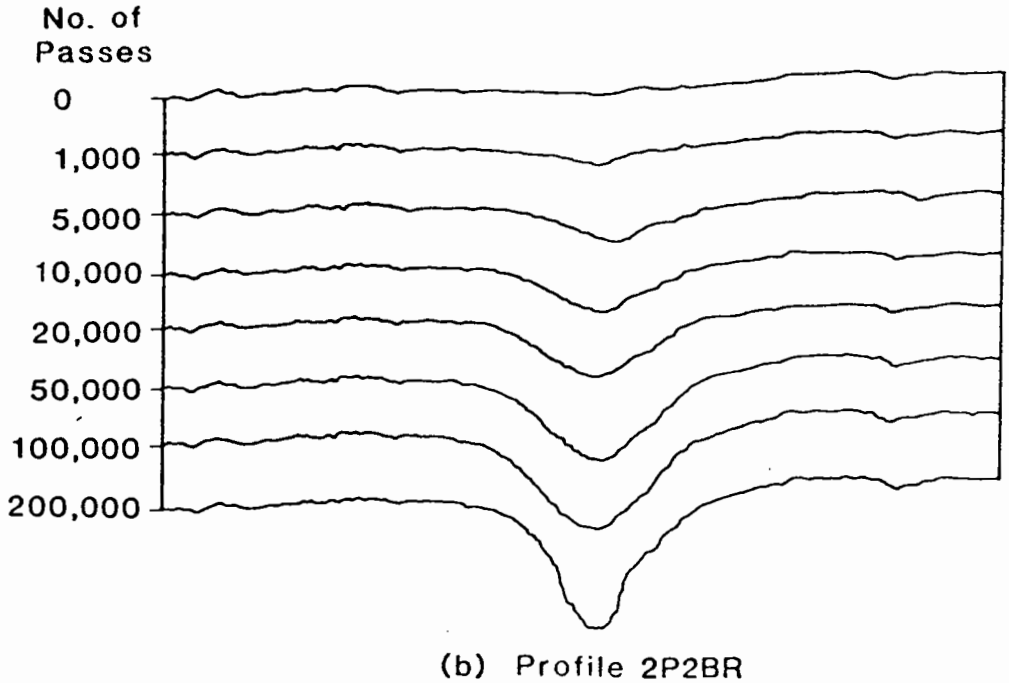

(b) Profile 2P2BR

Fig. 7.21 Rut Profiles for Section P2BR

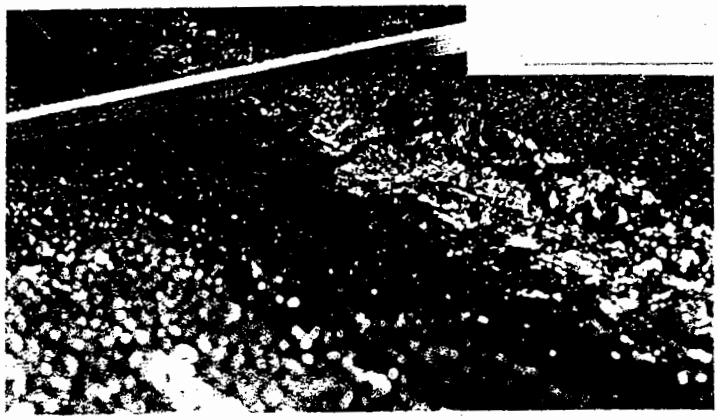

(a) Section P2

(b) Section P2MR

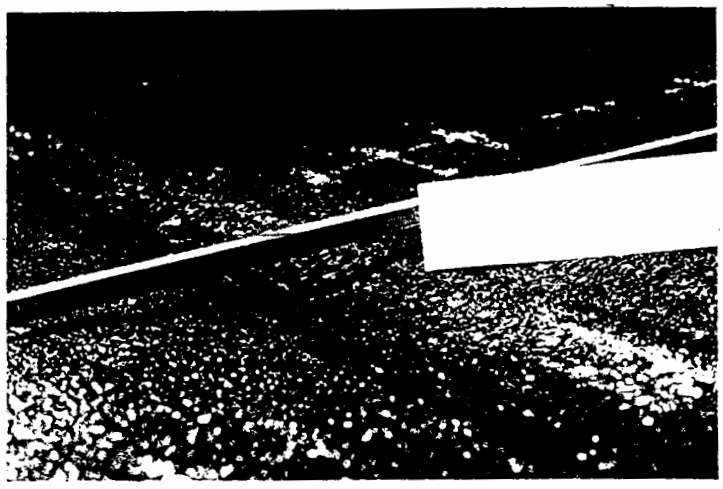

(c) Section P2BR

Fig. 7.22 Surface deformation at end of test

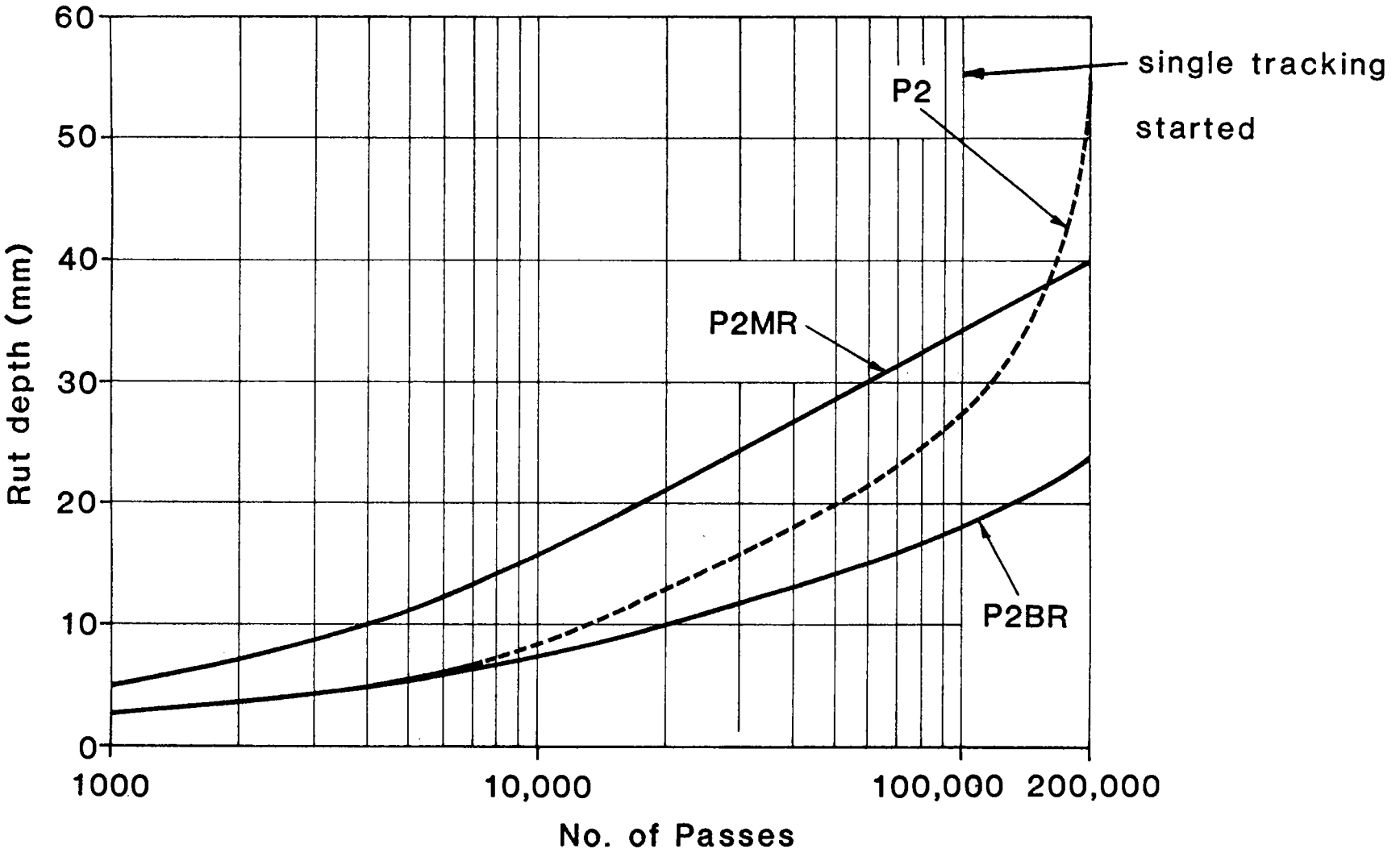

Fig. 7.23 Average Rut Depths for Pavement P2

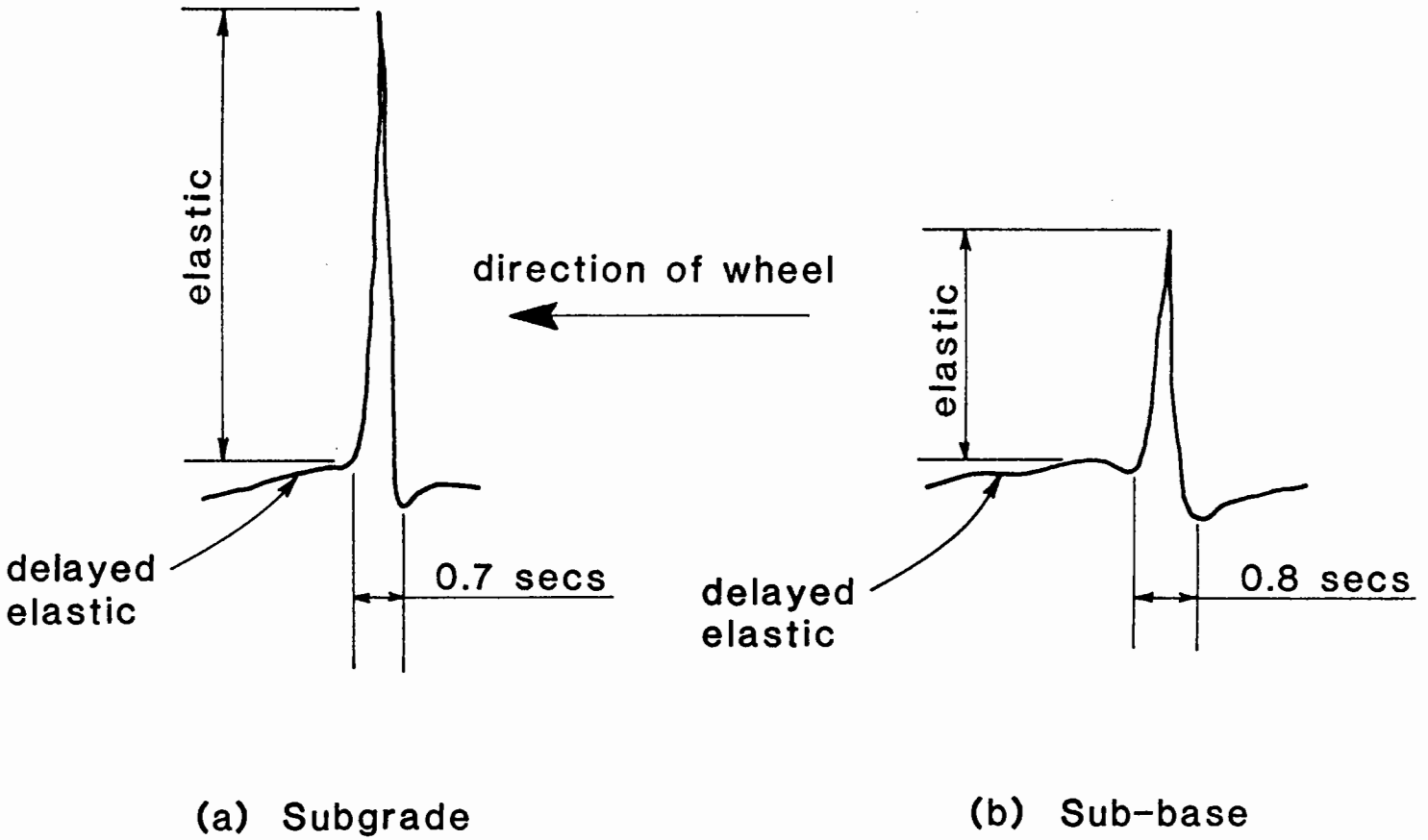

Fig. 7.24 Typical Elastic Strain Pulses Measured by Soil Strain Coils

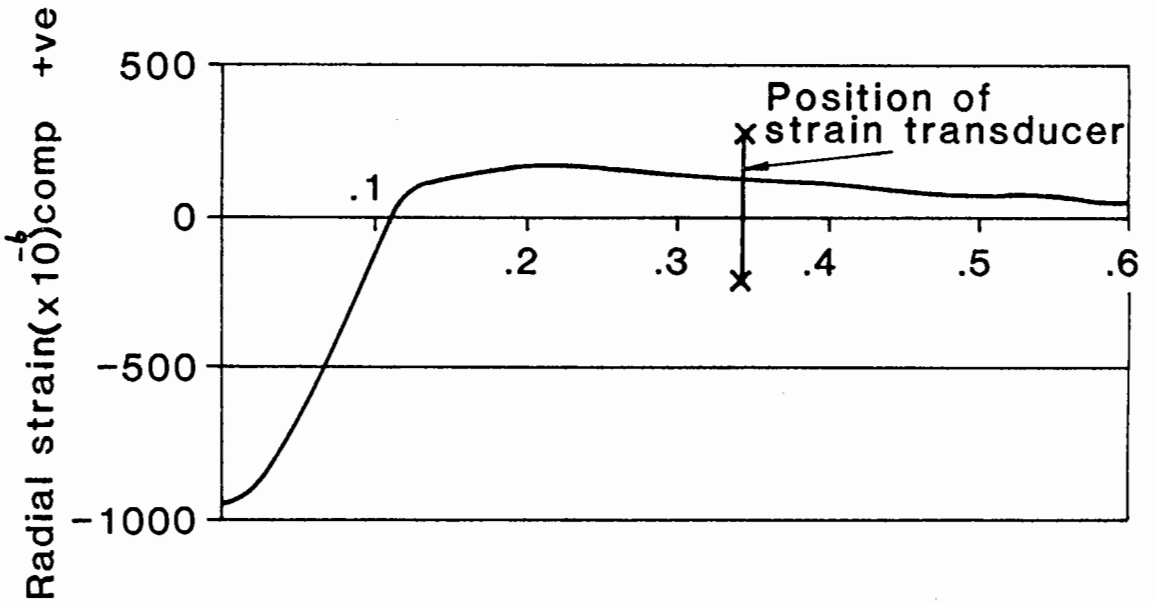

Fig. 7.25 Radial Strain at Base of Asphalt layer (BISTRO)

8 INTERFACE CONDITIONS

8.1 INTRODUCTION

A pavement structure is made up of several layers of different materials. The overall strength and stiffness of the pavement depends not only on the individual strength of each layer but also on the degree of bonding between them. Should the adhesion at any interface be reduced this would increase the levels of strains throughout the pavement for any given load and, hence, decrease the life of the pavement (Uzan, 1978; Brown and Brunton, 1984). This debonding effect is most noticeable when a wearing course slips over the underlying base course. Slippage occurs in cases where there is a higher than usual applied horizontal shear stress at the interface. This can be caused by traffic effects in braking, accelerating or cornering sharply or by a low stiffness road base (Brown and Pell, 1976). Since this effect can occur with conventional construction, it is particularly important to ensure that it is not a problem when a reinforcing grid is introduced to provide improved performance with respect to other parameters.

In order to assess the relative strength of various interface conditions, a large shear box was constructed for direct shear testing.

8.2 SHEAR BOX DEVELOPMENT

The limitations of the direct shear test are widely recognised and documented (Ansell, 1977 Sowers, 1963 Saada et al, 1980 Atkinson et al, 1978). Failure is along a predetermined plane and boundary displacements rather than strains within the sample are observed. There exists at the front and rear edges, a condition of

physical cutting of the specimen which results in considerable stress concentration at these positions. This gives rise to progressive failure along the shearing plane so that the full shearing strength is not mobilised simultaneously along the entire length of the plane. Fig. 8.1 shows the area of deformation and the non uniform distribution of strains in a shearing specimen. The shear box can therefore be seen to be unsatisfactory as a test apparatus for investigating the interrelation between strains and stresses and it is better suited to the determination of stresses which cause failure on a particular plane. It is, therefore, quite well suited to finding the strength of pre-existing failure surfaces and seemed appropriate for investigating the shear strength of interfaces in a bituminous sample on a comparative basis.

Large shear boxes have been developed in the past (Pike, 1973; Bishop, 1948) to investigate the properties of aggregates unsuitable for testing in the smaller standard soil mechanics shear box, which has plan dimensions 60mm x 60mm. Uzan et al, 1978, constructed a crude shear box to examine the shear strength of asphalt specimens of plan dimension 150 x 100mm but, since the grid reinforced failure surface had to carry a representative area of grid, this was considered too small. The dimensions of the asphalt specimen selected for the final tests were 320mm x 320mm x 150mm deep.

The shear box was constructed on a large steel base plate, Figs. 8.2 and 8.3, which was designed to allow 75mm x 75mm angles to be butted tightly against both the compaction mould and, on removal of this, the sample itself. This adjustment was provided by milling slots into the steel base plate along which bolts fixing the angles could slide. Both top and bottom platens of the shear box had a saw toothed profile (Fig. 8.4) to provide effective shear transfer between the asphalt and steel plates. The top plate was allowed to

move horizontally under an applied shear force by providing a roller carriage, Fig. 8.5 through which the normal load acted.

8.3 EXPERIMENTAL ARRANGEMENTS

The test specimens were constructed in two lifts, the bottom half being allowed to cool overnight before compacting the top half. This allowed the interface to be treated in the appropriate manner. A static compactive effort of 250kN (2440 kPa) acting on a rigid steel plate was applied for five minutes, Fig. 8.6. The braced wooden mould was removed after the specimen had cooled and the angles butted firmly against the asphalt base. Steel bearing plates were also secured to the top plate to confine the top half of the sample and to create a rigid platen through which the horizontal force acted Fig. 8.7.

Fig. 8.8 shows schematically the loading scheme during testing. Normal and shear forces were applied using hydraulic actuators and monitored using load cells. The normal load was held approximately constant and the shearing force was supplied at a constant rate of strain (5mm/min). Dilation (vertical upward movement) of the roller bearing carriage was monitored using four linear potentiometers arranged as shown in Fig. 8.5. A hard copy of this movement was obtained from an ultra violet recorder.

8.4 TEST PROGRAMME

The bituminous mix used in all the shear box tests was a continuously graded asphaltic concrete, the grading is given in Table 8.1. Five interface conditions were studied,

(a) " Chip seal" only. The interface was treated with a chip seal layer
(b) " Chip seal" and grid. The grid was held in place at the interface using the chip seal technique.

Table 8.1 Details of asphaltic concrete

Sieve Size (mm)	% Passing
14	100
10	87
5	62
2.36	40
1.18	27
.600	18
.300	12
.150	7
.075	4
Dust	0

14mm granite aggregrate
Specific gravity of aggregate 2.81
5.5% of 100 pen bitumen.

(c) Grid only. The grid was included at the interface
(d) No treatment. The interface received no treatment as in a normally constructed overlay.
(e) No interface. The sample was compacted in one lift and had no interface.

Where chip seal was used 100 pen bitumen was sprayed onto the compacted lower half of the sample and dressed with 6.3mm granite chippings, following the technique developed for site application. The bitumen was spread at 1.1 l/m^2 and the chippings were applied at approximately 5 kg/m^2. Due to the difficulty in applying the bitumen and chippings these values should only be considered as approximate. In reality, the bitumen tack coat was heavier than this and the stone dressing rather less, after the excess had been removed. A minimum of two tests were carried out for each interface condition and the complete series of tests repeated for two values of normal stress, of approximately 190 kPa and 430 kPa.

8.5 RESULTS

Table 8.2 gives the test numbers, together with the air void content for each specimen. The average void content for all the specimens was 10.4% with a variation between 8.7% and 12.3%. Normally the void content of asphaltic concrete is lower, around (6% to 7%) but due to the difficulty of compacting the material under a static load this could not be achieved.

Fig. 8.9 shows a typical plot of shear and normal stress monitored continuously throughout each test, against the relative displacement of the top platen. (The test results are given in full in Appendix G). The shear and normal stresses were calculated by dividing the recorded load by the total area of the sample (320mm x 320mm.) and no account was taken of shear non-uniformities across the interface. The observed values of shear and normal stress observed can, therefore, only be regarded as useful for comparative purposes

Table 8.2 **Interface Conditions**

Test number	Interface condition	Void content V_v (%)
4	Chip seal only	8.7
5	Chip seal only	9.4
6R	Grid and chip seal	12.0
7R	Grid and chip seal	11.3
8	No treatment	10.9
9	No treatment	9.9
10	No interface (i.e. compacted in one lift)	9.5
11		11.2
12		9.3
13R	Grid only	10.2
14R	Grid only	9.1
15	No treatment	10.3
16	No treatment	10.3
17R	Grid only	9.0
18R	Grid only	9.1
19	Chip seal only	10.8
20	Chip seal only	12.2
21R	Grid and chip seal	12.3
22R	Grid and chip seal	12.0
23	No treatment	10.7
24	No interface	10.1
25	No interface	10.2
26	No interface	10.7
		10.4 Average

and not an absolute statement of shear strength of the interface.

Fig. 8.10 shows the maximum shear stress recorded for each test, plotted against the corresponding (simultaneously occurring) normal stress.

The average maximum shear stress for each interface condition and both normal stresses, is given in Table 8.3. This is also represented as a percentage of the "no interface" and "no treatment" conditions in Table 8.4. The "no treatment" condition is more representative of the normal insitu state. No account has been taken of the slight differences of normal stress for either series of tests. At higher normal stresses the relative difference between interface conditions was less marked, and the "no interface" and "no treatment" interfaces showed virtually the same absolute strength. The average peak shear stress of the "no interface" condition was in fact 3% lower than the "no treatment" interface, although this was due to the exceptionally high value of shear strength exhibited by the "untreated" interface in Test 15 which increased the average significantly.

With respect to the "no treatment" condition, the specimens with "chip seal" at the interface showed a reduction in shear strength of approximately 19%. The addition of the grid reduced the shear strength only by a further 1%. The interface with grid only produced a 10% reduction in shear strength and the "no interface" condition was 8% stronger. These results imply that the "chip seal" in itself reduces the bond between layers in an asphalt construction but inclusion of the grid with the "chip seal" has very little additional effect.

Fig 8.9(b) shows the dilation of a sample, based on vertical movement of the roller bearing carriage during testing. The numbers refer to the position of the linear potentiometer (Fig 8.5). 1 and 2

Table 8.3 **Average Values of Peak Shear Stress for Two Values of Mean Normal Stress**

Interface Description	Average value of Peak Shear Stress (kPa)		Percentage of "no interface" condition		Percentage of "no treatment" condition	
	Mean Normal Stress		Mean Normal Stress		Mean Normal Stress	
	190 kPa	430 kPa	190 kPa	430 kPa	190 kPa	430 kPa
Chip seal only	237	464	60	94	72	91
Grid and chip seal	243	436	62	89	74	86
No treatment	327	509	83	103	100	100
No interface	394	492	100	100	120	97
Grid only	300	446	76	91	92	88

Table 8.4 **Average percentage shear strength of interfaces with respect to "no interface" and "no treatment" conditions**

Interface Description	Average percentage of "no interface" condition"	Average percentage of "no treatment" condition
Chip seal only	77	81
Grid and chip seal	75	80
No treatment	93	100
No interface	100	108
Grid only	83	90

were to the rear of the carriage and 3 and 4 at the front. In each case the sample dilated in the exaggerated manner shown in Fig. 8.11, tilting away from the direction of shear.

The dotted line shown in Fig. 8.10 used the data from the "untreated" interfaces to produce an angle of friction, $\phi = 39^{o}$ for the interface with the intercept at zero normal stress being 160kPa which represents a value of cohession.

8.5 DISCUSSION AND CONCLUSIONS

Both the "chip seal only" and "grid and chip seal" interfaces showed a reduction in shear strength of approximately 20% when compared to the "no treatment" condition. The chip seal interface is rich in bitumen and this, combined with the slow rate of loading in the test (5 mm/min), created a viscous failure along the predetermined failure plane (a feature of the shear box test). The grid when installed using the chip seal technique created no further weakness as the viscous failure in the chip seal was predominent.

The "grid only" condition reduced the shear strength of the interface by 10% when compared to the" untreated" interface. The area covered by the grid in the plane of the interface is approximately 14%. By considering the strengths of the asphalt/asphalt bond as 100%, to obtain a reduction of 10% in the shear strength of the interface including the grid, the actual asphalt/grid bond must be only 28% that of the asphalt/asphalt bond. It would be of some benefit to increase the effectiveness of the asphalt/grid bond so as to reduce the liklihood of a shear failure at an interface containing the grid.

In general it appears that the reduction in shear strength should not be a problem in general practice especially since rates of loading are significantly higher under traffic loading and viscous

failure of the chip seal unlikely.

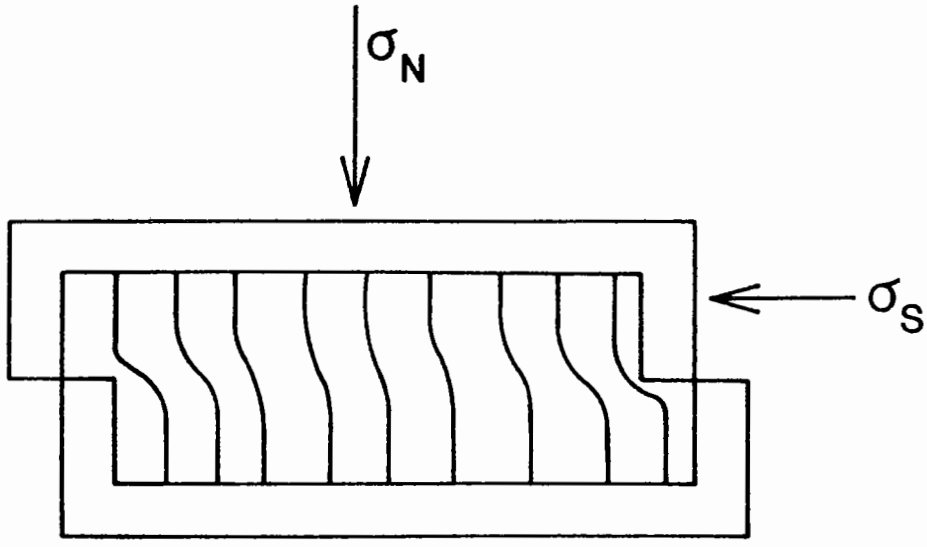

(a) Non Uniform Distribution of Shear Strains

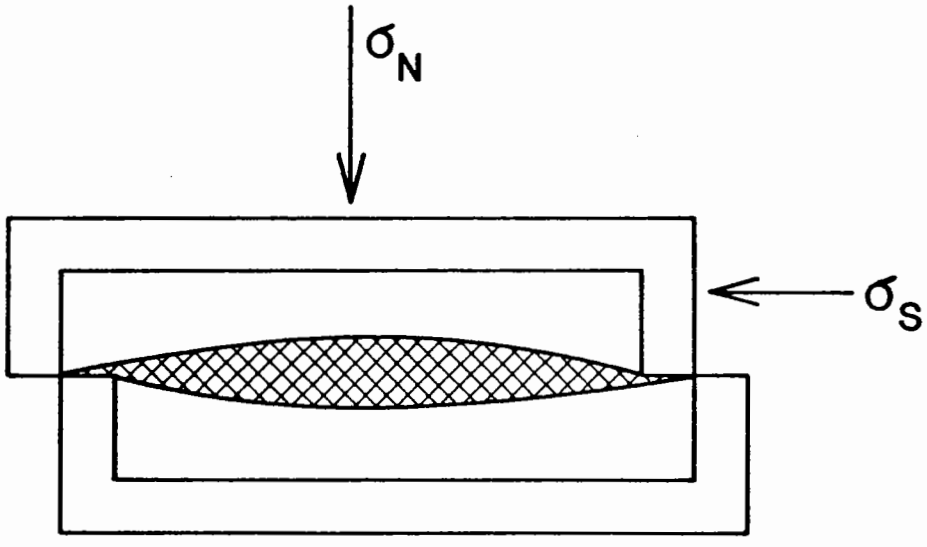

(b) Area of Deformation

Fig. 8.1 Strain distribution and area of deformation in the direct shear test

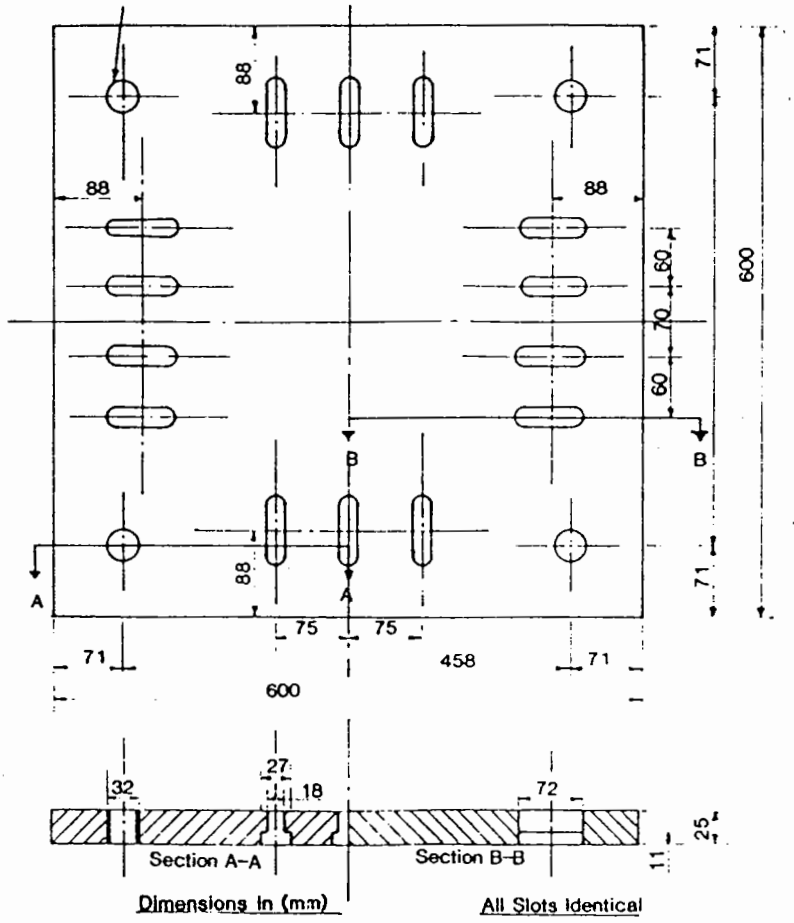

Fig. 8.2 Steel base plate

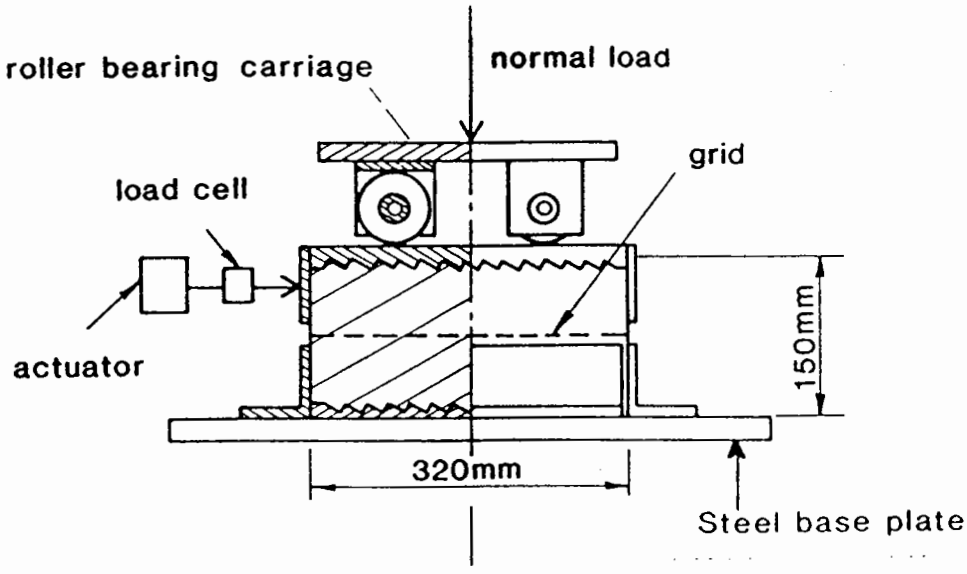

Fig. 8.3 Shear box apparatus

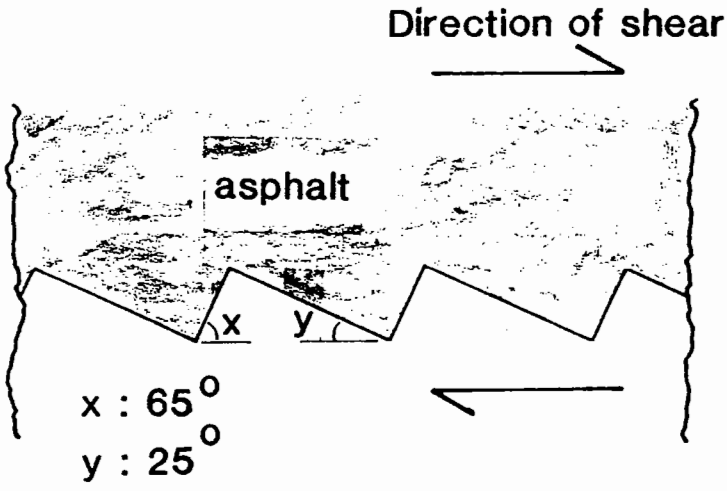

Fig. 8.4 Sawtooth profile steel plate

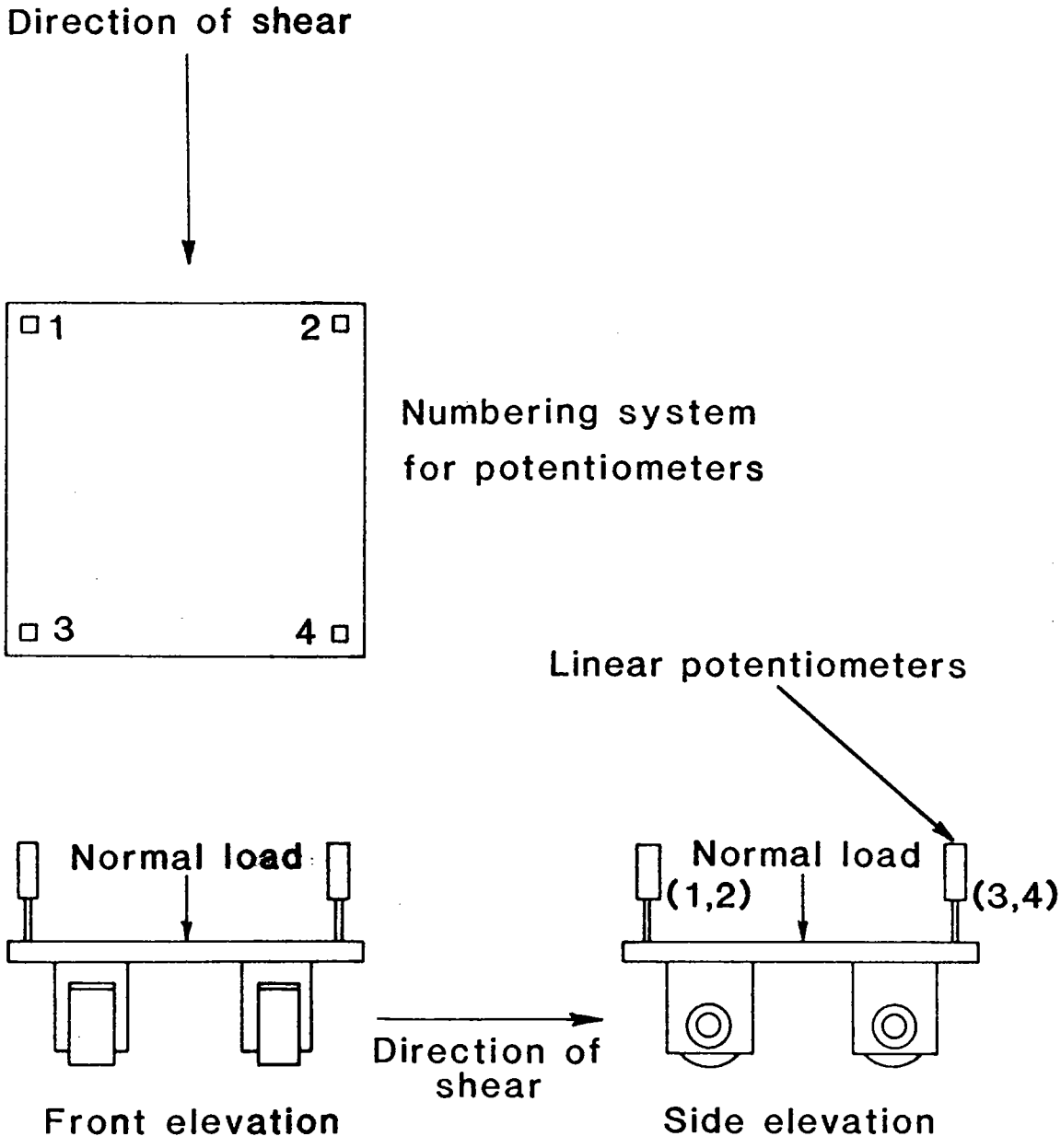

Fig. 8.5 Roller Bearing Carriage and Linear Potentiometer Arrangement

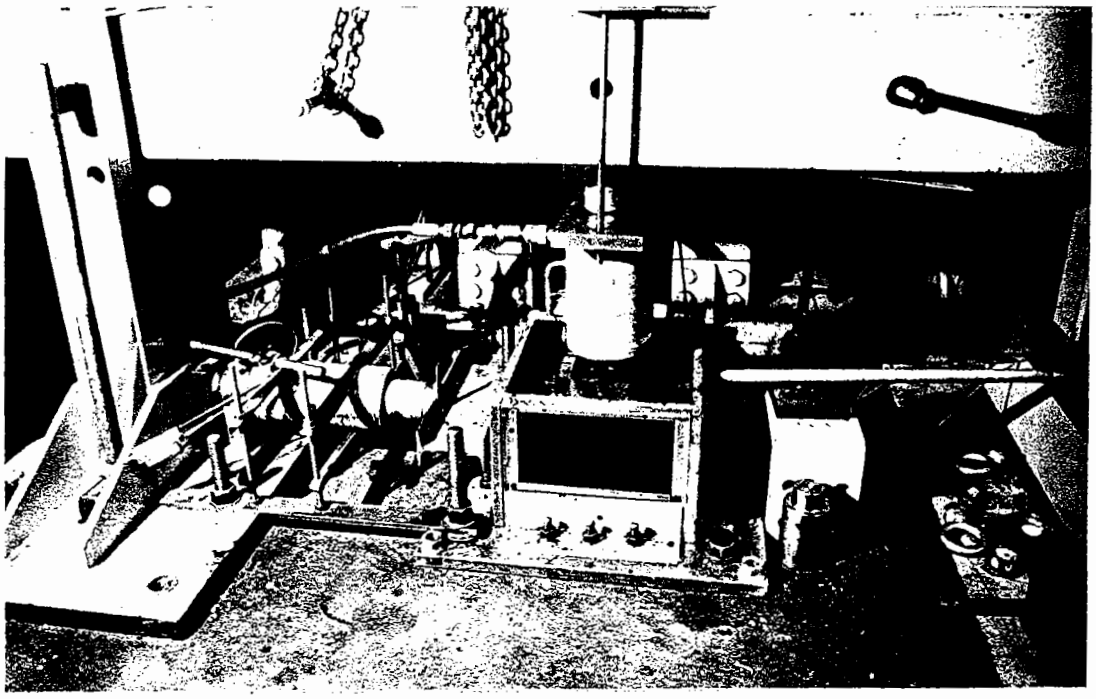

Fig. 8.6 Shear box during compaction.

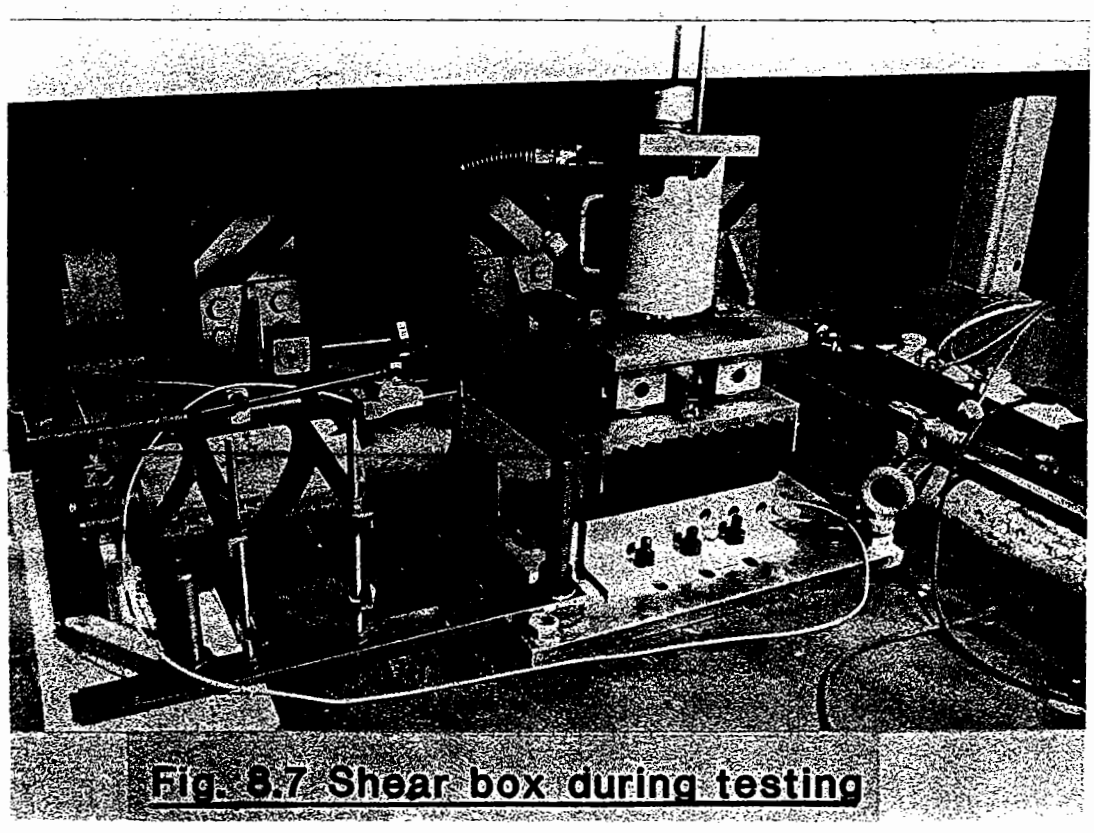

Fig. 8.7 Shear box during testing

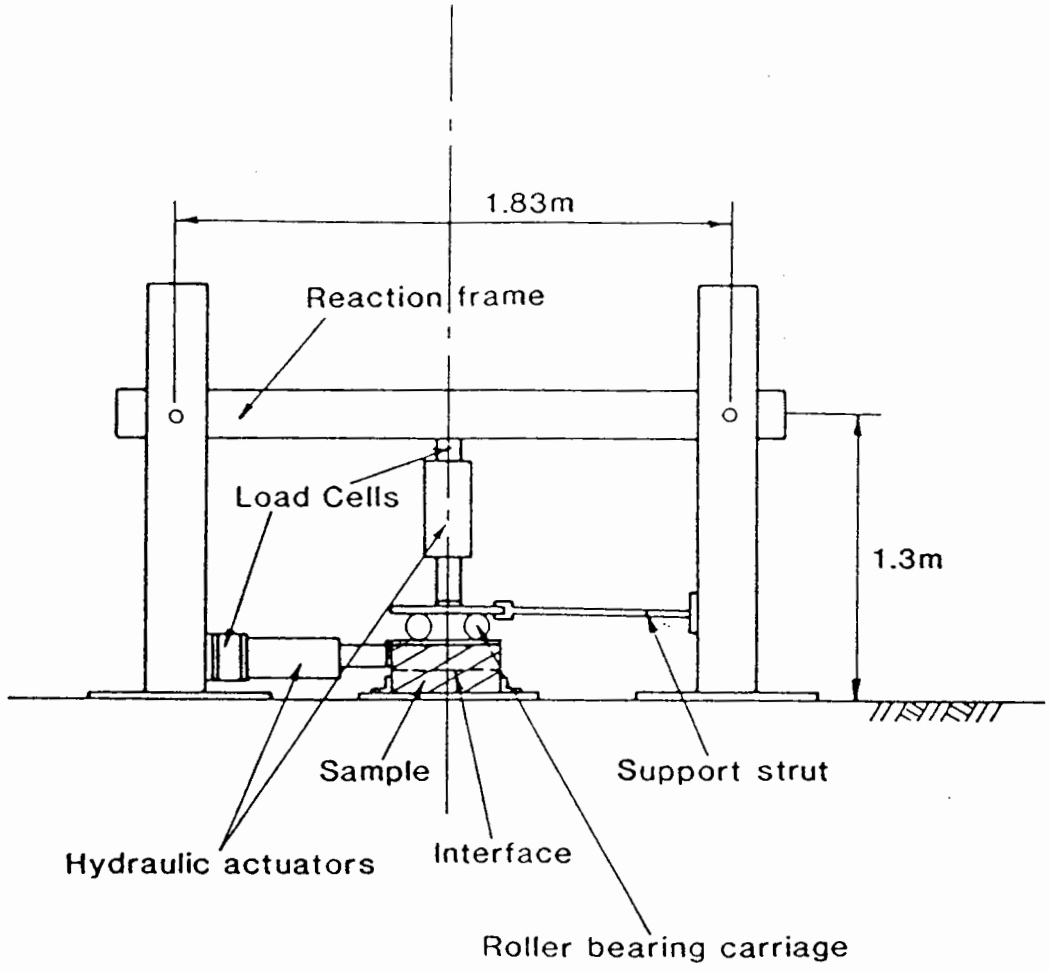

Fig. 8.8 Loading arrangement for large shear box.

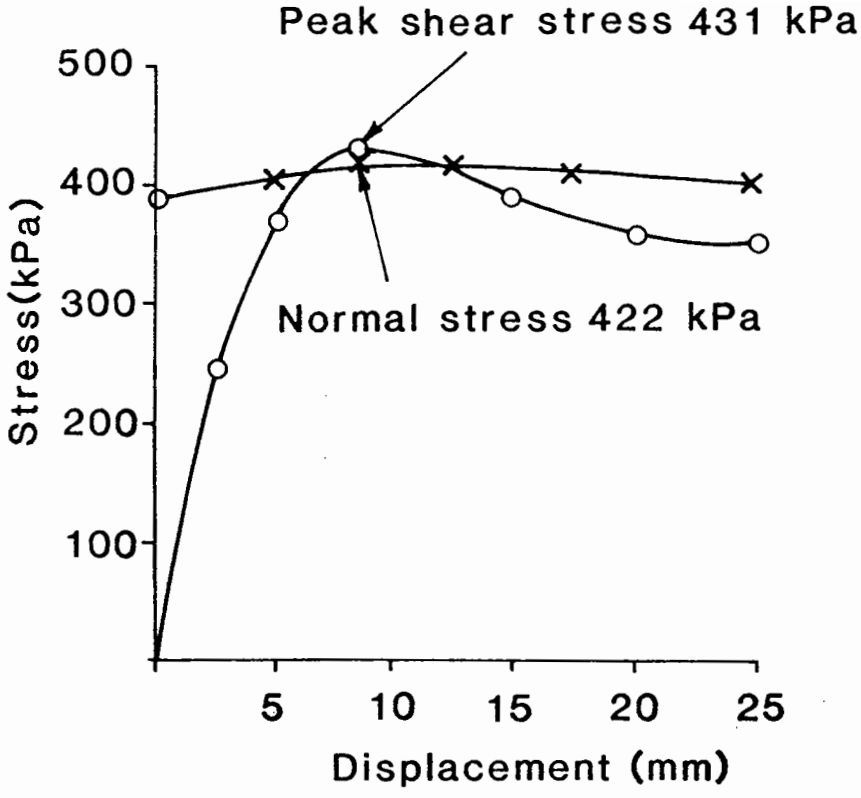

(a) Shear and Normal Stress During Test

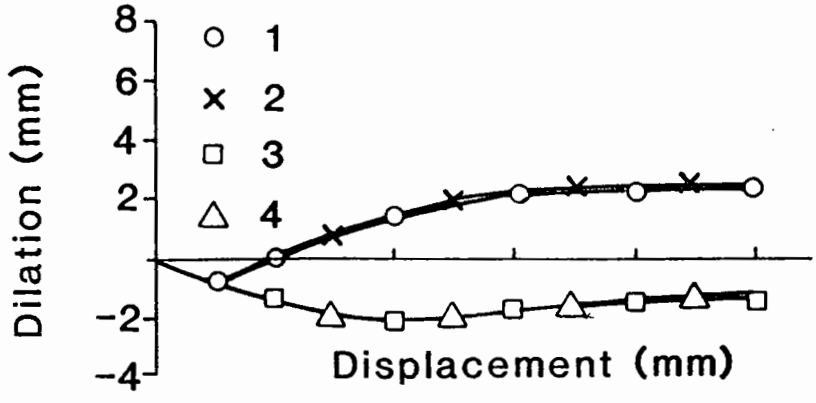

(b) Dilation of Sample During Test

Fig. 8.9 Test 22R Chip Seal and Grid at Interface

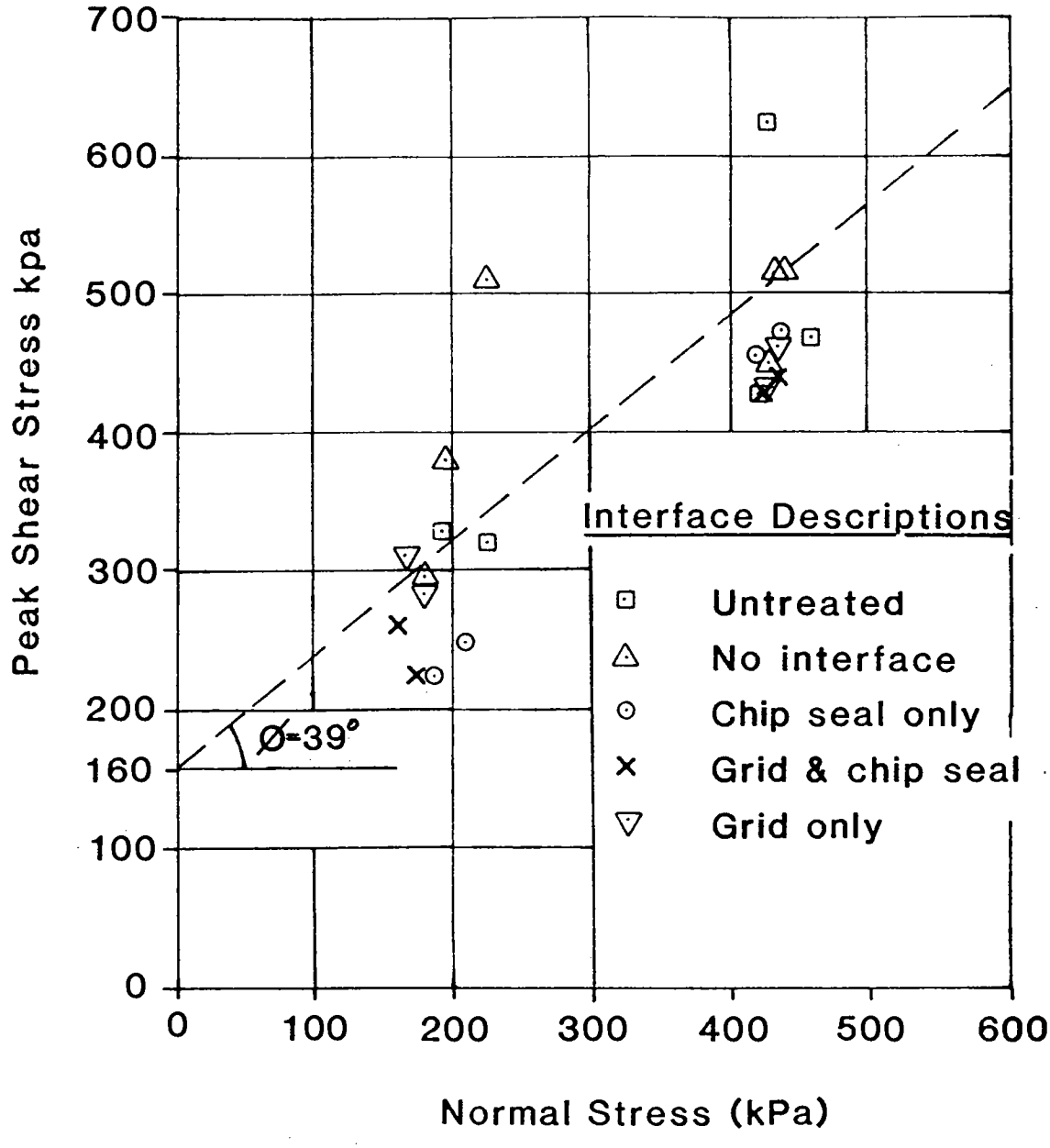

Fig. 8.10 Peak shear stress against normal stress for every test

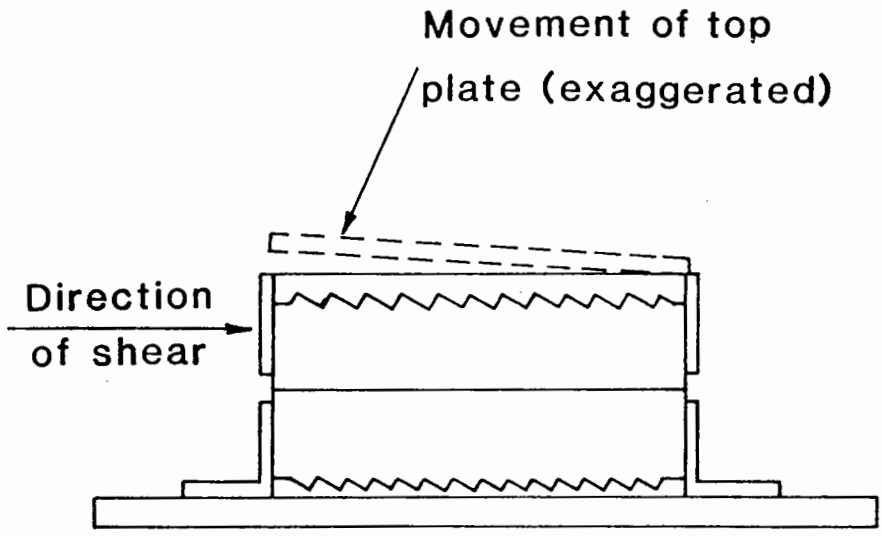

Fig.8.11Distortion of Top Platen
During Shearing

9 APPLICATIONS TO PAVEMENT DESIGN

9.1 INTRODUCTION

An Analytical design procedure for flexible pavements has been developed at Nottingham, (Brown and Brunton 1984 (b), Brown and Brunton 1984 (c) and Brown Brunton and Stock 1985), and has been modified to include the beneficial effects of including polymer grid reinforcement at various positions in the pavement. These benefits include an increase in design life for pavements susceptible to fatigue, and permanent deformation. Some guidelines for designing against reflection cracking are also presented.

Fig. 9.1 shows the possible locations and particular benefits of including the grid in a new structure. The use of the grid in asphalt overlays with respect to reflection cracking is illustrated in Fig 9.2(a) and with respect to rutting Fig 9.2 (b).

9.2 ANALYTICAL DESIGN OF PAVEMENTS

The computer program "ANPAD", (ANalytical PAvement Design) has been developed at Nottingham (Brunton 1983) to design flexible pavements from fundamental analytical concepts. The design procedure for ANPAD is outlined in Fig. 9.3. It incorporates as subroutines a linear elastic layered system solution, CHEVRON, (Warren et al 1963) for structural analysis, and a procedure for evaluating the elastic stiffness of asphalt based on the programme PONOS (De Bats 1972), based on Van der Poel's Nomograph (Van der Poel 1954). The required input data for ANPAD is shown in Table 9.1. The design criteria used in this approach to pavement design are;

(a) the maximum tensile strain in the asphalt, limiting fatigue cracking and

(b) the maximum compressive subgrade strain, limiting permanent

Table 9.1 Typical Input Data Required for ANPAD

Input Data
Text, date
No. of designs
Options
Air temperature
Average speed
Design life (msa) or design life (years) Initial no. of commercial vehicles Percentage growth rate Year of road opening No. of traffic lanes
Layer thicknesses
Binder content
Void content
Specific gravity of aggregate for each bituminous layer
Specific gravity of bitumen
Type of base material
Subgrade CBR
Sub-base to subgrade modular ratio

deformation.

In both cases the maximum allowable values depend on the number of repeated load applications of a standard wheel load. This is usually expressed in millions of standard axles (MSA), for the design life of a pavement.

The standard magnitude of axle weight is 80kN. A dual wheel load is therefore 40kN, represented in the analysis of a pavement as a pair of circular uniformly distributed loads, at 150mm centres, with a contact pressure of 500kPa.

9.2.1 The criterion for fatigue cracking

The design criterion to prevent failure by fatigue cracking is tensile strain (εt), and the maximum value occurs at the base of the asphalt layer. To prevent failure by fatigue the level of strain must be below the critical value which would cause failure over the life of the pavement, expressed as the Number of cycles to failure (Nf).

The fatigue life of a bituminous mix was found to be dependent on the volumetric proportion of binder (V_b), and its initial softening point (SPi). The Nomograph Fig. 9.4 has been developed from extensive laboratory data, for the purposes of defining the fatigue line for a given mix. (Pell, Cooper 1975, and Cooper, Pell 1974).

Alternatively the equations shown on Fig.9.4 may be used. Either the tensile strain for a given life, or the life for a given tensile strain may be calculated.

9.2.2 The criterion for permanent deformation

Prevention of excessive rutting is dealt with by limiting the maximum vertical strain on the subgrade (εz) and Fig. 9.5 shows the

relationship between the maximum allowable value of this parameter and the number of load applicatons in Million's of Standard Axles (M.S.A) This relationship applies when the road base is made from a standard hot rolled asphalt and was derived by back-analysis of trial pavements using this material (Brown 1974).

Material other than hot rolled asphalt road base offers different resistance to permanent deformation and will therefore achieve different lives in the same design situation. These are catered for by modifying the basic equations and introducing a rut factor (fr). These factors are presented here below for four mixes, the typical British Standard materials and modified versions of these developed at Nottingham (Brown, Cooper and Pooley 1985).

Hot rolled asphalt	1
Dense bitumen macadem	1.56
Modified rolled asphalt	1.37
Modified dense bitumen macadam	1.52

9.3 EFFECTS OF POLYMER GRID ON PERMANENT DEFORMATION

It has been demonstrated that polymer grids when located at the correct position in an asphalt layer control permanent deformation. Fig.9.6 shows the approximate experimental constructions investigated at Nottingham.

The tests conducted on slabs in the S.T.F. and P.T.F., described in Chapter Six were typically of the construction shown in Fig. 9.7(a). The slabs were constructed on a rigid, non deformable, plywood base. Only single wheel tracking was used and the bituminous material was tested at 30^{0}C. The grid in these tests was located in the middle of the asphalt layer, and deformation or rutting could only occur through lateral flow, or to a lesser extent, compaction of the asphalt. This situation is similar to an asphalt

overlay on a stiff pavement (i.e. concrete), but should only be equated to any situation where deformation is expected in the upper layers of the pavement. The extension in life of the reinforced slabs over the unreinforced slabs was a minimum of 3.9 times and a maximum of 30 times (i.e. 3.9 to 30 times the number of load applications were required to realize the same magnitude of permanent deformation in the reinforced slabs as the unreinforced slabs) (Table 6.4). Note should be taken of the negligible effect on permanent deformation when the grid was included at the asphalt/plywood interface in the reflection cracking tests in the S.T.F. (Section 5.3.4). The grid in this case, positioned away from the area of flow in the asphalt, showed no sign of controlling permanent deformation.

Deformation was also monitored on a full depth asphalt construction represented in Fig. 9.6(b), discussed in Chapter Seven. The grid was located at the base of a 150mm asphalt layer, wheel tracking was distributed across the pavement, and testing was conducted at temperatures between 17^{0}C and 34^{0}C. From Fig.7.5 and 7.6 the benefit from including the grid in this position was negligible with respect to permanent deformation. The test was continued with on overlay Fig. 9.6(c) reinforced at the asphalt/overlay interface. Only when single tracking and high temperatures (35^{0}C) were achieved, did any appreciable benefit occur through the inclusion of the grid. This is illustrated by the two data points at 10,000 passes shown in Fig. 7.6.

Further testing in the P.T.F. on a thin asphaltic concrete pavement constructed over a soft support Fig.9.6(d) (described in detail in Chapter Seven), was an example of deformation occurring in the foundation of the pavement, and not in the bituminous layer. The development of permanent deformation for the three sections in the test, (unreinforced, reinforced in the middle of the asphalt

layer, and reinforced at the base of the asphalt layer), is shown in Fig. 7.23. As the highest shear strains were occurring beneath the bituminous layer, the grid located at the base of the asphalt layer, played the most significant part in reducing permanent deformation. The number of passes of the wheel to form a rut of 20mm in the unreinforced section was at least 50,000, and in the section reinforced at the base of the asphalt layer 135,000. An increase in life of at least 2.7 times is therefore apparent.

From the laboratory investigations carried out at Waterloo (Haas 1983) on polymer grid reinforced pavements it was stated that

"The results show that for equal thicknesses, reinforced pavements would carry more than three times the number of loading cycles in order to reach the same level of limiting criteria of rutting."

It is clear that the grid will not be effective in controlling permanent deformation if it is too remote from the high shear strains developed in the pavement, which may occur either at the surface or in the lower layers.

In situations where deformation is likely to occur in the upper layers of the pavement i.e. overlays on rigid constructions, areas of high temperature or heavily canalised traffic, a depth of approximately 25% of the width of the loaded area on the pavement is likely to be an appropriate depth. Practically this may be between the wearing course and base course or at the base of an overlay. In situations where deformation is expected in the foundation of the pavement the grid should be located at the base of the asphalt layer.

Based on these experiences, an increase in life of three times for reinforced pavements was introduced into the design calculation for the control of permanent deformation.

9.4 RESISTANCE TO CRACKING

9.4.1 Reflection cracking

The ability of the grid to inhibit reflection cracking has been demonstrated in Chapter Five. In laboratory tests conducted on beams, the grid has reduced the propagation of cracking by a factor of three, (e.g. Fig. 5.9) when included within the asphalt mix. When located at the base of the asphalt beams, no cracking was evident at the end of testing.

In the tests conducted on asphalt slabs, those slabs which were reinforced at the base of the asphalt layer showed no signs of cracking at the conclusion of testing.

In both types of tests, on beams and slabs, debonding was noticed between the asphalt layer and the plywood base.

Thermal reflection cracking relative to areas with high diurnal, or seasonal variations in temperature has not been investigated. This type of reflection cracking involves large movements at the joints in concrete pavements over an extended period of time. The assumptions, therefore, on the inhibition of reflection cracking presented here should not be extended to areas where large thermal movements in pavements are expected and thermal reflection is the major cause of distress.

An increase in life of a factor of three was introduced for reinforced pavements with respect to reflection cracking. The grid when used for the purpose of reducing the severity of reflection cracking should be located as near to the tip of the existing crack or joint as possible. It is possible that the grid could be placed in one to two metre strips over joints easily identified otherwise a continuous roll should be used.

9.4.2 Fatigue cracking

The initiation of fatigue cracking is dependant on the level of repeated tensile strain in a bituminous material. The maximum strain occurs at the base of the asphalt layer and this is the location in which the grid should be positioned to inhibit fatigue. The research at Nottingham has shown that the elastic stiffness of reinforced pavements is unaltered from that of unreinforced pavements. The initial level of repeated tensile strain at the base of an asphalt layer must therefore be similar for reinforced and unreinforced pavements. The equivalent stiffnesses of reinforced and unreinforced bituminous material has also been demonstrated in four point bending tests (Brown and Brodrick 1980). The advantage of the high strength tensile element at the base of the asphalt layer, with regard to fatigue cracking is therefore to reduce the rate of crack propagation through an asphalt layer, and inhibit horizontal permanent deformation.

The thin asphaltic concrete pavement tested in the P.T.F. was one such pavement susceptible to fatigue. Surface cracking was noticed in both the unreinforced section and the section reinforced in the middle of the asphalt layer at between 20,000 and 30,000 passes of the wheel. In the section reinforced at the base of the asphalt layer, no cracking was evident after 200,000 passes, when the test was concluded. This suggests that a minimum factor of 10 for the increase in life of reinforced pavements over unreinforced pavements is suitable for fatigue. The importance of the grid location was also highlighted in this test as cracking was not inhibited in the section reinforced in the middle of the asphalt layer.

Further testing has been carried out at Nottingham (Brunton and Brown 1984), on the fatigue life of reinforced asphalt. The

experimental arrangement is shown on Fig. 9.7. An asphalt beam rested on a rubber support and was cyclically loaded through a semi-rigid loading platen. A small crack indicator was cast into each beam and the grid (Tensar AR1), when used, was placed immediately above it. Asphaltic concrete was used in each of the tests and a tenfold increase in fatigue life was realised for reinforced beams.

Haas 1983 also concluded on the testing conducted at Waterloo that, "Fatigue cracking was not observed on the surface of reinforced pavements, which suggests this criterion becomes secondary when reinforced pavements are considered."

9.5 ANALYTICAL DESIGN PROCEDURE FOR REINFORCED PAVEMENTS

9.5.1 Design of new construction

Using the modified design method a parametric study was carried out. This shows how the grid would affect the structural layer of the pavement, in new construction typical of that shown in Fig.9.1 (Brown, Hughes, Brodrick 1985). Four types of asphalt mix were used for the road base and are detailed in Table 9.2. Rut factors were available for these mixes (see Section 9.3) with respect to the development of permanent deformation, as each will deform to a different extent under trafficking.

The design conditions used were as follows:

(a) 40mm hot rolled asphalt wearing course

(b) Variable road base (Details in Table 9.2)

(c) 225mm granular subbase

(d) Subgrade of 5% CBR

(e) Average annual air temperature, $9.5^{0}C$

(f) Average speed of commercial vehicles, 50 km/hr.

The two hot rolled asphalt mixes provide pavements which are

Table 9.2 Details of Typical Road Base Materials

Mix type No.	Mix type	Binder Content (%)	Void Content (%)	VMA (%)	Initial Penetration of Bitumen
1	Typical Hot Rolled Asphalt	5.7	5.0	18.1	50
2	Typical Dense Bitumen Macadam	3.5	10.0	17.9	100
3	Modified Hot Rolled Asphalt	5.0	4.0	15.7	50
4	Modified Dense Bitumen Macadam	4.5	6.0	16.4	50

stronger with respect to cracking than rutting. Consequently when using a grid it should be located near the surface to increase life based on rutting. In this construction a convenient location would be immediately below the 40mm hot rolled asphalt wearing course, which is susceptible to permanent deformation.

Fig. 9.8 shows the variation in total thickness of road base as a function of design life for the rolled asphalt constructions, illustrating the savings when a layer of grid is installed. The computations are tabulated in Table 9.3. In this case the design life is increased three times for both the hot rolled asphalt and the modified hot rolled asphalt.

For a typical dense bitumen macadam, fatigue cracking is the more likely failure mode. Consequently, the grid would be most usefully located at the bottom of the roadbase. In the design computations the additional advantages, for this material, of including a second layer of grid below the wearing course were also considered. The design chart is shown in Fig. 9.9, and the calculations have been tabulated in Table 9.4. Particularly large benifits for Mix type 2 were noticed when the material was reinforced at the base of the layer. Additional benefit was gained when reinforcement was considered at both the base of the asphalt layer and immediately underneath the wearing course.

The modified dense bitumen macadam is much less susceptible to fatigue cracking (due to lower void content, and a higher percentage of harder grade bitumen). In this case most benefit was gained by reinforcing the pavement structure at the base of the wearing course.

The benefit of including grid reinforcement in new constructions can be assessed in various ways. The most pessimistic approach would be to use normal layer thicknesses and to regard the inclusion of a grid as an additional factor of safety or an attempt to reduce the

Table 4.3 Design computations for typical and modified hot rolled asphalt road bases

Mix Type	Thickness of Road base (mm)	Design life (m.s.a.)									S Design life reinforced / Design life Unreinforced
		Unreinforced						Reinforced			
					1 layer at bottom (for fatigue x10)			1 layer at top (deformation x3)			
		Nz	Nt	Nd	Nz	Nt	Nd	Nz	Nt	Nd	
1	100	1.0	11.7	1.0				3.0	11.7	3.0	3.0
	150	4.9	63.0	4.9				14.7	63.0	14.7	"
	200	18.5	27.3	18.5				55.5	273	55.5	"
	250	578	1009	57.8				173	1009	173	"
3	100	2.0	21.9	2.0				6.0	21.9	6.0	3.0
	150	11.1	124	11.1				33.3	124	33.3	"
	200	46.6	556	46.6				140	556	140	"

Where Nz is design life required for deformation m.s.a.)

Nt is design life required for fatigue (m.s.a.)

Nd is design life

S is maximum increase in design life due to inclusion of grid reinforcement

Table 9.4 Design computations for typical and modified dense bitumen macadam road bases

Mix Type	Thickness of Road base (mm)	Design life (m.s.a)												S = Design life reinforced / Design life Unreinforced
		Unreinforced			Reinforced									
					1 layer at bottom (for fatigue x10)			1 layer at top (deformation x3)			1 layer at top and bottom			
		Nz	Nt	Nd	Nz	Nt	Nd	Nz	Nt	Nd	Nz	Nt	Nd	
2	100	1.2	0.5	0.5	1.2	5.0	1.2				3.6	5.0	3.6	7.2
	150	4.8	1.5	1.5	4.8	15.0	4.8				14.4	15.0	14.4	9.6
	200	16.0	3.4	3.4	16.0	34.0	16.0				48.0	34.0	34.0	10.0
	230	30.5	5.5	5.5	30.5	55.0	30.5				91.5	55.0	55.0	"
	300	113	14.7	14.7	113	147	113				339	147	147	"
	400	488	49.2	49.2	488	492	488				1464	492	492	"
4	100	2.1	11.4	2.1				6.3	11.4	6.3				30
	125	4.9	26.2	4.9				14.7	26.2	14.7				"
	150	10.7	56.6	10.7				32.1	56.6	32.1				"
	170	19.4	100.6	19.4				58.2	100.6	58.2				"
	200	43.9	225.8	43.9				132	2258	132				"

Where Nz is design life required for deformation (m.s.a.)

Nt is design life required for fatigue (m.s.a.)

Nd is design life

S is maximum increase in design life due to inclusion of grid reinforcement

chances of pavement failure within a design period.

Alternatively, although less conservative, saving in thicknesses may be estimated from Figs. 9.8, 9.9, which would allow economic comparisons to be made. The cost of the grid and its installation is difficult to quantify precisely but is likely to be about £2.5/m^2 (1986 prices). An asphalt mix costs about £0.07/mm/m^2 (1986 prices) therefore any thickness saving in excess of 2.5/0.07, i.e. 36mm, shows economic benefit. Another approach to the design calculation might be to consider the grid as providing an extension in life to a pavement of conventional thickness for a nominal increase in initial cost.

9.5.2 Design of overlays

An overlay may be required over a cracked or failing concrete pavement, or a construction may need upgraded to meet a more demanding traffic flow. Overlays over concrete pavements may be particularly susceptible to rutting in the upper layers, or reflection cracking.

In any situation where reflection cracking is likely to be the main source of distress the grid should be positioned as close to the existing crack as possible, as illustrated in Fig. 9.2(a). Laboratory tests have also shown that under certain conditions (transient loads), reflection cracking can be eliminated by placing the grid at the base of the asphalt layer, or if placed within the asphalt layer an increase in life of three is realised.

The grids appear to be attractive for use in overlays on heavily trafficked areas with high concentrated wheel loads, and elevated temperature, i.e. in situations where normal mix design practise is inadequate to deal with permanent deformation. Fig. 9.2(b) shows two positions where the grid might be located. As stated previously the

grid must be situated in the area sustaining the highest shear strain, i.e. where asphalt flow is greatest. Over a rigid concrete pavement the majority of deformation must take place in the asphalt overlay, the grid should be positioned below the wearing course in a normal base course/wearing course overlay. Alternatively, if an overlay is on an asphalt pavement, itself susceptible to permanent deformation, the grid may be of better use positioned at the base of the overlay. A factor of times three is suitable for the extension in life realised by a reinforced pavement over an unreinforced pavement.

The situation might arise where a combination of reflection cracking and pavement deformation is a problem. A satisfactory solution is this case might be to place a strips of grid over existing cracks or joints in the pavement to reduce reflection cracking, apply a base course, and where permanent deformation is considered a problem, i.e. in bus lanes, approaches to traffic lights or junctions etc., to instal a layer of grid between the wearing course and base course. In any of these situations an increase in life of a factor of three would be a conservative estimate of the effect of including the grid, whether at the tip of an existing crack or within an overlay.

For design purposes the use of grids in overlays may be considered similar to the use of grids near the surface of new constructions.

9.6 CONCLUSIONS

Using the analytical design procedures developed at Nottingham, quantitive improvements in pavement construction can be estimated by including a polymer grid at various positions within a pavement. Design charts have been produced for four different road base

materials with the grid located either at the base of the construction, for fatigue, and in the top layers for permanent deformation and reflection cracking. The location of the grid is vital for the maximum benefit to be realised, and the likely failure mode must first be recognised before the position of the reinforcement is specified.

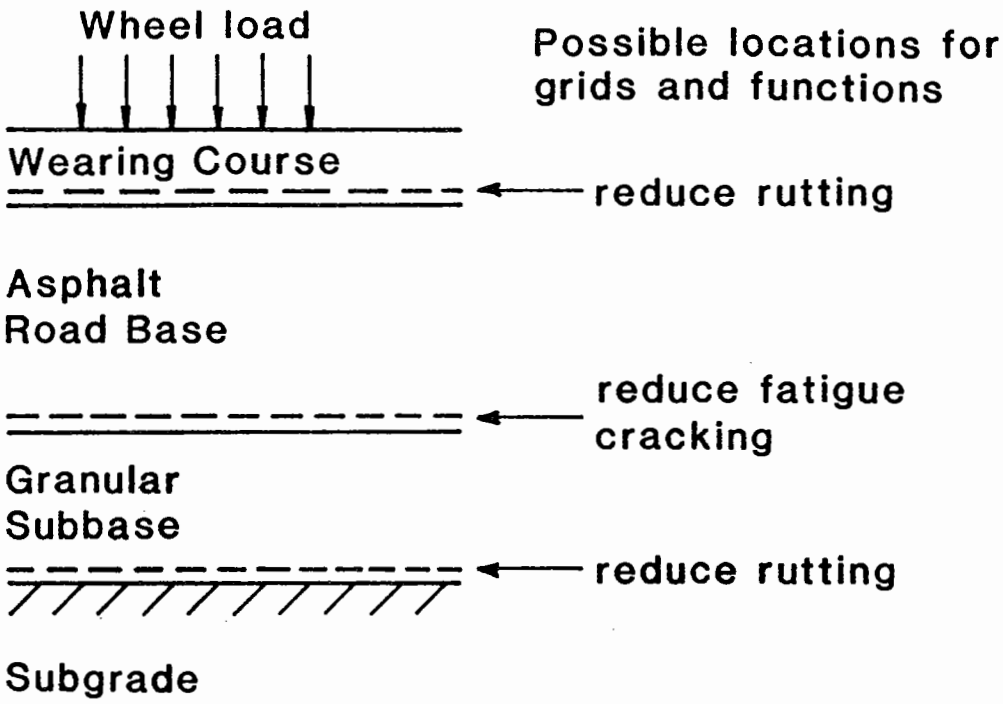

Fig. 9.1 Use of Grids in New Pavement Construction

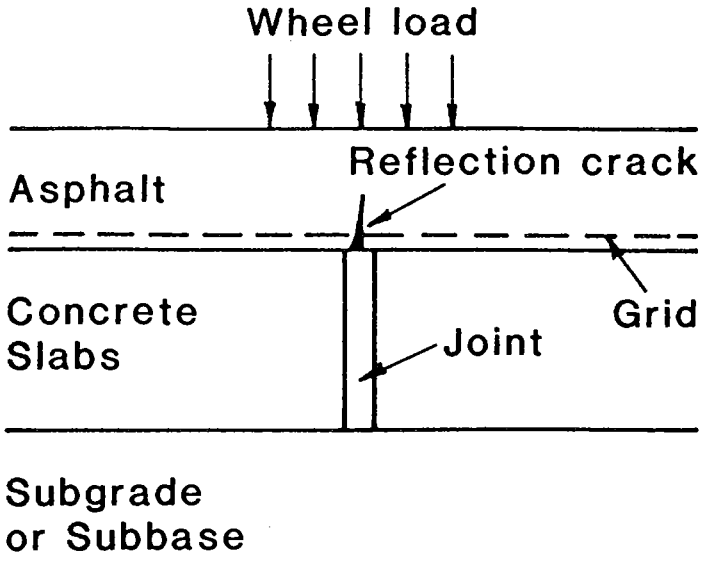

(a) Reflection Cracking

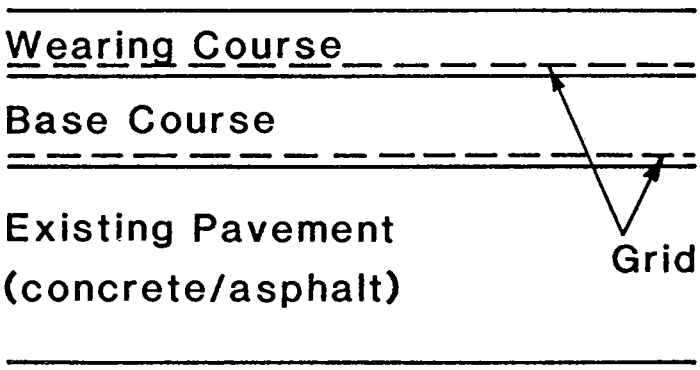

(b) Rutting

Fig. 9.2 Use of Grids in Overlays

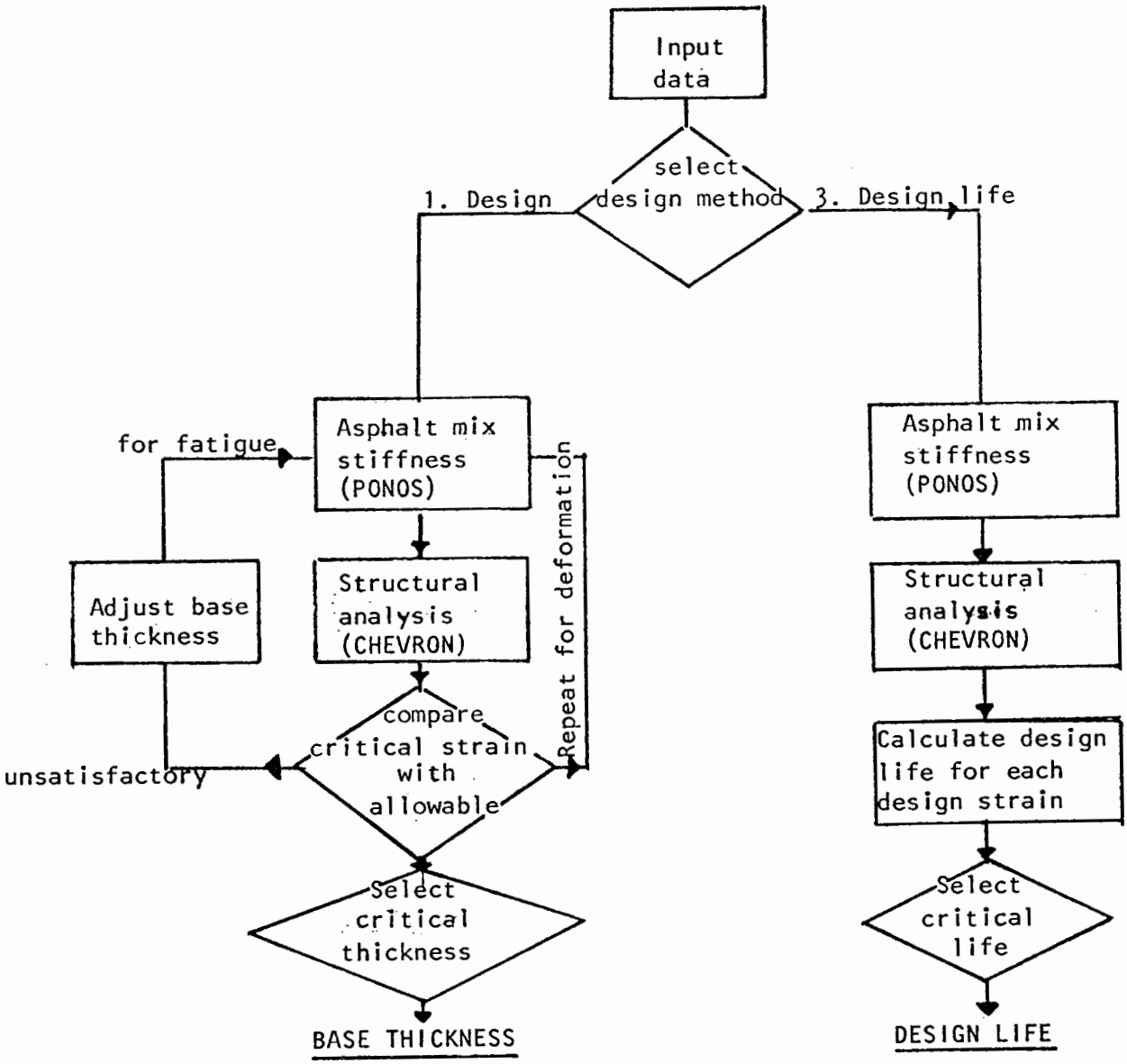

Fig. 9.3 Flow diagram for ANPAD

(After Brown and Brunton)

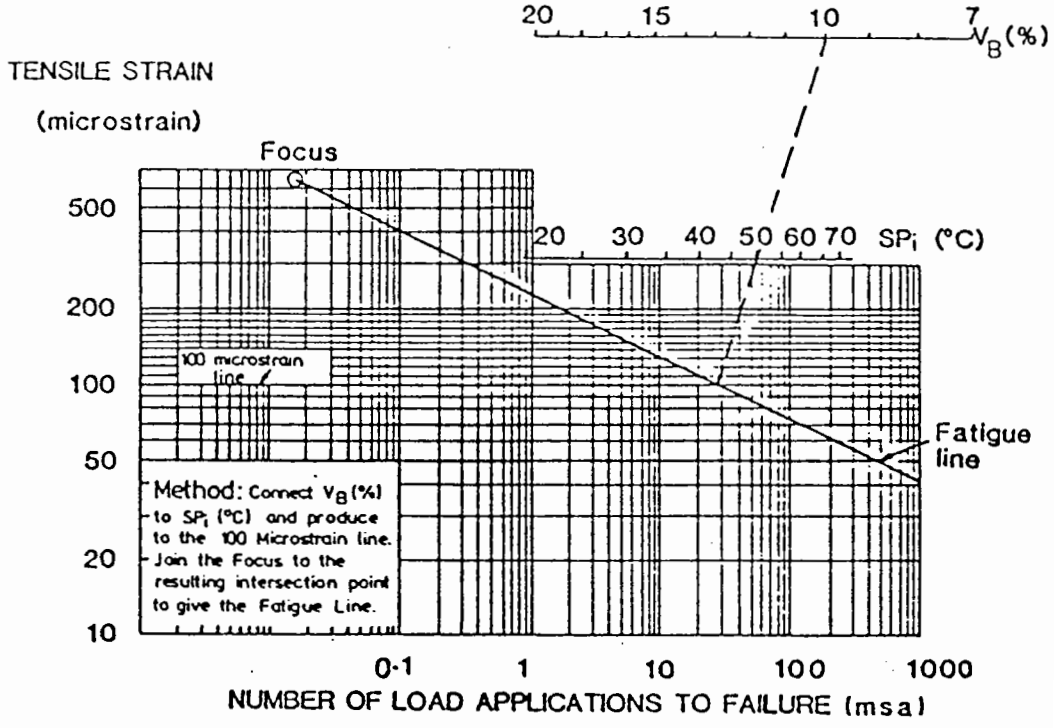

$$\log \varepsilon_t = \frac{14.39 \log V_B + 24.2 \log SP_i - 46.06 - \log N}{5.13 \log V_B + 8.63 \log SP_i - 15.8}$$

$$\log N = 15.8 \log \varepsilon_t - 46.06 - (5.13 \log \varepsilon_t - 14.39) \log V_B - (8.63 \log \varepsilon_t - 24.2) \log SP_i$$

Fig. 9.4 Nomograph for the Determination of Fatigue Strength (Derived from Cooper and Pell)

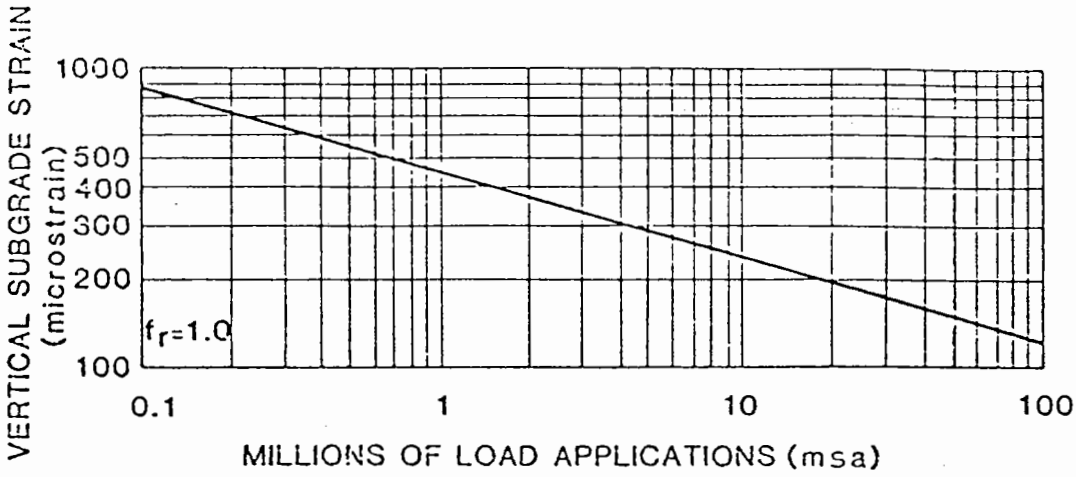

$$\varepsilon_z = \frac{451.3}{(N/f_r)^{0.28}} \qquad N = f_r \left(\frac{3 \times 10^9}{\varepsilon_z^{3.57}} \right)$$

Fig. 9.5 Maximum Allowable Subgrade Strain

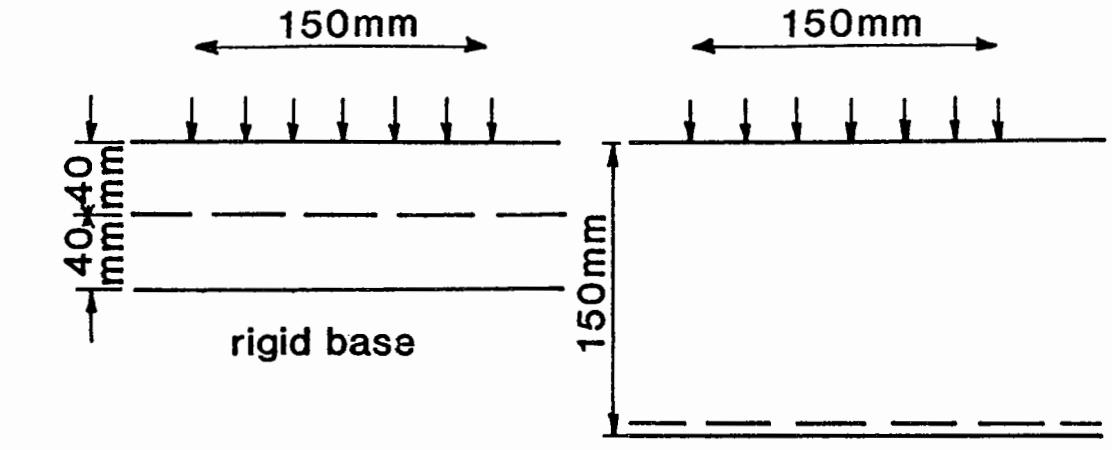

(a) Typical Slab Test (b) Full Depth Asphalt Test

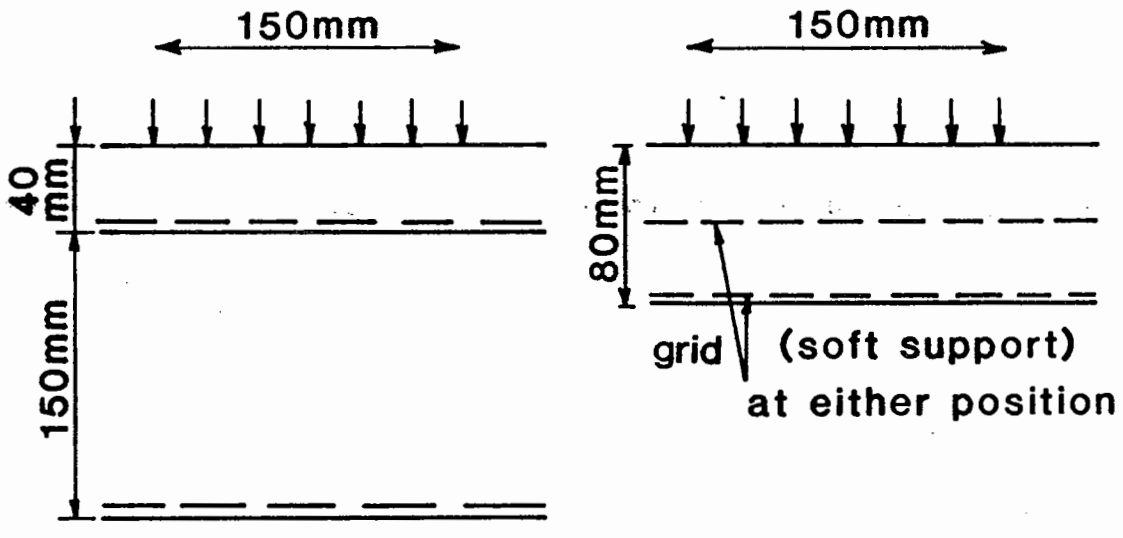

(c) Full Depth Test with Overlay

(d) Thin Asphalt Layer on Soft Support

Grid shown thus: — — —

Fig. 9.6 Grid Positions for Various Constructions

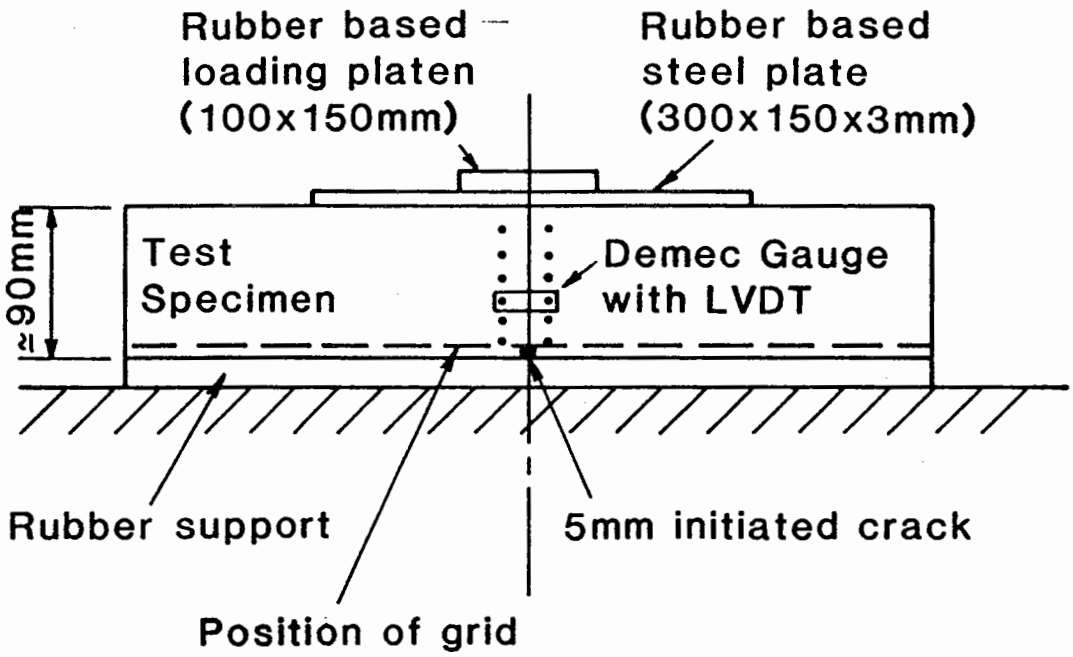

Fig 9.7 Experimental Arrangement for Fatigue Cracking Tests (After Brunton and Brown 1984)

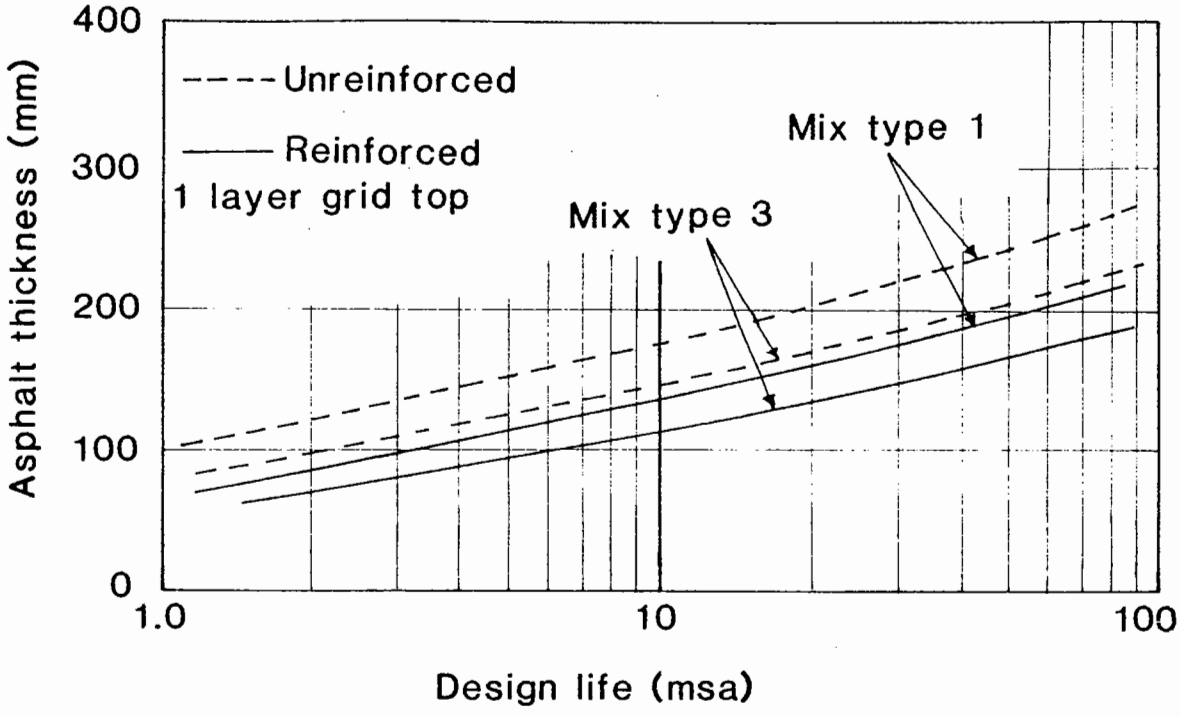

Fig 9.8 Design Thickness Requirements for Rolled Asphalt Road Base Mixes

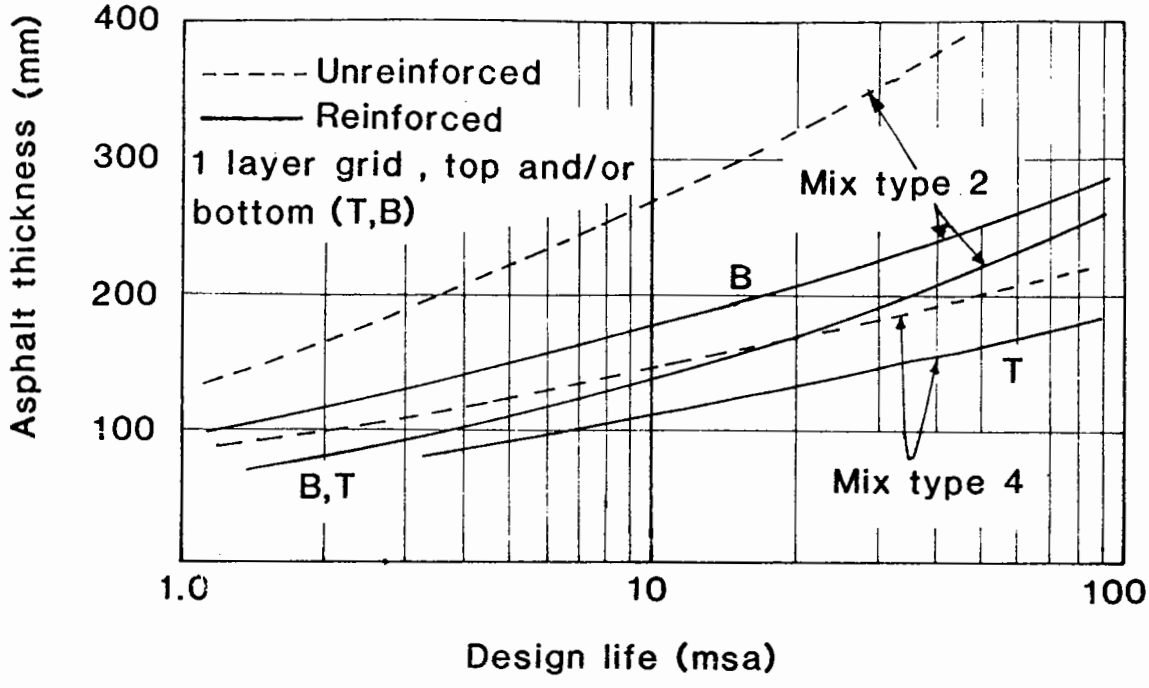

Fig 9.9 Design Thicknesses for Dense Bitumen Macadam Road Base Mixes

10 CONCLUSIONS AND RECOMMENDATIONS FOR FUTURE WORK

10.1 CONCLUSIONS

The conclusions which have been drawn from the research to date at the University of Nottingham on polymer grid reinforced pavements were as follows:

1. The elastic stiffness of "Tensar" AR1 is approximately 0.9MN/m.
2. The elastic stiffness of "Tensar" AR1 falls by approximately 50% over a temperature increment of 40°C (i.e. from 5°C to 45°C). Bituminous material is however, more temperature susceptible and, therefore, at high or abnormally high pavement temperatures the modular ratio between the grid and bitumen will be greater.
3. The effect of frequency on the stiffness of the grid was minimal between 1Hz and 30Hz.
4. The stiffness of the grid is not reduced by exposure to elevated temperatures such as those experienced during paving, provided shrinkage is prevented.
5. The grid will be insulated from extreme temperatures during paving by the "chip seal" layer, used in the installation procedure.
6. The grid, although prone to creep or load relaxation, was not susceptible to fatigue effects of importance in asphalt applications.
7. Reflection cracking tests on beams have shown that cracking may be prevented if the grid is included at the base of the asphalt layer, and reduced in severity if included within the asphalt layer.
8. Reflection cracking tests in the S.T.F. have shown that under loading similative of a moving wheel, cracking may be prevented when the grid is at the base of the asphalt layer.
9. Permanent deformation tests in the S.T.F. have shown that the

grid when sandwiched in an asphalt, reduces rutting. A large aperture grid used in this series of tests was also successful in reducing rutting.

10. The complete deterioration of unreinforced slabs tested in the S.T.F. showed the ability of the grid to inhibit cracking and lateral flow in the asphalt. The reinforced slabs, remained uncracked and coherent throughout each test.

11. The grid, when included at an asphalt interface using the "chip seal" method, reduced the shear strength by approximately 20%, at low loading rates.

12. Tests in the Pavement Test Facility.

(a) Testing on a full depth asphalt pavement have shown that the grid will not reduce rutting when positioned at the base of the asphalt layer in a heavy duty pavement.

(b) The grid, when included at the base of an overlay, does reduce permanent deformation under severe loading.

(c) The grid when included at the base of a thin asphalt pavement prone to high elastic and plastic strains, does significantly reduce the amount of permanent deformation and cracking.

13. The position of the grid in a structure is extremely important in reducing the severity of any particular mode of distress, in particular:

(a) To inhibit reflection cracking the grid must be at the base of an overlay, or the tip of an existing crack.

(b) To inhibit permanent deformation the grid must be located at the region of maximum shear strain in the bituminous layer, or in structures susceptible to deformation in the lower layers, at the base of the asphalt layer.

(c) To inhibit fatigue cracking the grid should be at the base

of the asphalt layer.

14. An increase in life of approximately 10 times for fatigue cracking seems appropriate for a reinforced structure over an unreinforced structure.

15. An increase in life of approximately 3 times for both permanent deformation and reflection cracking seems appropriate for a reinforced structure over an unreinforced structure.

16. The grid does not initially increase the elastic stiffness of a bituminous layer.

The ability of the grid to improve the performance of flexible pavements has been proven in the laboratory. Tests on asphalt slabs, beams and on typical constructions in the P.T.F. have shown the ability of the grid to inhibit both reflection cracking and fatigue cracking and to reduce permanent deformation. The grid typically performs to greatest advantage under conditions which are outside the normal limits set on asphalt design, i.e. areas of high ambient temperatures, extreme loading conditions, or constructions likely to sustain severe permanent deformation.

10.2 RECOMMENDATIONS FOR FUTURE WORK

To prove the undoubted benefits of polymer grid reinforced pavements, full scale trials must be carried out and the product proven in the field. Although laboratory testing is a good indication of likely behaviour in the field, restrictions on duration and scale of test amongst other things are obviously imposed.

Guidelines have already been developed for the design of reinforced asphalt pavements, and data from full scale trials would help to "tune" these guidelines to suit various pavement conditions.

Reflection cracking caused by the slow opening and closing of

concrete joints in an overlayed pavement due to diurnal or seasonal variations in temperature are a major cause of distress in extreme climates. Although this was not fully examined, a testing rig has been developed at Nottingham to simulate this movement. The test specimens were identical to those used in the reflection cracking beam tests described in Section 5.2. Unfortunately, owing to lack of time, no samples were tested. A full description of the testing rig is given in Appendix C. Further testing in this area would complement the results already obtained.

The polymer grid has other applications in pavement design which have not as yet been fully investigated. One such application is the use of the grid in roadbases stabilised with either lime or cement. These roadbases are susceptible to cracking and lead to reflection cracking in asphalt overlays. The grid might control cracking in the roadbase in the same manner as steel reinforcing in concrete controls cracking.

REFERENCES

A.S.T.M. "Rubber property - Durometer hardness, Test for", D 2240-75, Part 35, 1980.

ASPHALT INSTITUTE, The "Mix design methods for asphalt concrete and other hot mix types" MS-2, May 1984.

ABDELHALIM, A. O., "Geogrid Reinforcement of Asphalt Pavements", Ph.D. Thesis, University of Waterloo, 1983.

ABDELHALIM, A.O., HAAS, R., PHANG, W.A., "Geogrid Reinforcement of Asphalt pavements and verification of elastic layer theory". T.R.R. 949, Washington 1983, pp 55-65.

ANSELL,P., "Cyclic simple shear testing of granular material", Ph.D. thesis, University of Nottingham, 1977.

ATKINSON,J.H., BRANSBY,P.L., "The Mechanics of Soils - an Introduction to Critical State Soil Mechanics", McGraw Hill, 1978, pp 81-83, pp 167-172.

BETERSON, W.D., "Recycled Asphalt Concrete in Utah", Symp. Proc. Assoc. Asphalt Paving Technologists, Vol. 49, 1979, pp 261-271.

BICHER,G. and HARRIS,R., "An experimental investigation of the action of welded wire fabric in bituminous concrete overlays as related to its control of reflection cracking", MSc thesis, Massachusetts Institute of Technology, 1956.

BISHOP,A.W., "A large shear box for testing sands and gravels", Proc. 2nd Int. Soil Mechanics Conf., Rotterdam, 1948, pp.207-11.

BOHN,A., ULLIDTZ,P., STUBSTAD,R. and SORENSON,A., "Danish experiments with the falling weight Deflectometer", Proc. 3rd Int. Conf. on Structural Design of Asphalt Pavements, Vol.1, 1972, pp.1119-1128.

BRITISH STANDARDS INSTITUTION, "Specification for coated macadam for roads and other paved areas", BS 4987, 1973.

BRITISH STANDARDS INSTITUTION, "Specification for rolled asphalt (hot process) for roads and other paved areas" BS 594, 1973.

BRITISH STANDARDS INSTITUTION, "Hot rolled asphalt for roads and other paved areas", BS 594, 1973.

BROWN,S.F., "A simplified fundamental design procedure for bituminous pavements", The Highway Engineer, Vol.21, No. 8-9, 1974, pp 14-23.

BROWN,S.F., BRODRICK,B.V.,(a) "Grid reinforcement for asphalt pavements", Report No. 1, Submitted to Netlon/SERC, Nottingham University, 1982.

BROWN,S.F., BRODRICK,B.V.,(b) "Nottingham Pavement Test

Facility", T.R.R.810, 1981, pp 67-72.

BROWN,S.F., BRODRICK,B.V.,(c) "Instrumentation for the Nottingham Pavement Test Facility", TRR 810, 1981, pp 73-79.

BROWN,S.F., BRODRICK,B.V. and HUGHES,D.A.B., "Tensar reinforcement of asphalt - laboratory studies", Proc. Symp. on Polymer grid Reinforcement in Civil Engineering, SERC/Netlon Ltd., London 1984.

BROWN,S.F. and BRUNTON,J.M., "The Influence of bonding between bituminous layers", Journal Inst. Highways and Transportation, No.5, Vol.31, May 1984, pp 16-17.

BROWN, S.F., and BRUNTON, J.M.(a), "Improvements to pavement subgrade strain criterion", Journ. Transp. Eng., ASCE, Vol. 110, No. 6, 1984, pp 551-56

BROWN, S.F., BRUNTON, J.M.(b), "An Introduction to the analytical design of bituminolus pavements", University of Nottingham, 1984.

BROWN, S.F., and BRUNTON, J.M.(c), "Computer programs for the analytical design of asphalt pavements", Highways and Transportation, Vol. 31, No. 8/9, 1984, pp 18-27.

BROWN, S.F. and BRUNTON, J.M., "The Analytical Design of Bituminous Pavements", Proceedings Inst. of Civil Engineers, Pt. 2, 1985 (in press).

BROWN, S.F., BRUNTON, J.M., and STOCK A.F., "The analytical design of bituminous pavements", Proc. Inst. of Civil Eng., Pt. 2, Vol. 79, 1985, pp 1-31.

BROWN,S.F., COOPER,K.E., "The Mechanical Properties of Bituminous Materials for Road Bases and Base Courses", Proc. AAPT, Vol.53, 1984.

BROWN,S.F., COOPER,K.E., BRUNTON,J.M. and BRODRICK,B.V., "Development of improved procedures for asphalt pavement mix design", Report to Mobil Oil Ltd., Univ. of Nottingham, 1981.

BROWN, S.F., COOPER, K.E., and POOLEY, G.R., "Improved road base mixes for longer pavement life", Proc. Eurobitume Symp., 1985, The Hague, Netherlands.

BROWN, S. F., HUGHES, D. A. B., BRODRICK, B. V. "The use of polymer grids for improved asphalt performance", Eurobitume The Hague, 1985.

BROWN, S.F., HUGHES, D.A.B., BRODRICK, B.V., "Grid Reinforcement for Asphalt Pavements", Report No. 3, Submitted to Netlon/SERC, June 1985.

BROWN,S.F., PELL,P.S., "The potential for a theoretical approach to flexible pavement design", The Queens Highway, No.107, Oct. 1976, pp 11-16.

BROWNRIDGE,F.C., "An evaluation of continuous wire mesh reinforcement in bituminous resurfacing", Proc. Association of

Asphalt Paving Technologiests. Vol.33, 1964, pp 459-501.

BRUNTON, J.M.B., "Developments in the Analytical Design of Asphalt Pavements Using Computers", Ph.D. Thesis, University of Nottingham, 1983.

BRUNTON,J.M., BROWN,S.F., "Design of Asphalt Pavements with Polymer Grid Reinforcement for North American conditions". Submitted to the Tensar Corporation, University of Nottingham, October 1984. the art survey of reinforced asphalt paving" Proc. AAPT Vol.

BUSCHING, H.W., ANTRIM, J.D, "Fibre reinforcement of bituminous mixtures" Proc. AAPT Vol. 37 1968 pp 629-659

BUSCHING, H.W., ELLIOTT, E.H., REYNEVELD, N.G. "A state of the art survey of reinforced asphalt paving" Proc AAPT Vol. 39, 1970 pp766-798.

BUTTON,J.W., EPPS,J.A., LYTTON,R.L. and HARMAN,W.S., "Fabric interlayer for pavement overlays", Proc. 2nd Int. Conf. in Geotextiles, Las Vegas, 1982, pp 523-528.

COETZEE,N.F., "Some considerations on reflection cracking on asphalt concrete overlay pavements", PhD thesis, University of California, Berkeley, 1979.

COOPER, K.E. and PELL, P.S., "The effect of mix variables on the fatigue strength of bituminous materials", TRRL Report LR 633, 1974.

CRONEY,D., "Bituminous materials in road construction", HMSO, 1962.

DE BATS,F.Th., "The computer programs PONOS and POEL: a computer simulation of Van de Poels Nomograph", External report Koninkijke/Shell laboratorium, Amsterdam, 1972.

DEPARTMENT OF TRANSPORT, 'Specification for road and bridge works', HMSO, London 1976.

DEPARTMENT OF TRANSPORT, "Vacuum grouting of concrete road slabs", Roads and local transport directorate advice note HA 67/80.,1980

DYKES,J.W., "The use of fabric interlayers to retard reflection cracking", Proc. Association of Asphalt Paving Technologist, Vol.49, 1980, pp 354-366.

EATON,A.R. and GODFREY,R.N., "Reflection cracking studies at Thule Air Base, Greenland, using AC2.5 and fabrics", Proc. Association of Asphalt Paving Technologists, Vol.49, 1980, pp 381-396.

EPPS,J.A., et al, "Guidelines for recycling asphalt pavements", Proc. Association of Asphalt Paving Technologists, Vol.49, 1980, pp 144-176.

FOLEY,J.V. and WAGGENER,J.G., "The behaviour of welded wire fabric reinforcement in bituminous concrete", MSc thesis,

Massachusetts Institute of Technology, August 1957.

GERMANN, F. P., LYTTON, R. L.,"Methodolgy for predicting the reflection cracking life of asphalt concrete overlays" RR 207-5, Texas Transportation Institute, Texas A & M University, March 1979, pp 48-63.

GOTTSCHALL, A., HOLLSTEINER, S., "Steel fibre reinforced asphalt" Proc. 3rd Eurobitume Symposium, 'The Hague', Vol. 1 1985 pp 518-524.

GULDEN, W., BROWN, D., "Treatment for reduction of reflective cracking of asphalt overlays on jointed concrete pavements in Georgia," Transportation Research Record, 916, 1982.

HAYWOOD,A.T.J., "A review of the full scale road experiments with expanded metal under rolled asphalt laid on a concrete base", Research Report No. RN/2353/ATJH, Road Research Laboratory, Dept. of Scientific and Industrial Research, London, 1955.

HAAS, R, "Research and Development activities related to Tensar Geogrids", Progress Report for Tensar (Canada) Inc., November 1983.

HENSLEY,M.J., "Open graded asphalt concrete base for the control of reflective cracking", Proc. Association of Asphalt Paving Technologists, Vol. 49, 1980, pp 368-378.

HEUKELOM,W. and KLOMP,A.J.C., "Dynamic testing as a means of controlling pavements during and after construction", Proc. Int. Conf. on Structural Design of Asphalt Pavements, 1962, pp 667-679.

HORN,J.W., "The experimental use of welded wire fabric reinforcing in bituminous concrete resurfacing", MSc thesis, Massachusetts Institute of Technology, September 1956.

HUGO,F., STRAUSS,R. and SCHMITTER,O., "The control of reflection cracking with the use of a geotextile. A ten year case history", Proc. 2nd Int. Conf. on Geotextiles, Las Vegas, Vol.1,1982, pp 517-522.

JEWELL, R.A., MILLIGAN, G.W.E., SARSBY, R.W., DUBOIS, D., "Interaction between soil and geogrids". Proc. Symp. on Polymer grid reinforcement in Civil Engineering, SERC/NETLON LTD, London, 1984, pp 18-30.

JONES, C.M., "Recycling of Bituminous Pavements on the Road", Symp. Proc. Assoc. Asphalt Paving Technologists, Vol. 49, 1979, pp 240-250.

KANDHAL, P.S., "Asphalt cold recycling Technology in Pennsylvania", Proc. Assoc. Asphalt Paving Technologists, Vol. 53, 1984, pp 618-630.

KARI,W.J., et al, "Prototype specifications for recycling agents used in hot-mix recycling", Proc. of Association of Asphalt Paving Technologists, Vol.49, 1980, pp 144-176.

KENNEDY, C.K., FEVRE, P., CLARKE, C., "Pavement deflection: equipment for measurement in the United Kingdom", Dept of the Environment, Dept of Transport, TRRL Report LR 834, Crowthorne, 1978.

KENNEDY, C. K., LISTER, N.W., "Prediction of Pavement performance and the design of overlays", Dept. of Environment, Dept. of Transport, TRRL Report LR 833, Crowthorne, 1978.

KENNEPOL, J.A., LYTTON,R.L., "Pavement reinforcement with Tensar geogrids for reflection cracking reduction". Proc. Paving in cold areas, Canada/Japan Science and Technology consultations, Technical Memorandum of PWRI NJ 2136. October 1984, pp 863-882.

MACDONALD, C.H. "Recollections of early asphalt-rubber San Antonio, Texas, October 1982.

MAJIDZADEH, K., LUTHER, M.S., SKYLUT, H., "A mechanistic design procedure for fabric reinforced pavement systems", Proc. 2nd. Int. Conf. on Geotextiles, Vol. 2, AUGUST 1982, PP 529-534.

MARAIS, G.P. "The use of asbestos in trial sections of gap graded asphalt and slurry seals" Proc. C.A.P.S.A. Vol 1979 pp 172-175.

MARVILLET, J., VERSCHAVE, A., DUVAL, J., "Bitumen polymer binders for surface dressing" Proc. Eurobitume London 1978 pp 170-179.

McGOWN, A., ANCHAWES, K.Z., YEO, K.C., BUBOIS, D., "The lead-strain-time behaviour of Tensar Geogrids", Symposium Polymer grid reinforcement, SERC/Netlon Ltd, London, March 1984.

McGHEE, K.H., "Attempts to reduce reflection cracking of bituminous concrete overlays on portland cement concrete pavements". Virginia Highway and Transportation Research Council, Charlottesville, 1975.

MILLIGAN, G.W.E., LOVE, J.P., "Model testing of geogrids under an aggregate layer on soft ground". Proc. Symp. on Polymer grid reinforcement in Civil Engineering, SERC/Netlon Ltd, London, 1984.

MOLENAAR, A.A.A., "Structural Performance and Design of flexible road constructions and asphalt concrete overlays". pp 170-236.

MONTAGUE, S., "Fibres firm up fast rural repairs" N.C.E. 13th June, 1985, pp 20-21.

MOSEY, J.R., DEFOE, J.H., "In Place Recycling of Asphalt Pavements" Symp. Proc. Assoc. Asphalt Paving Technologists, Vol. 49, 1979, pp 261-171.

MULLEN, W.G., HADER, R.J., "Effectiveness of fabric and non Proc. Assoc. of Asphalt paving technologists, Vol. 49, 1980, pp 397-415.

MURRAY,C.D., "Simulation testing of geotextile membranes for reflection cracking", Proc. 2nd Int. Conf. on Geotextiles, Las Vegas, Vol.1, 1982, pp 511-516.

NIELSEN, D.L., RENSHAW, R.H., "Bitumen-rubber, the U.S.A. experience and its introduction to Southern Africa", Proc. Fourth C.A.P.S.A., Vol. 1, 1984, pp 335-353.

NIEVETT G. "The present position of the use of polymers in black top construction in Australia" Proc Eurobitume London 1978, pp 293-295.

PARIS, P.C., ERDOGEN, F., "A critical Analysis of Crack propogation Laws". Transections of the ASME, "Journal of Basic Engineering", Series D, Vol. 85, No. 3, 1963.

PATERSON, W.D.O. "Applications of rubber-bitumen membrane surfacing in pavement maintenance". Proc. Fourth C.A.P.S.A., Vol. 1, 1984, pp 397-405.

PELL, P.S., "Mechanical Properties of bituminous mixes" Conf. on The Analytical Design of Bituminous Pavements, Dept. of Civil Engineering, University of Nottingham, April, 1984

PELL, P.S., and COOPER, K.E., "The effect of testing and mix variables on the fatigue performance of bituminous materials", Proc. Assn of Asphalt Paving Technologists, Vol. 38, 1969, pp 371-422.

PEUTZ,M.G.F., VAN KEMPEN,H.P.M., JONES,A., (BISTRO) "Layered systems under normal surface loads". H.R.R. 228, 1968.

PEUTZ, M.G.F., VAN KEMPEN, H.P.M. and JONES, A., "Layered Systems under Normal Surface Loads", Highway Research Record 328, 1968, pp 34-45.

PIKE,D.C., "Shear Box tests on graded aggregates", TRRL Report LR584, Crowthorne 1973.

POOLEY, G.R. "Construction of a reinforced asphalt overlay at Canvey Island" Sym. on Polymer grid reinforcement in Civil Engineering: SERC/Netlon Ltd., Inst. Civil Engineers London 1984.

PORONI, G., PALLOTTA, S., LEGRANI, G., "Modified Bitumens" Proc. 3rd Eurobitume symposium, The Hague, Vol. 1985, pp 652-658.

POWELL, W.D., POTTER, J.F., MAYHEW, H.C., NUNN, M.E., "The Structural design of bituminous roads", Dept. of Transport, TRRL Report (LR1132 Crowthorne, 1984).

POWELL,W.D. and LEECH,D., "Rolling requirements to improve compaction of dense roadbase and basecourse macadam", TRRL, Report No.727, 1976.

RAITHBY,K.D. and STERLING,A.B., "Some effects of loading history on the fatigue performance of rolled asphalt", TRRL, Report LR 496, 1972.

"Recycling of asphalt mixtures", Symp Proc. of Asphalt Paving Technologist, Vol.48, 1979, pp 238-350.

ROAD RESEARCH LABORATORY, 'A guide to the structural design of pavements for new roads', Road Note 29, 3rd Edition, HMSO, London, 1970.

RUDDOCK, E.C., "Fabrics and meshes in roads and other pavements: a state of the art review", C.I.R.I.A., Technical Note 87, 1983.

SAADA, A.C., TOWNSEND, F.C., "State of the Art: laboratory strength testing of soils", A.S.T.M., Special Technical Publication No. 740, Chicago, June 1980, pp 7-77.

SCHEROCMAN,J.A., "Asphalt pavement construction: new methods and techniques", ASTM, Special Technical Publication, 1979.

SERVAS, V.P., CURTAYNE, P.C, WALKER, R.N., "Hot mix recycling - developments in the RSA and recommended approaches and contractural procedures", Proc. Fourth conf. on asphalt pavements for Southern Africa, Vol. 1, 1984, pp 353-363.

SCHAPERY, R. A., "A theory of crack growth in viscoelastic media" Report MM 2764-73-1, Texas A & M University, March 1983.

SMITH, R.D., "Laboratory testing of fabric interlayers for asphalt concrete paving: Interim Report", Transportation Research Record, 916, 1982.

SMITH,L.L. and GARTNER,W., "Welded wire fabric reinforcement for asphaltic concrete", Highway Research Board, Bulletin 322, 1959.

SOWERS,G.F., "Strength Testing of Soils", Proc. Conf. laboratory shear testing of soils, A.S.T.M., Special Technical Publication No. 361, Ottawa, Canada 1963, pp 3-22.

SZATKOWSKI,W.S., "Resistance to cracking of rubberised asphalt: full scale experiment on trunk road A6 in Leicestershire", TRRL Report LR 308, 1970.

TAM,W.S., "Design of Overlays for Bituminous Pavements", Internal Report No.WST/1. University of Nottingham, February 1985.

THOMPSON, R., COREY, D., CURRER, E.W.H., "The Alconbury Hill experiment and its relation to flexible pavement design". Proc. 3rd Int. Conf. on the Struct. Design of Asphalt pavements, Univ. of Michigen, Ann Arbor, 1972, pp 920-937.

TONS,E. and KROKOSKY,E.M., "A study of welded wire fabric strip reinforcement in bituminous concrete resurfacing", Proc. Association of Asphalt Paving Technologies, Vol.29, 1960, pp 43-76.

UZAN,J., LIUEH,M. and ESHED,Y., "Investigation of Adhesion Properties between Asphaltic Concrete Layer", Proc. AAPT,

Vol.47,, 1978, pp 495-521.

VAN DER POEL, C., "A general system describing the visco-elastic properties of bitumens and its relation to routine test data", Journ. App. Chem., 4, 1954, pp 221-236.

VAN DER POEL, C., "Time and temperature effects on the deformation of bitumen and bitumen-mineral mixtures", Journ. Soc. Plastics Engs, 11, 1955, pp 47-64.

WARD,I.M., "The Orientation of polymers to produce high performance materials", Proc. Symp. on Polymer Grid Reinforcement in Civil Engineering, SERC/Netlon Ltd., London March 1984, pp 1.

WARREN, H. and DIECKMANN, W.L., "Numerical computation of stresses and strains in a multi-layer asphalt pavement system", Unpub. int. rep., Chevron Research Corp., USA, 1963.

WAY, G.B., "Prevention of reflective cracking in Arizona", Proc. Assoc. of Asphalt paving Technologists, Vol. 49, 1980, pp 314-353/

APPENDIX A

THE INSTRON SERVO-HYDRAULIC TESTING FACILITY

The testing machine was used for "in isolation" tests on Tensar polymer grids and also for the reflection cracking investigation on asphalt beams. This machine, manufactured by Instron Ltd., can apply up to 100kN static loads and 50kN dynamic loads by means of a servo controlled hydraulic actuator of 100mm stroke, Fig 4.2. A control console monitors the applied load and actuator movement on a digital panel meter, and outputs are available for connections to a recorder so that permanent records can be obtained. Potentiometric controls on the console allow presetting of load or position or strain and frequency and a cycle counter records the progress of a test. By careful balancing it is possible to transfer from a load controlled test to a position or strain controlled test and limit switches are provided to prevent overload, overtravel and safety cut outs in all these modes.

For holding loads close to zero, a 10kN load cell is provided as the tolerances on the 100kN load cell output voltages could cause instability. This is because the load cell acts as a feed back to the servo control in a closed loop configuration. If zero is approached the loop may become apparently open and the actuator, when in load control, will become uncontrollable. In practise it is usually possible to apply a small load in position control (0.3kN) and then transfer to load control and operate between this value and the peak load required. Another important setting is the system gain which affects the response of the actuator to materials of different stiffness, i.e. different mechanical gain. This can be determined in two ways, firstly by increasing the gain until the loading system begins to oscillate and then backing off, or secondly applying a step

input at low gain and then increasing the gain until about 7% overshoot is obtained. Gain setting can be a problem for visco elastic materials as their properties may change with rate of loading and so must be determined for the prevailing test conditions.

The machine has a movable upper cross head to accommodate various specimen sizes and hydraulic jaws are used to locate loading platens. Hydraulic power is obtained from a 30kN water cooled oil pump.

APPENDIX B

RESTRAINT FORCE RESULTS

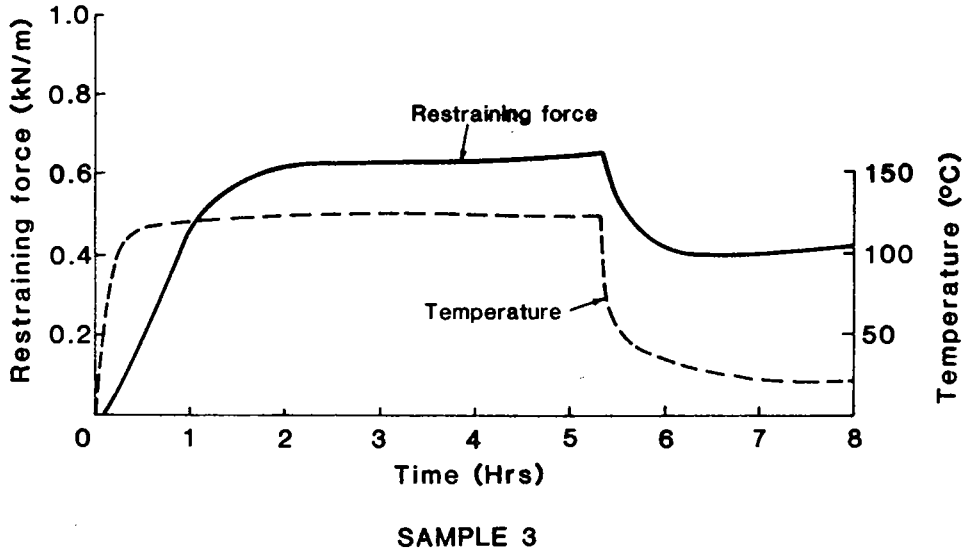

Fig. B1 Restraining Force With Temperature Changes in SS3

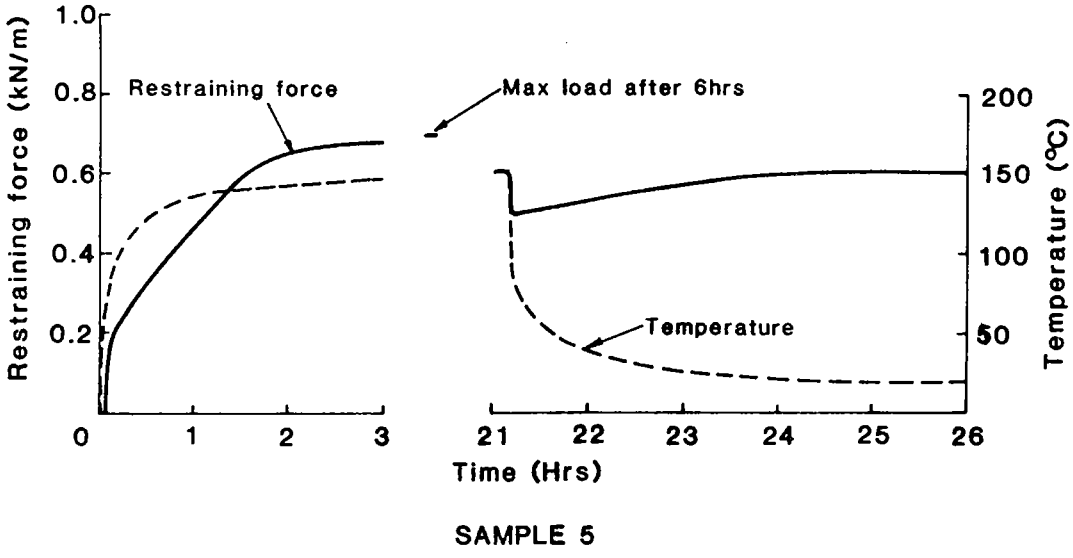

Fig. B2 Restraining Force With Temperature Changes in SS3

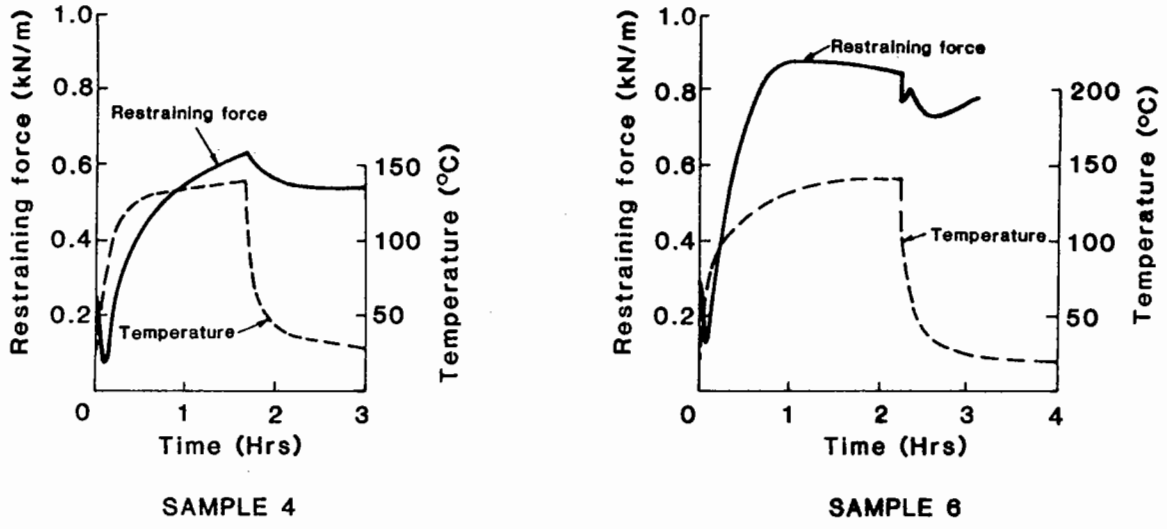

Fig. B3 Restraining Force With Temperature Changes In SS3

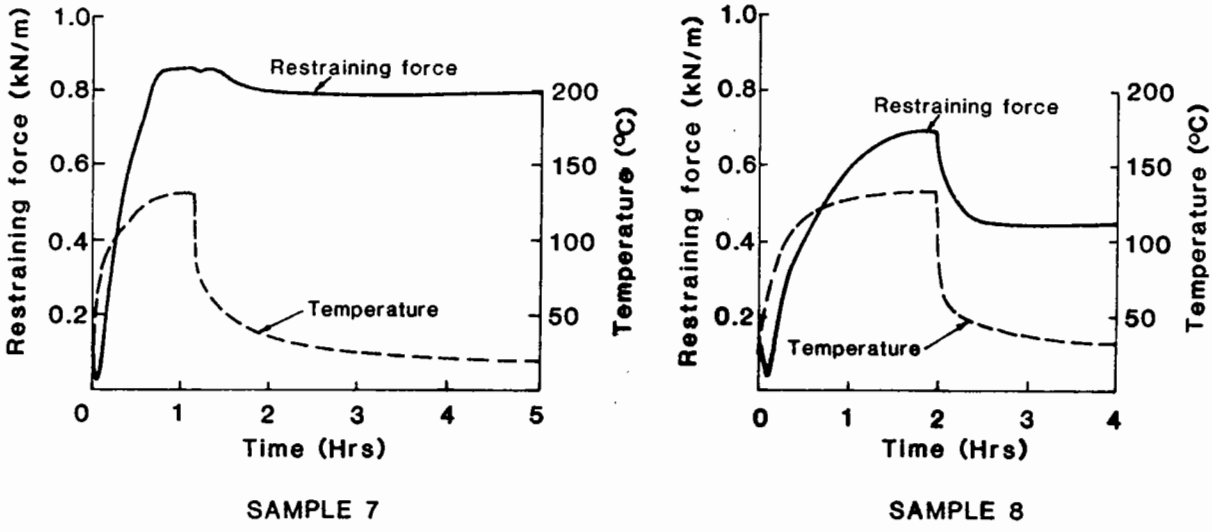

Fig. B4 Restraining Force With Temperature Changes in SS3

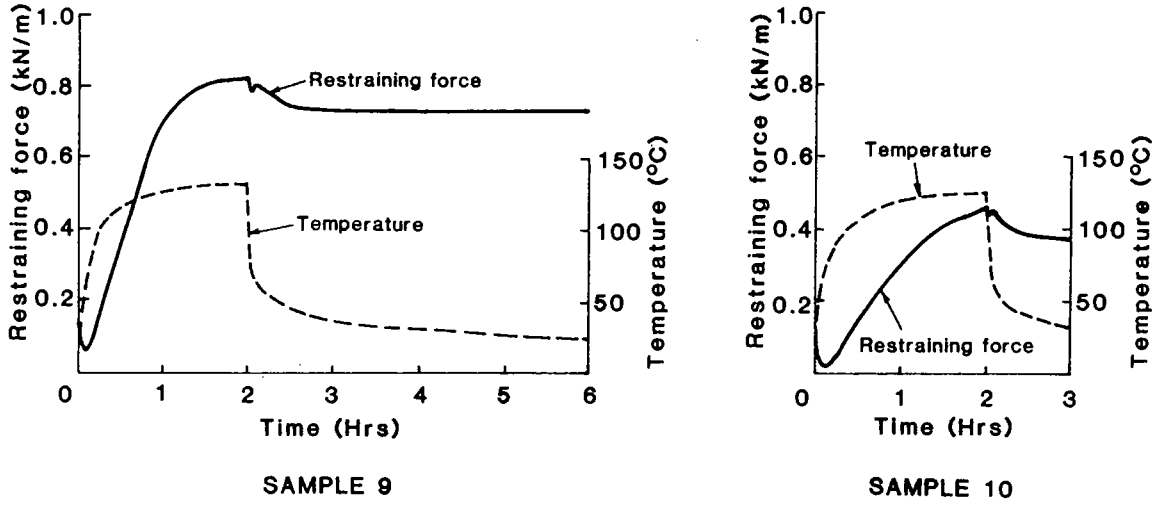

Fig.B5 Restraining Force With Temperature Changes in SS3

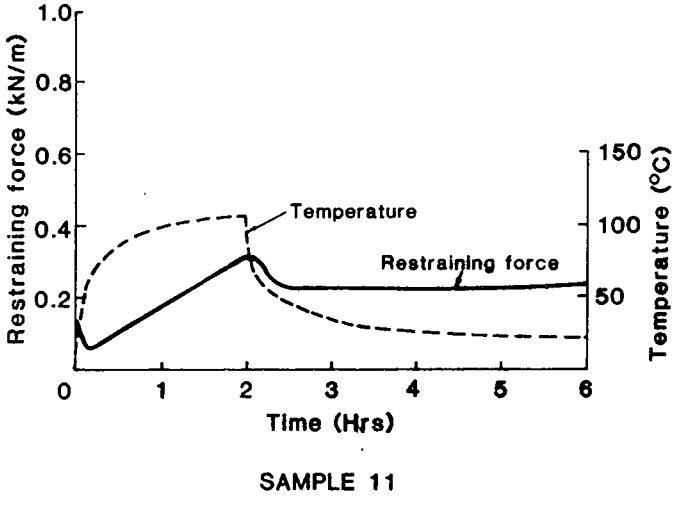

Fig. B6 Restraining Force With Temperature Changes in SS3

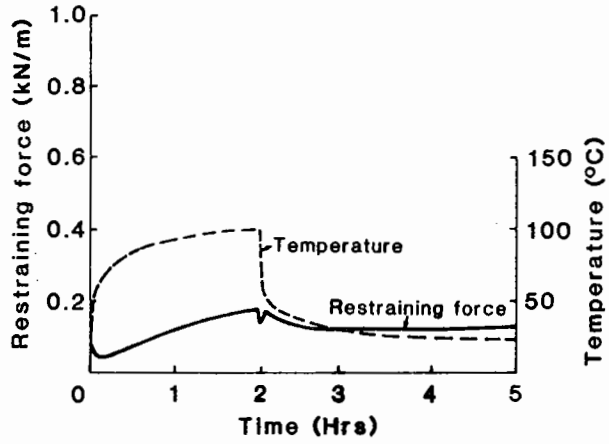

SAMPLE 12

Fig. B7 Restraining Force With Temperature Changes in SS3

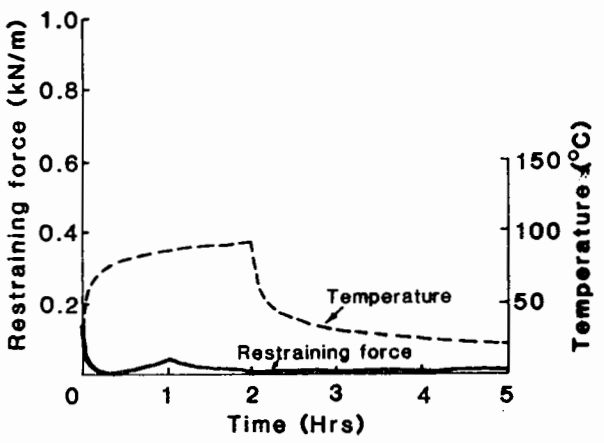

SAMPLE 13

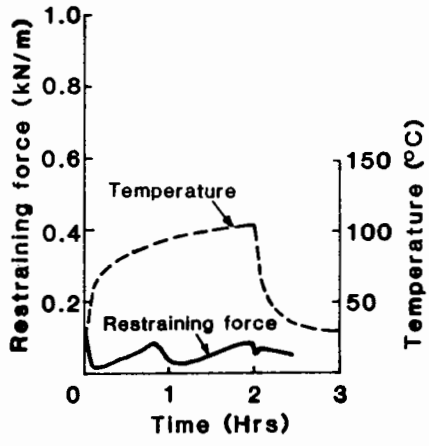

SAMPLE 14

Fig. B8 Restraining Force With Temperature Changes in SS3

APPENDIX C

C.1 THERMAL REFLECTION CRACK SIMULATOR

Reflection cracking may be caused by movements in underlying concrete slabs, caused by large diurnal or seasonal variations in temperature. In extreme climatic conditions, seasonal variations in temperature of 50^{o}C would not be unusual, although in a more temperate climate such as the U.K., pavement temperature may not vary this much. Experimental data on concrete pavements (Croney 1977) in England, has shown that the maximum season variations in temperature (Δt)in the centre of a concrete slab are approximately 30^{o}C with maximum daily fluctuations of 10^{o} C.

The magnitude of movement at a joint is dependent on the coefficient of thermal expansion of the concrete slab,(α) and the degree of restraint offered by the subgrade. The normal length (l) of a slab is between 5m and 10m, the coefficient of expansion (α) approximately, 10 x 10^{-6}/^{o}C. Neglecting the restraint due to the subgrade, the maximum seasonal movement at a joint, given by $l=\Delta t \times l \times \alpha$ for a 10m slab would be 3mm, and maximum daily movements, 1mm.

A facility has been developed in the laboratory to simulate this slow opening and closing of a joint, accompanied by temperature variations. A schematic diagram of the equipment is shown in Fig C.1. The specimens located in the rig are shown in Fig. C.2(a) and the control equipment Fig. C.2(b).

Two beam specimens are tested at the same time, the beams are similar to those that were used in the reflection cracking beams test and the procedure for manufacturing a specimen has been described elsewhere (Brown et al 1983). The asphalt beams (525 x 150 x 100mm deep), are cast onto plywood sheets, with a 10mm gap between them. The surface of the plywood sheets are roughened by glueing carborudom

paper to them, to create a suitable surface for asphalt to bonding. The beams were glued to steel sheets attached to the cross head and base of the testing rig. Clamps provided a positive "overburden" to prevent the beams separating from the plywood sheets. The crosshead of the testing rig could be either raised or lowered at a fixed strain rate, preset on the machine. When the crosshead was raised, tension was created in the asphalt at the 10mm gap. The position of the crosshead and, hence, the movement at the 10mm gap, was monitored using a linear potentiometer, while the temperature of the asphalt beams was measured with a thermocouple capable of delivering an analogue output. A load cell recorded the load required to move the crosshead. The facility was housed in a temperature controlled environment fitted with an electric heater and cooler and a fan to circulate air in the cabinet.

Fig. C.3 shows the arrangement whereby the analogue signals of load, temperature and position were converted to digital signals and read by a computer. A printer was also available to print the data at intervals during the test. The simulator was capable of varying the temperature of the test specimens while, simultaneously, moving the crosshead and, hence, opening and closing the 10mm gap.

A computer program was written to control the test facility; a brief flow chart is shown on Fig. C.4. The input data required was the minimum temperature, the temperature range, the amplitude of movement at the gap and the time period over which the temperature and movement were cycled. The strain rate had to be preset on the rig, and a suitable value manually calculated. The theoretical temperature and spacing of the gap was generated by the computer, and varied sinusoidally.

Initially, the specimens were heated to the maximum temperature of the test. During the first half of the cycle, immediately after

initialization, the specimens were cooled from maximum to minimum temperature, and the joint opened accordingly, creating tension in the asphalt beam. By continually comparing the theoretical temperature and position, generated by the computer, with the actual specimen temperature and joint spacing, the temperature and cross head were adjusted. The cooler, heater and crosshead movement were controlled through relays operated by the computer. During the second half of the cycle, i.e. when the temperature had reached its minimum and the joint was at maximum spacing, the crosshead was lowered and the temperature raised. Owing to an inefficient temperature control system, the time period over between maximum and minimum temperatures was over two hours. At intervals during the test, data on theoretical position and temperature, actual position and temperature and load were printed by the computer.

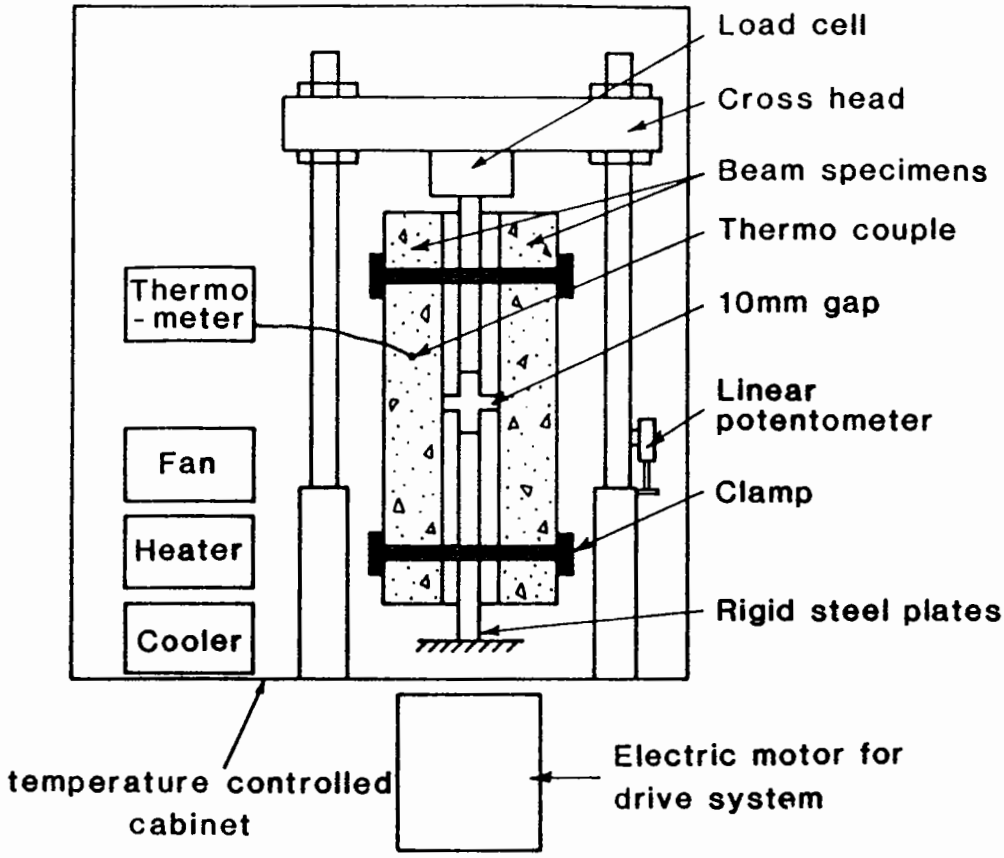

Fig. C1 Thermal Reflection Crack Simulator (Schematic)

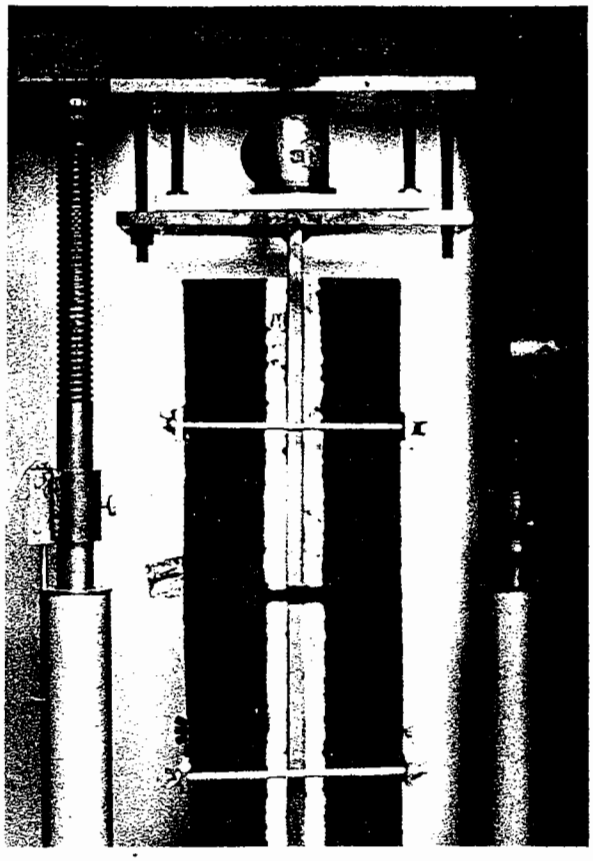

(a) Test sample

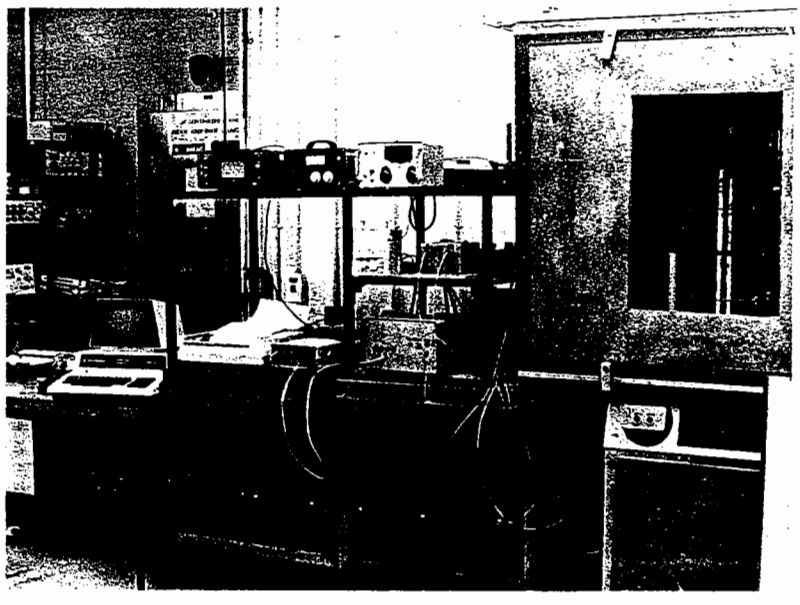

(b) Test apparatus

Fig C2 Thermal reflection crack simulator

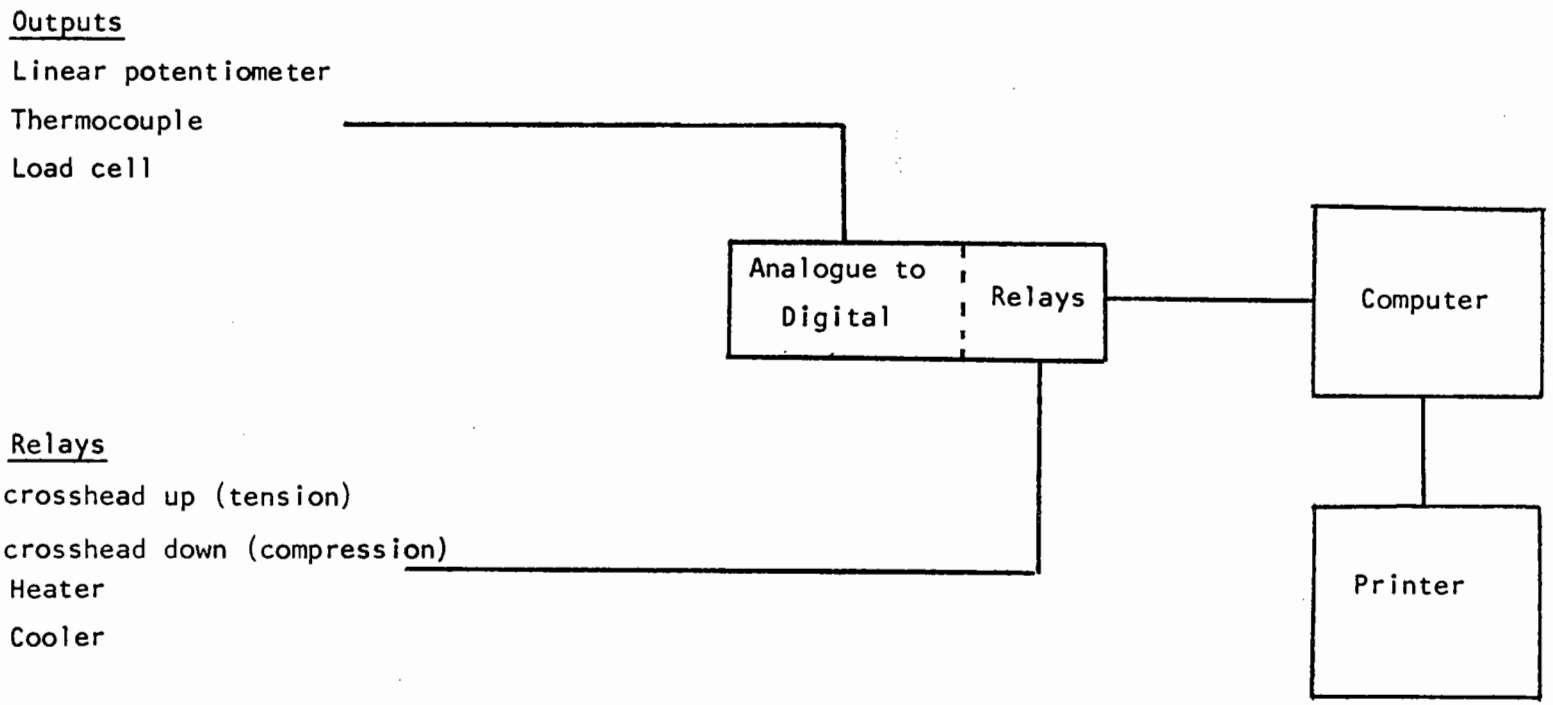

Fig.C3 Control system for Thermal reflection Crack Simulator

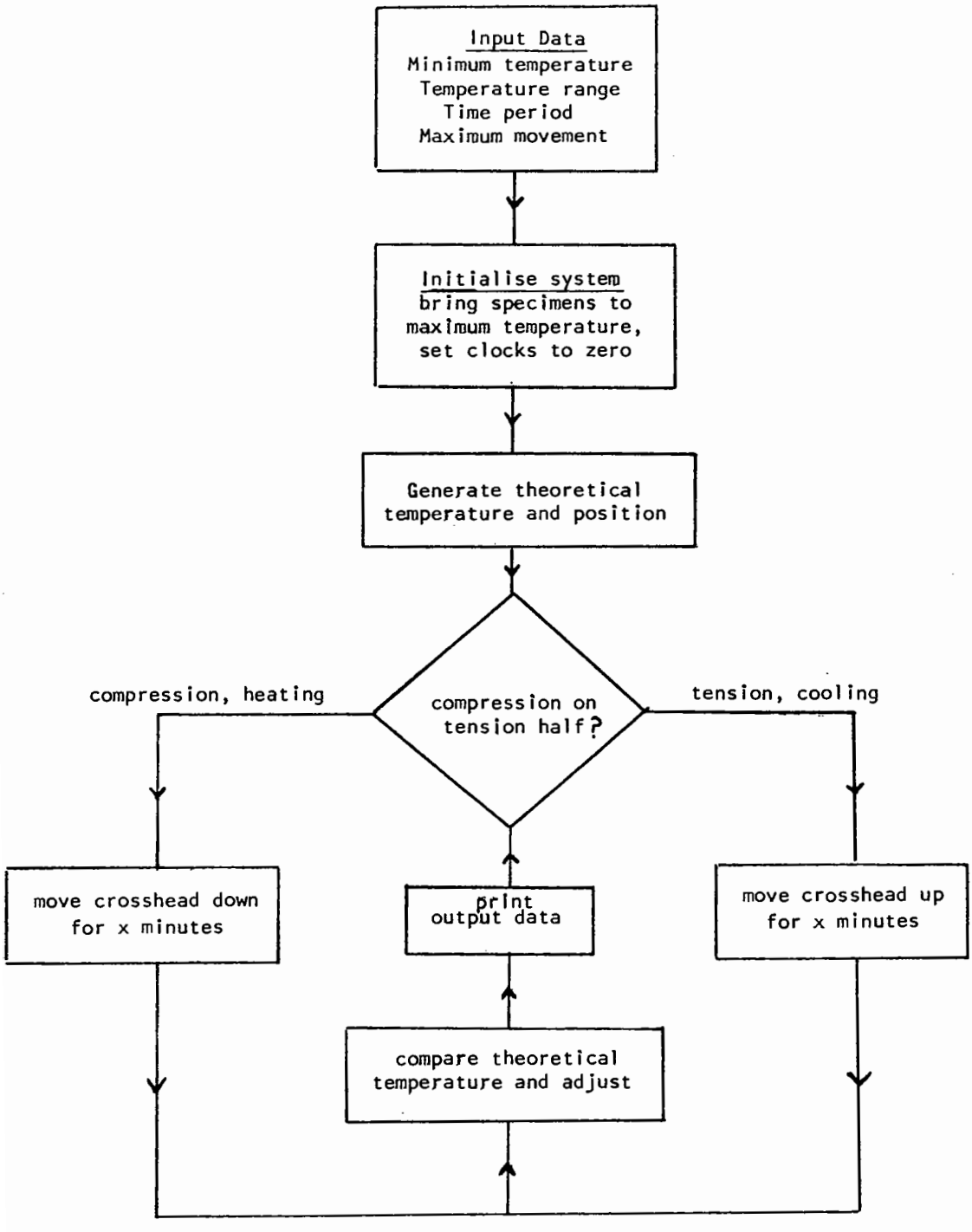

Fig.C4 Flow diagram for computer control of thermal reflection crack simulation

APPENDIX D

D.1 Mix Proportions

All bituminous mixes have three basic components; aggregate, binder and air. The mechanical properties of the mix are strongly dependent on their relative volumetric proportions. For practical reasons, proportions by mass are used to specify a mix for a particular job. Hence, conversions from mass to volume and vice versa are frequently needed and a sound grasp of the important mix parameters is required. The volume and mass components of a unit volume of compacted mix are shown below.

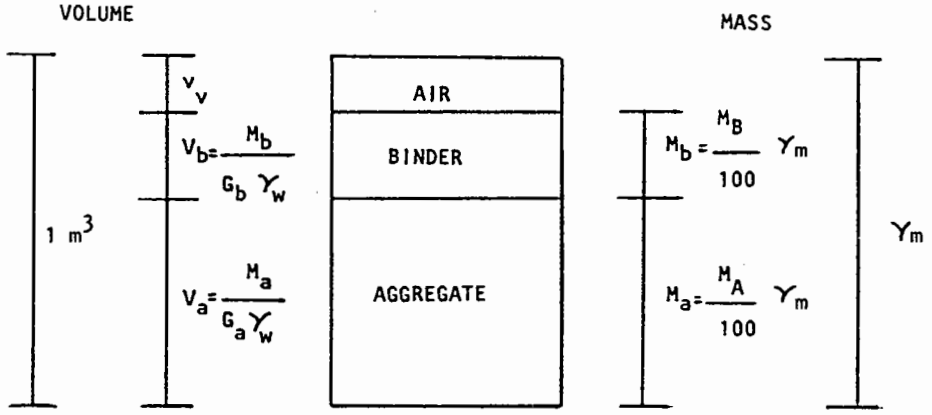

M_B = Binder content per cent by mass of total mix

$M_A + M_B = 100\%$

M_A = Aggregate content per cent by mass of total mix

M_b = Mass of binder, kg G_b = Specific gravity of binder

M_a = Mass of aggregate, kg G_a = Specific gravity of mixed aggregate

γ_m = Density of compacted mix, kg/m^3,

γ_w = Density of water (1,000 kg/m^3)

V_a = volume of aggregate, m^3

V_b = volume of binder, m^3 $V_a + V_b + V_v = 1 m^3$

V_v = volume of voids, m^3

V_A = volume of aggregate as %

V_B = volume of binder as %

V_v = volume of air voids as %

Note that upper case suffices imply quantities expressed as percentages.

Although aggregate grading and the type of mineral used form an important part of mix design, it is not necessary to consider them in detail in analytical design. Emphasis here is placed on proportions by volume and two particular parameters will need to be determined to evaluate the mechanical properties of mixes of significance for design. These are:

V_B, the proportion of binder by volume;

and

$VMA = V_B + V_v$, the 'voids in mixed aggregate'.

Given the binder content by mass and the void content of a mix as usual starting points, V_B is calculated from:

$$V_B = \frac{(100 - V_V)(M_B/G_b)}{(M_B/G_b)+(M_A/G_a)}$$

If the various portions of aggregate have different specific gravities, then an effective G_a for the mixed aggregate can be calculated from:

$$G_a = \frac{100}{(X/G_X)+(Y/G_Y)+\ldots}$$

where X, Y, etc., are the percentages by mass of each aggregate fraction having specific gravities G_x, G_Y, etc., or a number of "M_A/G_a" terms may be included in the denominator so long as all the mass proportions total 100%.

If it is necessary to calculate void content from measured density, (i.e. the density calculated from weighing a sample of mix in air and water to obtain it's volume and hence density), the following equation is applicable.

$$V_V = \frac{(\gamma_{max} - \gamma_m)}{\gamma_{max}} \times 100$$

in which γ_{max} is the theoretical maximum density which corresponds to zero void content. It is determined as follows:

$$\gamma_{max} = \frac{100\gamma_w}{(M_B/G_b)+(M_A/G_a)}$$

APPENDIX E

E THE SLAB TEST FACILITY

A side view of the Slab Testing Facility (S.T.F) is shown in Fig. E.1 with the hydraulic motor positioned at the opposite end to the loading actuator (see also Fig. 5.18). The carriage is driven by means of a wire rope tensioned around a drum, which is axially coupled to the motor. The drum rotation is transformed to linear motion by means of a screw in a sliding block. This operates a feedback displacement transducer which produces a voltage proportional to wheel position and, when differentiated, a signal proportional to velocity. Comparison of the differentiated signal with the command velocity signal produces an error voltage which is fed to a servo valve attached to the motor. The motor rotation continuously tries to minimise this error, which represents the difference between the command rate of change of position and actual rate of change of position, and effectively drives the carriage at the desired speed. Once over the slab, trigger voltages at each end, representing position, are used to stop the carriage and a circuit to detect zero speed then commands reversal. The result is a controlled reciprocation of the carriage at a constant speed over the slab. A tachogenerator is fitted to the drum shaft as part of the safety circuit to give a direct velocity output sensitive to a sudden increase in shaft speed should the drive cable start to break.

The loading arrangement is by means of twin beams acting as a lever on the moving carriage. Constant wheel load over the slab can only be achieved by applying an increasing actuator load of the correct "slope" as the wheel approaches the actuator. This was conveniently obtained by using the carriage position voltage as a command signal which increased (zero output was at the hinge) as the

carriage approached the actuator. An in-line load cell attached to the actuator shaft provided a feedback voltage proportional to the actuator load. It was thus feasible to control the actuator through a servo valve so that it maintained a constant wheel load during carriage movement over the slab. Actuator displacement must be responsive as it has to react to the lever deflection, tyre, slab and support compression during loading. Care had to be taken to prevent overload as the wheel approaches the hinge end, when the lever effect increases enormously.

Slab load was also measured by load cells placed under each corner of a steel pallet. The upper plate of the pallet was detached so that different reinforcing could be inserted between it and its supporting frame. This provided the option of a rigid support or a flexible support to simulate different foundation characteristics.

Initially, the S.T.F. was to come under total micromputer control, but the requirements were found to be incompatible with readily available systems (primarily made for on-off applications), and the software (programming) needed considerable development. Consequently, an advanced electronic control, Fig. E.2, which could eventually be brought under computer control, was constructed. The electronic design uses a three term servo control on both the wheel pass and load control. This improves accuracy and stability. The first term, is basically a direct amplication of the error signal which corrects general error changes. The second term is an integral term which acts like a long-term memory and tends to reduce the static error to zero and increases control accuracy. A differential term completes the three components and this corrects the tendency to overshoot which often occurs at high feedback gain. This brings about an improved dynamic actuator response to demand and command changes.

A lever arrangement for applying load was chosen as it is a simple concept allowing the carriage design to be straightforward. It has also been stated that keeping the wheel load constant would only require a simple ramp actuator load application, and this is basically true, although it has to be modified to compensate for the weight of the levers and carriage. However, in designing servo controls, account was also taken of the mechanical gain, for the dynamic system. That is to say, that the stiffness of the support under the wheel, the bending and resonance characteristics of the loading arrangement, must remain within the limits of the response of the hydraulic system. Clearly, the support conditions change as the wheel moves over the steel approach beams and on to the asphalt slab, but perhaps less obvious is the resonant frequency change of the lever system as its fulcrum changes with the wheel position. This means that, as the wheel moves, the electronic feedback gain has to vary in order to maintain mechanical stability.

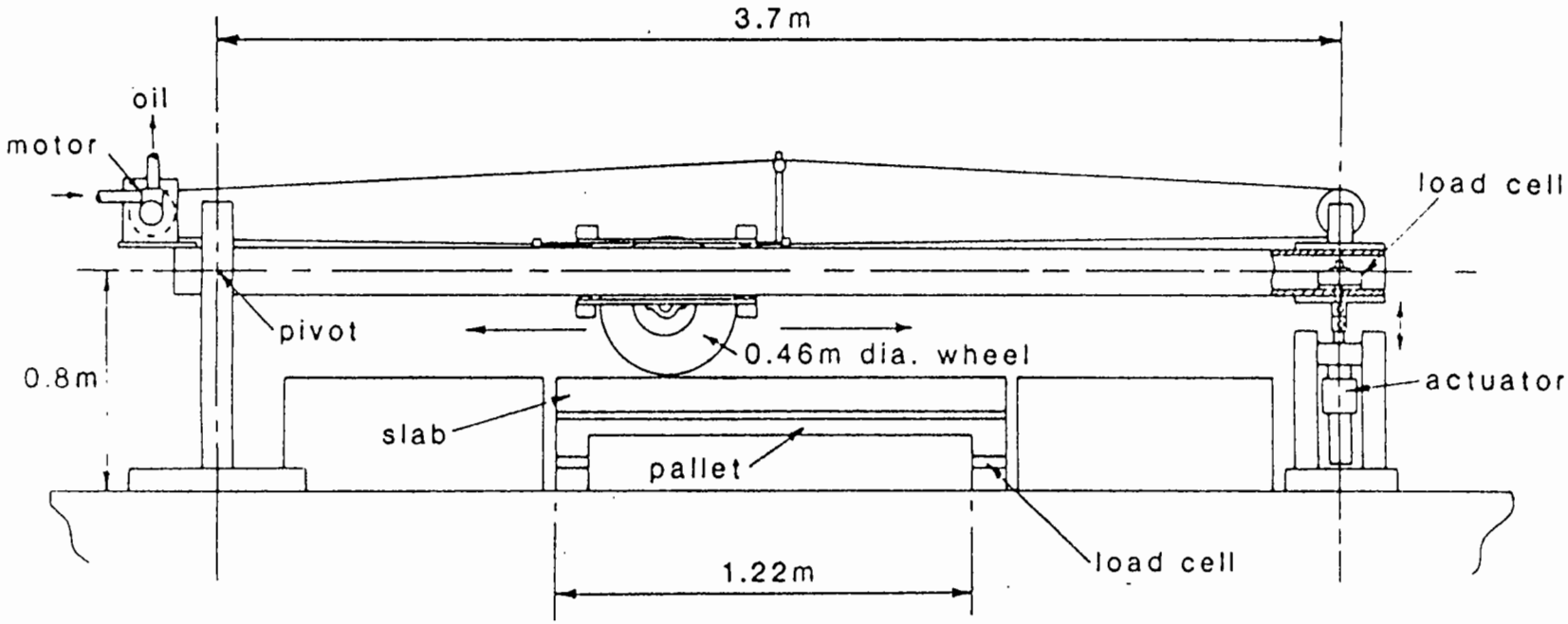

Fig. E1 Servo hydralic slab testing facility

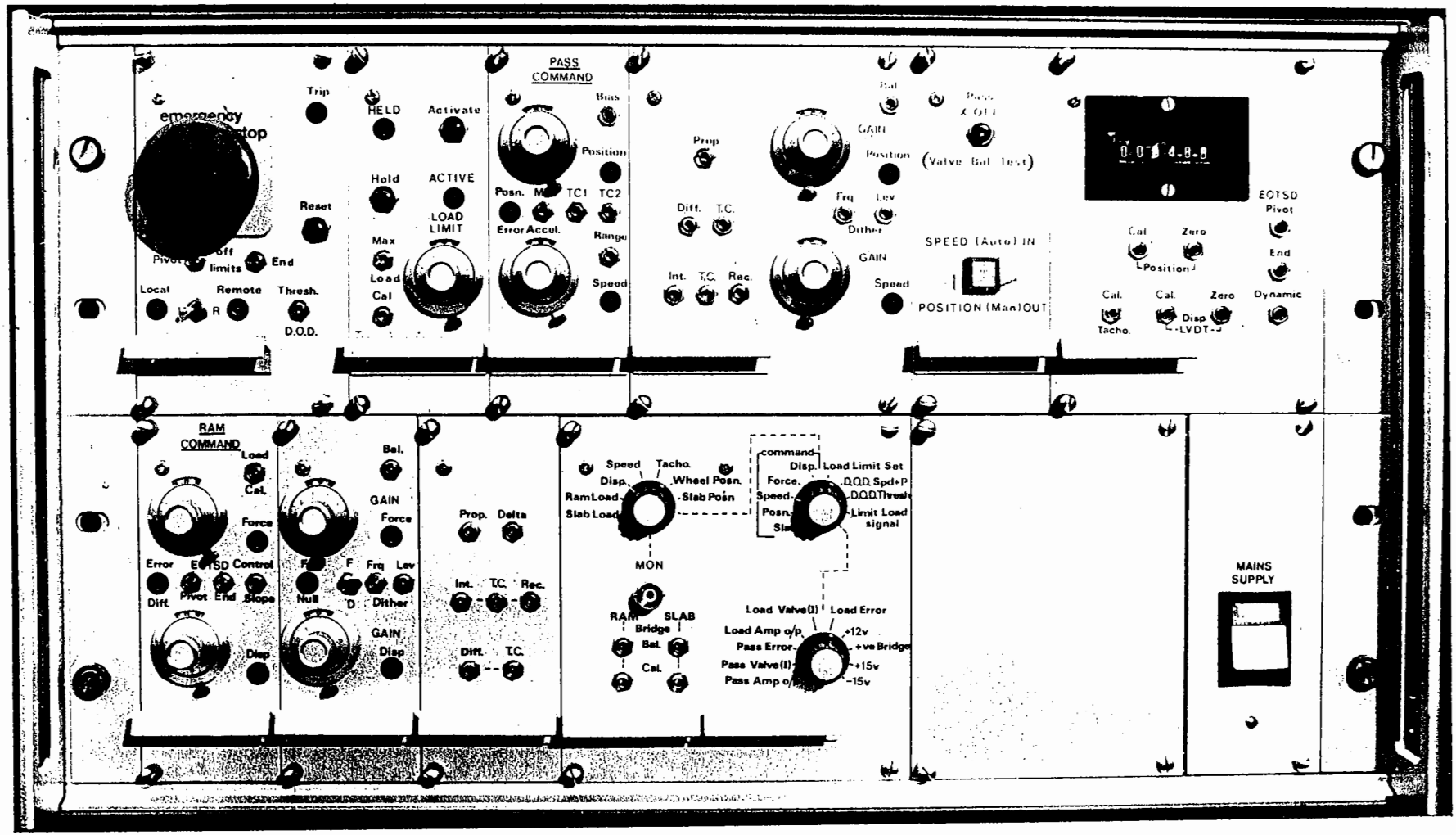

Fig E2 Electronic console for S.T.F

APPENDIX F

F.1 RESULTS FROM THE FALLING WEIGHT DEFLECTOMETER

A non destructive test using the Falling weight Deflectometer (F.W.D.) (Bohn et al, 1972) was carried out on both the pavements constructed in the P.T.F.

The F.W.D. applies a single load pulse, simulative of a vehicle loading, and has instrumentation capable of accurately measuring the deflected shape of the loaded surface. The load pulse obtained using the F.W.D. has an equivalent loading time, in terms of vehicle speed of 30 km/hr.

The shape of the deflection bowl is indicative of the stiffness of the various layers in the pavement and these may be calculated by comparing the measured shape to that obtained from a theoretical model. In this case the predictive model used to calculate the deflection was a linear elastic layered system within the computer program "Bistro" (Peutz, Van Kempen and Jones, 1968). The pavement is divided into a number of finite elastic layers and an approximate value of stiffness assigned to each. By adjusting these estimates a match can be obtained with the measured deflection bowl from the F.W.D. The resulting elastic stiffnesses are then assumed to be the insitu values for the various layers. One problem arising from this analysis is the marked non-linear elastic properties of the clay subgrade and this is overcome by subdividing the subgrade into layers of increasing stiffnesses with depth. A full description of the technique is given in a report by Tam (Tam, 1985).

Each of the pavements were analysed separately and are therefore presented separately. Reference should be made to Chapter Seven for the construction details of each pavement. The full depth asphalt construction will be referred to as pavement P1 and the thin

asphaltic concrete construction, Pavement P2.

(a) Pavement P1

The pavement structure is shown in Fig. 7.1. One test was conducted on the reinforced section and two on the unreinforced section before the application of the wearing course.

Fig F.1 shows how the pavement structure was subdivided into layers for the theoretical analysis. The base of the test pit and supporting material were included in the model.

The stiffnesses derived from this analytical method were compared with data obtained from laboratory testing of cores removed from the pavement, both in the subgrade and in the asphalt layer.

Fig. F.2 shows, graphically, the deflection bowls obtained in both the reinforced and unreinforced pavements. Assuming the stiffness of the subgrade and the thickness of the bound layer was the same in each case the similarity in the shape of the deflection bowls suggests that both the reinforced and unreinforced pavements had the same elastic stiffness. The deflections furthest away from the point of impact of the F.W.D. are influenced mainly by the stiffness of the subgrade and were identical in this case as expected.

The actual values of elastic stiffness obtained by matching the deflection bowl to that obtained with the F.W.D. are shown in Table F.1. The reinforced pavement had a marginally stiffer bituminous layer, 3,550MPa, than the unreinforced pavement 3,100MPa and a less stiff subgrade; 20MPa compared to 26MPa at formation level. The stiffness of the Dense Bitumen Macadam (D.B.M.) and the California Bearing Ratio (C.B.R.) of the subgrade were both tested in the laboratory. The C.B.R. of the subgrade was 3-4%. This can be approximately converted to an equivalent elastic stiffness of 10

Table F.1 Derived Stiffness for Each Layer of Pavement Test Facility.

(MPa)	(a) Location 1 Unreinforced	(b) Location 2R Reinforced	(c) Location 2R Reinforced	Mean reinforced
E_B	3100	3700	3400	3550
E_1	26	20	20	20
E_2	64	58	60	59
E_3	119	121	131	126
E_4	240	276	313	294
E_{conc}	20,000	20,000	20,000	20,000
$E_{H.C.}$	300	300	300	300
E_{clay}	175	155	155	155

times C.B.R. i.e., 30 to 40MPa (Heukelom et al, 1962) which compares reasonably with F.W.D. values.

The stiffness of the D.B.M. was measured in a repeated load uniaxial test on 100mm diameter cores taken from the pavement. The test temperature was 17°C and the loading frequency was 15Hz, corresponding to the loading rate experience by the pavement under the action of F.W.D. The average value of elasic stiffness obtained was 6,090MPa with a range from 2,190 to 14,100MPa. Hence, there is a significant difference between the predicted and measured values. Although the cores taken from the pavement were tested at 17°C, the temperature of the pavement when the F.W.D. was used on it was probably greater though not actually measured. It is considered that the temperature may have been about 23°C. A discrepancy of this order would explain the difference in stiffnesses. Other work with the F.W.D. has shown it to be very reliable for deducing insitu stiffness.

(b) Pavement P2

Three tests were conducted over section P2BR at different stress levels. Test 1 had a contact stress of 242 kPa under the loading platen, Test 2, 303 kPa, and Test 3, 354 kPa. The F.W.D. was positioned on the wheel track relative to the instrumentation as shown on Fig. 7.10. The vertical elastic strains in the subgrade and subbase and the transient stress pulses in the subgrade and subbase were measured during testing. The rut beneath the loading platen of the F.W.D. was filled with mastic asphalt to produce a level surface. This meant that the layer of asphalt beneath the platen was 100mm thick. (The analysis used in the F.W.D. is sensitive to the layer thicknesses.)

The layer thicknesses, and derived stiffnesses for each drop of

the F.W.D., are shown in Fig. F.3. Some slight differences were obtained in the stiffnesses observed between each drop, but are only a small percentage error in the structure as a whole. Using the average values of stiffness obtained from the F.W.D., BISTRO was used to compute the stresses and strains which had been monitored during testing. As the magnitude of strain varied considerably over the gauge length of the instrumentation, Simpsons rule was used to estimate an average value of strain from the BISTRO analysis. The measured and calculated values are compared in Table F.2.

The measured and calculated values of stress in the subgrade show best agreement, computed values being an average of 14% higher. The computed stress pulse in the subbase was, however, 20% of that measured . This may have been due to a stress concentration around the pressure cell, caused by aggregate contact on the diaphragm of the cell after the large deformations which occured during the course of the test.

The measured and calculated strains in the subgrade agree less well than those in the subbase due, perhaps, to the large strain gradient in the subgrade layer.

The PONOS Computer program (De Bats, 1972) was used to estimate the stiffness of the asphalt layer for the F.W.D. and rolling wheel loading conditions. The F.W.D. has an equivalent loading speed of 30 km/hr and the rolling wheel speed was 7 km/hr. The test temperature for the F.W.D. was 17^{o}C and for the rolling wheel, 20^{o}C. The estimated values for stiffness were 1517 MPa for the F.W.D. and 491 MPa under the rolling wheel. The values from the F.W.D. loading agree well with the average obtained from back analysis (1667 MPa).

BISTRO was used to model the pavement structure in the P.T.F. under the conditions experienced during loading with the wheel. The value of stiffness obtained from PONOS was used for the asphalt layer

Table F.2 Comparison of measured (M) and calculated (C) transient stresses and strains under F.W.D.

Test No.	Vertical Stress (kPa)						Vertical Strain ($\mu\varepsilon$)					
	Subgrade*			Subbase**			Subgrade***			Subbase***		
	M	C	$\frac{C}{M}$	M	C	$\frac{C}{M}$	M	C	$\frac{C}{M}$	M	C	$\frac{C}{M}$
1	10.9	13.2	1.21	125	25.5	0.20	1300	2496	1.92	600	779	1.30
2	15.2	17.2	1.13	165	33.7	0.20	1850	3140	1.69	700	805	1.15
3	18.5	19.9	1.08	198	38.8	0.20	2450	3750	1.54	700	955	1.19

* radial distance of pressure cell from F.W.D. = 190mm

** radial distance of pressure cell from F.W.D. = 380mm

*** strain coil directly under F.W.D.

(491 MPa). The elastic moduli for the subbase and soft clay layer were predicted using the initial values of transient stress and vertical elastic strain measured in the pavement for each section, (Table 7.2 and 7.3), using the following equation.

$$E = \frac{1}{\varepsilon v}(\sigma v - 2\nu\sigma r)$$

where $\sigma r = k\sigma v$

E = elastic stiffness

εv = vertical elastic strain

σv = vertical transient stress

σr = radial transient stress

k = coefficient of earth pressure

ν = poissons ratio

The angle of friction ϕ for the Keuper Marl is approximately 30^{o} and for granular material, up to 57^{o}. For the analysis an average value of 45^{o} was taken which resulted in a coefficient of earth pressure of approximately 0.3, using the emperical relationship;

$$k_o = 1 - \sin \phi$$

Poisson's ratio for the granular subbase was estimated at 0.3 and for the other layers was taken as 0.4. The wheel contact stress used in the analysis was 500 kPa, radius 76mm.

The stiffnesses used for the lower layers were taken as an average of those obtained from the F.W.D. analysis. The three sections analysed, representative of structures P2, P2MR and P2BR are shown in Fig. F.4.

Fig F.5 and Fig F.6 show the predicted levels of vertical strain and stress using BISTRO, for each of the three structures. The initial values of transient stress and elastic strain measured in the pavement are given in Table 7.2 and Table 7.3 and are superimposed onto these figures.

The measured subgrade strains were consistently higher for each section than the calculated elastic strains, especially in section P2MR where the measured elastic strain was 6142$\mu\varepsilon$ and the calculated value, approximately 2700$\mu\varepsilon$. The subbase strains were, however, in reasonable agreement with those predicted.

The measured subbase stress in section P2 is within 10% of that calculated, while the measured stresses in sections P2MR and P2BR are much greater than the calculated values.

The measured subgrade stress agrees well with that predicted.

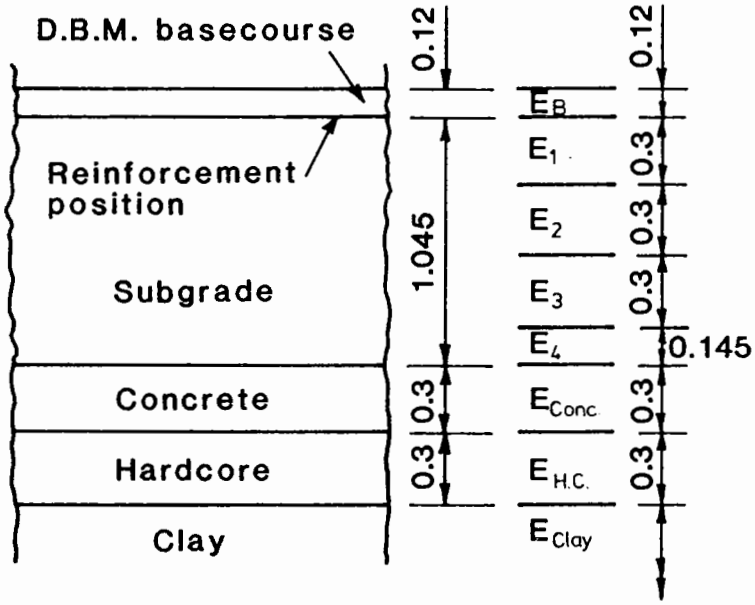

Fig F.1 PAVEMENT CONSTRUCTION IN P.T.F. AND LAYERS USED IN 'BISTRO' MODEL

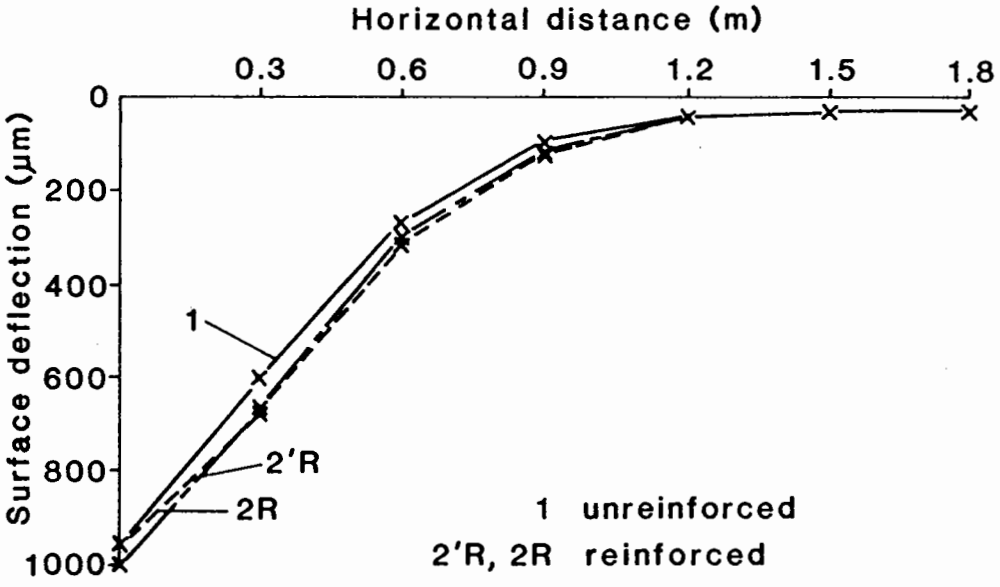

Fig F.2 MEASURED SURFACE DEFLECTION FROM F.W.D.

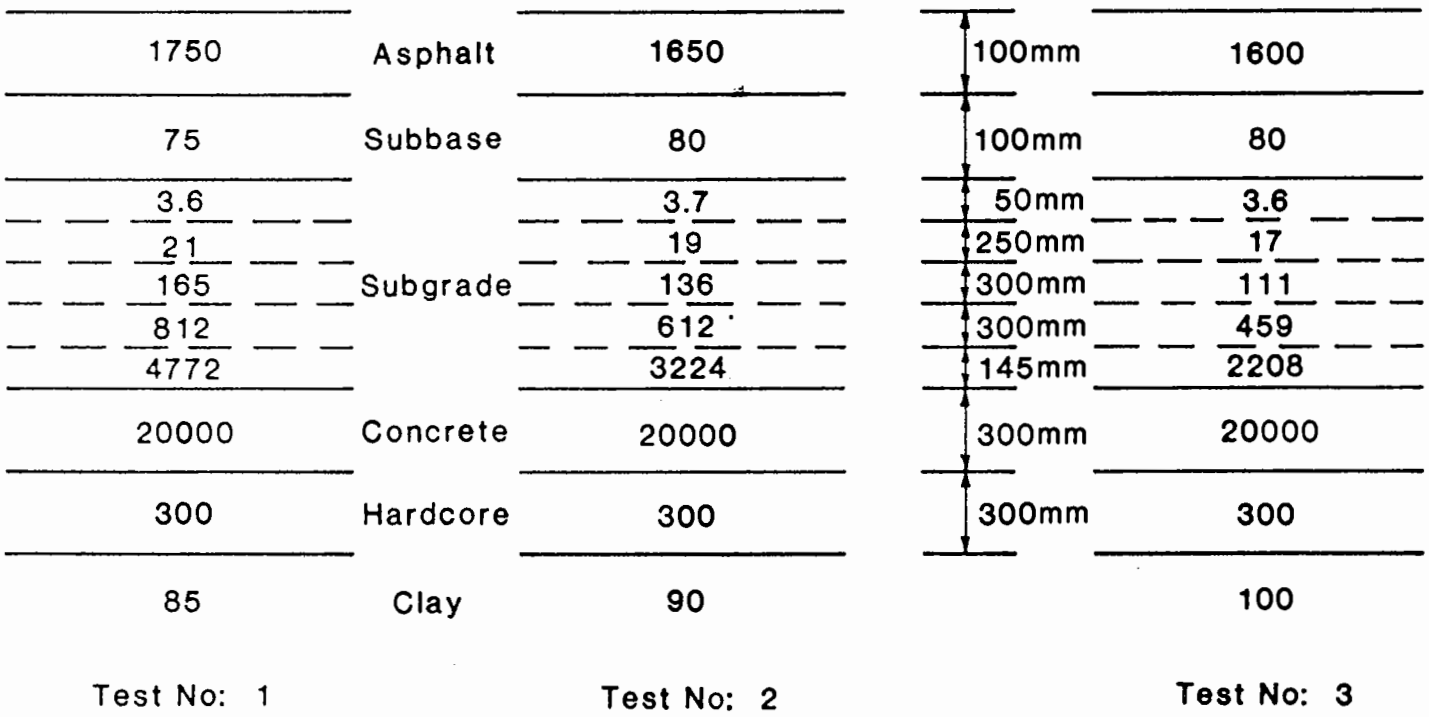

Fig F.3 Derived Stiffness moduli (MPa) of Each Layer of P.T.F., Section P2BR

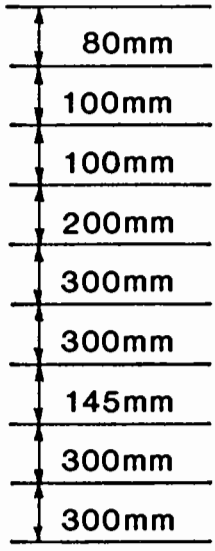

	Material	Stiffness (MPa)		
		P2	P2MR	P2BR
80mm	Asphalt	491.0	491.0	491.0
100mm	Subbase	49.2	88.8	107.9
100mm	Soft clay	5.1	4.7	6.8
200mm	Subgrade	19	19	19
300mm	Subgrade	137	137	137
300mm	Subgrade	628	628	628
145mm	Subgrade	3400	3400	3400
300mm	Concrete	20,000	20,000	20,000
300mm	Hardcore	300	300	300
	Clay	92	92	92

Fig F.4 Pavement Analysis Using BISTRO

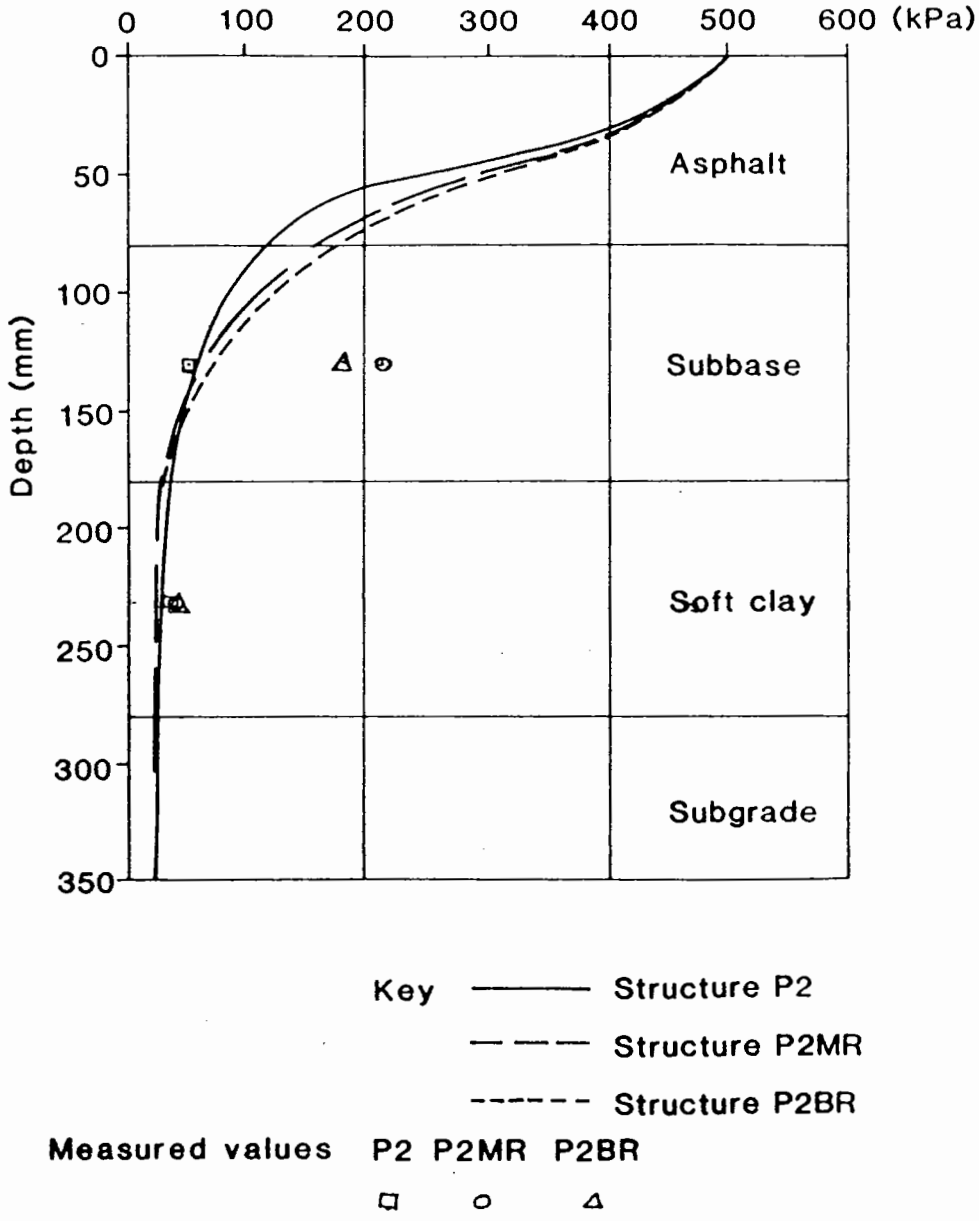

Fig F.5 Vertical Stress in Pavement P2

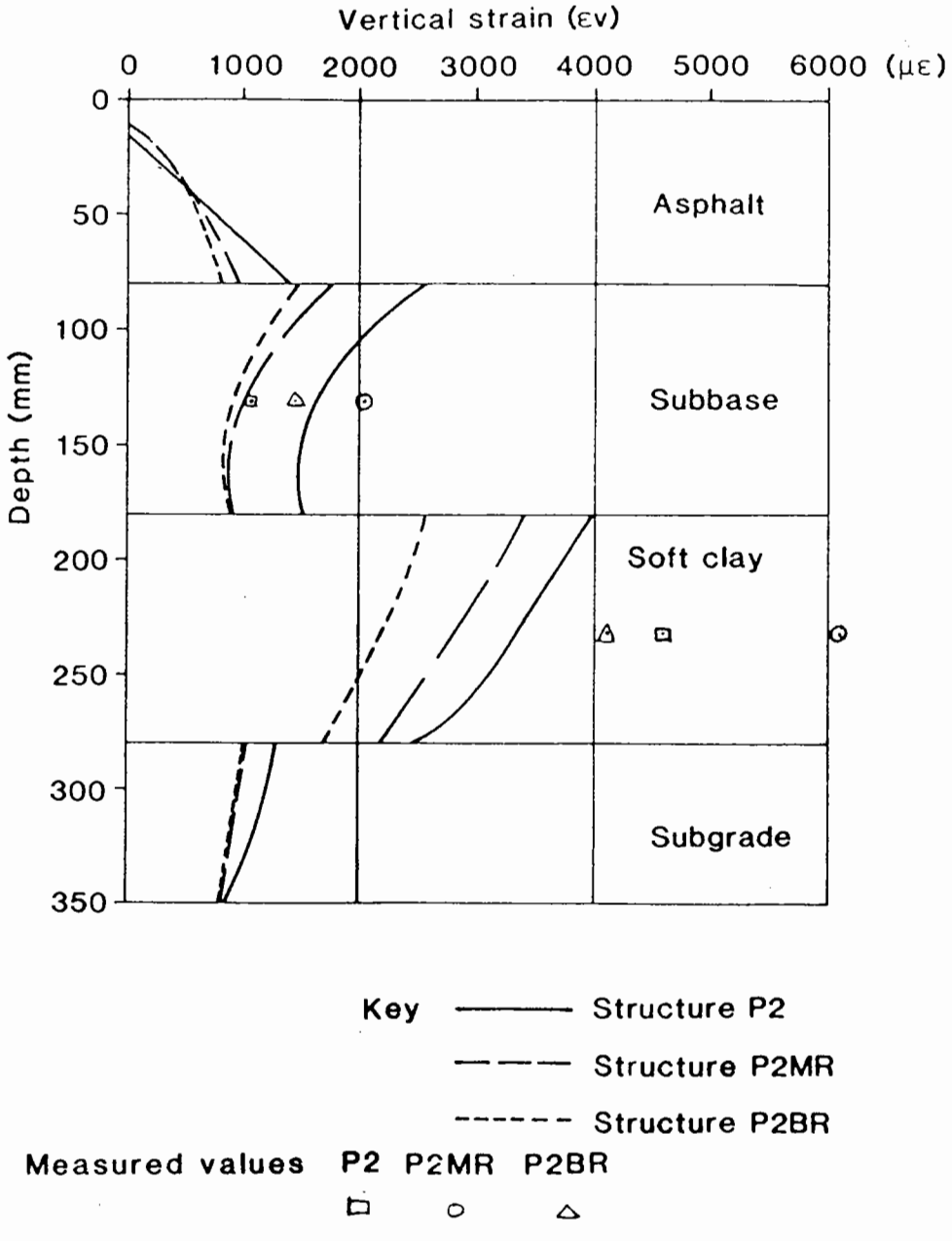

Fig F.6 Vertical Strain in Pavement P2

APPENDIX G

SHEAR BOX RESULTS

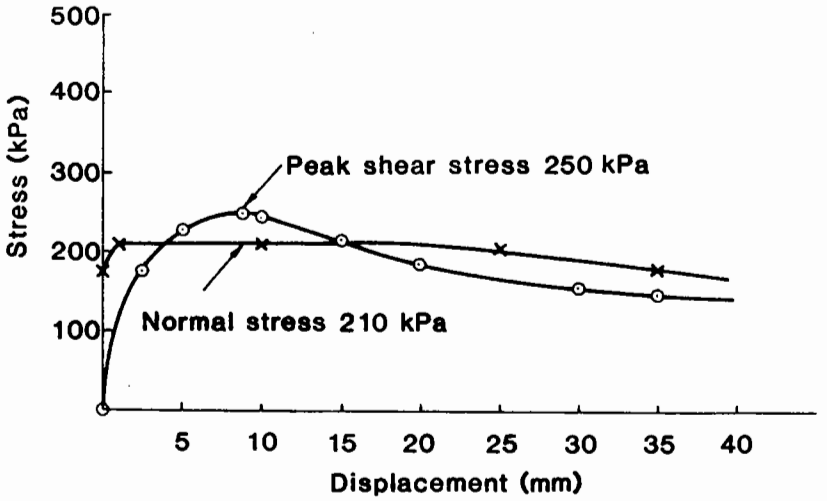

(a) Shear and Normal Stress During Test

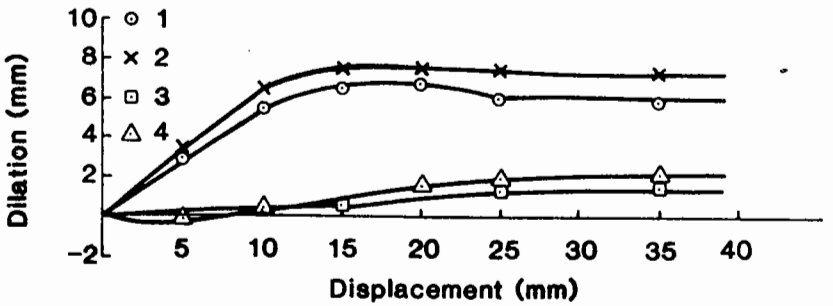

(b) Dilation of Sample During Test

Fig. G.1 Test 4. Chip Seal only at Interface

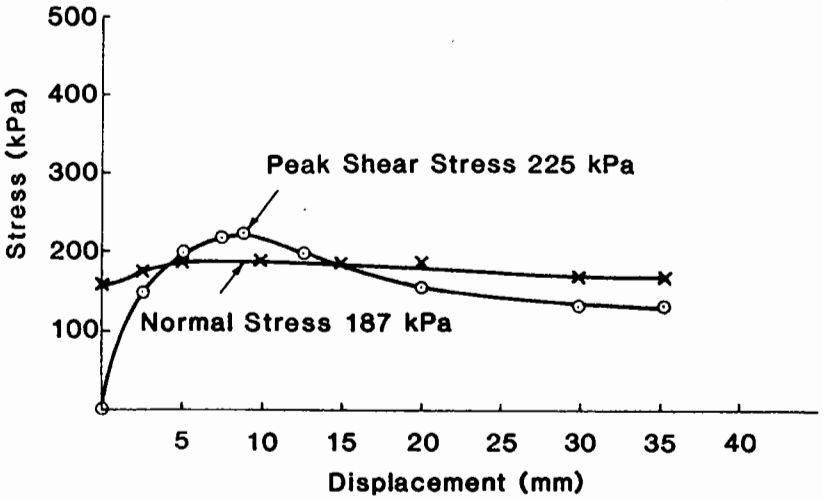

(a) Shear and Normal Stress During Test

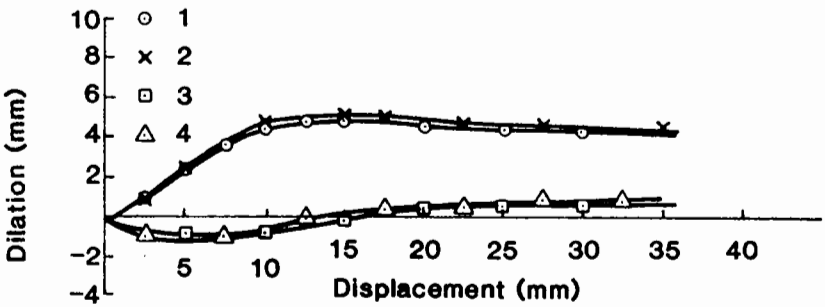

(b) Dilation of Sample During Test

Fig. G.2 Test 5. Chip Seal only at Interface

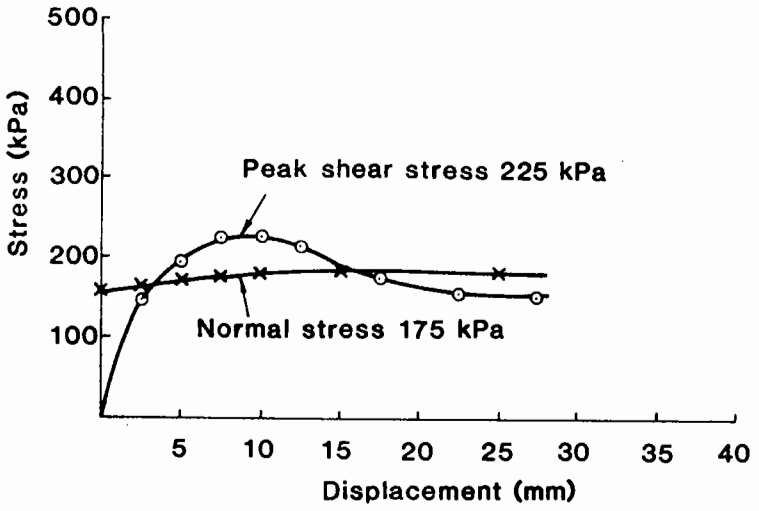

(a) Shear and Normal Stress During Test

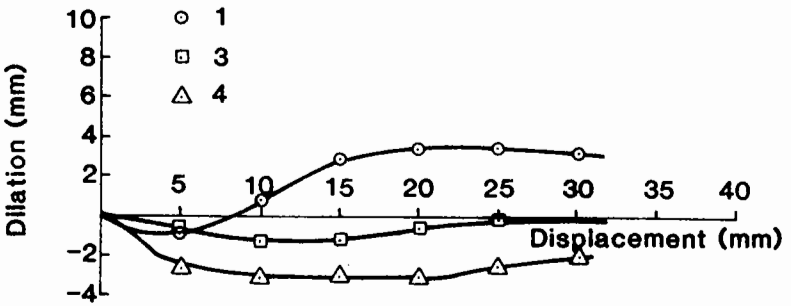

(b) Dilation of Sample During Test

Fig. G.3 Test 6R. Chip Seal and Grid at Interface

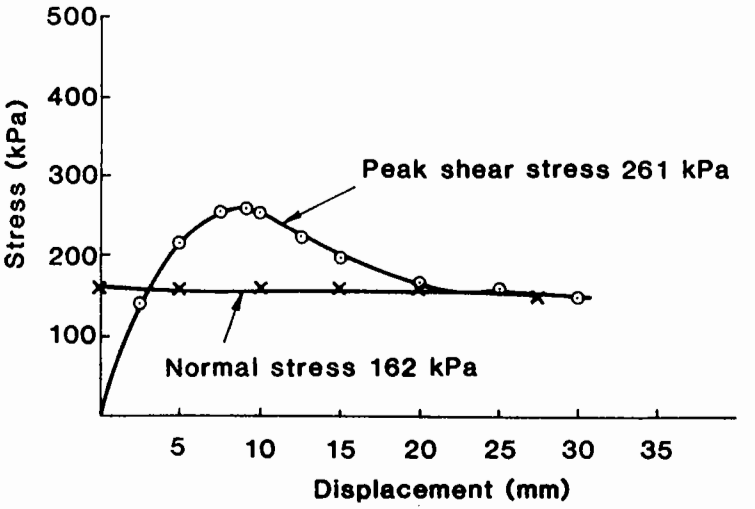

(a) Shear and Normal Stress During Test

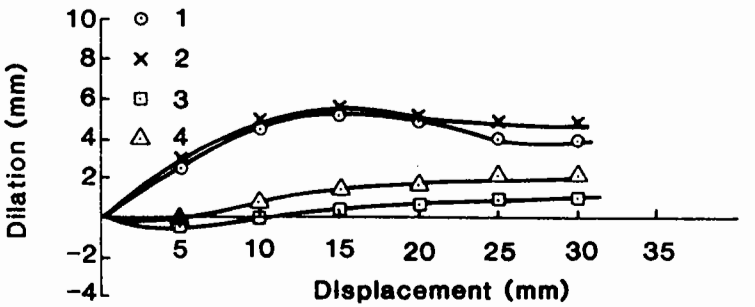

(b) Dilation of Sample During Test

Fig. G.4 Test 7R. Chip Seal and Grid at Interface

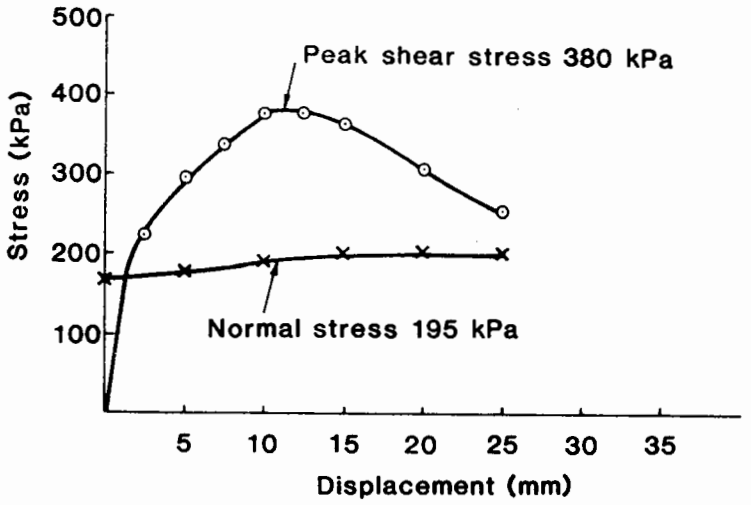

(a) Shear and Normal Stress During Test

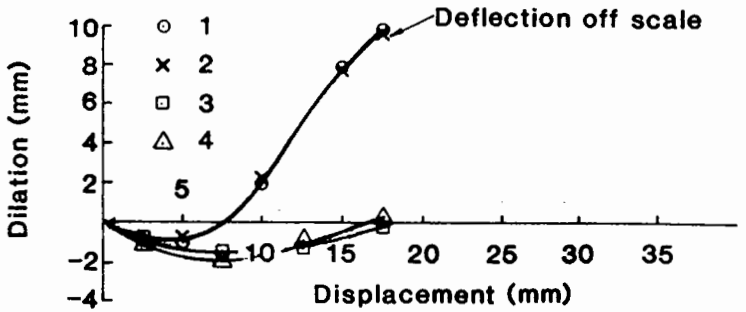

(b) Dilation of Sample During Test

Fig.G.7 Test 10. No Interface

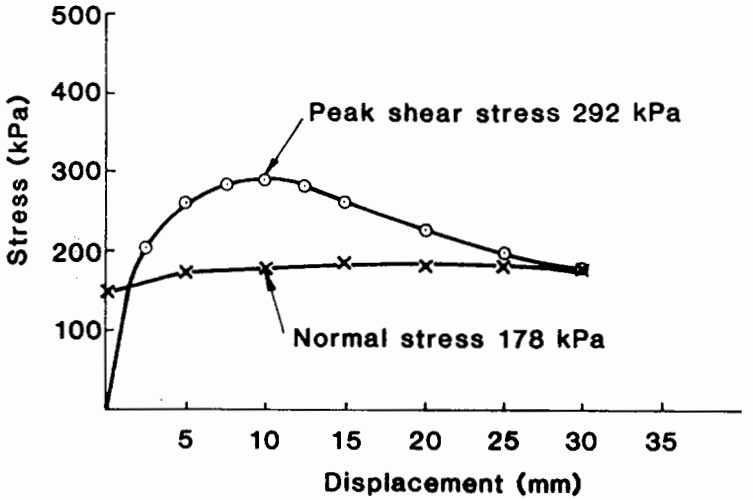

(a) Shear and Normal Stress During Test

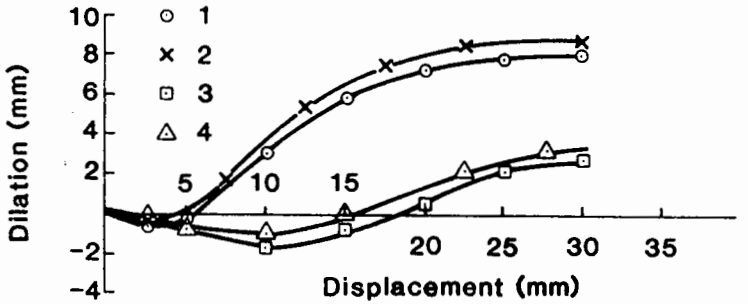

(b) Dilation of Sample During Test

Fig.G.8 Test 11. No Interface

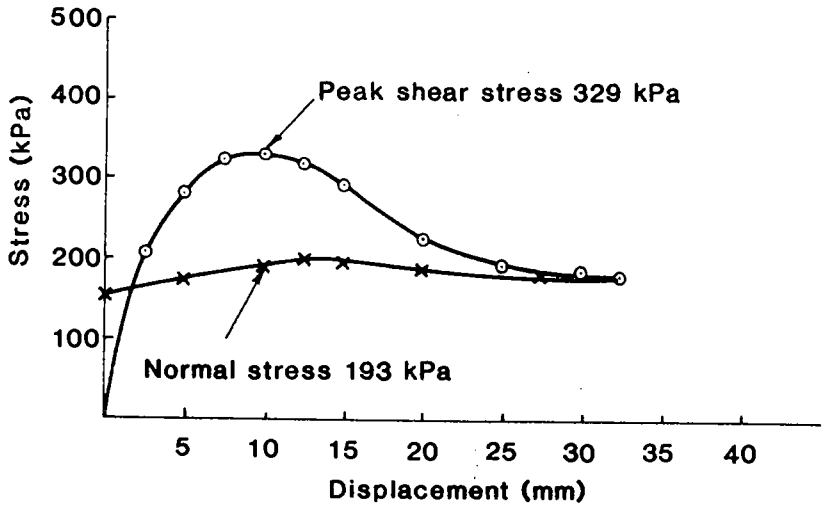

(a) Shear and Normal Stress During Test

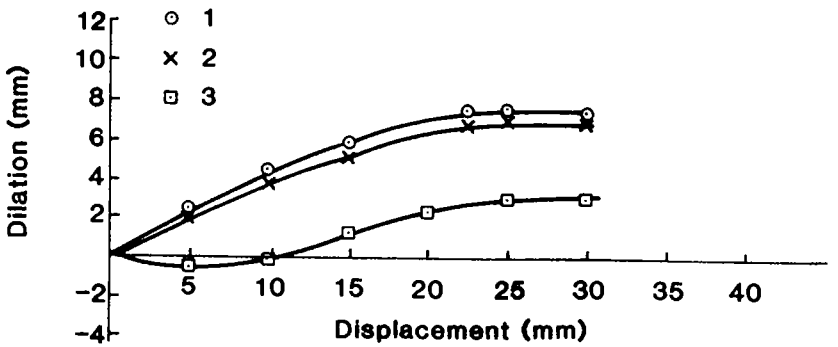

(b) Dilation of Sample During Test

Fig. G.5 Test 8. Untreated Interface

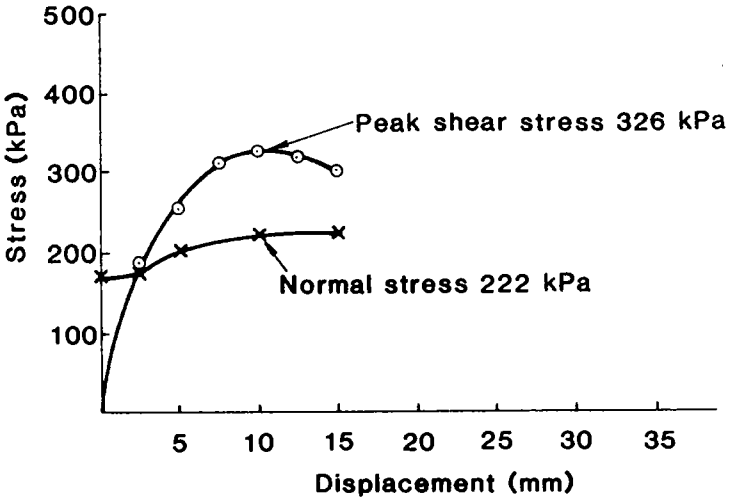

(a) Shear and Normal Stress During Test

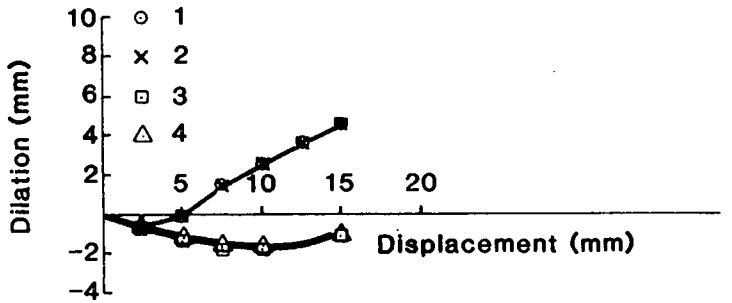

(b) Dilation of Sample During Test

Fig. G.6 Test 9. Untreated Interface

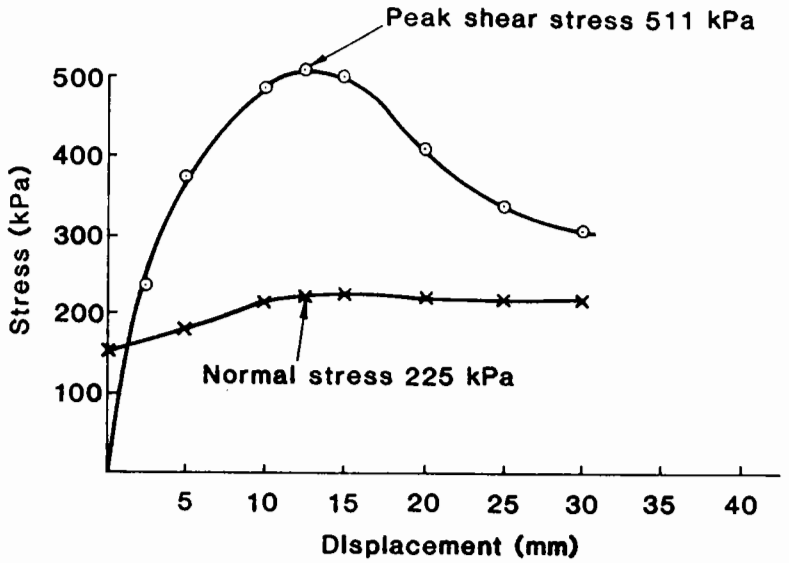

(a) Shear and Normal Stress During Test

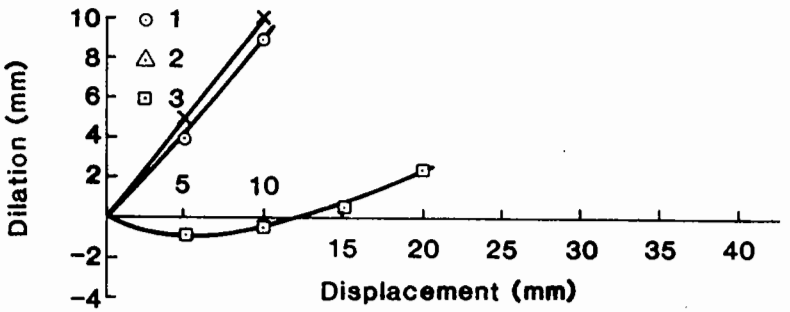

(b) Dilation of Sample During Test

Fig. G.9 Test 12. No Interface

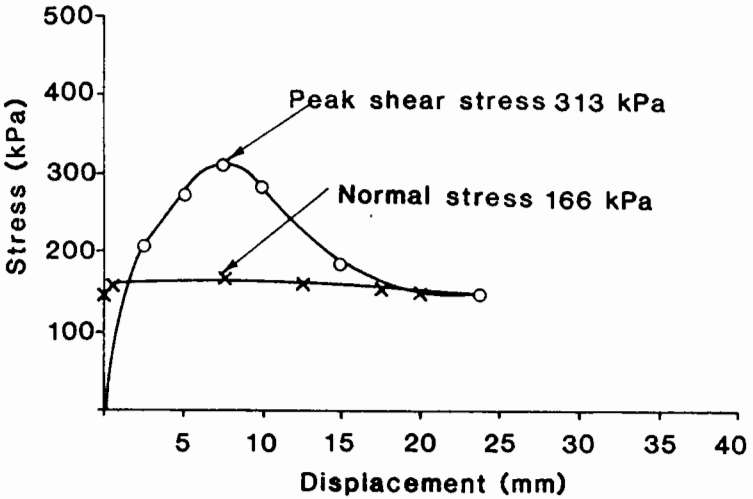

(a) Shear and Normal Stress During Test

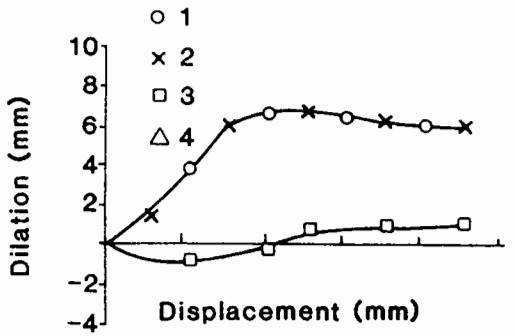

(b) Dilation of Sample During Test

Fig.G.10 Test 13R. Grid only at Interface

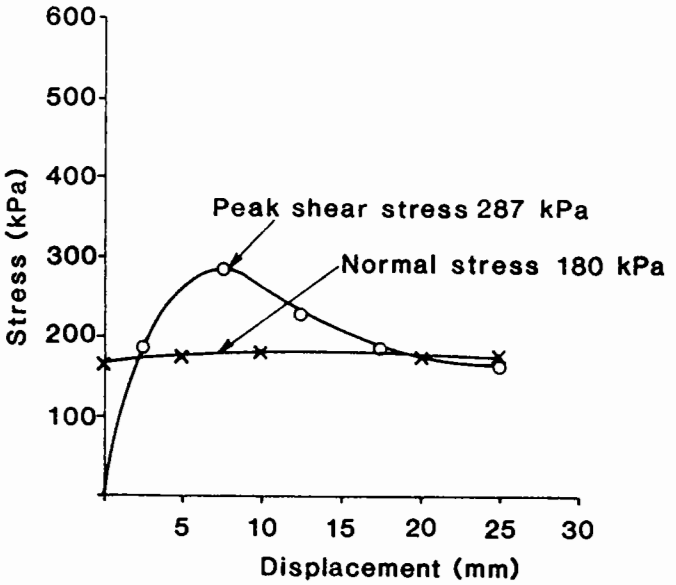

(a) Shear and Normal Stress During Test

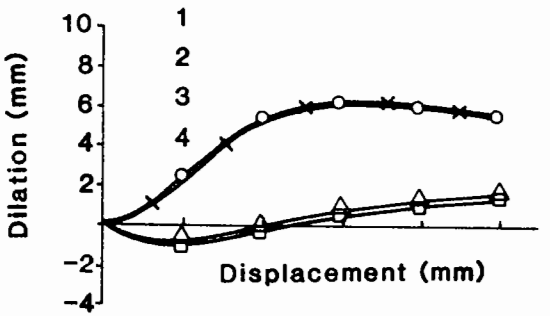

(b) Dilation of Sample During Test

Fig.G.11Test 14R. Grid only at Interface

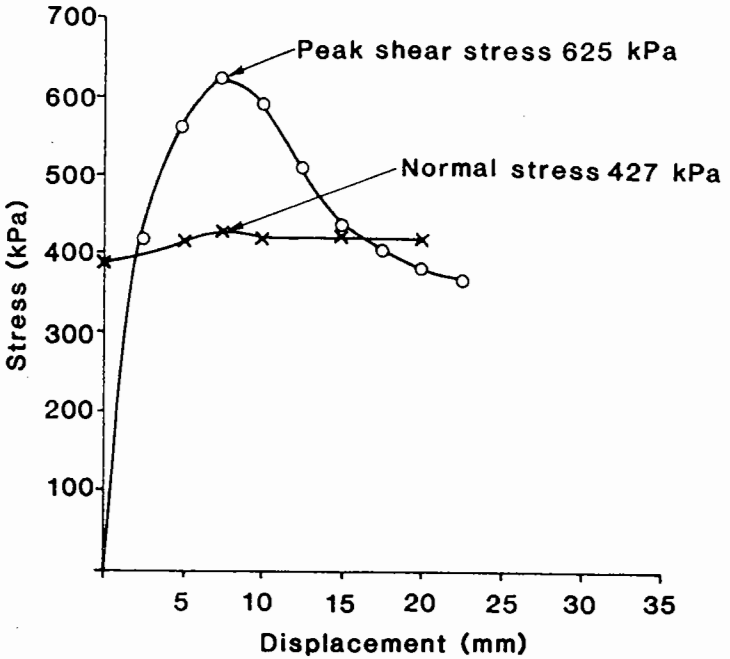

(a) Shear and Normal Stress During Test

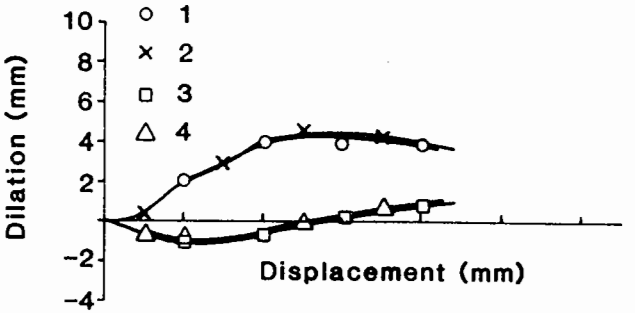

(b) Dilation of Sample During Test

Fig.G.12 Test 15, Untreated Interface

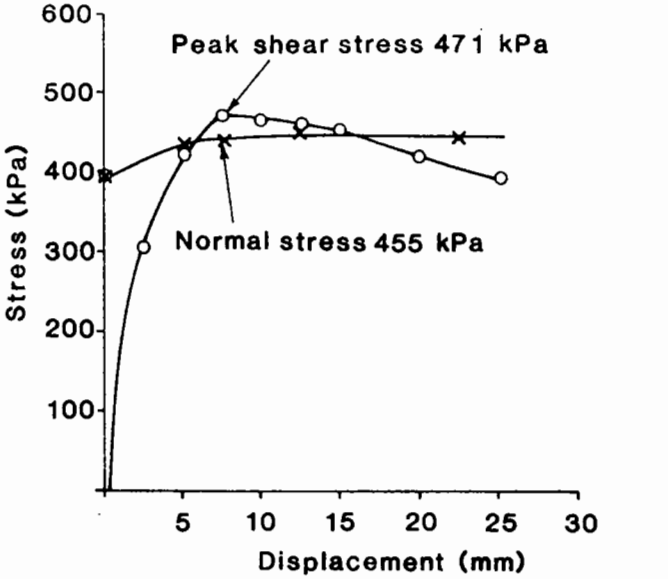

(a) Shear and Normal Stress During Test

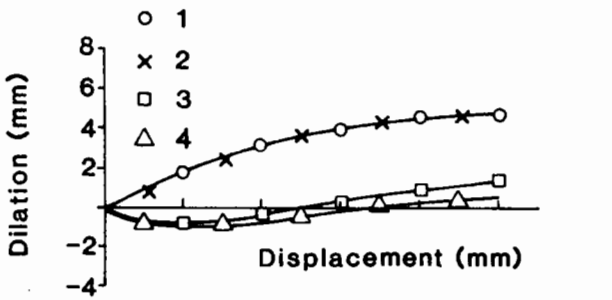

(b) Dilation of Sample During Test

Fig.G.13 Test 16, Untreated Interface

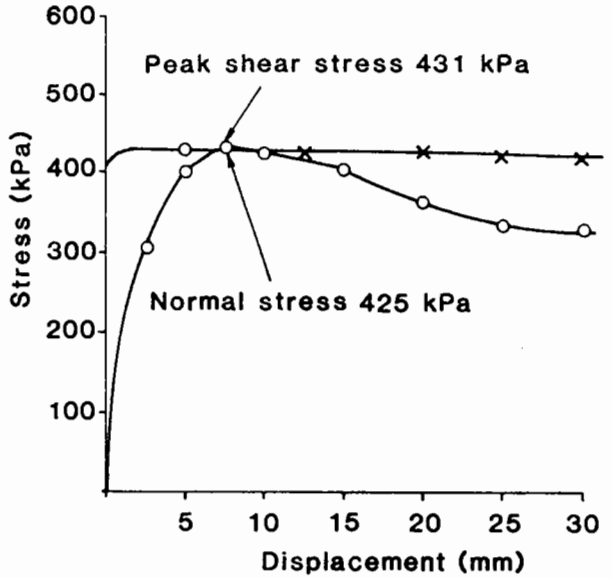

(a) Shear and Normal Stress During Test

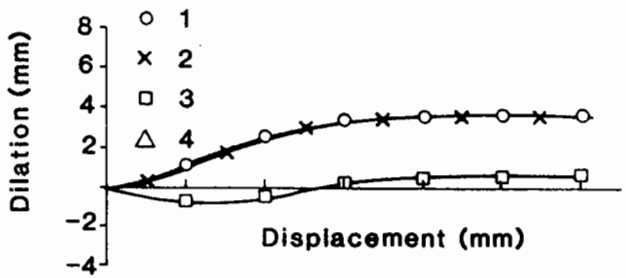

(b) Dilation of Sample During Test

Fig.G.14 Test 17R Grid only at Interface

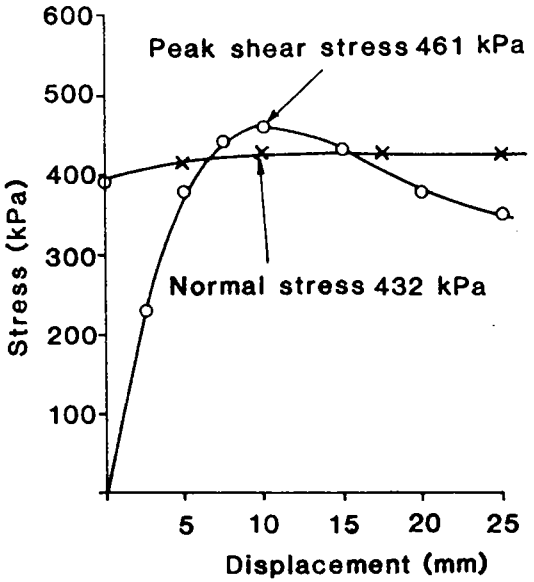

(a) Shear and Normal Stress During Test

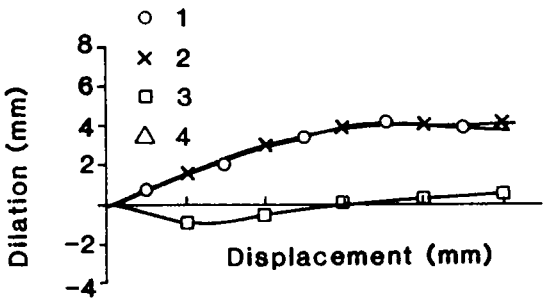

(b) Dilation of Sample During Test

Fig.G.15 Test 18R, Grid only at Interface

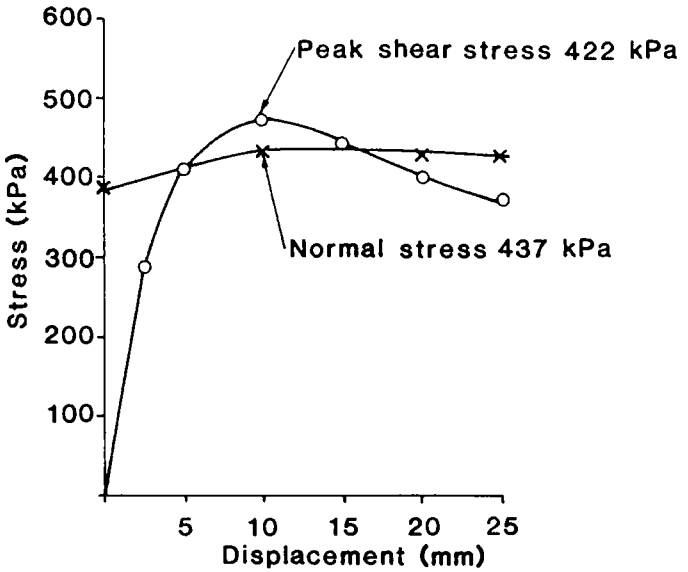

(a) Shear and Normal Stress During Test

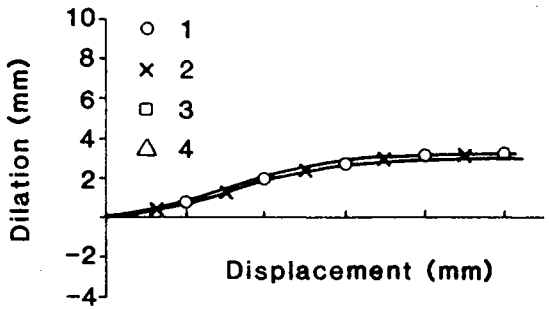

(b) Dilation of Sample During Test

Fig. G.16 Test 19, Chip Seal only at Interface

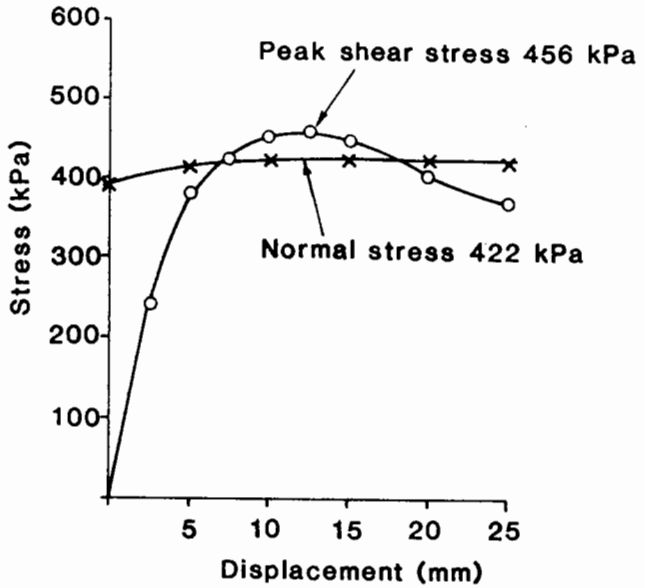

(a) Shear and Normal Stress During Test

Fig.G.17 Test 20 Chip Seal only at Interface

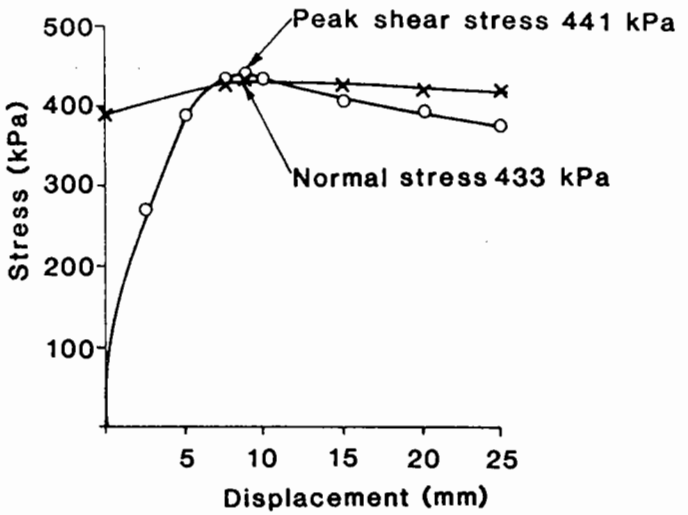

(a) Shear and Normal Stress During Test

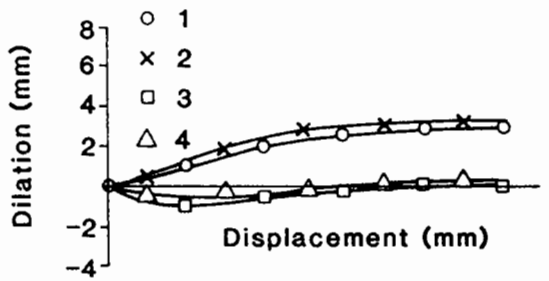

(b) Dilation of Sample During Test

Fig.G.18 Test 21R, Chip Seal and Grid at Interface

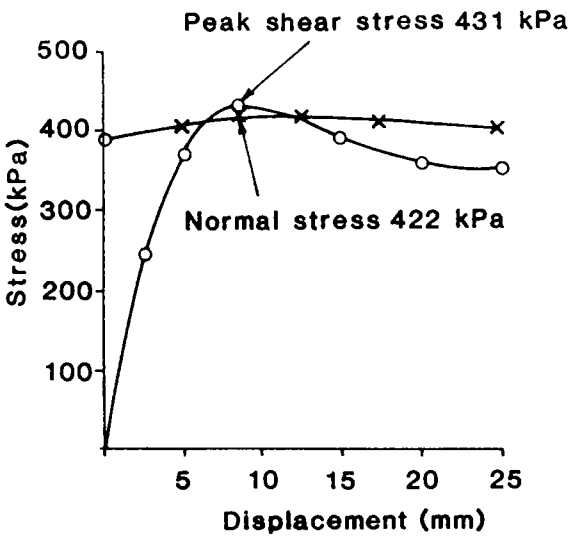

(a) Shear and Normal Stress During Test

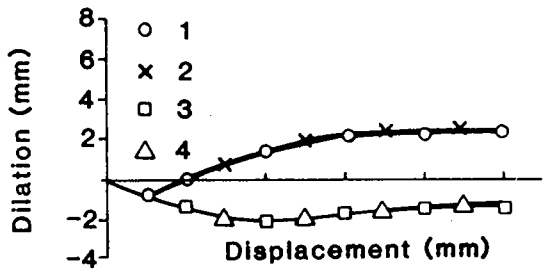

(b) Dilation of Sample During Test

Fig G.19 Test 22R Chip Seal and Grid at Interface

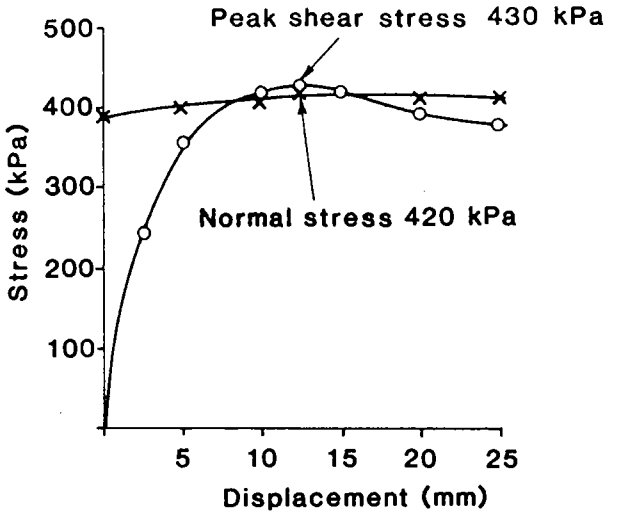

(a) Shear and Normal Stress During Test

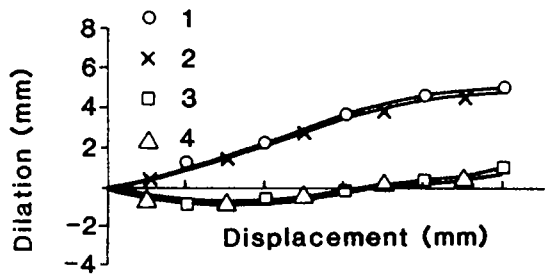

(b) Dilation of Sample During Test

Fig G.20 Test 23, Untreated Interface

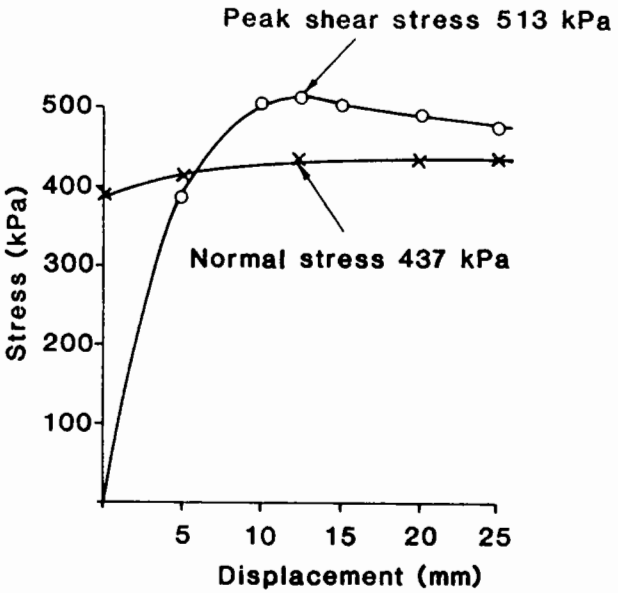

(a) Shear and Normal Stress During Test

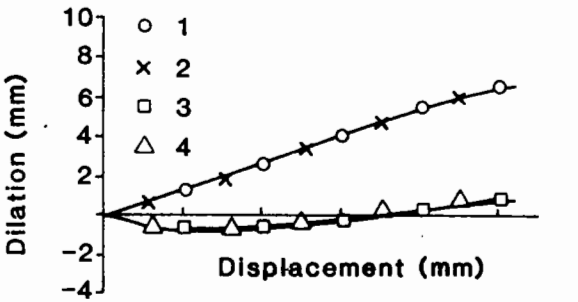

(b) Dilation of Sample During Test

Fig.G.21 Test 24, No Interface

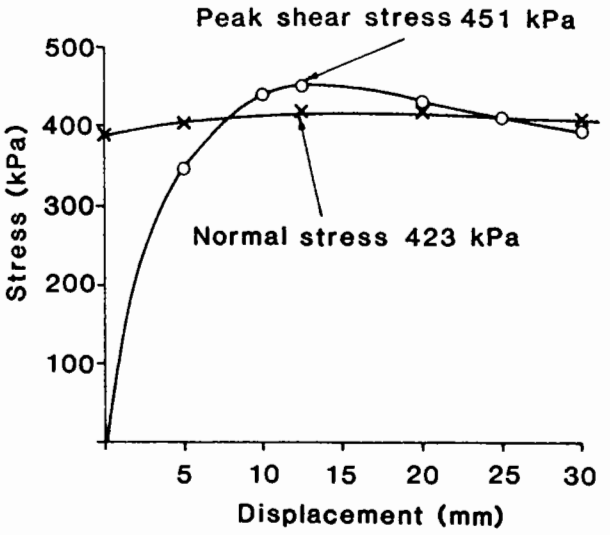

(a) Shear and Normal Stress During Test

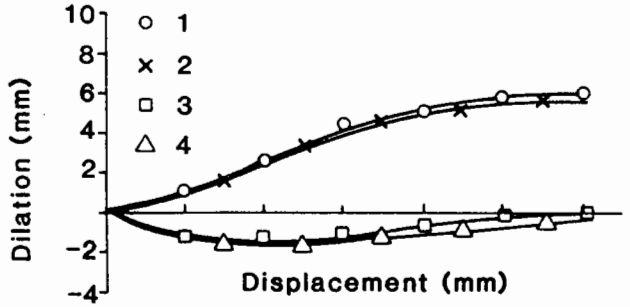

(b) Dilation of Sample During Test

Fig.G.22 Test 25, No Interface

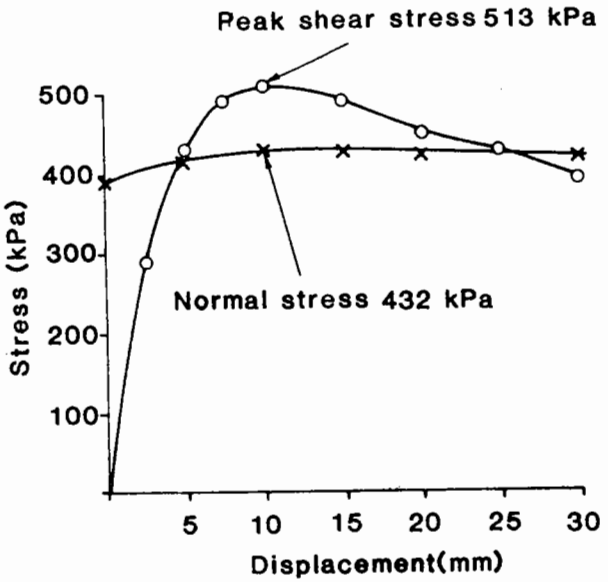

(a) Shear and Normal Stress During Test

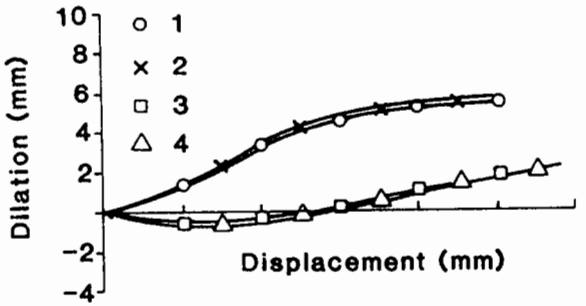

(b) Dilation of Sample During Test

Fig.G.23Test 26, No Interface

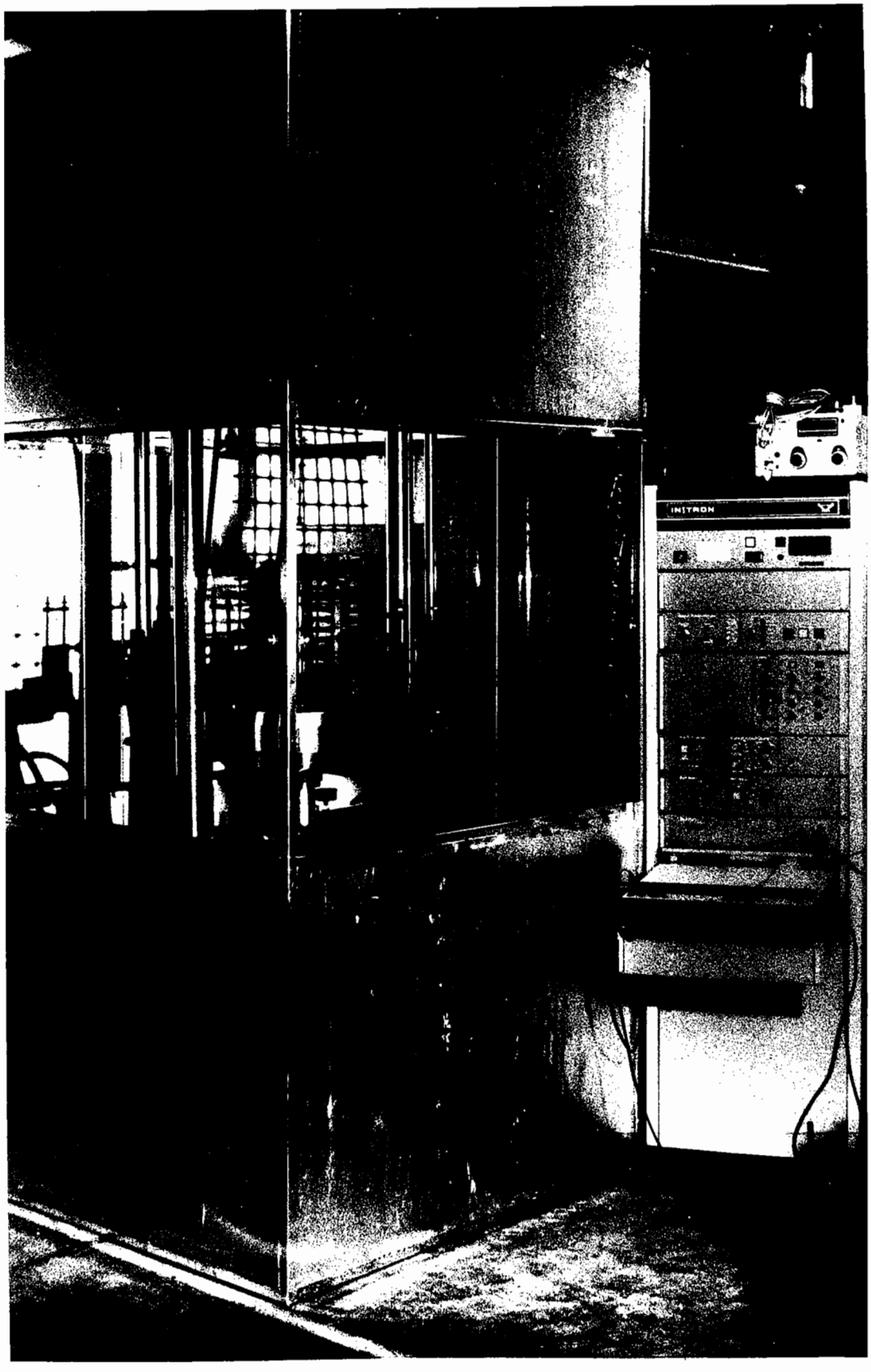

Fig. 4.2 Instron testing facility

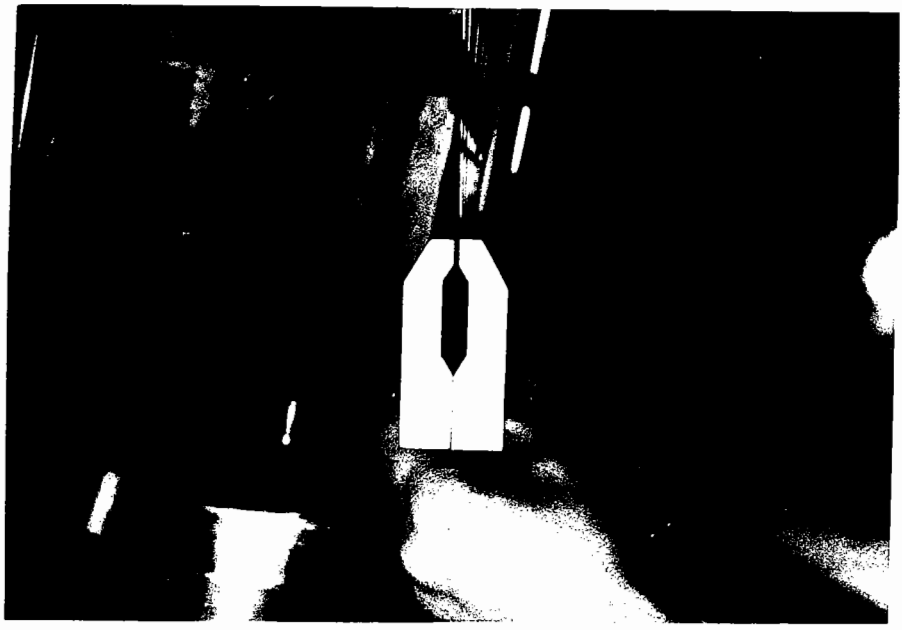

Fig. 4.3 clamps for polymer grid

Fig. 4.4 Grid in testing facility

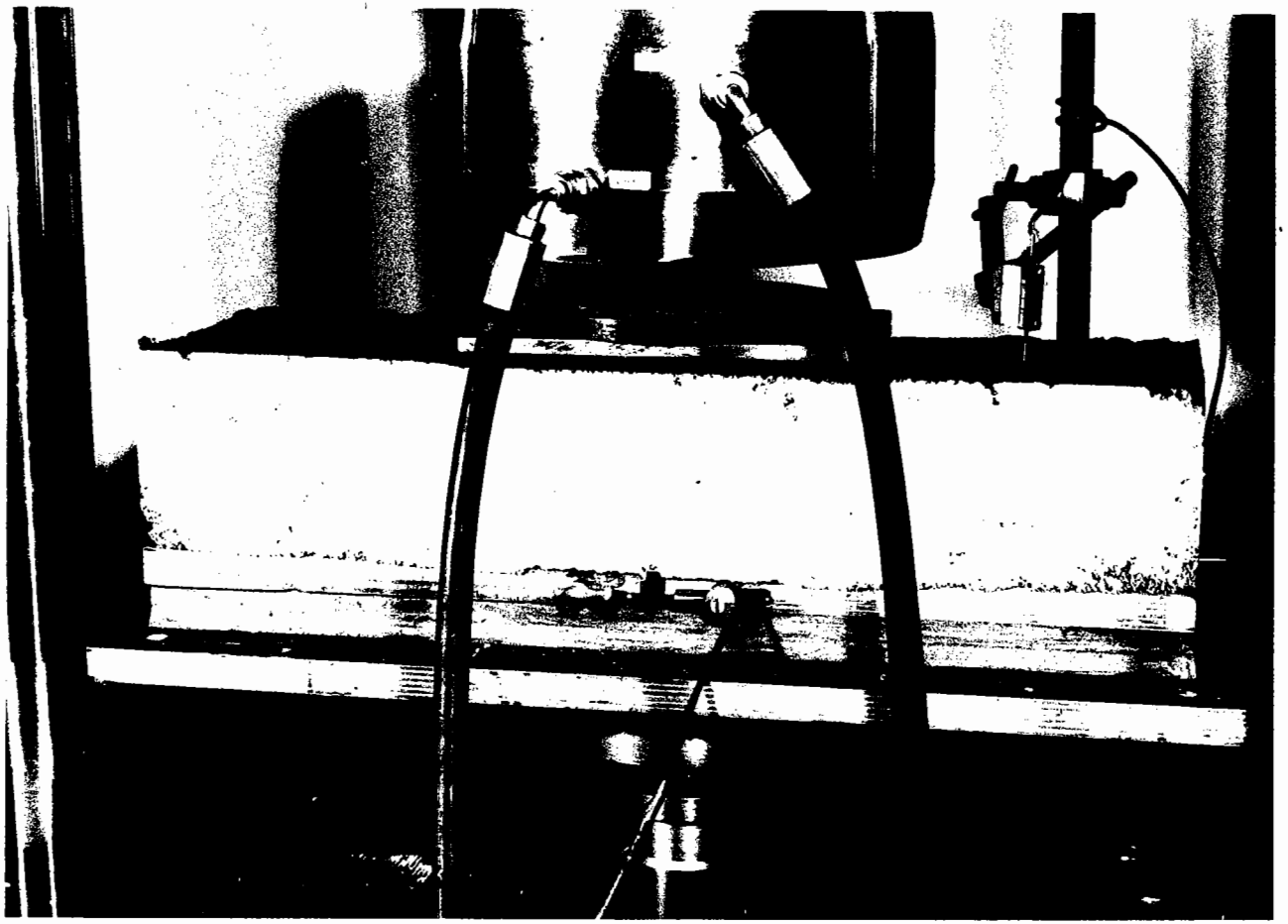

Fig 5.3 A general view of the reflection cracking beam test

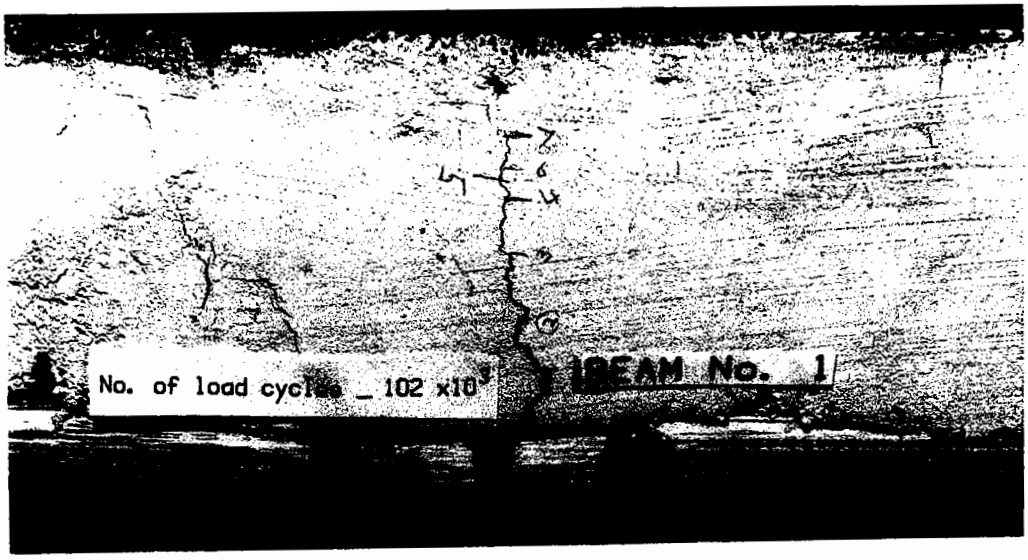

(a) unreinforced

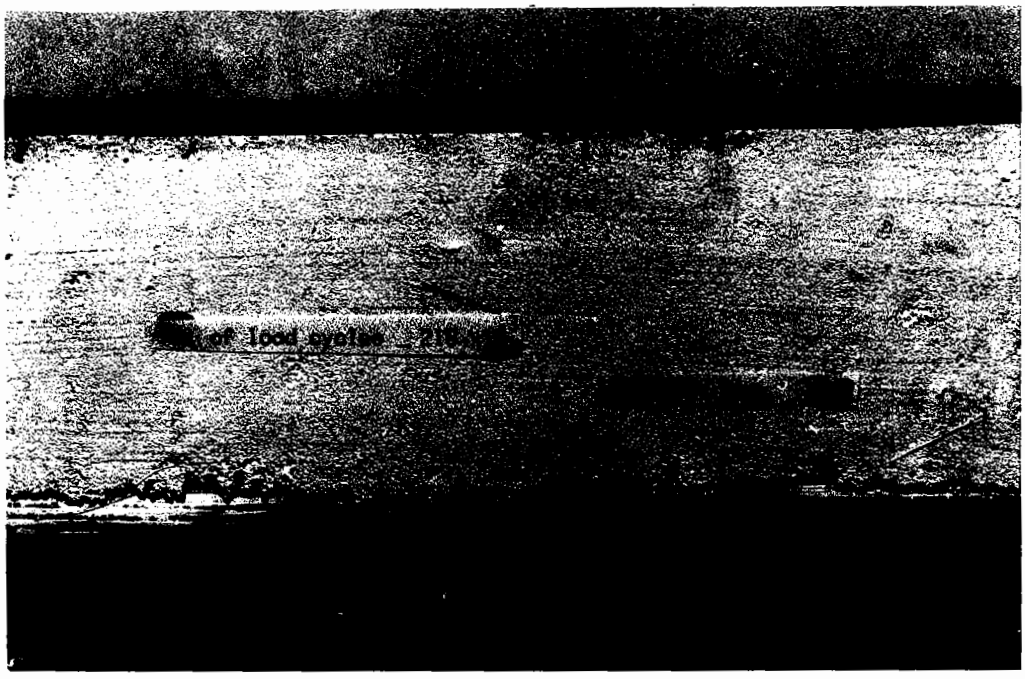

(b) reinforced at base of asphalt layer

Fig 5.5 H.R.A. beams reinforced & unreinforced

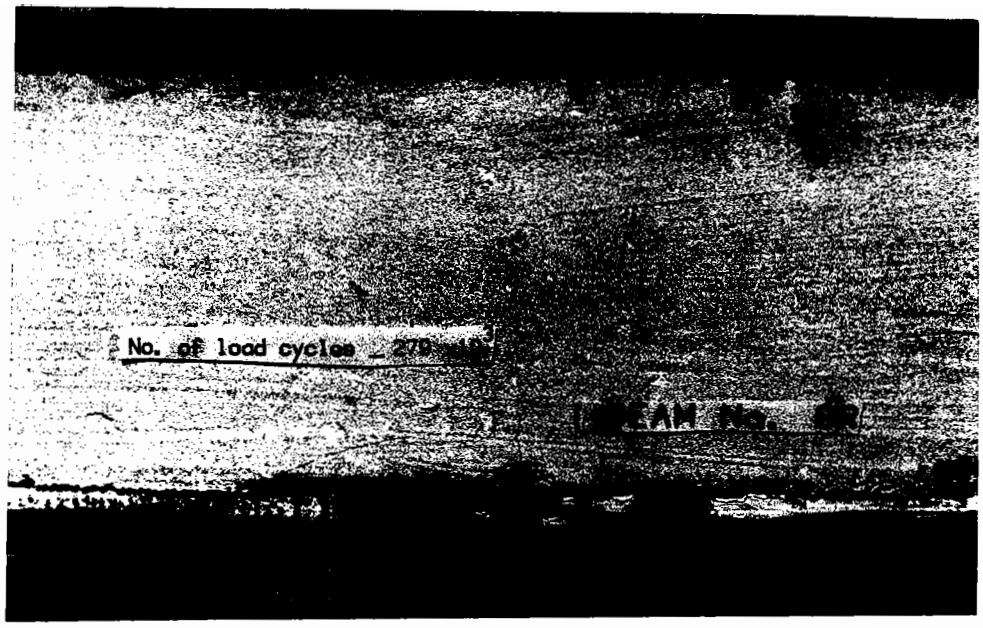

(a) reinforced 25mm from base of asphalt

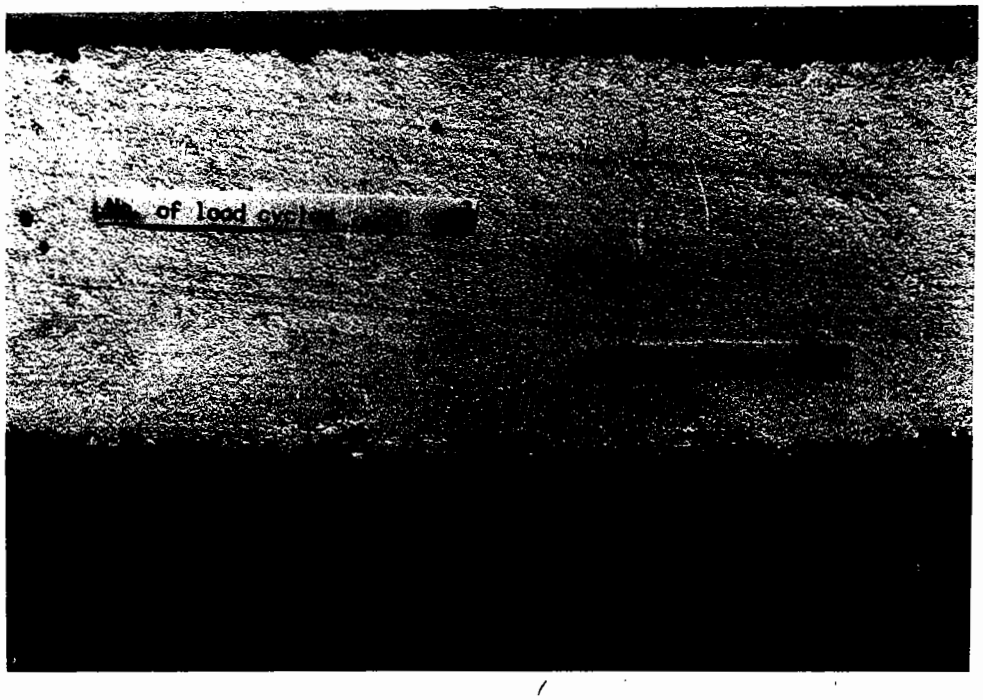

(b) reinforced 50mm from base of asphalt

Fig 5.8 Reinforced H.R.A. beams

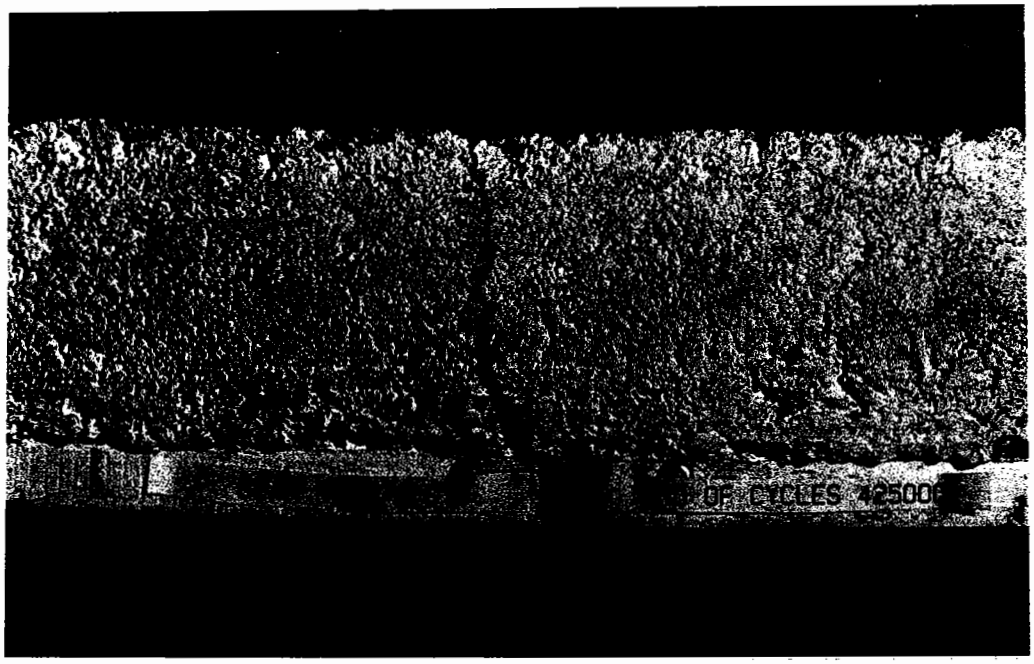

(a) unreinforced

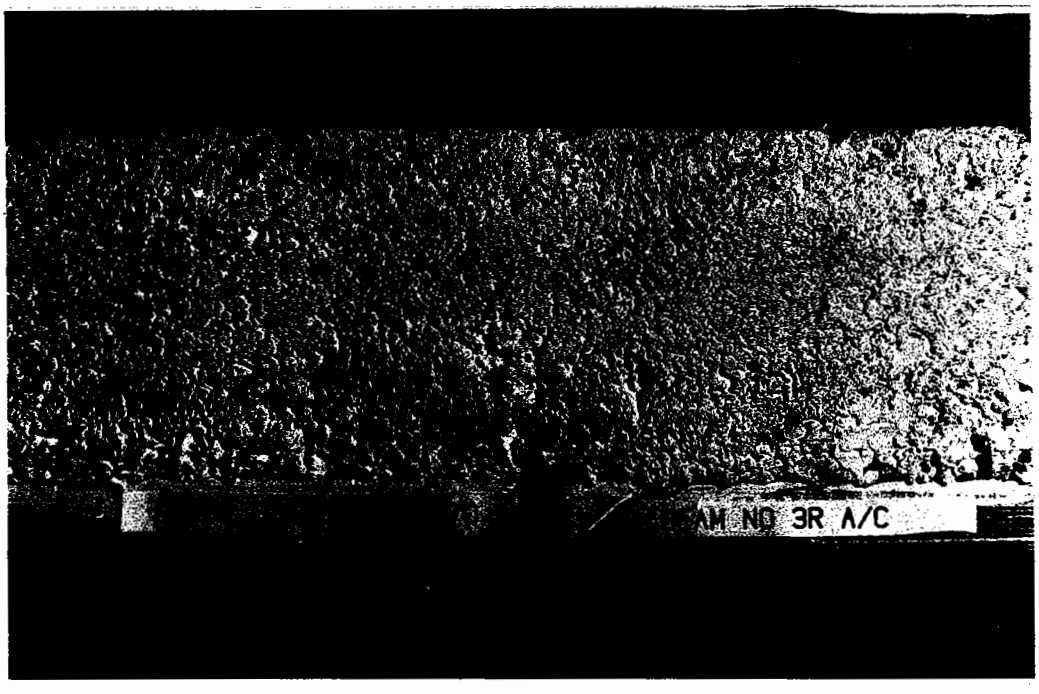

(b) reinforced at base of asphalt layer

Fig 5.11 Asphaltic concrete beams, reinforced & unreinforced

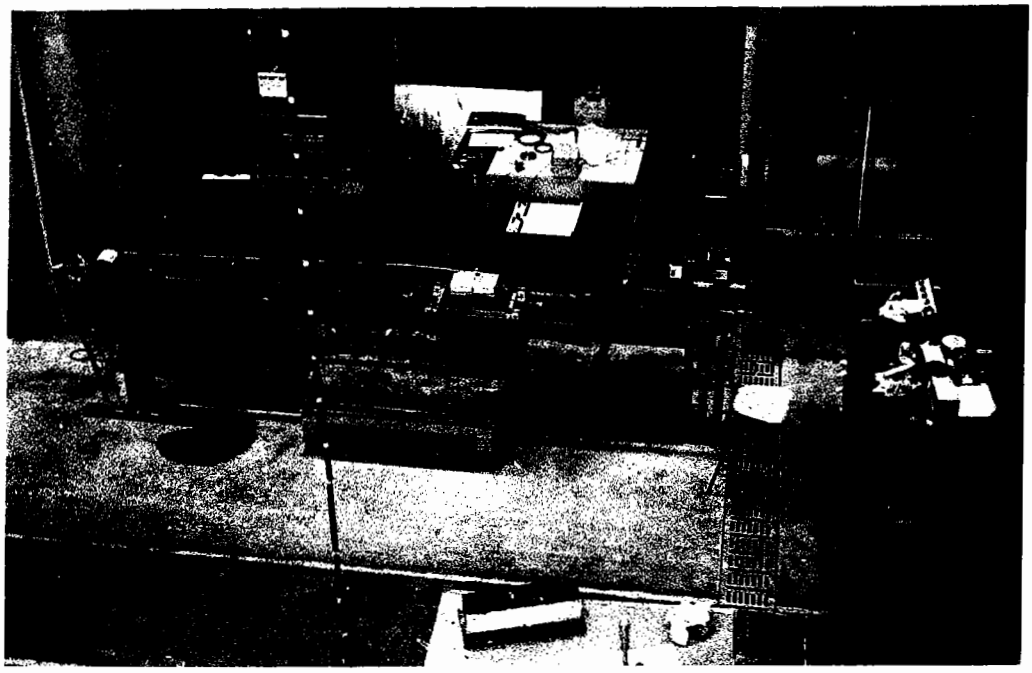

Fig 5.18 Views of the slab testing facility

Fig. 5.22 Steel mould for slabs

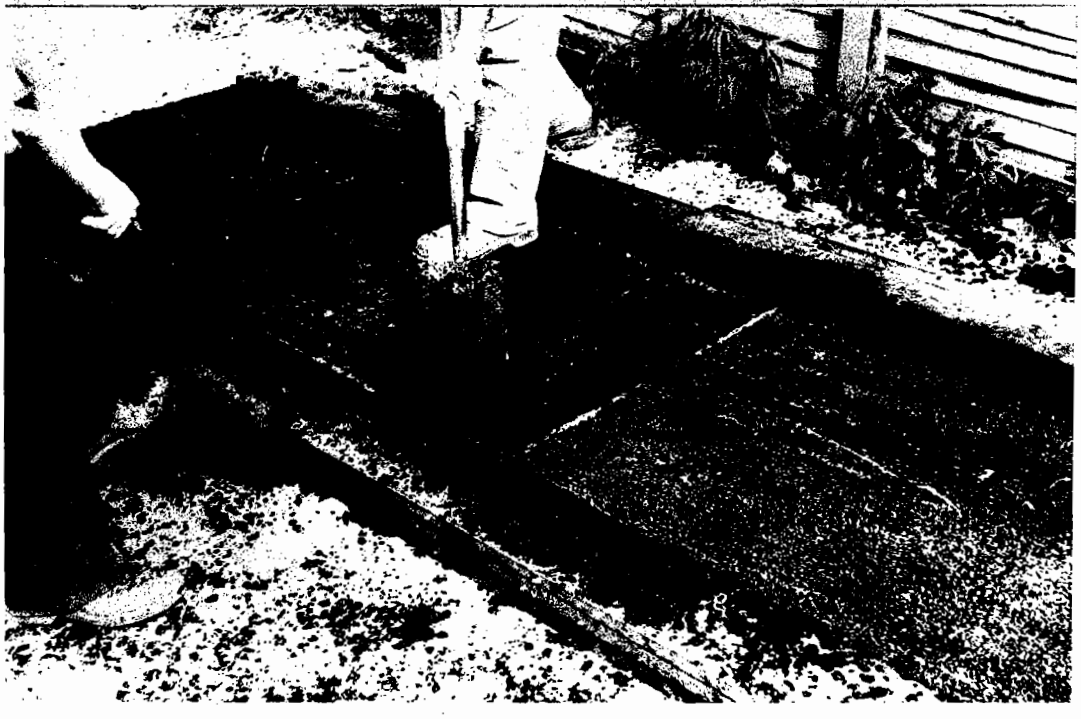

Fig. 5.23 Construction of slabs

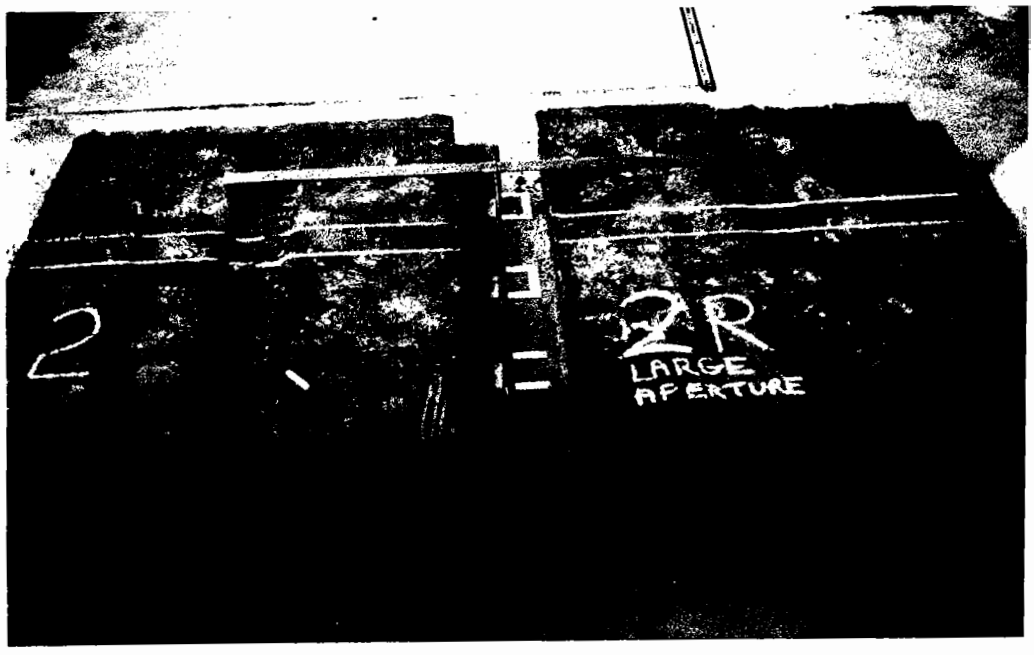

(a) Rutting: unreinforced left, reinforced right

(b) Cracking: unreinforced left,reinforced right

Fig. 6.9 Comparison of reinforced and unreinforced slabs

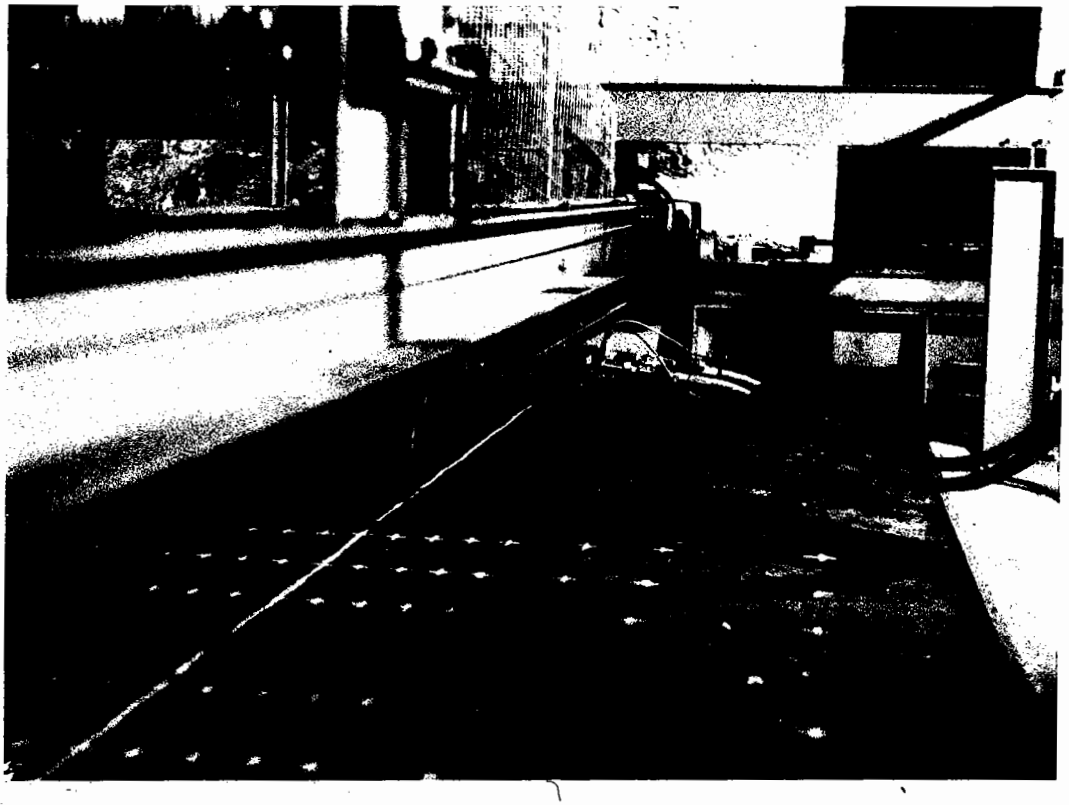

Fig. 7.2 The pavement test facility

Fig. 7.3 Grid anchored with a reinforcing bar

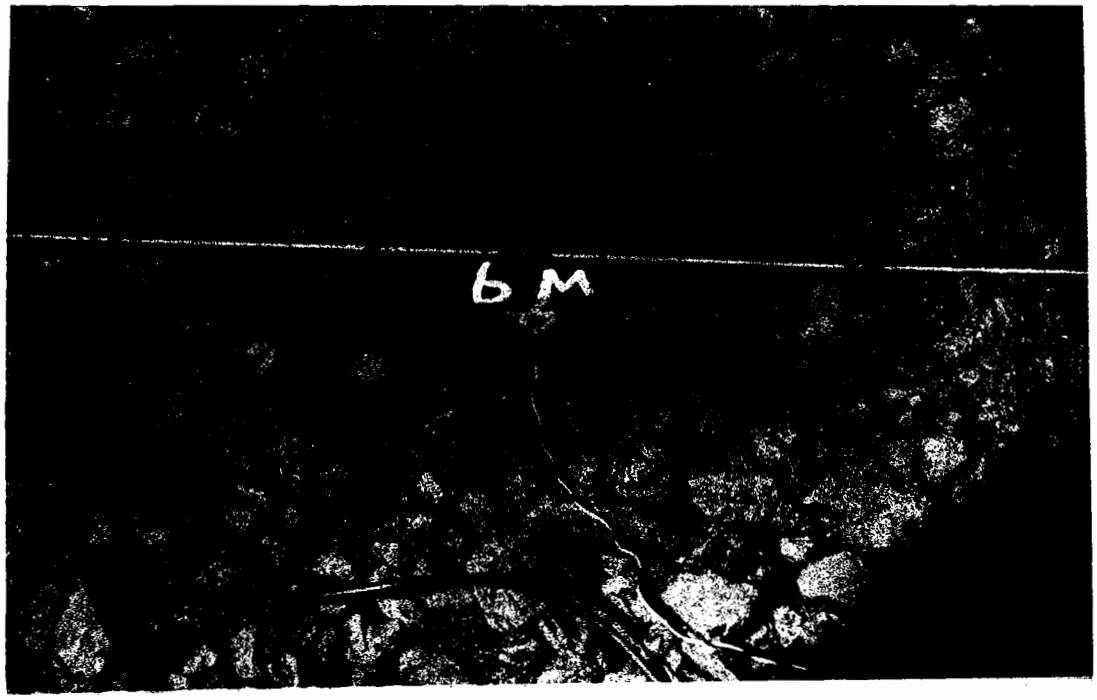

Fig. 7.11 Soil strain coils in subbase

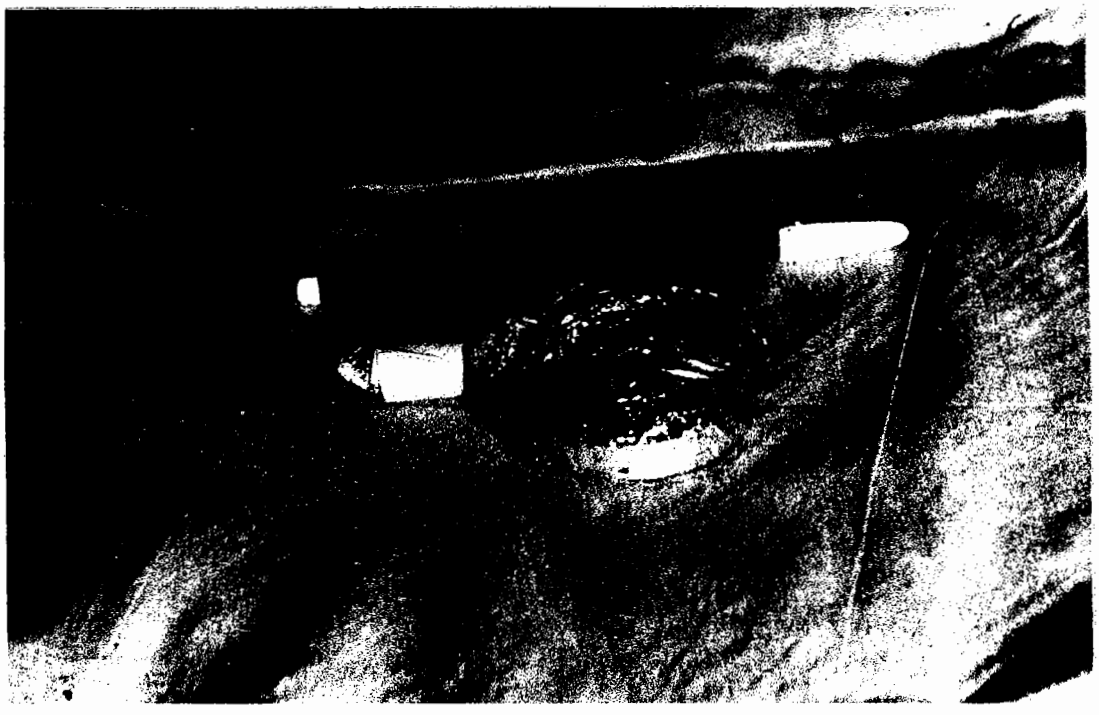

Fig. 7.12 Diaphragm pressure cell in protective sheath

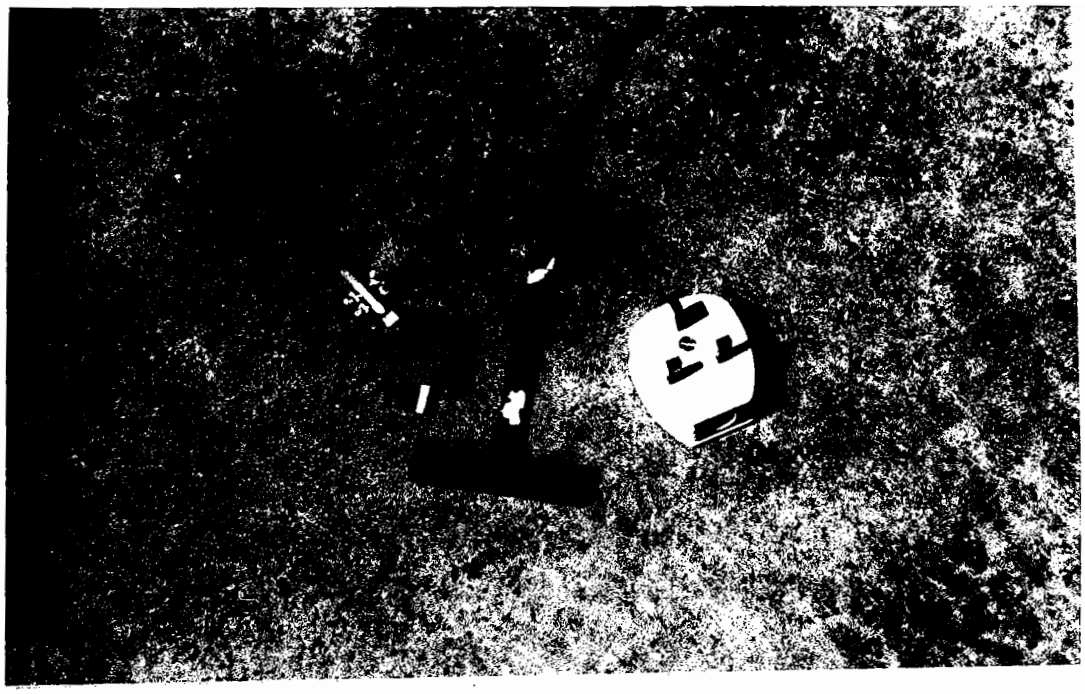

Fig. 7.13 Strain transducers (FTCII)

Fig. 7.14 Strain transducers in bed of mastic

(a) Section P2

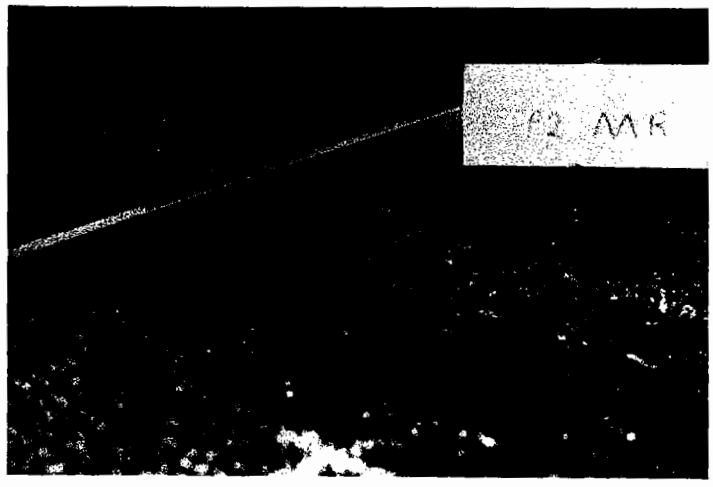

(b) Section P2MR

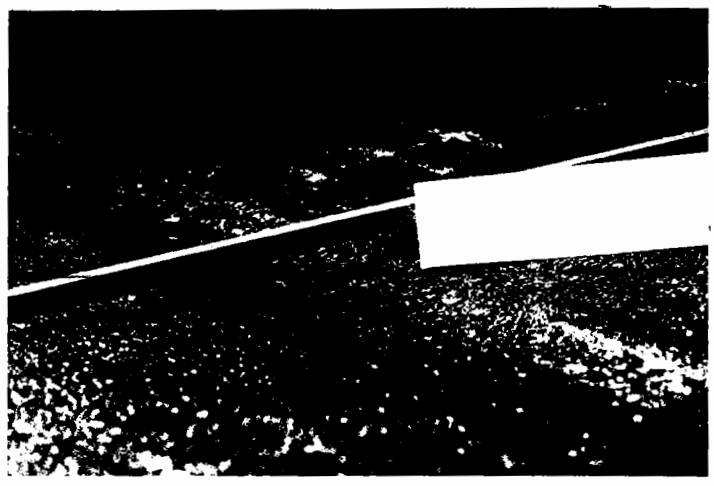

(c) Section P2BR

Fig. 7.22 Surface deformation at end of test

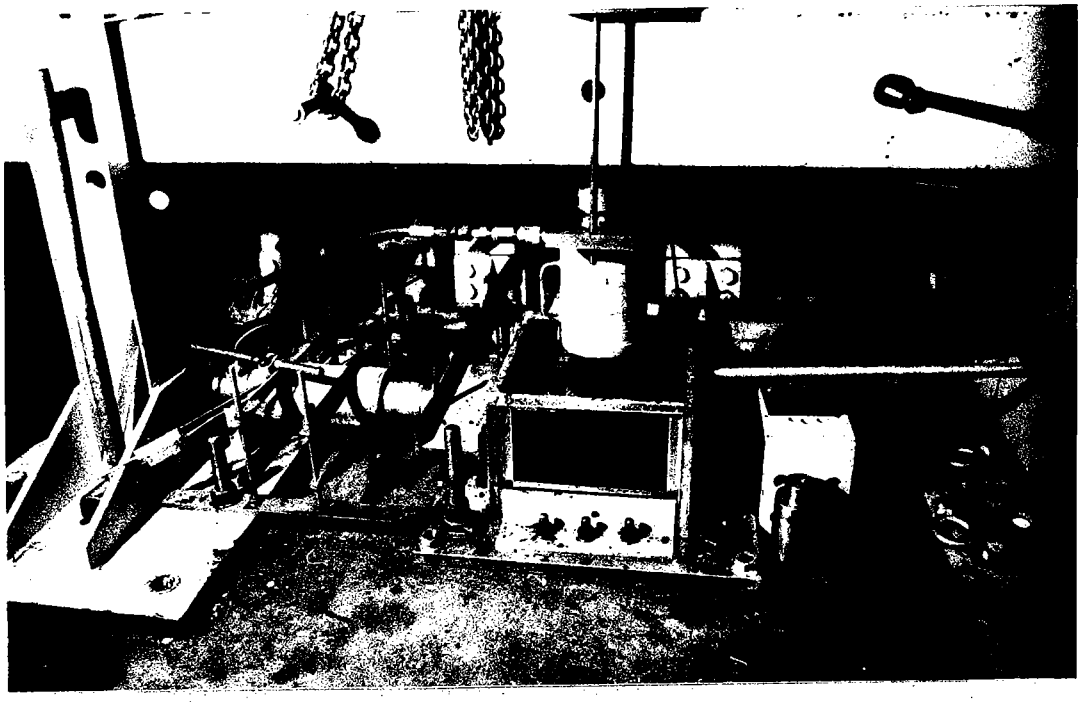

Fig. 8.6 Shear box during compaction.

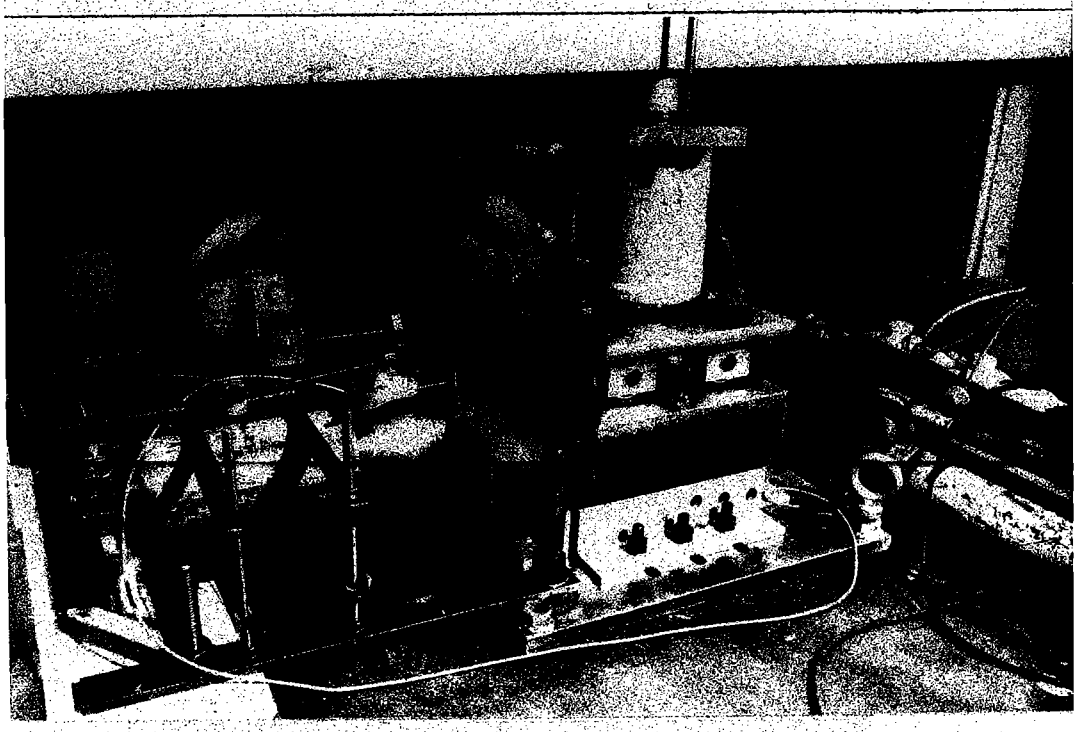

Fig. 8.7 Shear box during testing

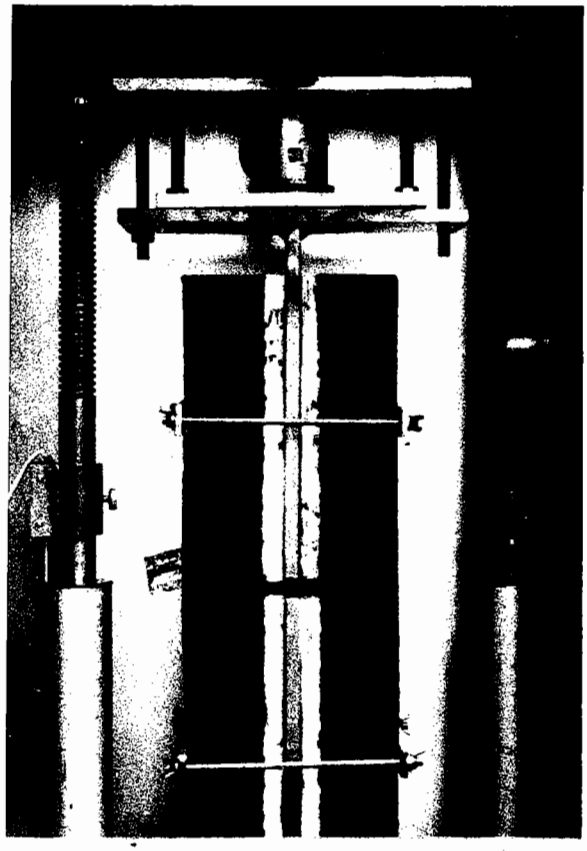

(a) Test sample

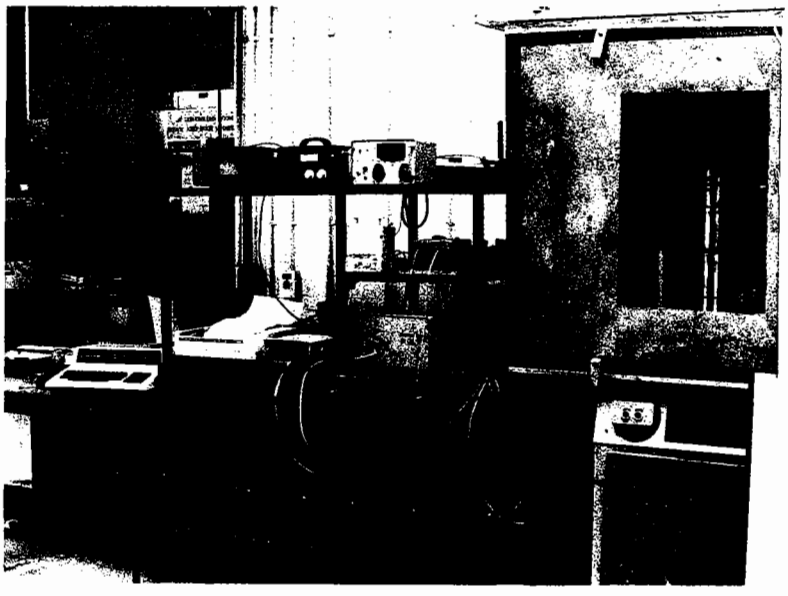

(b) Test apparatus

Fig C2 Thermal reflection crack simulator

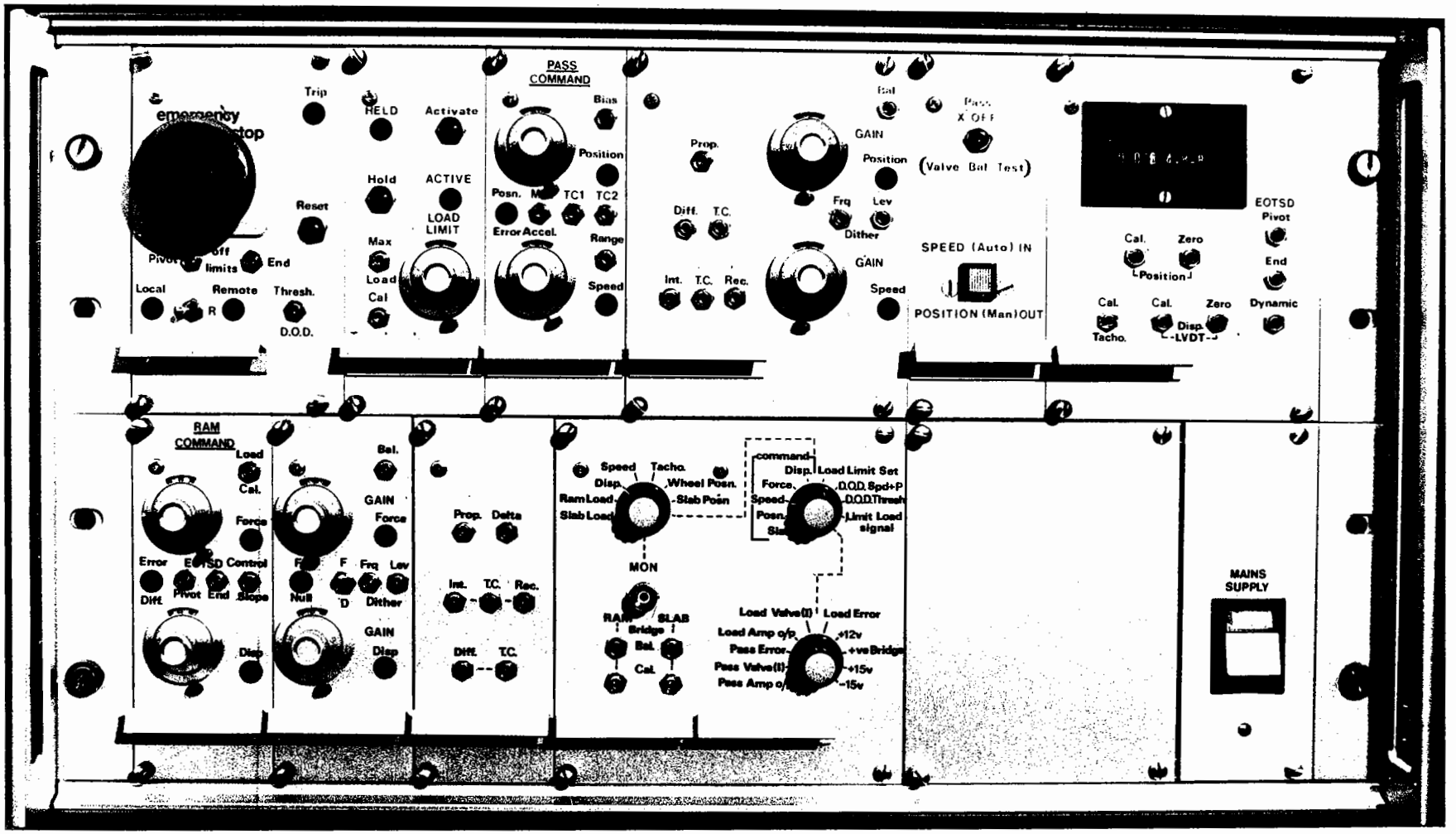

Fig E2 Electronic console for S.T.F